The effect(s) of dose and dose-rate of ionising radiation on early lens epithelial cell response and cataractogenesis

STEPHEN GREGORY RAYMOND BARNARD

The effect(s) of dose and dose-rate of ionising radiation on early lens epithelial cell response and cataractogenesis

A thesis submitted for the degree of Doctor of Philosophy

by

Stephen Gregory Raymond Barnard

Research conducted at Public Health England, Chilton, Oxfordshire UK

Thesis submitted to Durham University, School of Biological and Biochemical Sciences

September 2019

The effect(s) of dose and dose-rate of ionising radiation on early lens epithelial cell response and cataractogenesis

Stephen Gregory Raymond Barnard

Submitted for the degree of Doctor of Philosophy

September 2019

Abstract

The lens of the eye is thought to be one of the most radiosensitive tissues. Cataracts were one of the first observed biological effects following ionising radiation exposure. The recent change in regulations for eye lens dose limits has led to the urgent need to make sure our biological understanding is sufficient. The anterior of the lens is covered by lens epithelial cells (LEC), that are critical to maintaining normal lens function and producing fibre cells. Damage or disruption to LECs can have detrimental consequences to the lens. Low dose (<500 mGy) radiation-induced DNA damage and repair, cell proliferation and lens opacity were investigated post-exposure in or amongst four mouse strains (C57BL/6,129S2, BALB/c and CBA/Ca). Mice were sacrificed up to 24 hours post-exposure and lenses removed and epithelia isolated for analyses. Immunofluorescent staining for DNA double strand break (DSB) repair (53BP1) and cell proliferation (Ki67) were performed. Dose, dose-rates were varied during exposures to seek experimental evidence to support the epidemiological studies. Peripheral blood lymphocytes were collected for comparison with LEC. 120 female mice were irradiated and their lenses analysed for opacity at monthly intervals over 18 months. An inverse dose-rate effect was observed in the DSB repair response, as well as slower repair at low IR doses and a significant strain dependency. A nonlinear response to IR was observed for LEC proliferation that was bimodal; inhibition at low dose (<50 mGy), and a significant interaction effect between dose-rate and region. Lens opacity also increased over time. These results give the first biological evidence for an inverse dose-rate response in the lens. They highlight the importance of dose-rate in low-dose cataract formation represent the first evidence that LECs process radiation damage differently to blood lymphocytes. More work is needed to support lens dose limits.

Contents

List of Tables:

List of Figures:

Abbreviations:

µSv – Microsievert

53BP1 - Tumour suppressor p53-binding protein 1

^{60}Co – Cobalt 60

ANOVA – Analysis of variance

ARC – Age related cataract

ASPA – Animals Scientific Procedure Act

Atm - Ataxia–telangiectasia mutated

AWERB – Animal Welfare and Ethical Review Body

BER – Base excision repair

BMP – Bone morphogenetic pathway

BSA – Bovine serum albumin

BSS – Basic Safety Standards

CDKN1A – Cyclin dependant kinase inhibitor 1A

cGy – Centigray

CO_2 – Carbon dioxide

CT – Computed tomography

CtIP – C-terminal interacting protein

DAPI - 4', 6-diamidino-2-phenylindole

DDR – DNA damage response

DDREF – Dose and dose-rate effectiveness factor

DNA - Deoxyribonucleic acid

DNA-PKcs - DNA-dependent protein kinase, catalytic subunit

DSB – Double strand break

ECDF – Empirical cumulative distribution function

ECM – Extracellular matrix

ECRP – Endoscopic retrograde cholangiopancreatogrophy

EdU - 5-Ethynyl-2´-deoxyuridine

EHR – Excess hazard ratio

EMP – Extracellular matrix protein

Ercc2/XPD - Excision repair cross-complementing

ERK - extracellular-signal-regulated kinase

ERR – Excess relative risk

EU – European Union

eV – Electron volt

EV – Extracellular vesicle

EYA – Eyes absent

FA – Formaldehyde

FGF – Fibroblast growth factor

Gy – Gray

GZ – Germinative zone

H2AX – Histone variant H2

H_2O_2 – Hydrogen peroxide

HLEC – Human lens epithelial cells

HR – Homologous recombination

HSE – Health & Safety Executive (UK)

Hsf4 – Heat shock factor 4

IAEA – International Atomic Energy Association

ICRP – International Commission on Radiological Protection

IR – Ionising radiation

KeV – Kiloelectron volt

Ki67 – antigen KI-67

kVp – Peak kilovoltage

LDLensRad – Low dose lens radiation

LEC – Lens epithelial cell

LEDGF – Lens epithelium derived growth factor

LET – Linear energy transfer

LFC – Lens fibre cell

LOCS III – Lens Opacity Classification System

mA – Milliamps

MAPK - Mitogen-activated protein kinases

MCM – Minichromosome maintenance proteins

mGy – Milligray

MIP – Major intrinsic protein

MMP – Matrix metalloproteinases

MP18 – Membrane protein 18

MRC – Medical Research Council

mSv – Millisievert

NBS – Nijmegen breakage syndrome

NER – Nucleotide excision repair

NHEJ – Non-homologous end joining

OFZ – Organelle free zone

OGG1 – 8-oxoguanin DNA glycosylase 1

ORAMED – Optimisation of Radiation Protection of Medical Staff

P53 or TP53 – Tumour suppressor protein

PBS – Phosphate buffered solution

PCNA – Proliferating cell nuclear antigen

PDGF – Platelet derived growth factor

PFGE – Pulse field gel electrophoresis

PHE – Public Health England

PPE – Personal protective equipment

PPL – Personal project licence

Prkdc - Protein Kinase, DNA-Activated, Catalytic Subunit

PSC – Posterior subcapsular opacity

Ptch1 – Patched 1

rAML – Radiation-induced acute myeloid leukaemia

RBE – Relative biological effectiveness

RIF – Radiation-induced foci

RNA – Ribosomal nucleic acid

ROS – Reactive oxygen species

Scid – Severe combined immune deficiency

SSB – Single strand break

Sv – Sievert

TGF – Transforming growth factor

TLD – Thermoluminescent dosimeter

TX – Triton-X

UV – Ultraviolet

Wnt – Wingless Int-1 pathway

WT – Wild-type

XRCC1 – Chinese hamster cells 1

α – Alpha

β – Beta

γ – Gamma

Declaration

The work in this thesis is based on research carried out at Public Health England, Centre for Radiation, Chemical and Environmental Hazards, Chilton, Oxfordshire, U.K. and the Department of Biosciences, Durham University, U.K. No part of this thesis has been submitted elsewhere for any other degree or qualification and it is all my own work unless references to the contrary in the text.

Acknowledgments

Firstly, I would like to give my thanks and gratitude to my PhD supervisors Roy Quinlan and Liz Ainsbury. Both have supported me throughout my thesis and given me this opportunity to study alongside my continued working commitments at PHE – it is safe to say I have not always found the balancing of both work and my PhD easy, but thank you both for always being understanding and pragmatic. You have both given me critical input that has pushed both my thesis and my career to become a better scientist. Given the topic of my PhD, I could not have wished for a better 'dream team' of supervisors.

I must thank Simon Bouffler (and Public Health England) for giving me the opportunity to study and for continued feedback which has strengthened my writing, research, and this thesis greatly. I would like to thank MRC Harwell for allowing me and my project access to the gamma irradiation facility, particularly Mark Hill and James Thompson of Oxford University for regularly calibrating the sources to my requirements. I would also like to think Bob Sokolowski for helping organise the logistics of irradiating animals in another facility. I would like to thank Tim Daniels for assisting in further calibration at both the MRC and the X-ray facility at PHE.

I would to express my gratitude to the LDLensRad project and all its partners, with my thesis and the project being closely interlinked. I need to give special mention to Claudia Dalke for help and advice with setting up aspects of these experiments. I would like to thank my research group for creating a great environment to work in and lots of cake. I need to especially thank Roisin McCarron for all her help with imaging of mice for days on end in a windowless room, and Jayne Moquet who has read everything I have written, given advice, support and been my general 'agony aunt' when I need to vent!

This PhD would not have been possible without the support of my partner Jennifer, who continually supports me in everything I do! Thank you for the experiences and adventures we've still could have during this PhD. I would also like to thank my parents Joan and Steve for supporting all my ventures, and Greg for finding any excuse for us to visit a pub when I really shouldn't, sometimes a beer was just what was needed! I would also like to thank the constant encouragement and support from Alex and the whole Thomas family.

List of publications

Some of the work presented in this thesis has been the object of publication:

Barnard S.G., Ainsbury E.A., Quinlan R.A. and Bouffler S.D. (2016). Radiation protection of the eye lens in medical workers – basis and impact of the ICRP recommendations. *British Journal of Radiology.* 89 (1060). (Chapter 1).

Barnard S.G.R., Moquet J., Lloyd S., Ellender M., Ainsbury E.A. and Quinlan R.A. (2018). Dotting the eyes: mouse strain dependency of the lens epithelium to low dose radiation-induced DNA damage. *International Journal of Radiation Biology*. 94(12). (Chapter 3).

Barnard S.G.R., McCarron R., Moquet J., Quinlan R.A. and Ainsbury E.A. (2019). Inverse dose-rate effect of ionising radiation on residual 53BP1 foci in the eye lens. *Nature Scientific Reports.* 18;9(1). (Chapter 4).

Forward

"Radiobiology is the study of the action of ionizing radiation on living things" (Hall 1973).

This sentence explaining radiobiology from Eric Hall's 'Radiobiology for the radiobiologist' is a very fitting description, as this thesis is an investigation of the effects of radiation upon *in vivo* exposed lenses of living animals. Therefore, the following introduction addresses several key topics which need some understanding in order to fully appreciate the findings of the studies that are subsequently described.

This thesis aims to increase understanding to ensure the knowledge is there to make informed judgement for radiation protection, so the undoubted benefits of ionising radiation, in both medicine and industry, can be realised while radiation workers and the population are given the best possible protection regarding radiation-induced cataractogenesis. The influence of genetics upon radiation-induced cataract are largely unknown, as are the mechanistic and biological pathways causing cataract following radiation exposure. Effects to the DNA damage responses, as well as proliferation rates post-exposure in the lens epithelium have been hypothesised as having a role in the progression of cataract. The use of multiple strains of inbred mice following low dose radiation exposure will aim to identify the influence of genetics at low doses of radiation upon DNA damage response and proliferation. The effect of dose-rate is unclear but also hypothesised, therefore *in vivo* exposure to multiple dose-rates will aim to identify any significance.

Cataract represent the most iconic non-cancer effect of ionising radiation exposure. They were one of the earliest side-effects on ionising radiation exposure observed, however the mode of action from exposure to visually impairing cataract remain largely unclear.

1. Introduction

1.2 Radiation

1.2.1 Ionising radiation

To understand the influence and effects radiation have on living organisms, it is first important to have some understanding of what radiation is and how it can interact with biological targets, such as the lens of the eye.

The absorption of energy from radiation in biological target material can lead to excitation or ionisation. Excitation occurs when an electron in an atom is raised to a higher energy level without the electron being ejected from the atom or molecule (Hall 1973). If the radiation has enough energy to eject the electron(s) from the atom or molecule, this process is called an ionisation, and the whole action referred to as ionising radiation (Hall 1973). Radiation tends to be divided into two categories; ionising (IR) or non-ionising (see figure 1.1). These categories refer to the energy of the radiation, with ionising radiation being stronger. During IR, the energy dissipated per ionising 'event' is thought to be approximately 33 electron volt (eV), more than capable of breaking chemical bonds (Hall 1973). When IR passes through an object, electrons are ejected from its atoms leaving positively charged ions. IR has enough energy to remove electrons from atoms, with this process producing ions. This ability to induce chemical changes has repercussions for biological functioning, with disruption to cellular function affected.

Figure 1.1: Comparison of non-ionising and ionising radiation

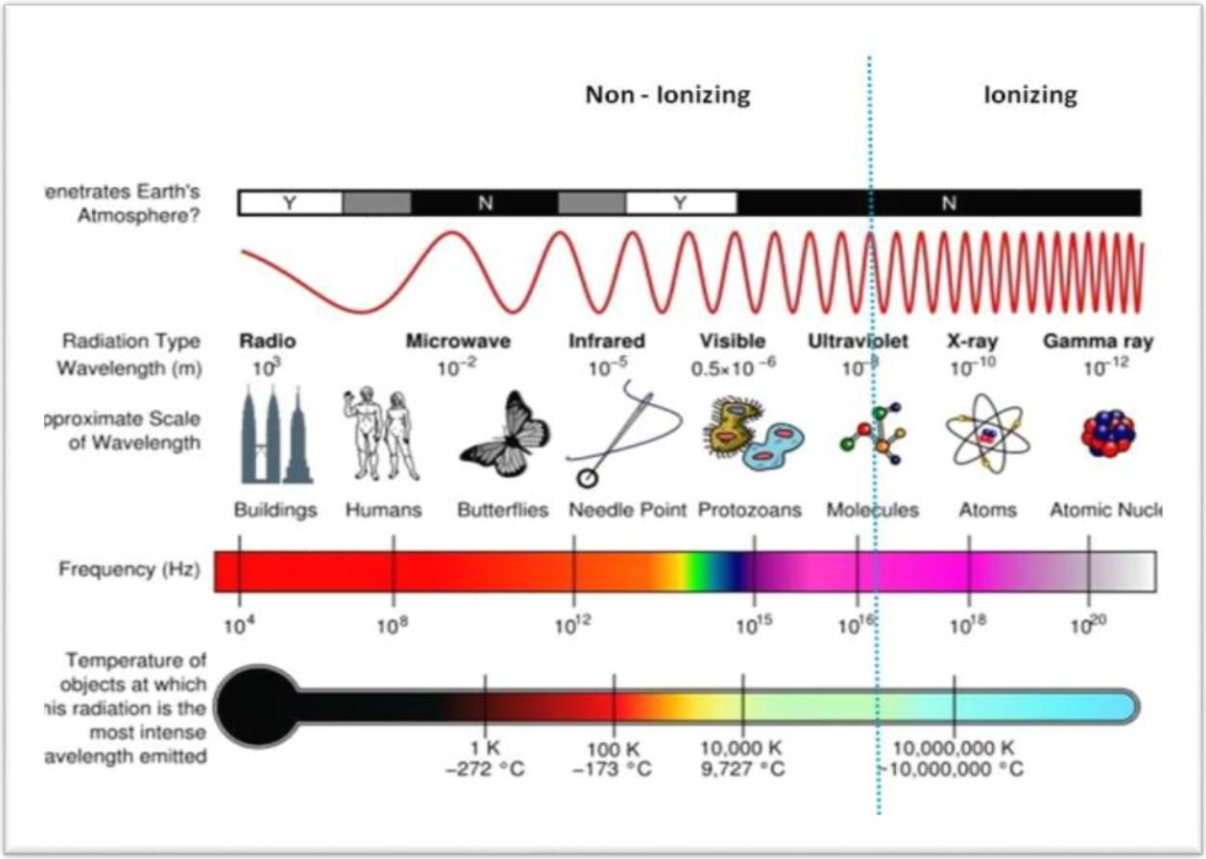

Figure 1.1: Comparison of non-ionising and ionising radiation, note the difference in wavelength of X-ray and γ-ray IR and their atomic scale.
(https://diamondenv.wordpress.com/2011/01/10/non-ionising-radiation/)

This chapter aims to outline the effect of IR on the lens of the eye. Experimental data were generated using IR exposures with both x- and γ-radiation sources. Whilst X- and γ-radiation do not differ in terms of nature or properties, the way in which they are produced differentiates them. The easiest way to explain this; X-rays are produced extranuclear, whereas γ-rays are produced intranuclearly. X-rays require an electrical device that can accelerate the movement of electrons at high energy. The electrons collide with a target material, often tungsten or gold, and upon impact some electrons are released to produce x-rays (Hall 1973). On the other hand, γ-rays are emitted, rather than produced, from radioactive isotopes. The emission of γ-rays is due to excess energy in the source material due to an unstable nucleus releasing electrons to achieve stability (Hall 1973).

Humans, but also other organisms, are exposed to IR through natural background sources (see figure 1.2) throughout life. To some extent organisms have adapted to such exposures, as natural radiation has been present since life first appeared on earth, from both terrestrial and extra-terrestrial sources (Mc Laughlin 2015). Most natural radiation exposure comes from natural gases,

such as radon, which get released from the ground. Humans have, over many years, facilitated the release of further gases during the extract of stones and soil etc. primarily for building resources. Another larger source of exposure is from direct radiation, for example radionuclides such as those found in rocks and soil. Radionuclides can be 'harvested' to create the IR sources used today for controlled exposures in nuclear, medical and diagnostic imaging, as well as experimental exposures.

Figure 1.2: Sources of ionising radiation in the world

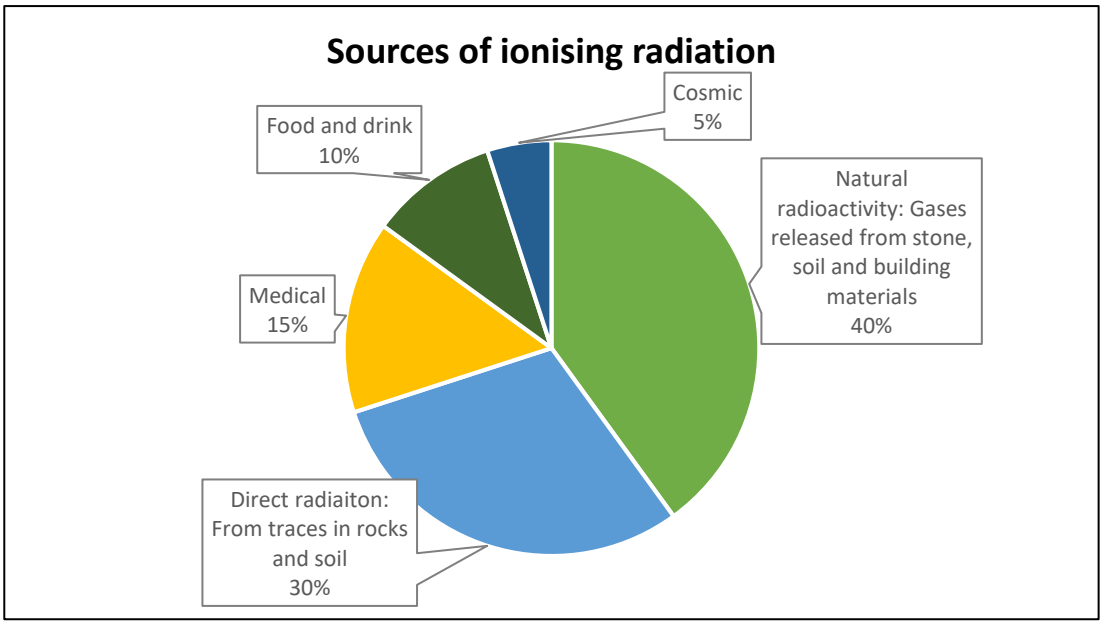

Figure 1.2: Sources of ionising radiation exposures, in brief. Values obtained and adapted form http://www.concert-h2020.eu/en/Stakeholders/natural_sources

X-radiation is the most well known source of IR for most persons given the abundant use and subsequent familiarisation when it is referred to. X-radiation was first discovered by Wilhelm Conrad Roentgen in 1895, who discovered that X-rays could pass through tissue but not bones, revealing a technique for imaging the skeleton. Over the next few decades, X-rays became increasingly used in medicine and dentistry. This improved knowledge and understanding of X-rays soon led to its use in industrial settings, along with improvements in X-ray tubes allowing them to deliver higher voltages. Fast forward to the present day and the use of radiation in medical, dentistry and industrial application is ever advancing and exposures are increasingly common. With this increasing use and reliance of IR in medicine came the inevitable risk of over-exposure and accidental exposure to IR, particularly for those exposed occupationally with IR on a regular basis.

This brief overview of the uses and sources of radiation exposure which humans are subjected has inevitably led to the introduction of radioprotective measures and safe working dose limits. To this extent, there is an increasing need for suitable radiation protection which is a topic that was discussed at length during this thesis (later in this chapter).

Exposure to IR results in a biological interaction in organisms. This interaction can have both a direct and/or indirect effect on a given cell. The direct effect, or direct ionisation, is the ionisation of a 'critical target' within the cell, with the DNA in chromosomes representing the most likely object. The individual particles have enough energy to directly disrupt the atomic structure of the object through which they pass (Hall 1973). This in turn starts a chain of events that lead to a biological change or loss of function in the cell. The indirect effect is the interaction of IR with other objects in the cell, for example water. Both X- and γ-IR are indirectly ionising. They do not produce chemical or biological damage themselves, but when absorbed by the target material as they pass through it, they give up or release their energy, producing fast-moving charged particles (Hall 1973). As an example, this energy release could be an electron from the water molecule (which accounts for 80% of a cell), producing a free radical. These free radicals can then cause damage to the critical target or other targets within the cell (Hall 1973).

During this thesis, experimental IR exposures were performed using both X- and γ-rays. X- and γ-radiation were the most appropriate exposures for the research questions this thesis aims to answer based on literature. However, it is worth considering heavy ion exposures, as these types of exposure are increasingly incorporated within medical and occupational exposures. Heavy ions are charged particles which directly ionise the object which they pass through, as described above. As the particle travels it produces ionisations, and these increase in density as the particle begins to come to rest, finally depositing a large amount of energy and ionisations (Hall 1973). These properties of heavy ion radiation therefore make them an attractive tool for radiotherapy treatments, where they can be used to treat tumours located within the range of this high ionisation range, sparing 'normal' tissue.

The direct and indirect effects of IR are due to excitations and ionisations in biological objects, but what else can influence these events? Such interactions are not random, but are dictated by, and localised to, the 'track' with which the particle travels along. This track is also dependant on the type of IR. Linear energy transfer (LET) is a term used to describe the amount of energy transferred per unit length of the track the particle travels along (Hall 1973). LET is a measure of quantity of energy transferred per unit length of the track. Therefore, the LET value is influenced by both the energy of IR and the length of the track itself. LET is essentially a measure of radiation quality, for example both the 250 kV x- and ^{60}Co γ-radiation used during the studies of this thesis are considered low-LET as they have values of around 0.3 keV/µ, whereas heavy ions such as neutrons are considered high-LET with a greater value of 12 keV/µ. IR is therefore often referred to has high- or low-LET based on such values.

IR-induced cataract was historically observed as one of the first side-effects of IR exposures; resulting in the lens since being considered a particularly radiosensitive tissue (Ainsbury et al. 2016; ICRP 2007a; Stewart et al. 2012). This radiosensitive classification is currently supported by the International Commission on Radiological Protection (ICRP), who, in 2012 proposed a significant reduction in annual exposure limits to the lens of the eye in occupational exposures (Stewart et al. 2012), discussed in more detail later.

1.2.2 IR quality and dose delivery

One potent property of IR is that sufficiently high enough energy is produced, enabling the breaking of chemical bonds. Whilst the direct and indirect ionisations that can occur with x-, γ- and heavy ion IR, as well as the differences between high- and low-LET, just as critical as the dose being delivered during an exposure is the way in which it is delivered. This determines the severity or complexity of the damage produced. Electron track structure, does rate and relative biological effectiveness (RBE) represent variations in IR that can have significantly different effects on the target site (i.e. DNA). The RBE of a radiation type uses 250 kVp X-rays as a standard, with RBE being a measure of dose of another radiation type required to achieve the same lethal dose as these x-rays (Hall 1973). The ICRP state that the stochastic effects of IR depend not only on dose, but also on the type and energy of the IR delivering the dose (ICRP Publication 60). Throughout this thesis, experimental data were produced using both x- and γ-radiation. Whilst these two types of IR do not differ in terms of linear energy transfer (LET), X-rays are thought to be more biologically effective (a higher RBE) than γ-radiation due to the production of secondary electrons (Hill 2004). This was demonstrated by an increased yield in chromosome aberrations following X-radiation exposure (Agency 2011). As discussed in this chapter, dose-rate is an important consideration when investigation radiation-induced cataracts. Dose-rate is the time in which the dose is delivered. Historically, the focus of IR-induced cataract research has been on the effect of dose and threshold, to improve understanding of whether cataract induction was stochastic or deterministic (a 'tissue effect') in nature (Hamada et al. 2014; Hammer et al. 2013). The effects of chronic, fractionated or protracted exposures remain unclear (Hamada 2016) but recognition that the lens may be more radiosensitive than previously thought means that these were increasingly of interest, particularly in the contexts of medical and occupational exposures (Barnard et al. 2016).

1.2.3 Radiation Protection and the lens

The 'radiosensitive' nature of the eye lens has been recognised for many decades, cataract were one of the first side effects of radiation exposure to be observed. This led to a huge amount of research into radiation-induced cataractogenesis in the last century.

Historically, cataract was thought to be induced by acute low-LET exposures of under 2 Gy for acute, and under 5 Gy for protracted (longer term) exposures (Ainsbury et al. 2009). These doses were thought to be deterministic; below this threshold of radiation dose, radiation-induced cataract did not occur (Hall 1973). In 1996, the UK National Radiation Protection Board (NRPB) (Edwards and Lloyd 1998) and similarly the German Radiation Protection Board suggested that radiation-induced opacities were potentially induced at less than 2 Gy. The International Commission on Radiological Protection (ICRP) had also classified radiation-induced cataract as a deterministic effect of exposure, with a threshold of 2 Gy for acute, and 4 Gy for fractioned exposures. This threshold was higher for protracted exposures ('1990 Recommendations of the International Commission on Radiological Protection' 1991; ICRP 2007b).

Since these publications issued guidance and recommendations, several studies, both epidemiological and experimental, have been published as compiled by Ainsbury *et al.* in 2009 (Ainsbury et al. 2009). These studies contain conflicting evidence against the threshold doses for cataract induction and questioned whether the deterministic status of radiation-induced cataract was correct. A reanalysis of epidemiological studies upon which these historical thresholds were founded was recommended, based on increased knowledge of latency periods and statistical analysis, suggesting that these historical studies were carried out too soon post-exposure, making judgements on low dose difficult to extrapolate and conclude.

There was a response from the ICRP in 2007 with the release of report 103 (ICRP 2007a), which details a review of the epidemiological and (limited) mechanistic literature suggesting that the lens of the eye may be more radiosensitive than previously thought. However, insufficient information was available from which to draw a firm conclusion on eye sensitivity. Since that report the ICRP made further comment in the form of a statement on tissue reactions (ICRP 2012) and report 118 (ICRP 2007b) that suggested an assumed absorbed dose threshold reduced to 0.5 Gy for the lens and a recommendation for reduced occupational equivalent dose limits for the lens from 150 mSv yr^{-1} to 20 mSv in a year, averaged over 5 years, with no single year exceeding 50 mSv. This was a dramatic reduction in recommended dose limits, attracting much attention. Those revised dose limits have since been incorporated into the current European Basic Safety Standard (BSS) which were incorporated and implemented by EU member states in February 2018.

This ‘paradigm shift’ regarding lens radiosensitivity initiated by ICRP 103 (ICRP 2007a) and the subsequent radiation protection recommendations led to increased research interest of the induction of cataract following IR exposure. In addition to several major epidemiological analyses and reanalyses, published studies have now considered type and extent of exposures, mechanisms of initiation of primary opacification of the lens, and the subsequent development through to clinically relevant cataracts, with techniques/equipment suggested to improve lens protection.

Particularly important have been studies in occupational medical settings, where individuals receive readily measurable exposures, and thus decreased dose limits have the potential to genuinely impact individual working hours and patterns. Probably the most common use of radiation within the medical setting is for diagnostic assessments. Medical radiation procedures are becoming increasingly frequent and advances in treatments in recent years have also led to increased complexity and variability in both patient and medical staff exposure scenarios. Those most likely to be affected by the new BSS lens exposure limits are interventional radiologists, cardiologists and individuals involved in nuclear medicine production who are also most at risk of frequent exposure (Frey 2014; Seals 2015; Bitarafan Rajabi 2015; Ciraj-Bjelac 2012).

During this chapter, many studies are discussed where eye lens radiation doses have been assessed in cohorts of medical staff and the occupationally exposed over time. The recent evidence from the literature allowed conclusions to be drawn regarding the likely spectrum of medical and occupational exposure types and doses. Ultimately the particular focus for studies of workers in the medical sector aims to help address questions surrounding the ease of compliance with the revised BSS, including the UK Health & Safety Executive (HSE), and others (Martin 2011).

One particular challenge in medical occupational exposure settings is the availability of relevant radiation protection tools (Bouffler 2012). Current methods of eye dosimetry need to be assessed to ensure that it will be feasible to maintain accurate records of eye lens doses - suitable and accurate dosimetry will be crucial to dose limit compliance.

The ICRP acknowledge that their conclusions regarding the increased radiosensitivity of the lens rely heavily on the weight of epidemiological evidence, while direct mechanistic evidence is somewhat lacking (ICRP 2012). Thus, it was highly relevant to consider new experimental studies, which would inform on mechanisms of cataract initiation and development to strengthen current radiation protection judgements. The aim of this thesis is to provide evidence and better understanding of early biological and mechanistic effects of IR within the lens and the relevance to cataract formation as a result.

1.2.4 Lens dose limits and impact

The mechanistic and biological effect of IR exposure upon the lens, particularly at low doses, were a key focus of this thesis. However, it is important to understand who is affected by low dose and how such exposure will impact on their working life, society and the general public. After all, the recommendations of the ICRP to reduce lens dose limits have driven the recent interest in low dose IR effects upon the lens.

Recently, there has been an influx of studies specifically relevant to low doses during occupational exposures, and this is partly due to the revisions made by ICRP on the recommended occupational eye lens dose limit and subsequently BSS regulations for working with radiation safely. The aims of the BSS were to ensure standardised safety procedures for those exposed to radiation occupationally and to a wider extent the public. As with ICRP (2012), the contributors to the BSS felt that given the increasing weight of evidence for induction of cataracts at doses lower than 2 Gy, the lower lens dose limit needed to be put in place regardless of the remaining research uncertainties, to keep doses as low as reasonably practicable. This has always been the philosophy applied in radiation protection practice.

Lower working dose limits and increased protection and monitoring will inevitably bring a financial cost which should be viewed in terms of the potential benefit to health. Such changes can also be expected to bring some savings as a result in the long term when considering future healthcare and interventions. Within the UK, the initial cost required to comply with new regulations would be around £8 million for both the medical occupational and nuclear worker settings. This is then estimated to equate to around £24 million over a three decade period to implement (www.hse.gov.uk).

According to the revised BSS, workers with lens exposures likely to exceed 15mSv/year are classified at category A workers. Category A workers are those working in areas where radiation exposure levels are higher, creating controlled areas with greater restrictions on access. The impact on radiation protection here would mean a very thorough and systematic process for regular monitoring of workers, with each person requiring individual dosimetry. This is likely to result in the introduction of new procedures and dosimeters with a financial cost attached for both the product and additional service charges to satisfy the new criteria for safety and monitoring.

In response to the BSS and ICRP revisions on the recommendations for eye lens doses, the UK based Health & Safety Executive (HSE) compiled a report outlining the impacts on those affected, concerning costings and benefits of the changes. The document can be found at

www.hse.gov.uk. To summarise some of the key findings relevant to the UK, the HSE predicted a relatively small number of individuals to be at risk of significantly high lens doses, but there was also a warning that some work could be prohibited if persistent over-exposure occurred. The incorporation of further monitoring using optimised lens dosemeters will remedy this issue. Education and training in understanding the importance of radiation protection of the lens cannot be underestimated for those individuals occupationally exposed.

Cataract surgery (the removal of the opacification usually by laser) is now a common procedure across the world. Upon development of a visually impairing opacity, surgery can be performed to lase a hole through the opaque cells to allow light to pass through. This procedure is usually performed in less than 10 minutes and is reportedly pain-free, with patients expecting around a two hour visit in total. The success rate of cataract removal is very high, but it does come with risks associated post-surgery. In around a quarter of patients, the artificial lens inserted to replace the damaged lens became cloudy due to lens epithelial cells (LECs) attempting to populate the lens once more. This can result in a posterior capsular opacity which requires further treatment (www.visionaware.org). To put cataract surgery into perspective, in the US alone, Medicare estimates costs for cataract extraction in the region of $3.6 billion per year, accounting for 60% of visually impairing disorders (Chodick 2008).

Although the proposed lens dose limits have raised some concerns over the likelihood of compliance and the impact of workload and staffing, a recent survey found that 93% of medical physicists and radiation protection officers were aware of the proposed reduction and a further 55% of those were actively participating to some degree to monitoring of specific eye lens dose monitoring studies (Carinou et al. 2014). Interventional radiologists and cardiologists who typically receive the highest doses of radiation during their associated procedures had been identified as most at risk of over-exposure under the new dose limits (Broughton. J. 2013). Similarly a study conducted by Public Health England (Ainsbury 2014) regarding UK workers across three radiology departments involving over 1000 individual procedures used optimised lens dosemeters alongside questionnaires were also included to assess the likelihood of compliance. In total 68 persons took part in that pilot study, only two individuals received extrapolated doses of slightly greater than the 20 mSv/year limit, although these two individuals were not using protective lead glasses. There are an increasing number of imaging techniques that require close personal contact between operator and patient, especially in paediatric settings, and the risk of exceeding dose limits are a potential hazard as throughput increases.

Eye lens monitoring, personal protective equipment (PPE) availability and enforcement, as well as education and training are and will continue to be paramount to ensuring a minimum number of workers are over-exposed to radiation in the lens (Le Heron 2010).

Furthermore, in support of the ICRP and BSS, implementation of the revised dose limits for the lens of the eye will also affect most radiation workers in a positive manner - whether that is through increased awareness and training or introducing new dosimetry and radiation protection measures to ensure compliance. Recommendations are relevant across Europe and raise discussion internationally. It must be noted the HSE also raised the valid point that these new dose limits would not only affect occupational medical exposures but also those working within the nuclear sector including reactor vessel entry, fuel dismantling and industrial radiography. On an individual level, if education, protection and monitoring fail in reducing the lens dose limits, then alterations to work patterns may be necessary.

What was clear is that those workers affected, as well as the general population, have an interest in the effects of low dose radiation and the risk to the lens, and it is those particularly working in medical imaging that are the most at risk, with subsequent repercussions for airline crew, pilots, astronauts etc.

1.2.5 Medical and occupational exposures

Medical and occupationally exposed persons are most affected by low dose eye lens exposures and limits, as well as the general population. With IR-induced cataract being one of the largest non-cancer effects of exposure to radiation, there was a large interest in understanding the impact effects of low dose radiation and the risk to the lens, and the justification and application of reduced lens dose limits.

Prospective epidemiological studies take time to collate, but offer the most solid data on incidence of cataracts amongst the occupationally exposed. The most relevant epidemiological data for medical occupational exposures available to the ICRP reviewers was a 20-year study of this kind, published in 2008, based on almost 36,000 radiologic technologists in the US (Chodick 2008). An increased incidence of cataracts was found in workers of whom the majority received a cumulative dose lower than 500 mGy, supporting studies amongst the atomic bomb survivors and other populations, and the conclusions were presented in ICRP 118 (2012). Since then, a further follow up of this cohort of US radiologic technologists reported an excess risk of cataract at even lower doses, below 100 mGy cumulative dose (Little et al. 2018). A low dose and possible low dose-rate

excessive risk of cataract were suggested, strengthening the relevance of the investigations conducted within this thesis.

Interventional cardiologists and radiologists make up one of the largest and most diverse group of occupationally exposed individuals within the medical setting (Table 1.1). Procedures such as CT fluoroscopy – leading to mean whole body doses of between 0.007–0.048 mSv for the radiologist (Paulson 2001) - are widespread throughout the world and are often conducted in dedicated large departments allowing high patient throughput required by these procedure types in modern medical care. Seals et al (2015) reviewed the recent literature relating specifically to exposures of interventional radiologists and drew general conclusions regarding the risk of radiation-induced cataractogenesis in this cohort. The study found that with current workloads and radiation protective measures in place, there was a potential for lens doses to exceed the recommended limit of 20 mSv/y. Adherence to lens dose limits may not always be accurate in such studies, there is a further suggestion that current data with regards to interventional radiologists (but likely to be relevant to any studied cohort) reflects an underestimation of actual exposure, given the possibility that studied individuals were likely to alter their behaviour to reduce dose once they were aware of being a test subject.

A recent study identified a significant increase in the development of posterior subcapsular cataract (PSC) amongst a large cohort of 106 interventional cardiologists from a range of centres across France, with a further 99 age-matched unexposed control subjects (Jacob 2013). It is also noteworthy that no difference was seen in other opacification types between the two groups. Interestingly the risk of opacity increased with activity duration but not with workload. A summary of recently published assessments of interventional radiologists has been compiled (Omar 2015) including the work of previously published clinical cohorts (Ciraj-Bjelac 2012) and (Vano 2015). The concluding remarks from these studies revealed that using current monitoring techniques, workers were likely to exceed the new recommended occupational dose limits. A similar but larger retrospective study in Saudi Arabia analysed 34 staff including primary cardiologists and also assisting staff based on thermoluminescent dosimeter (TLD) badges worn at collar level (Al-Haj 2015). Cardiologists received the highest doses as expected but these were within the ICRP recommendations. There is substantial uncertainty using such a method whereby conversion coefficients due to different clinical set ups and X-ray tube angulation may significantly affect exposure.

The ORAMED (Optimisation of Radiation Protection of Medical Staff) project was set up to investigate low dose medical exposures and assess the risk and hazards these may pose including

those affecting the eye lens with a particular objective to optimize radiation protection in interventional cardiology and radiology settings (Vanhavere 2015) following recent interest in the potential lowering of exposure thresholds by the ICRP. A number of studies were conducted monitoring eye lens dose using specific dosimeters and extrapolation to yearly doses received by workers covering 34 European hospitals and 1,300 procedures. Lens annual dose is likely to exceed the 20 mSv/year limit, although there were some overestimations in these studies due to TLD positioning, highlighting the importance of effective dosimetry monitoring and PPE. ORAMED have developed a more accurate monitor optimised for eye lens dosimetry, the EYE-D dosemeter dedicated to lens specific exposure by incorporating Hp(3) measurements (Bilski 2011). The EYE-D monitor was demonstrated in use in 2013 (O'Connor 2013) and indicated likelihood to exceed 20 mSv/year in gastroenterologists, although the study concluded that this could be remedied by a reconfiguration of equipment in order to stay within the revised limits of eye lens exposure.

Interestingly, the survey discussed previously by (Carinou et al. 2014) found that of the respondents claiming to receive doses above the ICRP recommended limit of 20 mSv annually, 40% of them based this assumption on eye lens dosimeters already being worn, and these (being non-specialist eye dosimeters) may lead to inaccurate exposure amounts.

It can be difficult to predict the likelihood of over-exposure to the lens or have a general rule, as each medical centre will have varying levels of procedure throughput and radiation protection approaches. In a recent multicentre study, during fluoroscopic procedures it is estimated to take around 23.4 hours of exposure time before the eye lens receives a dose of 20 mSv (Attigah et al. 2016).

Table 1.1: Lens doses from recent studies of radiation dose in medical scenarios

Study	Country	Procedure	Avg. lens dose/procedure	Min/max lens dose/procedure	Dosimeter
O'Connor et al 2013 (22)	Ireland	Endoscopic retrograde cholangiopancreatography (ECRP)		0.01/0.09 mSv	EYE-D™
Jacob et al 2013 (16)	France	Various interventional cardiology		0.046/0.23 6mSv	TLD
Vano et al 2015 (18)	Spain	Catheterizations		0.044/0.067 mSv	APD
Al-Haj et al 2015 (19)	Saudi Arabia	Cardiologists	0.02 mSv	0.005/0.08 mSv	TLD
Ainsbury et al 2014 (13)	United Kingdom	Various Radiologist	0.03 - 0.05 mSv		Eye Lens
Romanova et al 2015 (24)	Bulgaria	Fractura femoris	0.046 mSv	0.02/0.0 7mSv	EDD30
		Fractura cruris	0.002 mSv (0.023 mSv with C-arm)	0.01/0.043 mSv	EDD30
Zagorska et al 2015 (25)	Bulgaria	Endoscopic retrograde cholangiopancreatography (ECRP)	0.034 - 0.093 mSv		EDD30
Rathmann et al 2015 (26)	Germany	Radiologists	0.018 mSv	0.012/0.029 mSv	TLD
Khoury et al 2015 (27)	Brazil A	Hepatic Chemoembilisation	0.017 mSv	0.007/0.041 mSv	TLD
	Brazil B	Hepatic Chemoembilisation	0.02 mSv	0.016/0/025 mSv	TLD
	Brazil C	Hepatic Chemoembilisation	0.08 mSv	0.012/0.148 mSv	TLD
Cemusova et al 2015 (35)	Czech Republic	Radiologists		0.013/0.070 mSv	EYE-D™

Table 1.1: Recent studies reporting lens doses of medical occupational exposures.

Orthopaedic procedures pose an exposure risk to the surgeons performing them. A recent Bulgarian study found average exposure per procedure to be 47.2 and 77.1 µSv for 3 and 5 minute procedure durations respectively (Romanova 2015). Given consistent workloads similar to those during the study period, compliance to the revised dose limits would be achievable, however if the workloads and working patterns alter, this could result in overexposure and is likely to occur in medical centres with higher throughputs. Similarly another study from Bulgaria, the same monitoring was applied to medical workers during endoscopic retrograde

cholangiopancreatography (Zagorska et al. 2015) with eye lens doses ranging from 34.9 µSv and 93.3 µSv per procedure. This study highlights the potential for the gastroenterologist performing the procedure and the associated anaesthesiologist to exceed the revised annual dose limit if protective equipment is not adhered to.

Not only can eye lens doses be assessed from retrospective studies of human cohorts, but phantom models can also be a useful investigative tool for current studies assessing exposures. These can have some limitations compared to human subjects, but useful data can be gathered on positioning and quality of measurement tools. Phantoms were used to estimate doses received to the eye lens, umbilicus and ankle of the interventional radiologist whilst performing percutaneous biopsy using modern C-arm computed tomography (CT) system incorporating laser guidance (Rathmann 2015). Whilst the eye lens was not the most sensitive tissue during these procedures, a significant dose of 180 µSv can be delivered per procedure. C-arm CT systems are becoming increasingly attractive and likely to be used more frequently in future, although the current data does not suggest eye lens dose being exceeded initially, a significant throughput and increased use of such a system would require a high level of eye lens monitoring and sufficient shielding to reduce the potential of over exposure.

A study performed in Brazil (Khoury 2015) monitored a number of interventional radiologists during hepatic chemoembolization, a common non-surgical technique where surgery is not an option. This multi-centre investigation found mean exposure values to be between 17.6 to 80 µSv per procedure. Furthermore, the researchers used this data to calculate the number of procedures that could be performed each week to keep within the revised annual dose limit of the lens, a novel approach which allows for workload and procedure throughput to be dictated by potential exposure.

Medical occupational exposures clearly represent the largest population of individuals most at risk of excessive lens radiation doses, with an obviously large variation in potential lens dose exposures due to differences in procedures and their lengths. These individuals are primarily who are affected by reduced lens dose limits. Another smaller but significant body of individuals are those handling radionuclides working within nuclear medicine (Bruchmann 2015). These situations have a variable degree of exposure and are likely less predictable than the working patterns and procedures of diagnostic and hospital related procedures. Specifics regarding nuclides used and the working environment are extremely important in determining eye exposures. Situations like those were why it is important to understand the influence of not only dose, but the quality and length of exposure.

1.2.6 Occupational radiation: dose-rates and exposures

One of the problems identifying potential risks of such exposures is the lack of epidemiological data to support investigations of dose, dose-rate and radiation quality. To date information on these factors has been obtained predominately from *in vivo* animal models, and to a lesser extent *in vitro* cellular models where exposure conditions can be controlled. Animal models can provide a useful source of lifespan data following radiation exposures (Dalke et al. 2018; Puk, de Angelis, and Graw 2013).

The new thresholds do not consider dose-rate effects largely because of a lack of epidemiological data supporting this at the time of print (Hamada et al. 2014). Therefore, it is important not to overlook the potential influence of dose-rate during this thesis. It has been hypothesised that there could be a significant dose-rate dependence of IR-induced cataract (Little et al. 2018; Hamada 2017b). Typically tissue damage following radiation exposure leads to an initial accumulation of DNA damage, followed by some degree of cell death and cell turnover, thus reducing some of this accumulated damage burden. Dose-rate and cellular turnover are both intrinsic in calculating the dose-rate effect. The lens is unique in that there is no cell death or degradation of cells, and early lens fibre cells are likely to be some of the oldest cells in the body. The dose-rate effect may not apply here. Rather than a dose-rate effect, it is proposed that a stationary or progressive cataract type develops caused by the accumulation of DNA damage. The ICRP have highlighted the need for further information to inform current judgements on the dose and dose-rate effectiveness factor (DDREF) applicable to the eye lens (Rühm 2015). DDREF values could be different for individual health endpoints, depending on the mechanisms that operate. DDREF as currently formulated by ICRP applies on to the stochastic effects of cancer and heredity effects. The use of the DDREF remains a matter of some debate as to whether dose and dose-rate should be pooled or considered as separately given potential differences in biological effects.

Another very important factor which is particularly relevant to medical and occupational exposure is the type of radiation exposure. Different radiation qualities are effective to different degrees in terms of inducing damage or biological endpoints, including cataracts. The relative biological effectiveness (RBE) of x-, γ- and β-radiation is similar, whereas α and neutron exposures have a broader, less well-defined, RBE. Most of what is known about the RBE values relevant for lens opacification is derived from epidemiological studies of human cohorts such as atomic bomb survivors and nuclear radiation workers. Given the radiosensitive nature of the lens as a tissue, the effects seen from neutron exposure within the atomic bomb survivor cohort demonstrate a different threshold of effectiveness compared to cohorts involving other types of radiation

exposure (Otake 1990). Mice exposed to neutron radiation (Di Paola 1978) have shown an increased susceptibility to cataractogenesis compared to γ-radiation exposure particularly at lower dose levels (Medvedovsky 1994). Heavy ions are a form of high linear energy transfer (LET) radiation quality found mainly in space but also encountered in heavy-ion beam therapy during medical procedures, although less common in recent years.

1.2.7 Monitoring eye lens doses

It is well known that experimental studies using radiation rely heavily on accurate dosimetry of dose during exposures, to strengthen the quality of the research and subsequent findings. Likewise, the same is required of epidemiological studies and occupational exposure monitoring and dose recording, such as those introduced and discussed above. A brief overview of how lens doses can be monitored is therefore useful to understanding the strengths and weaknesses these studies.

There is evidence in the literature that with current working practices, lens doses received by interventional cardiologists, in particular, may be close to or exceeding the new eye lens dose limit of 20 mSv yr^{-1}. To ensure accurate compliance monitoring, it is apparent that changes to current dosimetry practices may be required. The use of both medical personnel and phantoms are useful in providing data on exposure doses, but also for testing the suitability of monitoring techniques. Typically, the standard method of monitoring consists of a TLD worn around the chest area, giving a representation of whole body dose but not specifically for the radiosensitive eye lens. This strategy have been discussed elsewhere (Cemusova 2015).

The need for optimised dosemeters using an eye lens tissue relevant measuring technique, namely Hp(3) tissue equivalent dosimetry is a concern that has been raised previously (Behrens 2015), and dosemeters specifically developed and optimised for the eye lens are now increasing in availability. Of chief concern is the necessity to have a dosemeter than can account for the unique characteristics possessed by the lens, including the nature of the lens structure and tissue composition.

As well as pre-existing models for measured lens dosimetry, the incidence of reported and predicted cases of dose limit exceedances also indicate that not only eye dosimetry but novel approaches and updates to established methods of eye protection are needed. For instance, the risk of developing PSC opacities can be significantly decreased by regular use of protective lead glasses, as demonstrated amongst a large cohort of French interventional cardiologists, and modern glasses are much lighter, more comfortable and afford much better vision than earlier

versions (Jacob 2013). The use of radiation shielding over the eyes would further reduce the received lens dose. For instance, ceiling mounted face shielding using lead has been proven to significantly reduce lens dose using phantoms and humans (O'Connor 2013).

1.2.8 Conclusions of eye lens dose limits

The increasing number and quality of human studies demonstrating that doses of radiation < 2 Gy can induce clinically relevant cataracts prompted ICRP to review and subsequently reduce their recommendations for occupational eye lens dose limits. A key point is that the new limits do not rule out the possibility of a no-threshold model. This is a clear indication as to where research needs to be focused, on low dose and dose-rate exposures. In line with ICRP 118 (2012), the recent literature suggests that medical radiation workers may develop cataracts because of occupational exposures. Furthermore, the studies that have been discussed indicate that eye lens doses to occupationally exposed individuals in the medical sector may in some cases exceed 20 mSv annually. The epidemiological evidence is supported by a small number of animal studies investigating early lens changes, for example. However, although there have been recent advances in our understanding of specific steps in radiation cataract initiation and development (Ainsbury et al. 2016), it is still very difficult to draw conclusions on the relevant issues such as whether radiation cataractogenesis may most appropriately be viewed as a stochastic or deterministic effect for radiation protection purposes.

The discussion surrounding eye lens dose limits for occupational exposures indicates two key issues that have driven the aims of the research within this thesis; the need for low dose mechanistic and biological evidence for lens opacities and IR-induced cataract. Secondly, there is a demand for knowledge and support of the reduced lens dose limits, form researchers, occupational exposure and epidemiologists to support and justify the implementation.

1.3 The lens of the eye

To understand the interaction between IR exposure and the lens, it is important to appreciate the anatomy, function and biological mechanisms of this tissue. The lens has long been thought of as a radiosensitive tissue (ICRP 2007a; Ainsbury et al. 2009), with this chapter aiming to explain how and why this might be the case. Historically, the lens became a much studied model tissue for the study of cellular differentiation processes that take place in early embryogenesis (Duncan 1981). It has been extensively researched over the decades and is one of the model systems for developmental biologists. The human lens is a unique tissue for a multitude of reasons. The lens continues to grow throughout life, however this growth is not linear (Brown and Bron 1996), with the majority of growth occurring prenatally, and slowing down upon birth. This nonlinear, or biphasic, growth of the human lens has been recently demonstrated by weighing the lens at different ages (Mohamed and Augusteyn 2018). Growth of the lens, as measured by weight, appears to be not only biphasic but can be described as having a pre- and post-natal growth phases (Mohamed and Augusteyn 2018). The most striking property of the lens is its transparency, essential for allowing the passing and focussing of light onto the retina. This transmission of light also regresses with age, with an increase in light absorption and scattering (Brown and Bron 1996).

1.3.1 The anatomy of the lens

The lens is a transparent round to oval tissue (vertebrate dependant) whose primary purpose is to transmit and refract incoming light and direct it towards the retina (Duncan 1981; Andley 2007; Bassnett 2009; Brown and Bron 1996). Lens shape varies from vertebrate to vertebrate (Figure 1.3), with the size and the space it occupies in relation to the eye varying. For example, a human lens is much smaller and more oval compared to the relatively large and spherical murine lens. Figure 1.3 demonstrates these differences by comparing mouse (the lenses used in the studies described in this thesis), dog, and human.

Figure 1.3: The vertebrate lens

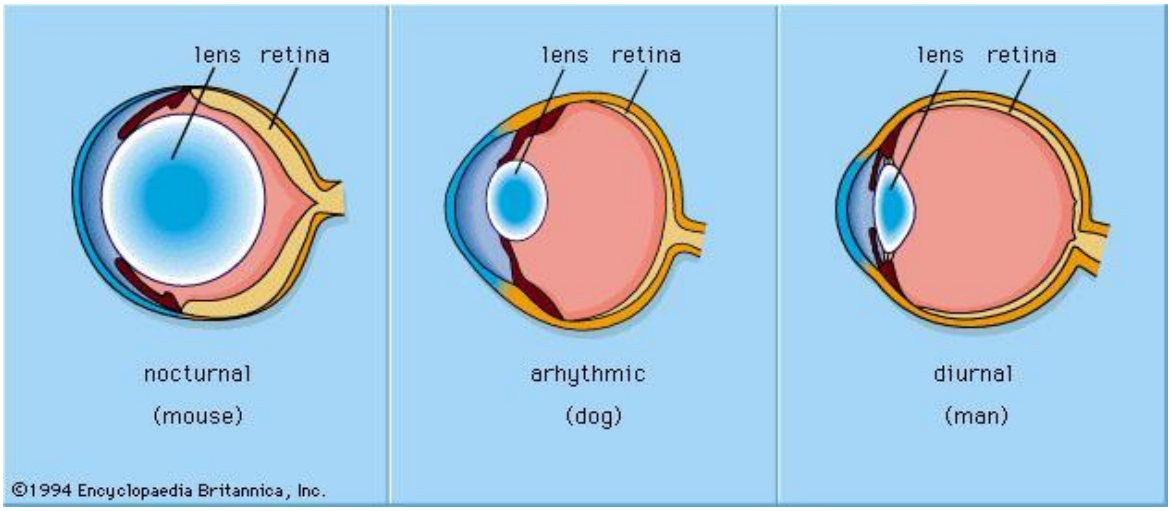

Figure 1.3: Comparison of the lens relative size and shape in different vertebrates. https://azretina.sites.arizona.edu/node/246 *- 1994 Encyclopaedia Britannia, Inc.*

The lens is made up essentially of a single cell type, lens epithelial cells (LEC). These LECs reside in a single cell monolayer covering the anterior hemisphere of the lens fibres, closest to the cornea of eye (Treton and Courtois 1981). LECs cover the lens all the way around to the equator of the lens. LECs can terminally differentiate into lens fibre cells (LFC) by a tightly regulated process, and these LFCs form the body of the lens (Duncan 1981). The monolayer of LECs can be further divided into morphologically distinct regions (Figure 1.4). The central (region) and largest area of the lens epithelium consists of largely quiescent LECs in the adult lens. Whilst these centrally located LECs are still metabolically active, they are not as actively in cell cycle and proliferate very infrequently (Wu et al. 2015; Wu et al. 2014). A small population of stem or progenitor cells were thought to reside in this central region as suggested by a small number of studies due to partial lens regeneration seen after the removal of the lens content (Henry and Tsonis 2010; Lin et al. 2016; Zhou et al. 2006). Surrounding the central region of the epithelium is the peripheral region, consisting of the germinative and transitional zones (Treton and Courtois 1981; Tholozan and Quinlan 2007), and then on the very outer of the monolayer, the meridional rows. This whole peripheral region is compact and appears approximately 20-30 cells wide (Barnard et al. 2018; Markiewicz et al. 2015) in the mouse lens, however this region is wider in bovine (Wu et al. 2015; Wu et al. 2014) and human lenses.

Within the peripheral region, the germinative zone contains some LECs that are actively cycling. These cycling LECs in the peripheral regions do so at a much higher frequency than the those of the central region. This allows the cells to divide, proliferate and repopulate. When LECs cycle, they can produce progeny cells that eventually get displaced and shuffled towards the lens

equator, where the transitional zone lies. Here they gradually begin a terminal differentiation process (Rafferty and Rafferty 1981; Wormstone and Wride 2011; Wu et al. 2015) in preparation to become LFCs, lining up in structured and organised rows (the meridional rows) prior to elongation and subsequent organelle breakdown, amongst other cellular processes. This process of differentiation takes place throughout life, hence the continual growth of the lens as introduced earlier, but becomes slower as the organism ages, and so LFCs are continually added to the lens (Markiewicz et al. 2015) but not linearly. The maintenance and continuation of lens growth is therefore largely the responsibility of a controlled proliferation and differentiation process (Duncan 1981).

Figure 1.4: The orientation of the lens epithelium

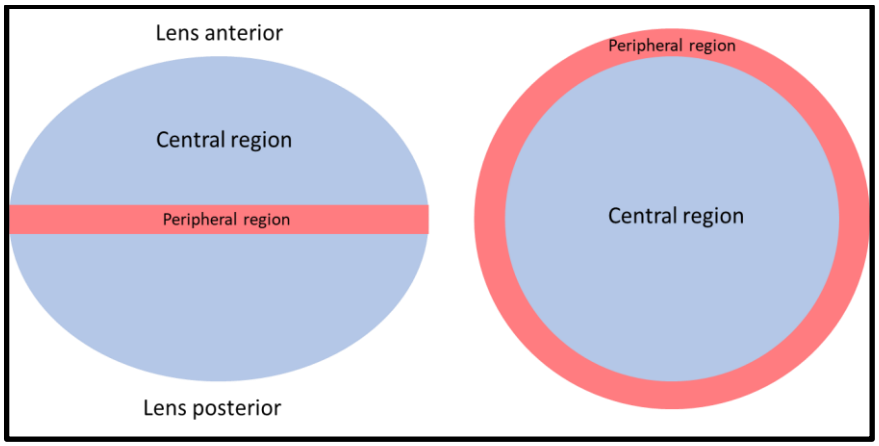

Figure 1.4: The side (left) and top view (right) of the lens depicting the locations of the central and peripheral regions of the lens epithelium in relation to one another.

The peripheral region of LECs sits close to the equator of the lens body, and is bathed in a transparent liquid known as the aqueous humour (Duncan 1981). It is likely that cell proliferation is partly dictated and controlled by growth factors released into this fluid, with fibroblast growth factor 2 (FGF2) being closely associated with LEC proliferation induction (Chang et al. 2000; Iyengar and Lovicu 2017; Robinson 2013). Similarly, a range of insulin-like growth factors have also been shown to stimulate cell division of the LEC residing in the peripheral region (Reddan and Dziedzic 1982; Liu, Chamberlain, and McAvoy 1996) as well as platelet derived growth factors (PDGF) (Iyengar et al. 2006). For FGF to influence the cells, the MAPK/ERK signalling pathway must be in operation, allowing receptors of the LECs to communicate this signal (Lovicu and McAvoy 2001).

The aqueous humour is thought to play a key role in orchestrating cellular proliferation in the peripheral region of the lens epithelium. Similarly, the stimulation of LEC differentiation is thought to be induced by factors contained within the vitreous humour, bathing the posterior of the lens, in contact with the existing LFCs (Iyengar and Lovicu 2017; Lovicu, Chamberlain, and

McAvoy 1995). This is where the early differentiating cells migrate and begin to elongate. Again, FGFs have been shown to play a role in this fluid also. To date, FGF is the only known growth factor able to induce cell differentiation, unlike the multiple possible factors influencing cell proliferation (Iyengar and Lovicu 2017). Once LECs exit the peripheral region and migrate towards the elongation compartment, they are exposed to the vitreous humour. This posterior area of the lens is also bound by the retina, it is thought that the presence of the retina and its contact with the lens are needed for normal formation of fibre cells (Duncan 1981). Inducing LECs to differentiate is certainly not straightforward *in vitro*, which may also be related to a lack of retina tissue presence. Whether FGF within the aqueous or vitreous humour, the factor stimulates LECs in a dose dependant fashion (McAvoy and Chamberlain 1989).

Figure 1.5: The lens epithelium

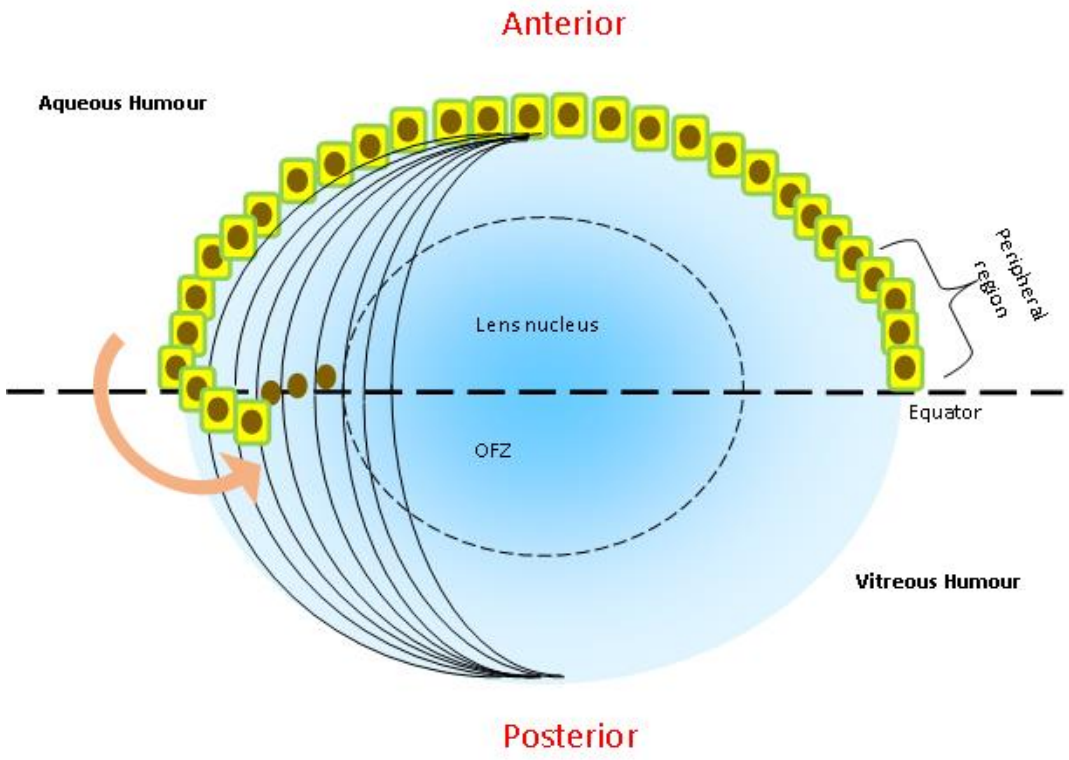

Figure 1.5: The lens epithelium covering the anterior surface of the lens. LECs become more compact at the peripheral region of the lens epithelium and begin to elongate and differentiate into LFCs (image simplified).

Figure 1.6: Layout and distribution of the LECs

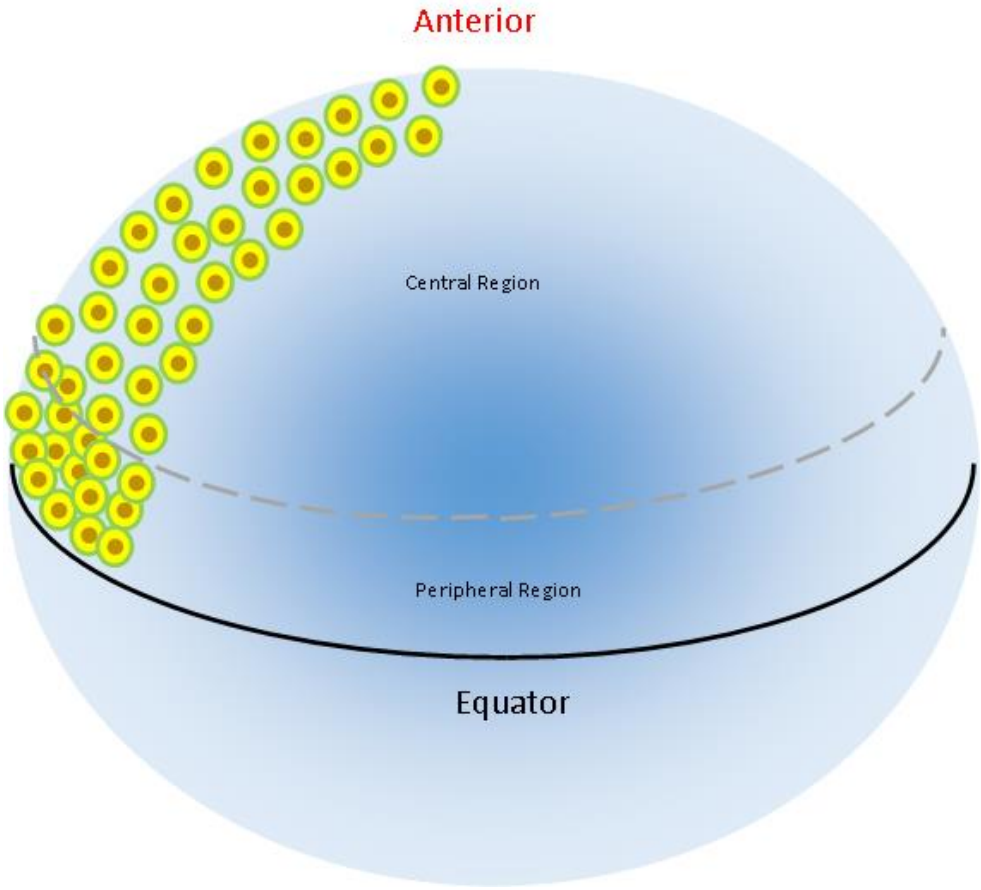

Figure 1.6: The formation and distribution of the LECs within the lens epithelium. The LECs cover the anterior surface of the lens, becoming more compact in the peripheral region towards the equator.

1.3.2 Development of the lens and morphogenesis

Whilst this thesis does not investigate early neonatal or juvenile lenses in mice, it is important to have a brief understanding of the development of the lens during embryogenesis and why the lens is such a unique and well studied tissue.

The lens has become a model tissue for developmental biologists due to its unique control and regulation of cell proliferation and fibre cell generation via differentiation (Duncan 1981) as have been described (see section 1.3.1 above). The early embryogenesis phase of vertebrate lens development is critical for function of the tissue and aids understanding of biphasic lens growth (Mohamed and Augusteyn 2018).

The lens initially forms from the head ectoderm in mammals (not all vertebrates), which covers the optic vesicle. This lens ectoderm becomes closely associated with the optic vesicle. Within the middle of these two tissues lies a matrix of collagen and glycoprotein. This matrix contains a fibrous network that joins the basement membrane of the two tissues. The ectoderm cells that are associated with the optic vesicle elongate to form a lens placode, which eventually dips to form a lens pit which gradually deepens and breaks away from the ectoderm and optic vesicle for form the independent lens vesicle. Cells closest to the posterior of this lens vesicle begin to elongate to fill the cavity that has developed during the break away of the vesicle, forming the primary LFCs. It is these primary LFCs that are often referred to as the oldest cells in the body; under normal circumstances, these cells will remain in the centre of the lens body for life. Proliferation of the posterior cells begins to increase rapidly providing cells to fill this cavity space, upon which proliferation eases off and eventually stops mitotic activity of posterior cells. Proliferation became restricted to the anterior part of the lens vesicle, the presumptive epithelial cells. Now only these LECs divide and provide progeny cells for LFC generation, forming the distinct regions of the lens epithelium, namely the central and peripheral regions, with proliferation eventually becoming restricted to the latter. This anatomical difference and separation of the anterior and posterior located cells signals the compartmentalisation of LEC and LFC. The defining separator of these two cells types is the border of the optic cup, about halfway up the lens resembling an 'equator' line. The posterior of the lens now sits within the optic cup, and that is where LEC elongation is restricted for future growth. It is therefore believed that the optic cup is an inducer of cell differentiation and elongation (Duncan 1981).

1.3.3 Continued growth and transparency

One of the primary roles of LECs is to regulate and maintain the process of LFC generation via differentiation. This constant production of LFCs keeps the lens growing throughout life. It is important to understand this process and its critical role in ensuring healthy lens maintenance, as ineffective differentiation can play a role in cataractogenesis, in both age related and IR-induced circumstances. This process of differentiation is a tightly coordinated and controlled chain of events involving both biochemical and morphological changes to the LEC (Wride 2011).

1.3.3.1 LFC differentiation

The process of differentiation begins in a very narrow zone on the very outskirts of the peripheral region; the transitional zone. This zone opposes the meridional rows, a region where the epithelial cells begin to line up in orderly rows prior to differentiation. As discussed, the primary

objective of the lens is to be as transparent as possible, a quality that is essential for the function of the tissue. Differentiation is a process whereby LECs begin a gradual degradation of organelles and light scattering objects (including the nucleus), alongside a gradual increase in crystallin proteins (Hejtmancik and Shiels 2015) and elongation. The lens is often referred to as the 'crystalline lens' due to the tissue's high content of crystallin proteins. LECs also undergo a dramatic morphological change, becoming thin, elongated fibres, with a hexagonal shape (if cross-sectioned through the middle) to aid compaction and reduce extracellular spaces (Hejtmancik and Shiels 2015). This organisation also helps with cellular exchanges and signalling.

Fibre cells essentially make up the bulk of the lens, forming a tightly packed lens nucleus in the centre of the lens. The fibres are very carefully organised, forming to create a 'Y' shaped suture where the fibre cells meet each other (Kumari et al. 2011). LFC must undergo cytoskeletal and intermediate filament reorganisation to reshape themselves into hexagonal elonged tubes, allowing them to 'interlock' within each other as they now sit within the LFC compartment of the lens, gradually moving inwards towards the centre of the lens nucleus (Bassnett 2009; Wride 2011; Song et al. 2009). The rate of apoptosis in the lens is very low; therefore, the LFCs in the centre of the lens nucleus are likely to be some of the oldest in the human body, as the development of the lens is an increasing accumulation of LFCs. LFCs organise themselves along junctions, known as sutures, originating at the posterior and anterior end of the lens. LFCs aligning themselves with these sutures is imperative for transparency (Delaye and Tardieu 1983). Mature LFCs contain a high concentration of crystallin proteins, which can be divided into three classes – α, β and γ-crystallins (Takemoto and Sorensen 2008). These crystallins fill the cytoplasm of the LFCs once occupied by organelles prior to degradation and aid transparency. Expression of membrane associated proteins such as the major intrinsic protein (MIP) which participates in the formation of water channels (Gorin et al. 1984). Similarly, membrane protein (MP)18 has increased expression in LFC, where it is thought to help with the organisation of LFC junctions (Louis et al. 1989). Water content of the cells decreases during differentiation, resulting in a loss of aquaporin 1 (present in the LECs), replaced by an increase in aquaporin-0 presence (Kumari et al. 2011; Varadaraj, Kumari, and Mathias 2010; Hamada 2017a), both of which are predominately expressed in the lens (Kumari et al. 2011). Aquaporins are membrane proteins that act as channels for water to pass in and out of the cell (Takata, Matsuzaki, and Tajika 2004). It is thought that aquaporin-0 has some function in lens transparency, hence the switch from aquaporin-1 in the LEC (Schey et al. 2017). Knockout of aquaporin-0 in zebrafish results in cataract formation (Froger et al. 2010). Although LFC differentiation is often characterised and described as cellular organelle loss, this is one of the final, but perhaps most dramatic steps in the process. The nucleus, Golgi apparatus, endoplasmic

reticulum and mitochondria are all gradually degraded (Bassnett 2009; Wride 2011) as the LFCs mature, leaving a zone in the centre of the lens filled with cells devoid of organelles and high in crystallin proteins ready to allow the passage of light.

1.4 Classification of cataract

Cataracts are defined clinically as a progressive opaqueness of the lens, leading to a loss of vision (Ainsbury et al. 2016). The process of cataractogenesis is a lengthy and complex one, whereby the lens becomes progressively cloudy (Ainsbury et al. 2016). Cataracts are the leading form of blindness worldwide (50% of blind persons in middle- and low-income countries, just 5% in developed countries), with an estimated 95 million people affected by the condition (Liu et al. 2017). Whilst cataract is classified as a disease, cataract removal is ever improving to the point where a simple non-invasive procedure is now performed (in development countries) whereby the lens is replaced by a plastic replacement.

Most recently, the Lancet (Liu et al. 2017) described cataract as being classified, based on cause, into three distinct groups: age-related, paediatric or secondary cataract. Depending on the location within the lens that the opacity occurs, cataract can further be sub-divided and classified as nuclear (forming in the lens nucleus), cortical (appearing in the lens cortex) or posterior subcapsular (forming towards the back of the lens) (Duncan 1981). Figure 1.7 depicts the locations where each opacity leading to cataract form. Congenital cataract, whereby the opacity is present at birth, were also reported. Nuclear cataract have a ‘hard’ phenotype, thought to be induced by non-enzymatic post-translational modifications with fluorescent chromophores accumulating, which all make the lens more sensitive to oxidation and cross-linking, eventually causing light to scatter (Truscott 2005). The ability to transport antioxidants is thought to decrease as a result of aging, leading to the formation of a glutathione barrier to develop around the lens (Michael and Bron 2011). Cortical cataract is thought to form due to mutations in the LECs, where the membrane permeability and enzyme function of the cells hinder LFC function and increases oxidative stress, with telomere shortening and lipid peroxidation both suspected as possible causes (Michael and Bron 2011; Babizhayev, Deyev, and Linberg 1988; Sanders et al. 2011).

Figure 1.7: Typical cataracts and their location of formation

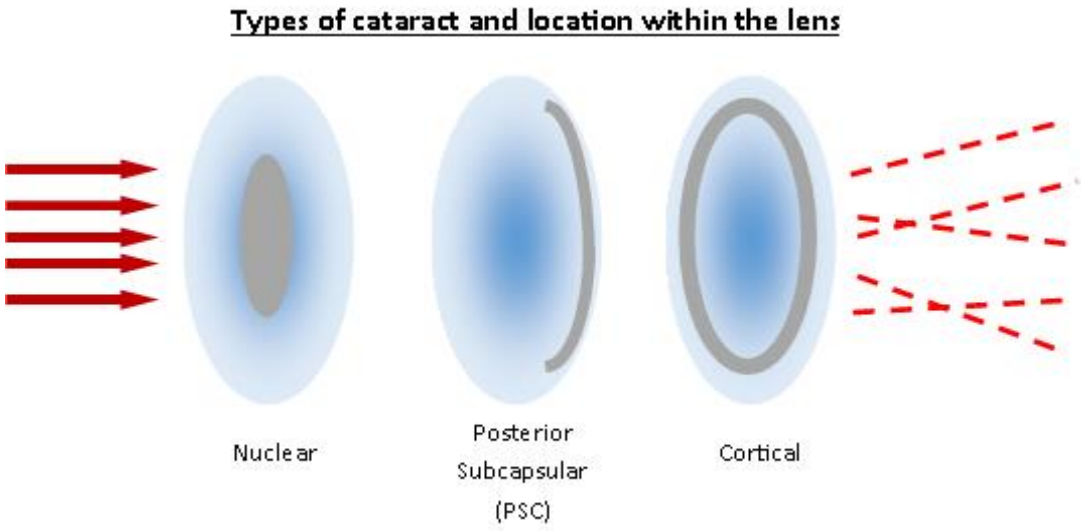

Figure 1.7: Depiction of the location of opacity within the lens in the three main classification of cataract types. All result in the refraction of light rather than focusing it towards the retina.

There are some common biological processes thought to be involved in most cataract forms, chiefly involving abnormal LEC growth (Eldred, Dawes, and Wormstone 2011). Inefficient organelle loss will lead to light scattering in LFCs if the differentiation process is hindered (Sandilands et al. 2002), likewise if apoptosis signals became uncontrolled (Wride 2011). Several drugs and medications are known to induce cataract in humans, but this is generally a side-effect of treatment from serious injury or disease. A substantial number of gene mutations have been identified as linked to early cataract onset which can be viewed via an online database (http://cat-map.wustl.edu). Diabetes is a well-known disease that also leads to increased incidence of cataract formation, with higher levels of glucose leading to auto-oxidation of glucose and a non-enzymatic glycation of lens proteins, causing them to have higher molecular weights and thus aggregating causing light-scattering (Katta, Katkam, and Geetha 2013). There is a lack of correlation between cataract phenotype and IR-exposure, as are apparent in the next couple of sections. This is in part due to the interconnected nature of lens cells (Stewart et al. 2013), accounting for variation in cataract phenotype whilst also being influenced by lifestyle, genetic and environmental factors (Ainsbury et al. 2016; Shafie, Barria von-Bischhoffshausen, and Bateman 2006).

1.4.1 Age-related cataractogenesis

Age-related cataract are increasingly mentioned in the same context as IR-induced cataract due to the concept of cataractogenic load (Alice Uwineza and Hamada 2019), whereby IR accelerates age-related cataract. Therefore, it is important to understand the similarities and differences between naturally developing and radiation-induced cataract.

It is said that if every human lived long enough, we would all develop age-related cataract. This is evident when looking at the distribution of cataract prevalence; 3.9% in persons aged 55-64, increasing up to 92.6% for those aged 80 plus (Liu et al. 2017). Cataract are therefore one of the most common and well known age-related diseases. Not just applicable to humans, most mammals and birds are thought to be affected by some form of cataract development towards the latter stages of life (Wolf et al. 2005). Age-related cataract is by far the most common type of cataract in adult humans, with a typical onset around the late 40 to early 50 years old. Age-related or congenital, hereditary cataract tend to form in the nucleus of the lens, however nuclear cataract has been reported in airline pilots exposed to IR via cosmic radiation (Rafnsson et al. 2005). The role of oxidative stress and reactive oxygen species is thought to play an important role in the development and progression of age-related cataract (Wolf et al. 2005).

1.4.2 Radiation-induced cataract

Epidemiological studies over the last several decades have demonstrated increased incidence of cataract in surviving persons exposed to doses of IR during nuclear accidents and incidents. As a result, the lens was thought of as one of the most radiosensitive tissues in the body, and highly responsive to IR (Ainsbury et al. 2016). However, cataract are considered deterministic, or tissue reactions, whereby cataract only occur once a threshold of radiation dose is reached, below which there is no significant effect (Stewart et al. 2012). The status of lens dose limits and thresholds are discussed (see section 1.2 of this chapter). Historically, the most prevalent (but not exclusive) type of cataract reported following IR exposure had been the posterior subcapsular cataract (PSC) (Chumak et al. 2007; Worgul et al. 2007; Nakashima, Neriishi, and Minamoto 2006; Miller, Fujino, and Nefzger 1967; Bouffler 2012; Worgul, Merriam, and Medvedovsky 1989). PSCs are certainly not unique to IR exposure, their development can also be influenced by other factors, such as aging (Michael and Bron 2011), steroids and other risk factors (Michael and Bron 2011; James 2007). Cortical cataract has also shown an increased prevalence in Chernobyl clean-up workers, but not nuclear cataract (Worgul et al. 2007). Less than 1 Gy of IR leads to loss of visual quality and the appearance of cataract (Neriishi et al. 2012). There is much less evidence for doses of <0.5 Gy. Until recently, cataracts were thought to be induced above thresholds of 2 Gy and 8 Gy

for acute and protracted exposures, respectively (ICRP 2007b). In 2012, the assumed threshold for cataract induction was lowered to 0.5 Gy absorbed dose for radiation workers (ICRP 2012; Barnard et al. 2016), resulting in new occupational exposure recommendations (Dauer et al. 2017) and limits for the eye lens (Barnard et al. 2016; Broughton. J. 2013), resulting in the implementation of a 20 mSv per year dose limit for the lens (averaged over 5 years, with no single year exceeding 50 mSv) within the EU Basic Safety Standards. This was based upon the evaluation of epidemiological data from nuclear incident survivors and various clinical cohorts. Questions still remain regarding the mechanism(s) of both cataract formation after the initial damage and also the low dose sensitivity of the lens itself (Barnard et al. 2016). The regulatory changes provided and additional legislative impetus to establish a mechanistic link between radiation exposure and cataract formation (Barnard et al. 2018).

1.4.3 Diabetic cataract

Persons with diabetes were reported to have a risk of developing cataract five times greater than non-diabetics (Peterson et al. 2018). Cataract can occur up to 20 years earlier in diabetic persons, and also develop more aggressively, so a significantly reduced latency period is expected and an increased progression to visual imparity (Peterson et al. 2018). Diabetic cataract is associated with hyperglycaemia, which produces advanced glycation end products, elevated oxidative stress factors, and the activation of the polyol pathway (the conversion of glucose to fructose) (Hashim and Zarina 2011).

Other noteworthy but less extensively studied lens disorder is the appearance of vacuoles and retrodots. Vacuoles are non-opaque lens changes that are reported to appear within the lens, appearing as clear fluid-filled spaces within the lens cortex. Similarly, retrodots appear as small lobular objects in the cortical regions of the lens. Both are reported to have little impact on visual function (Tan et al. 2012). Vacuoles are less well studied, and have been linked in PSC cataract although they also appear in cases of no cataract (Tan et al. 2012). Both vacuoles and retrodots increase in prevalence with age. Increased incidence of both at baseline subsequently increases the incidence of cataract surgery. The presence of vacuoles at baseline increases the likelihood of developing PSC over a 10 year period (Tan et al. 2012).

1.4.4 Self-repair and regeneration

The lens can develop opacities and cataracts when the processes that maintain proper lens function and growth are disrupted. However, several studies have reported the self-repair or regeneration of the lens, suggesting that the lens has some combative measures to prevent damage. Radiation exposure is another form of damage, and the repair and regeneration of damaged cells or to the lens has a whole is particularly interesting to the latency of IR-induced cataract.

Stem cells are known to be crucial in the repair and regeneration of many tissues, and it seems that the lens may not be an exception, with a small population of stem/progenitor cells reported in the lens epithelium. Newts and frogs have been demonstrated to regenerate lenses from cells within the corneal endothelium upon removal of the lens (Henry and Tsonis 2010; Freeman 1963). Following removal of the lens in adult newts, pigment epithelial cells of the dorsal iris appear to de-differentiate, lose pigmentation, and differentiate into lens cells, with subsequent differentiation into LFCs (Kimura et al. 2003; Kanao and Miyachi 2006). However, mammals are only able to regenerate the lens when the lens capsule has been left behind (Gwon 2006), as it is the LECs that are needed for regeneration. This has been demonstrated in the vertebrate lens following the removal of lenses from rabbits and macaques, whilst leaving a small population of endogenous LECs. Lenses were seen to regenerate (Lin et al. 2016). However, in mammals, the regenerated lens often has some defects (Gwon 2006). A few pathways involved in lens regeneration and transdifferentiation of corneal cells to lens formation have also been identified, including FGF, bone morphogenetic pathway (BMP) and wingless Int-1 pathway (Wnt) (Tseng 2017; Day and Beck 2011).

Vimentin driven wound healing is also known to occur within the lens epithelium. Upon physical injury of wounding, the epithelial cell quickly repopulates the area, known as collective migration (Menko et al. 2014).

1.5 Evidence of radiation exposure and the lens

From the topics and studies that have been discussed so far, the relationship between IR exposure and the lens of the eye is of significant interest. There has been extensive research in this area for many decades, and increasingly so given the recent re-evaluation of threshold doses and the stochastic vs deterministic nature of IR-induced cataract induction.

The most significant and well known non-cancer effect of IR is cataract, and the IR induction is hard to dispute given the mounting epidemiological data. The difficulty comes with low dose and

low dose-rate exposures, where data are much sparser, although recently there have been evidence for low dose and dose-rate excessive risk to cataract reported for the first time (Little et al. 2018). Mechanistically, for the induction of IR cataract there is a lack of understanding as to how exposure leads to lens opacity and cataract. Epidemiological studies demonstrate a strong latency period between exposure and cataract, however little is known as to what is actually happening during this time frame (Bouffler 2012).

During this chapter, the focused evidence between IR exposure and reported effect in the lens are discussed with a recap of the key epidemiological studies and *in vivo* and *in vitro* mechanistic findings.

1.5.1 Epidemiological studies

Historically, our knowledge of radiation-induced cataracts derives from observations of lens opacity and cataract following persons exposed to radiation either accidentally or intentionally and it was such studies that have contributed towards the radiosensitive 'status' of the lens and the evidence of radiation-induced cataract.

1.5.2 Nuclear incidents

Perhaps two of the most well-known nuclear incidents and significant contributors to the observation of radiation-induced cataract are the atomic bomb survivors and the Chernobyl clean-up workers. The atomic bomb survivors (over 6,000 persons used in study) showed increased incidence to cataract following exposures to less than 1 Gy (estimated threshold dose of 0.5 Gy) (Neriishi et al. 2012). Chernobyl clean-up workers (over 8,000 persons included) also showed increased incidence to cataract to doses below 1 Gy (Worgul et al. 2007). Both cases demonstrate a clear increased incidence of cataract following relatively low-dose exposure, above the expected age-related cataract frequencies. Such early observations in nuclear accident/incident cohorts led to the introduction of safe lens dose limits, as defined by the International Commission for Radiological Protection, ICRP (ICRP 2007b; Stewart et al. 2012). A cohort of workers from the Russian Mayak region demonstrated increased risk of cataract, particularly PSC types, because of chronic occupational exposures to external gamma IR (Azizova et al. 2018). Reduced lens dose limits also focus research on low dose effects, and increasingly investigated topic over the last decade or so.

1.5.3 Occupational exposures

Here is a brief recap as to the importance of persons routinely exposed occupationally to doses of IR to the lens, as introduced extensively in section 1.2.6 of this chapter. Thankfully, nuclear accidents such as those discussed during this thesis are few and far between, with a general decline since 1980 (Coeytaux et al. 2015). Occupational exposures such as in industrial and medical workers represent the largest cohort for individuals to potentially be over-exposed to IR currently. Occupational exposures have the second largest probability to over-exposure and will feel the largest impact from reduction in lens dose limits (Barnard et al. 2016). Occupational exposures have been extensively discussed in this thesis, with the impact of dose limits particularly in the UK and Europe, and are the primary justification for the need for low dose and mechanistic understanding of IR-induced cataract as investigating during this project (Barnard et al. 2016). Very recently, one of the largest cohort studies of radiologic technologists in the United States reported an excess risk of cataract from low dose (<100 mGy cumulative lens exposure) and low dose-rate exposures (Little 2013; Little et al. 2018).

1.6 Experimental findings

1.6.1 *In vitro* models

In vitro tools are often used when trying to understand the mechanisms and biological intricacies of IR effects. They are important tools for the investigation of radiation cataract, particularly LECs as are discussed below.

Primary cell culture and cell lines are well documented using reliably characterised LECs in IR related research studies. These cells are isolated mostly from early foetus or neonates from either mouse or human lenses (although rabbit and bovine have been used), allowing for the cells to successfully take to culture conditions before immortalisation (Dalke et al. 2018; Markiewicz et al. 2015; Fujimichi and Hamada 2014; Hamada 2017a). Several isolated LECs are available commercially including a few donor HLEpiC (www.innoprot.com) (Bains et al. 2019) and human lens epithelial (HLE)-B3 cells (www.lgcstandards-atcc.org) (Andley et al. 1994). A number of *in vitro* models have yielded useful findings to help our understanding of the biological processes occurring post-exposure to IR. It is from such studies that most of our current knowledge regarding the role of genomic damage comes from, thought to be one of the key mechanism affecting LECs as a result of IR exposure (Ainsbury et al. 2016). A full summary of the most relevant *in vitro* studies to shed light on the mechanistic processes occurring during radiation-induced cataract was recently

published by Ainsbury *et al.* (2016) (Ainsbury et al. 2016), some relevant examples are discussed here.

In vitro investigations have observed the effects of IR in several processes and pathways, with some key experimental studies outlined here. Cultured human lens epithelial cells (HLEC) from three separate donors have demonstrated genetic changes in telomere length and oxidative stress following low dose IR exposures (Bains et al. 2019). The DNA damage response has also been modelled *in vitro*, allowing for low dose and early time point study (Markiewicz et al. 2015; Bains et al. 2019; Dalke et al. 2018; Kunze et al. 2015; Bannik et al. 2013). Markiewicz et al (Markiewicz et al. 2015) could observe linear DNA damage responses in both mouse and human FHL124 lens epithelial cells. These studies used markers for DSBs induced by IR, thus they need rapid repair by the LEC, and efficient repair to reduce mis-repair or un-repaired persisting damage. As well as IR, ultraviolet (UV) radiation exposure has also been demonstrated to affect eh DNA damage response *in vitro*, inducing significant single strand breaks (SSBs) in rabbit derived LECs, with similar repair kinetics to other cells types, repairing using an initial fast phase, following by a slower phase of repair. However UV exposure was concluded to have other toxic effects besides inducing DNA damage (Sidjanin, Zigman, and Reddan 1993). Hydrogen peroxide exposed bovine LECs result in higher levels of oxidative stress, which in turn have been observed to induce DNA damage (Kleiman, Wang, and Spector 1990).

Increases in proliferation and growth factor FGF2 have been observed in HLEC, along with changes in transcription factor cyclin dependant kinase inhibitor 1A (CDKN1A), which has a known role in cell proliferation (Chang et al. 2000; Chang et al. 2005). IR induces oxidative stress in some cases, which is thought to result in altered proliferation, cell migration and problems in differentiation, all could lead to promotion of cataract (Wride 2011; Jarrin et al. 2012). Excessive proliferation in LECs is documented following IR exposure *in vivo* (Markiewicz et al. 2015). Proliferation is not easy to study *in vitro* due to the carefully regulated nature of cell division and differentiation in the lens, and the compartmentalisation of such metabolic activities to specific regions of epithelium (Ainsbury et al. 2016; Jarrin et al. 2012; Wride 2011). Proliferating cells in the peripheral of the epithelium are thought to be radiosensitive (Markiewicz et al. 2015), therefore cultured cells with unregulated cell division could be difficult to translate to *in vivo* models.

Changes in gene expression following IR exposure have also been studies *in vitro*, which would be extremely difficult *in vivo*. One example of this is the altered expression of the gene transforming growth factor beta (TGFβ), which dictates the expression of tropomyosin 1 and 2 (cytoskeletal proteins) in LECs deficient in the gene peroxiredoxin-6, encoding antioxidant protein

and therefore protection from oxidative stress. These LECs were taken from mice that have increased incidence of IR-induced cataract compared to wild-types (WT) (Worgul et al. 2002; Fatma et al. 2005). If this altered gene expression could be detected *in vivo*, it has the potential to be a possible predictor of PSC. Polymorphisms to X-ray repair complementing defective repair in Chinese hamster cells 1 (XRCC1) and 8-oxoguanin DNA glycosylase 1 (OGG1), genes involved in DNA repair, have both been identified as having a role in age-related cataract development (Hamada and Fujimichi 2015). Difficulties comparing genes identified *in vitro* and *ex vivo* compared to human age-related cataract lenses have been reported, with little similarity between up- or down-regulated genes (Ruotolo et al. 2003). The role of matrix metalloproteinases (MMPs), enzymes that aid degradation of extracellular matrix proteins (EMPs) are likely to be important in the mechanisms of IR-induced cataract, as identified as being downregulated in *in vitro* bovine and human cell lines (Wu et al. 2014).

Differentiation of human LECs can be achieved in-vitro using extracellular matrix (ECM) coated plastic (Blakely et al. 2000). Several morphological changes can also be induced by UV exposure including apoptosis and necrosis in human LECs (Shui et al. 2000) which could be useful in understanding repair mechanisms as well as cell signalling within the microenvironment. Senescence and telomere shortening were identified as possible accelerators of age-related cataract and therefore a possible pathway of IR-induced cataract, using cultured human LECs (Bains et al. 2019; Babizhayev, Vishnyakova, and Yegorov 2011; Babizhayev and Yegorov 2010; Chodick 2008).

Whilst not involving IR exposure, *in vitro* studies have demonstrated that protein aggregation and protein folding are a large contribution to lens transparency loss and cataract formation (Ainsbury et al. 2016; Kosinski-Collins and King 2003). αA- and αB-crystallin have been shown to accumulate light scattering aggregates due to IR-induced oxidative stress (Fujii et al. 2007). IR induced oxidative stress has been shown to affect cell division, migration and LFC differentiation (Wride 2011; Jarrin et al. 2012). Cultured cells have also been demonstrated to modify their microenvironment to promote the migration of LECs by expressing transforming growth factor beta (TGFβ) and fibroblast growth factor 2 (FGF2) (Kayastha et al. 2014).

The *in vitro* studies highlighted here demonstrate the wide array of potential mechanisms that can be investigated using cultured LECs without the need for animal models, allowing the investigation of processes that are not able to be observed in living vertebrates. These studies also highlight the vast amount of unknown biological effects IR exposure has on the LECs and their continued function (Ainsbury et al. 2016).

What is clear from the studies discussed during this section is that *in vitro* models are not always the suitable method for investigating the effects of IR, having several drawbacks, and work is needed to establish *in vitro* models that behave under the same characteristics as the lens (Ainsbury et al. 2016; Markiewicz et al. 2015; Augusteyn 2008). These *in vitro* cell culture models need to have a proven reproducibility to increase the reliability in their findings. *In vitro* conditions vary significantly from the natural lens environment within a vertebrate. The complex physiology of the lens and the compartmentalisation of the epithelial cells, with specific cell cycle states, make it difficult to replicate *in vitro* (Augusteyn 2008).

1.6.2 In vivo models

In vivo models, particularly rodents, still represent the most effective way to study radiation-induced cataract and relatable to human (Lett, Cox, and Lee 1986), largely since, as previously discussed, the structure and function of the lens and LECs are difficult to model outside of the organism. The pros and cons of *in vitro* models have been outlined above. The complex homeostatic environment that regulates LEC cell cycle state, proliferation, differentiation and transcription, to name a few key processes, is most accurately observed in living animals. Whilst the findings of *in vitro* methods have strengthened our knowledge of early mechanistic effects and pathway alterations, they remain limited and often short-lived due to the different behaviour and characteristics of LECs *in vitro* and *ex vivo* (Ainsbury et al. 2016).

Most *in vivo* studies are carried out under experimental and laboratory conditions. In 2013 a study was published whereby over 1000 birds from the Chernobyl contaminated areas had their lens opacity measured (Mousseau and Moller 2013). Whilst this study is a difficult direct comparison to human cohorts, due to the vast contamination of this area, and increased incidence of morbidity related to radiation-induced cataract was reported. Although studies in animal models, particularly the mouse, show a strong degree of transferrable information in the understanding of human cataract formation, there are several key differences between rodent and human lenses, animal eyes are primarily used in low-light conditions and therefore the pupil and retina have some differences (Malmstrom and Kroger 2006). However, mice reach a similar age of ocular development as humans in relative terms (Ainsbury et al. 2016).

1.6.3 Mouse models

Most *in vivo* studies of radiation-induced cataract in recent years have used mice, as these represent the most diverse (in terms of strains) and cheapest model for investigation. As has been discussed above (see section 1.6.2 of this chapter), one advantage of mice is the ability to perform *in vivo* observations and grading of cataract and opacity formation and progression in the living animal. This is a significant setback in *in vitro* investigations, as large latency periods from radiation exposure to cataract formation make *in vitro* findings difficult to translate to cataract. *In vitro* studies however are useful tools for identifying potential biological responses that may lead to cataract, able to focus concurrent *in vivo* investigations. This thesis involves *in vivo* exposures of several mouse strains to investigate early post-exposure effects of LECs to DNA damage response and repair, changes to LEC proliferation and lens opacity changes over an 18 month period.

Possibly one of the earliest studies highlighting the potential of the mouse as an effective research model for radiation-induced cataract came from an extremely comprehensive study by Upton et al. (Upton et al. 1956) in 1956. The researchers exposed mice, rats, guinea pigs and rabbits to neutrons, x- and γ-rays, observing the production of lens opacities post-exposure. The mouse was found to be the most radiosensitive of all there vertebrates (Upton et al. 1956) due to small dot-like vacuoles observed along the posterior subcapsular sutures of the fibre cells in irradiated mice at around 8 months, but not seen in controls. Although mice are significantly strain dependant (although this can be an advantage when looking and genetic influences as are discussed), in general the lifespan of a research mouse is 2 – 3 years (Yuan, Peters, and Paigen 2011). However, the large variation of the different strains of mice can sometimes make it difficult to compare studies without complicated discussion (Ainsbury et al. 2016)

Given the discussion regarding the large latency periods expected for radiation-induced cataract to develop, the lifespan of the mouse required careful experimental and exposure planning in lifetime studies (Ainsbury et al. 2016; Dalke et al. 2018). Several studies investigating the effect of radiation exposure on cataract and possible pathways or mechanisms of cataractogenesis in mice have been performed. Heightened incidence of spontaneous and IR-induced (following 0.5 Gy X-rays) cataract have been reported in both ataxio-telangiectasia mutated (Atm) and MRad9 heterozygous black Swiss Webster mice (Kleiman et al. 2007; Hopkins et al. 2004), both genes involved in DNA damage response. Homozygous Atm deficiency also increases the speed at with lenses develop cataract compared to WT and heterozygous controls following 0.5 – 4 Gy IR exposure (Worgul et al. 2002). Heterozygous mice for the Patched 1 (Ptch1) gene (on a CD1 background), a gene involved in cell signalling including a role in cell proliferation, cell fate and

epithelial-to-mesenchymal transition, show a raised incidence of both spontaneous and IR-induced cataract development (De Stefano et al. 2015). C57BL/6J mice have demonstrated an increased dose response in the LECs compared to lymphocytes following as low as 25 mGy of γ-IR, suggesting a possible sensitivity of these cells to IR-induced DSBs (Bannik et al. 2013). Similar results were seen in the same cells at a low dose range of 20 – 100 mGy, where peripheral LECs repaired DSBs slower than peripheral lymphocytes form the same animals, also suggesting non-linear dose response post-24 hours after exposure (Markiewicz et al. 2015). The peripheral region has often been observed as more radiosensitive to IR induced DSBs (Markiewicz et al. 2015; Bannik et al. 2013), with these different regions of the lens epithelium difficult to recreate *in vitro* due to cell cycle differences.

1.6.3.1 Mouse strain dependency

Little is known about the effect of strain in radiation exposed lens studies other than the murine models mentioned above. No studies to date appear to have made direct comparisons between strains of mice, with focus tending to be on using knock-out or mutant strains in comparison to WT counterparts.

For example the studies on the XPD/*Ercc2* mice (Kunze et al. 2015; Dalke et al. 2018) and the Ptch1 mice (De Stefano et al. 2015) demonstrate animals susceptible to radiation-induced cataract by selecting heterozygous knock out mice following genotyping of the neonates born as a result of carefully planned breeding. The potential for strain dependency in IR-induced cataract would be highly applicable to genetic differences in humans; murine models simply provide a better platform for looking as such effects. Genetic differences appear to be of greater importance at lower doses of IR (Ainsbury et al. 2016), when comparing $Atm^{+/-}$ or $Atm^{-/-}$ mice with their exposed WT counterparts (Kleiman et al. 2007; Worgul et al. 2002; Worgul et al. 2005), heterozygote mice show a greater incidence of cataract compared to WT following 0.5, 1 and 2 Gy exposures. When both heterozygotes and WT mice are exposed to a high dose of 8 Gy, there is not significant difference between them. This is an important observation highlighting the significance of the genetic component and low dose exposures. The identification of sensitive in-bred strains would allow for large scale, reliable and reproducible studies to be performed on a cohort that resembles that of humans more closely as opposed to genetic mutants. The genetic effect of IR became apparent in subsequent chapters introducing and discussing relevant studies.

The use of inbred or outbred mice are also an important considering in murine models. Inbred strains generally have less inter-individual variation, making them useful experimental models as fewer animals are needed to obtain significant results, such as power calculations.

Outbred strains have greater heterogeneity; mice are genetically more diverse from each other. Therefore, it has been suggested in broader studies that inbred strains underrepresent the complexities of the human population (Martin et al. 2017; Carreras et al. 2019; Ainsbury et al. 2016)

The strain dependency, and influence of inbred versus outbred and mutant mice, of IR-induced effects and in the broader sense cataractogenesis has been raised in previous commentaries and is not well understood currently (Ainsbury et al. 2016; Hamada and Fujimichi 2015). Historically, most *in vivo* studies of IR-induced cataract studies have used heterozygous mutants, specifically with deficiencies in DNA damage repair (Kleiman et al. 2007; Dalke et al. 2018; Worgul et al. 2002; Worgul et al. 2005; Kunze et al. 2015; De Stefano et al. 2015). Such mutants require extensive breeding programmes and are not greatly representative of the general human population. WT inbred strains, whilst claimed to be mostly genetically identical, offer a more representative alternative for investigating the effects of low dose IR on the early effects of DNA damage and repair in the LECs. To investigate the influence of inbred murine strain, radioresistant C57BL/6 mice were exposed to low doses of X-radiation (0, 10 and 25 mGy) alongside radiosensitive 129S2, CBA/Ca and BALB/c mice (Newman et al. 2014; Darakhshan et al. 2006; Peng et al. 2009; Roderick 1963; Wolf et al. 2005; Makharashvili and Paull 2015; Patel et al. 2016; Rithidech, Cronkite, and Bond 1999; Boulton et al. 2001; Verbiest, Bouffler, and Badie 2018; Hamasaki et al. 2007), as per chapter 2: Materials and Methods. Mice were sacrificed at 2, 4 and 24 hours post-exposure and the lenses fixed and immunofluorescently stained with DNA damage and repair marker 53BP1 (Asaithamby and Chen 2009; Bartova et al. 2018; Fradet-Turcotte et al. 2013; Kim and Yim 2018; Noon and Goodarzi 2011; Rothkamm et al. 2015; Zimmermann and de Lange 2014). 53BP1 foci within the LEC nuclei of both the central and peripheral regions of the epithelium were scored and analysed.

1.6.4 In vivo murine lifetime studies

One of the research questions within the field of IR-induced cataract is the mechanism(s) that lead to cataract following initial radiation exposure (Ainsbury et al. 2016). As discussed above, there is evidence to support the effects of IR exposure on both the behaviour of proliferation and the induction and repair of DNA damage including DSBs in LECs. However, conclusions as to how these observations are involved in a mechanism(s) leading to the formation of cataract can only be hypothesised for now. Cataract have been detected in repair-deficient heterozygous mice vie slit lamp observation following 0.5 Gy of X-rays, with 50% of WT mice developing cataract after 1 year, and an even higher frequency in the mutant mice (Kleiman et al. 2007). This finding formed the basis of a recent lifetime study (Dalke et al. 2018) in mice using the more advance Scheimpflug

imaging technique, shown to be a more accurate method for analysing and track lens opacity and cataract formation in mice (Fuchs et al. 2011; Puk, de Angelis, and Graw 2013). This lifetime study takes 0.5 Gy as a maximum dose for use as a positive control, with additional lower doses, exposed at a dose-rate of 0.063 Gy/min (Dalke et al. 2018). The mice used were also *Ercc2* gene heterozygous mutants (involved in DNA repair) alongside WT (bred on a B6C3F1 mice, a C3HeB/FeJ x C57BL/6J) (Kunze et al. 2015). It should be noted that Scheimpflug imaging systems are significantly advanced compared to slit lamp observation, the technique used in most historic murine IR-induced cataract studies which report cataract following 0.5 Gy doses (Hall et al. 2006; Kleiman et al. 2007; Worgul et al. 2002; Worgul et al. 2005). The study by Dalke et al. (Dalke et al. 2018) was unable to detect IR-induced lens opacity, this is possibly unexpected but not necessarily surprising given the advancements in imaging technique. The study detected 2% increases in lens opacity of irradiated and non-irradiated mice, but this is the expected increase because of aging.

This study has been extremely helpful in providing a basis for an improved and modified study to try addressing the question of what is happening between IR exposure and cataract manifestation. Additional dose-rates would allow observations as to its effect, as suggested in recent literature (Little et al. 2018). The use of 0.5 Gy as a positive control is valid, however the limited lifespan of the mouse (Yuan, Peters, and Paigen 2011) coupled with the lack of evidence to determine the latency period of cataract formation would suggest that increased dose of IR could shed some light on these areas. No significant effect of gender was seen in this study.

A modified study is proposed and undertaken during this thesis. The study will consist of only female mice, as no significant effect of gender has been seen previously. The effect of dose-rate is of interest and so multiple dose-rates were performed (see chapter 2: Materials and Methods). Doses up to 2 Gy were exposed to allow for observations regarding the latency of cataract formation, increasing the likelihood of effects being seen. Whilst the lifespan of experimental mice is estimated at around 2 – 3 years of age (Yuan, Peters, and Paigen 2011), doses of 0.5 Gy are reported to reduce murine lifespan over a 2 year period (Dalke et al. 2018) in DNA repair deficient mice. Therefore, it is proposed the observable lifespan of mice be reduced to 18 months, and the use of a 'radioresistant' strain is used (Roderick 1963), the C57BL/6, a favourable strain based on early findings of this thesis, see Chapter 3 (Barnard et al. 2018).

1.7 Evidence for DNA damage and repair in the lens

Like many other tissues, DNA damage in the LECs from natural and environmental insult results in the formation of DSBs and subsequently needs repairing just like most other cells (Ainsbury et al. 2016). The role of DNA damage and repair in the lens following IR exposures is a

topic of increasing interest given the improved understanding of IR-induced cataract. Studies have demonstrated a probable role of DNA damage in the lens having a role to play in cataract formation. A higher frequency of DNA single strand breaks was reported in lens epithelial cells of cataractous patients compared to age matched controls (Kleiman and Spector 1993). There has been discussion regarding base and nucleotide excision repair genes in cataractogenesis (Fujimichi and Hamada 2014). Polymorphisms in two genes involved in BER, *OGG1* or *XRCC1* result in an increased risk of senile cataract in humans. Similarly, polymorphisms in the nucleotide excision repair (NER) associated *XPD* gene show the same increase in risk. In mice, mutated *Xpd*/*Ercc2* genes result in sensitivity to ionising radiation (Kunze et al. 2015). The congenital disorder Nijmegen breakage syndrome (NBS), resulting in defective homologous recombination and chromosomal instability, reports lens opacities in a proportion of patients (Gralek et al. 2011). Heat shock transcription factor 4 (Hsf4) mutated mice develop cataract and abnormal lens fibre cell development. This protein has an important role in the gene *Rad51* upregulation, crucial for DSB repair (Fujimoto et al. 2004). In humans, mutations in Hsf4 are associated with inherited cataract, the gene is considered critical to proper lens development (Bu et al. 2002). Ataxia-telangiectasia mutated protein (Atm) is recruited by DSBs to activate repair. Atm haploinsufficency in mice leads to development of cataract more rapidly than WT controls following 500 mGy exposures of X-rays (Kleiman et al. 2007). Mice defective in either MRad9 or Atm were more susceptible to cataractogenesis (Kleiman et al. 2007).

Ionising radiation has multiple effects on the lens including, but not limited to, induction of DSBs in nucleated cells (Markiewicz et al. 2015; Bannik et al. 2013). These are detectable as y-H2AX/53BP1/Rad51 foci (Markiewicz et al. 2015; Kunze et al. 2015; Bannik et al. 2013; Horn et al. 2013). DNA damage foci are localised accumulations of response proteins, visualised at sites of DSBs via immunocyto- and/or immunohistochemical detection (Rothkamm et al. 2015). In most instances, the induction of DSBs increases linearly with dose following radiation exposure in human and cellular studies (Barnard, Bouffler, and Rothkamm 2013), however, the dose response and dose-rate effects in lens cells is not as well documented (Hamada 2016). Most DSBs are repaired quickly, but there is an inherent risk of mis-repair or unrepaired damage persisting (Barnard, Bouffler, and Rothkamm 2013). 53BP1 foci induction has recently been demonstrated in the mouse lens epithelium by flat-mounting the tissue (Markiewicz et al. 2015) and using lens sectioning (Kunze et al. 2015). This DNA damage marker has been demonstrated to co-localise with y-H2AX (Ding et al. 2016; Horn et al. 2013). 53BP1 and yH2AX show an almost identical dose response in the lens epithelium following *in vivo* radiation up to 24 hours post-exposure (Markiewicz et al. 2015). The repair of DSB has been reported to be slower in the peripheral region of the epithelium

when compared to peripheral blood lymphocytes following low doses of x-irradiation (Markiewicz et al. 2015) suggesting that DNA damage might persist as a result.

IR-induced DNA damage triggers (and is part of) the DNA damage response (DDR), and as such, can have effects beyond the initial induction and repair of DSBs. Recent studies have suggested a link between IR exposure and the initiation of the DNA damage response (DDR) to telomere length and telomerase activity (Bains et al. 2019; Dalke et al. 2018). There are some suggestions that telomeres may play a role in cataractogenesis, namely a decrease in telomere length and telomerase activity in HLE cells *in vitro* (Babizhayev and Yegorov 2010), although this role is not fully understood at present. However, these observations highlight the importance of understanding the DDR during initial radiation exposure (including different exposure doses and dose-rates) and that there may be lasting effects which could contribute to the explanation of the latency period between exposure and visually-impairing cataract manifestation.

1.7.1 The influence of dose-rate

Historically, dose-rate has only been considered in only a very limited number of studies looking at cataract risk in IR exposed populations. A very recently published epidemiological study, by Little *et al.* (2018), has suggested an excess hazard ratio of 0.69 (0.27 – 1.16) per Gy of IR to the formation of cataract in radiologic technologists following mean cumulative occupational exposures to low doses (<100 mGy) accumulated over an average 5-year lagged eye lens absorbed dose (Little et al. 2018) (using self-reported cataract history as an endpoint). This excess hazard ratio (EHR) was significantly different from the lowest dose exposure cases (<10 mGy cumulative exposure) used as a control group. Excess hazard ratios are difficult to compare between epidemiological studies due to a variety of factors including varying models and parameters, and the authors found that the observed risks were statistically similar to those reported on the Japanese atomic bomb survivor reanalysis (Neriishi et al. 2012), for example, where a lower EHR of 0.32 (0.17 – 0.52) was reported. However, the Little *et al.* (2018) (Little et al. 2018) study does incorporate a relatively large number of persons, over 12,000 cases, alongside well characterised dosimetry – a key consideration for effective IR epidemiology (Ainsbury et al. 2009; Ainsbury et al. 2016) . Whilst there is little biological evidence for a dose-rate influence in the lens to date, it has been suggested as potentially having a large impact, particularly during fractionation (Hamada 2016), and even more so given this latest epidemiological finding (Little et al. 2018). The ICRP do not draw conclusions regarding the effect of dose-rate on the lens due to a lack of evidence currently (Stewart et al. 2012; Hamada 2017a).

The mechanism(s) of IR-induced cataractogenesis are still largely unknown, however, several possible mechanisms have been identified, with a combination of processes likely to play roles (Ainsbury et al. 2016). The mouse has been identified as a highly appropriate *in vivo* tool for such investigations on the lens for both early, short term biological effects (Barnard et al. 2018; Markiewicz et al. 2015; Kunze et al. 2015), as well as longer term studies of cataract formation (Dalke et al. 2018; Kunze et al. 2015; Bakthavachalu et al. 2010; De Stefano et al. 2015; Kleiman et al. 2007; Kohale et al. 2004). LECs are organised as a single cell monolayer covering the anterior surface of the lens, where they are critical to the homeostatic function of the lens (Wormstone and Wride 2011). The epithelium can be morphologically and functionally defined by two distinct regions, the central and peripheral regions; the former made up largely of quiescent cells, whilst the latter consists of cells with a proliferative ability but not necessarily actively cycling (Tholozan and Quinlan 2007; Treton and Courtois 1981). The role of DNA damage and its potential impact on cataractogenesis in the lens is documented (Barnard et al. 2018; Markiewicz et al. 2015; Bannik et al. 2013; Kleiman et al. 2007; Kleiman and Spector 1993; Kunze et al. 2015). Notable examples include; cataractous lenses showing a high frequency of single strand breaks (Kleiman and Spector 1993), base and nucleotide excision repair genes having a suggested role in cataractogenesis (Fujimichi and Hamada 2014) and mutated *Xpd/Ercc2* genes (involved in DNA repair) result in sensitivity to IR (Kunze et al. 2015). LECs appear to employ both non-homologous end joining and homologous recombination to repair DNA damage, observed in the dose responses of both 53BP1 and Rad51 for both pathways respectively (Markiewicz et al. 2015). Reduced levels of Atm and Rad9 have been demonstrated to increase the radiosensitivity of the lens (Kleiman et al. 2007; Worgul et al. 2005).

IR-induced DNA double strand break (DSB) formation and repair can be quantified using several protein biomarkers, most commonly y-H2AX, Rad51 or 53BP1 (Chua and Rothkamm 2013; Horn et al. 2013; Rothkamm et al. 2015). IR-induced DNA damage assessed by y-H2AX and 53BP1 foci quantification in LECs demonstrated a clear response at a range of doses (Barnard et al. 2018; Markiewicz et al. 2015).

The dose-rate at which IR is delivered is influential in the repair of DSBs. IR is generally considered to be less effective when administered over a longer period, as opposed to an acute delivery, i.e. within minutes (Hall and Brenner 1991). For decades it has been well understood that, certainly for x- and y-IR, a lowering of dose-rate and extension of exposure time reduces the biological effect of a given dose particularly in cellular experiments (Hall 1973), and decreasing dose-rate generally correlates to a decrease in the number of detectable un-repaired DSBs post-exposure (Ruiz de Almodovar et al. 1994). Low dose-rate is typically defined as being 5 mGy/hr or

lower (ICRP 2007b). Results from studies using y-H2AX demonstrate lower frequencies of residual DSB induced with lower dose-rates in lymphocytes (Turner et al. 2015; Kato et al. 2006). The study of Turner et al. (Turner et al. 2015) compared two dose-rates (1.03 Gy/min and 0.31 mGy/min), of x-irradiation and subsequent y-H2AX foci yields in the peripheral blood lymphocytes of C57BL/6 mice. At 24 hours post irradiation, the acute dose-rate produced a significantly higher frequency of unrepaired damage in the lymphocytes from mice exposed to 1.1 and 2.2 Gy.

1.7.2 Non-targeted and bystander effects

Most mechanistic studies of IR-induced effects on the lens investigate the effects on the target tissue, the lens, or target cells, with the LECs likely to be a highly susceptible target of IR. However, non-targeted and bystander effects are increasingly discussed (Ainsbury et al. 2016). In brief, here is what is currently known about such effects.

Non-targeted effects of IR are described as effects exhibited in cells or tissues that are not the target of IR. Radiation-induced genomic instability is a well-known example of this, for example progeny cells of irradiated cells by carry post-irradiation damage or mutation. Therefore, the nature of the LECs to proliferate and differentiate could be effected (Ainsbury et al. 2016). Oxidative stress is known to influence genomic instability, which is also induced by IR (Kadhim, Moore, and Goodwin 2004). Oxidative damage has also been associated with reactive oxygen species produced via lip peroxidation is a major cause of spontaneous DNA damage, which can influence genomic instability also (Clutton et al. 1996). In general, the proliferating cells of the peripheral region, which are heavily investigated during this thesis, are thought to be most likely to be radiosensitive and therefore susceptible to radiation induced genomic instability via non-targeted effects (Markiewicz et al. 2015). Oxidative stress driven DNA damage has been observed in the LECs of cataract lenses (Osnes-Ringen et al. 2013) which could have induced genomic instability resulting in cataract, however the role of genomic instability in cataract remains unclear (Ainsbury et al. 2016).

The potential role of bystander effect(s) in the LECs and the progression of cataract following IR exposure are also a topic of discussion in literature. The bystander effect is essentially the link or communication between and irradiated cell to a non-irradiated cell, or vice versa. The bystander effect has been reported in a few studies using other tissue and cell types, with cytokines, gap junctions and reactive nitrogen species just a few of the known mechanisms involved (Ainsbury et al. 2016). For example, an LEC damaged by IR by communicate to an unirradiated cell nearby, resulting in an IR response or effect in the unirradiated cell in the absence of IR exposure to it. Evidence for the bystander effect in LECs is lacking. However, the pathways identified as involved

in the bystander effect are present in the LECs, with communication via gap junctions occurring (Lovicu and McAvoy 2005). Connexin proteins have also been demonstrated to have a role in bystander effects in glioma cells, with the LECs also known to use connexin channels (Sanson et al. 2002).

The role of bystander and non-targeted effects in the lens are unclear, but there is plausible hypothesis that would suggest they are not disregarded as being involved somehow in IR-induced opacities and cataract. Whilst this thesis does not specifically investigate the effect of these, they are a consideration during discussions of results.

1.7.3 Effects of IR on LEC proliferation

Whilst one of the aims of this thesis is identify the possible role of IR induced DNA damage in the lens, the effects exposures may have on the rate of LEC proliferation will also be investigated. Changes in cell proliferation regardless of IR exposure is known to alter the morphology of the lens (Upadhya, Ogata, and Reneker 2013; Matsuyama et al. 2013). The formation of new LFCs is also known to be highly dependent on cell proliferation within the peripheral region (specifically the germinative zone (GZ)) of the lens epithelium (Hayden et al. 1980), also termed the proliferation compartment in historical literature (Duncan 1981). The effects of IR on cell proliferation and cell cycle are not well documented for the lens.

As has been introduced above, the LECs in the peripheral region of the monolayer (including germinative zone cells) are thought to be the most critically sensitive to IR exposure and cataract induction (Ainsbury et al. 2016). As mentioned earlier, cycling cells are known to be more sensitive to IR induced damage due to a greater relaxation state of chromatin, and this is observed as a radiosensitivity of the peripheral region LECs (Von Sallmann, Grimes, and Mc 1962; Rafferty and Rafferty 1981). The critical nature of the germinative zone cells may also be explained by suggestions of a small population of stem cells residing in this area (Oka et al. 2010), with any effects of IR in these cells likely to have large ramifications in lens homeostasis.

Of the few studies that document the effects of IR *in vivo*, low doses were first shown to increase LEC proliferation in rabbit lenses following x-irradiation 1952 (Von Sallmann 1952). In 1980, it was suggested that IR-induced cataract occurred due to a ‘pathological morphogenesis’ in peripheral region LECs following x-radiation, meaning that mitotic changes demonstrated by abnormal cell densities in this region resulted in cataract. However, these observations were seen in experiments using frogs (Hayden et al. 1980), a much less characterised model of the lens compared to humans and rodents. Nevertheless, observations in frogs demonstrate the

importance of cell proliferation, with frogs having an advantage in terms of experimentation windows not available during human epidemiological cohorts, or in other animal models. The study does also not report doses of radiation, but rather dose-rate and the conclusions are rather crude. Regardless, changes in peripheral region cell density and the organisation of the meridional rows are only seen in frogs with actively dividing LECs, and not in hypophysectomy frogs whose LEC have ceased to proliferate. More recently, low doses of IR (less than 100 mGy x-radiation) increased proliferation in murine lenses using proliferation markers cyclin D1 and 5-Ethylnyl-2'-deoxyuridine (EdU) labelling (Markiewicz et al. 2015). Increased cell density was also observed following IR exposure, along with lens shape changes observed using aspect ratio measurements. The LECs in the peripheral region of the monolayer (including germinative zone cells) are thought to be the most critically sensitive to IR exposure and cataract induction (Ainsbury et al. 2016). Cycling cells are known to be more sensitive to IR induced damage due to a greater relaxation state of chromatin, and this is observed as a radiosensitivity of the peripheral regions LECs (Von Sallmann, Grimes, and Mc 1962; Rafferty and Rafferty 1981).

The LECs in the peripheral region of the monolayer (including germinative zone cells) are thought to be the most critically sensitive to IR exposure and cataract induction (Ainsbury et al. 2016). Cycling cells are known to be more sensitive to IR induced damage due to a greater relaxation state of chromatin, and this is observed as a radiosensitivity of the peripheral regions LECs (Von Sallmann, Grimes, and Mc 1962; Rafferty and Rafferty 1981). Ki67 became a well-characterised marker for proliferation, particularly in the classification and grading of tumour growth (Bosch et al. 2017; Denkert et al. 2015; Jurikova et al. 2016; Li et al. 2015; Miller et al. 2018; Penault-Llorca and Radosevic-Robin 2017). Ki67 is also being increasingly investigated for use as a quantitative and automated standard assessment tool for scoring and grading cancers, particularly breast (Koopman et al. 2018; Miller et al. 2018; Yuan et al. 2015). The marker therefore has a broader recognition amongst clinicians and a suitable marker for the study of proliferation in the LECs. Although proliferation under natural and unirradiated control conditions is thought to be a slow process, with divisions occurring once every 17 – 20 days (Griep 2006), the effect of IR on this process is largely unknown. To observe the potential effect of IR-induced proliferation, it is essential to understand unirradiated spontaneous rates. Proliferation has been reported to respond to radiation at 24 hours post-exposure using EdU and cyclin-D1 markers (Markiewicz et al. 2015), therefore mice are sacrificed at 24 hours post-exposure, as well as an additional 4 hours post-exposure time point (to incorporate DNA damage and repair detection; see Methods). The investigation of both dose and dose-rate and their influence upon LEC proliferation was performed

in conjunction with endpoints for DNA damage and repair. Therefore, the experimental procedures are identical.

In vivo studies are at present the most suitable approach for studying the effects of IR on cell cycle. The lens is a very precisely organised and controlled tissue, which is needed to maintain its unique function and characteristics. Proliferation of LECs in the lens is therefore difficult to replicate and study *in vitro*. Further experimentation is needed to establish cell lines and primary cell cultures that demonstrate the same characteristics as *in vivo* LECs (Ainsbury et al. 2016; Markiewicz et al. 2015).

The stimulation of LEC proliferation has further been demonstrated *in vitro* (Hamada 2017a; Fujimichi and Hamada 2014) following IR exposure. Both an increase and inhibition of cell growth have been seen, and although initially this may seem at odds, it has been hypothesised as a probable result of two separate subsets of LECs being present in the HLEC1 human lens epithelial cells used, each subset having differential responses. However, *in vitro* cultures are difficult to translate to *in vivo* responses due to almost all cells proliferating and therefore the rate of proliferation making it difficult to relate even to the peripheral region of the lens epithelium.

1.8 Radiation-induced DNA damage

DNA damage induced by IR exposure is well characterised in several tissues and cells types. The specific role of DNA damage at inducing radiation-induced cataracts is unclear. Previously, DNA damage within the lens, and LECs, have been introduced (see section 1.7 of this chapter), with a clear indication of an influence in les opacity. However, many questions remain as to the exact mechanism, and the effect low dose and dose-rate have on this endpoint. IR induced DNA damage in the form of DSBs, a hallmark of IR exposure. To understand the effects of DNA damage in the lens, it is important to appreciate the intricacies of DNA damage induction and repair, and why these have important repercussion in the lens.

1.8.1 Double strand breaks

Double strand breaks (DSBs) occur when both strands of the DNA helix are broken in close proximity (figure 1.8). They arise from exogenous agents not limited to IR, but also chemical exposure and in some cases, during the immune response (Scully and Xie 2013). DSBs are considered the most harmful of DNA lesions, due to the subsequent effects that can be caused if unrepaired (Panier and Boulton 2014).

Figure 1.8: DNA double strand break (DSB)

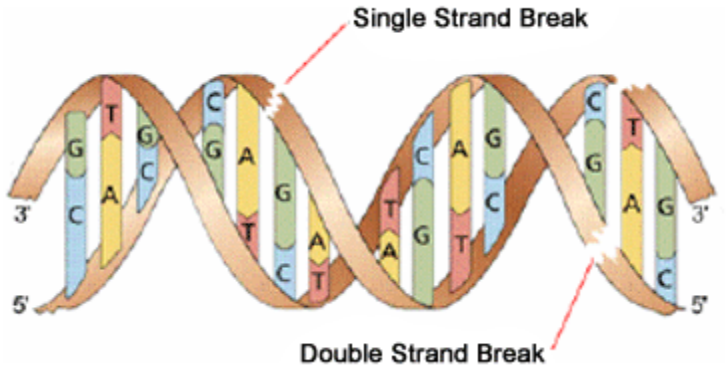

Figure 1.8: Comparison of single strand versus more harmful double strand breaks on the double helix of DNA (http://team3rocksz.blogspot.com/2011/11/types-of-damages.html)

1.8.2 Induction by ionising radiation

The target site for IR tends to the nucleus of the cell, as this contains the chromosomal DNA (Hall 1973). IR can induce a number of harmful lesions in the DNA, including abasic sites, oxidated bases and sugars, strand breaks and cross-links within or between the complementary DNA strands or between DNA and surrounding proteins (Barnard, Bouffler, and Rothkamm 2013). IR lesions tend to be distinguishable from other genotoxic substances as it can cause multiple lesions very close together (within 1 -2 helical turns of the DNA strand), which produces clustered lesions, one of with are double strand breaks (DSB) (Barnard, Bouffler, and Rothkamm 2013; Rothkamm et al. 2015). When a DSB is induced, both complimentary strands of the DNA are damaged. IR induced DSBs have been and still are highly studied, partly because they are harmful and contribute to many of the toxic, mutagenic, clastogenic and carcinogenic effects of IR, and partly due to the broad range of methods available to detect and subsequently quantify them (Barnard, Bouffler, and Rothkamm 2013). During IR-induced DSBs, the sugar phosphate backbone of the DNA is damaged by direct radical production, or indirectly by radicals formed through water radiolysis, which occurs around the site of the DSB (Barnard, Bouffler, and Rothkamm 2013). When two such events occur is very close proximity (as mentioned, within two helical turns of the DNA strand), a DSB is formed. Each direct or in-direct event tends to consist of multiple radical hits as oppose to single 'hits' (Barnard, Bouffler, and Rothkamm 2013; Milligan et al. 1995). IR doses up to several hundred Gray show linearity with DSB induction due to radicals originating from the same radiation track (Lobrich, Rydberg, and Cooper 1995; Barnard, Bouffler, and Rothkamm 2013). It should be noted that whilst DSB are the most commonly studied and quantified of IR-induced damage, due to their harmful nature, single strand breaks (SSB) are also produced in the order of 25 – 40 fold more than DSBs,

possibly even higher once quantification limitations are improved (Balagurumoorthy, Adelstein, and Kassis 2011).

1.8.3 Repair of DSBs

DSBs need to be repaired or attempted to be repaired to ensure there is no loss of function in the cell. The DDR coordinates a well-orchestrated system to repair IR induced DSBs almost immediately after induction (Noda 2017). DSBs are firstly detected by a group of proteins, the MRN complex, consisting of MRE11, Rad50 and NBS1 (Jackson and Bartek 2009). This complex encourages the binding of phosphorylated Atm and also the phosphorylation process of H2AX (now γ-H2AX) (Rothkamm and Horn 2009); this is the fundamental structure of repair foci, the cluster of proteins that accumulate around the site of DSBs. However, the complexity of a DSB compared to a SSB, makes it much harder to repair as there is no complimentary opposing strand to use as a template. DSB repair is via two main pathways: alternative and classical non-homologous end joining (NHEJ) and/or homologous repair (HR). The choice of repair pathway is mostly dictated by the state of cell cycle; G0 and G1 cells preferentially repair using NHEJ, whereas DSBs induced during cycling S1 phase opt towards HR (Zimmermann and de Lange 2014). Regardless of how they are induced, most DSBs are repaired quickly and effectively, but there is a chance of breaks being mis-repaired or potentially un-repaired. Both may result in cell death to protect the cell from further harm. The DDR directs the cell, based on the severity and complexity of the DSB(s) induced, whether to repair, undergo cell death (via apoptosis) or become senescent (the cell ceases to divide via cell-cycle arrest)(Noda 2017). Mis-repaired or unrepaired DSBs that persist can result in a loss of cell viability due to translocated chromosomes and other genome rearrangements which become stable within the cell and reproducible during cell division (Zimmermann and de Lange 2014).

Foci assays have revealed a biphasic repair of DSBs in operation, with fast repair of γ-H2AX foci occurring up to 1.5 hours post-exposure, extending to 1.5 Days for slow repair in human lymphocytes (Horn, Barnard, and Rothkamm 2011). Its these slower, unrepaired, DSBs that are more difficult for the cell to repair that carry a greater risk. These are often termed ‘residual’ DSBs as they persist long after fast repair has ended and can potentially be retained by the cell unless cell death or senescence is activated (Noda 2017).

1.8.4 Biomarkers of DSB repair

The study of DSB induction at low IR doses (those relevant to occupational and medical exposure levels) is a fairly recent development, as DSB detection methods have increased in sensitivity particularly with advances in fluorescent microscopy imaging techniques and the ability to quantify DSBs (Barnard, Bouffler, and Rothkamm 2013).

DSBs can be visualised as radiation-induced foci (RIF, mostly just termed foci), which represent hundreds to thousands of individual proteins that accumulate at the site of the a DSB. The introduction of the foci assay over the past two decades has greatly improved the sensitivity of DSB detection, particularly in occupational and medical situations, where the relative dose is fairly low. The assay is a vast improvement on the previously available methods of pulse-field gel electrophoresis (PFGE) or the neutral filter elution methods, which measured DSB indirectly via molecular weight or chromosome DNA length (Barnard, Bouffler, and Rothkamm 2013). RIF represent hundreds to thousands of individual proteins that are involved in the DNA damage response following DSB induction (Bekker-Jensen and Mailand 2010; Costes et al. 2010), with many of these proteins firmly established as surrogate markers (Feuerhahn and Egly 2008).

Whilst there are a large number or surrogate markers for IR-induced DSBs, the most commonly referred to and widely used remain the phosphorylated histone variant γ-H2AX (Horn et al. 2013; Rothkamm and Horn 2009), the auto-phosphorylated DNA damage kinase Atm-pS1981 (So, Davis, and Chen 2009) and the mediator protein 53BP1 (Noon and Goodarzi 2011), the latter of which are discussed in more detail to follow. These markers are used to detect RIF using immunofluorescent microscopy techniques which allow visualisation of foci and subsequent quantification by counting, either manually or using automated image analysis, the fluorescent foci. This also makes the assay accessible to a large number of investigators due to minimal requirements (fluorescent microscope and relatively inexpensive antibodies). In recent years, live cell imaging has improved RIF detection and understanding by allowing the patio-temporal dynamics of protein recruitment to be studied (Neumaier et al. 2012; Asaithamby and Chen 2009).

RIF assays using fluorescent microscopy demonstrate the most sensitive technique to detect and quantify DSBs, particularly during low dose and early time point investigation. The assay has been demonstrated to detect doses as low as 1 mGy using γ-H2AX as a marker (Rothkamm and Lobrich 2003). DSB induction by IR can conceptually be expected to occur linearly as dose increases, but there are a few factors in the assay that may affect linearity. This includes the occurrence of spontaneous or 'background' foci, which will be higher in cycling cells compared to non-cycling or quiescent cells (importantly cycling cell state is a key defining feature of lens epithelial cells)

(Barnard, Bouffler, and Rothkamm 2013). This is thought to be due to DNA breaks that occur as part of the process of DNA replication, and DSBs being passed over in later stages of the cell cycle (Barnard, Bouffler, and Rothkamm 2013; Rothkamm et al. 2003). Assay and reagent quality can also introduce non-specific staining and aggregate formation – a common issue in immunofluorescent protein detection (Barnard, Bouffler, and Rothkamm 2013). Foci size can also be a point of contention when scoring, multiple DSBs in close proximity are thought to more closely together, creating a cluster of damage (Neumaier et al. 2012). In theory this effect can result in lower foci yields, if a foci is quantified regardless of size (Barnard, Bouffler, and Rothkamm 2013), and influence the shape of the dose response curve as non-linear.

RIF represent a biological response to DNA damage, and as such require a period of several minutes post-exposure before they can be reliably detected with immunostaining and fluorescence (Rothkamm and Horn 2009).

Whilst the formation of DSBs in irradiated cells is well reported, and the spontaneous background foci because of replication is discussed, foci have also been observed in bystander cells. Bystander cells are not directly exposed to radiation but are in close proximity to those that have. Increased frequencies of γ-H2AX foci have been reported in these cells following IR exposure (Dickey et al. 2011; Burdak-Rothkamm, Rothkamm, and Prise 2008).

1.8.5 53BP1

There are a number of surrogate markers established for the detection of IR-induced DSBs. Tumour suppressor p53 binding protein 1 (53BP1) represents one of the most widely used of such markers, thought to be involved in the chromatin remodelling specifically at the break site (Noon and Goodarzi 2011; Zimmermann and de Lange 2014). It is a large protein containing a number of interaction surfaces for several DSB response proteins (Panier and Boulton 2014). The protein is abundant in the nucleoplasm of the cell, but is rapidly localised at the site of damaged chromatin at the site of DSBs (Kim and Yim 2018; Panier and Boulton 2014). Here it promotes repair by NHEJ (Panier and Boulton 2014) whilst inhibiting the HR pathway, and colocalises with gamma-H2AX during the protein cascade of foci formation, with the phosphorylation of H2AX being the initiator (Panier and Boulton 2014). 53BP1 has recently been revealed as directly engaging in the ubiquitylated form of H2AX, prior to phosphorylation, hence why it localises at DSB sites (Fradet-Turcotte et al. 2013), although the two proteins can form independently of each other (Zimmermann and de Lange 2014). 53BP1 has also been demonstrated to also recruit EXPAND1 (Huen et al. 2010)and RIF1 (Silverman et al. 2004) DSB response proteins to the damage site. 53BP1 also recruits PAXIP1, another downstream response protein to DSBs and thought to be critical for

cell survival following DNA damage (Gong et al. 2009). It is thought that if 53BP1 is particularly integral in amplifying ATM during low levels of DNA damage induction and promote checkpoint signalling, with 53BP1 failure to localise at damage sites resulting in G2-M checkpoint defects (Panier and Boulton 2014). ATM appears to be stimulated by 53BP1 through direct interaction with the RAD50 component of the MRN complex (Lee and Paull 2007). Besides being involved in the repair of DNA DSBs, 53BP1 also has a role in maintaining the integrity of centrosomes (Kim and Yim 2018). The role of 53BP1 in the DNA damage response and repair of DSBs is clearly integral, demonstrated by the number of downstream proteins that interact and are promoted by 53BP1. It is also clear that the protein has roles beyond simply repairing DSBs, including checkpoint signally and repair pathway choice.

1.9 Research questions

The aims of this thesis can be divided into four distinct questions to help focus the results and discussions. Lens sensitivity at low doses remain unclear, however epidemiological results have led to reduced lens dose limits based on mounting evidence. IR exposures induce cataract, however there remains a substantial gap in mechanistic and biological knowledge as to how and why this happens over a long latency period. Biological for the revised lens limits is needed.

1: The effects of low dose IR exposure on the lens are not fully understood. Evidence suggests a possible differential response at low compared to high dose IR. The DNA damage response at low doses is investigated across four strains of mice *in vivo* to determine the effect of low dose IR in inducing DNA DSBs and repair in the lens epithelium. Strain dependency of the lens in response to IR can help to explain population variance and individual susceptibility. Genetics are thought to have a greater influence in low dose IR response. Thus, the hypothesis to be investigated in this thesis is that low dose IR impacts the DNA damage response in the lens epithelium in a strain-dependant manner.

2: The effect of not only dose, but also dose-rate is not well understood. The ICRP recommend dose limits but do not make comment on the delivery of that dose. Recent epidemiological studies suggest the effects of low versus high dose-rate may not be uniform in IR-induced cataract. Thus, the hypothesis to be investigated is whether the use of different dose-rates affects the DNA damage response.

3: LEC proliferation and differentiation are naturally well-regulated and controlled, a characteristic essential for lens function. The impact of IR on LEC proliferation behaviour has been demonstrated in historic studies, however the impact of dose and dose-rate in proliferation has not been well described. Thus, the hypothesis to be investigated in this study is whether IR causes disruption to normal proliferation of LEC, leading to aberrant differentiation and cell migration.

4: Scheimpflug imaging is a proven sensitive technique for quantifying and tracking lens opacity in mice. This technology allows for the monitoring of lens opacity *in vivo* in mice over a period. Dose-rate effects have never previously been addressed using this method, and current studies can be significantly modified to offer an optimum study for detection of IR-induced cataract. Thus, the hypothesis to be investigated during this study is that dose and dose-rate impact upon lens opacities over time.

2. Materials and Methods

2.1 *In vivo* ionising radiation exposures

The LECs are highly organised, with proliferating cells compartmentalised in a way that is difficult to recreate during *in vitro* cell culture (see chapter 1; section 1.3). Exposing lenses *in vivo* during whole body irradiations represents the most appropriate method for accurately assessing the response of this tissue to IR. Consideration is given to the identification of appropriate strains of mice and methods for analysing cell proliferation, DNA damage and the tracking of lens opacities, outlined during this chapter. Different strains of mice have different genetic backgrounds, and have differing sensitivity or resistance to radiation-induced effects.

2.1.1 Mice used during studies

The strain dependency of radiation-induced cataractogenesis in mice is not well understood (Ainsbury et al. 2016). Most *in vivo* radiation-cataract studies have been performed using specific heterozygous or homozygous knockout models, with comparisons to wild-type counterparts (Kleiman et al. 2007; Worgul et al. 2002; Worgul et al. 2005; De Stefano et al. 2015; Dalke et al. 2018; Kunze et al. 2015). These mice chiefly have reported deficiencies in the repair of DNA damage amongst other pathways, and are therefore useful in determining the role of this pathway(s) by providing a sensitive model. However, genetically altered strains are not representative of the human population; not all persons will carry such unique genetic defects. Therefore, several inbred (nearly genetically identical) strains are compared to identify the role of strain dependency to low dose IR. Inbred strains are likely to still underestimate human complexities, but allowed for stronger power calculations due to their genetic similarities, an important consideration during experimental studies (Ainsbury et al. 2016; Martin et al. 2017; Carreras et al. 2019). The genetic background of mice is a significant factor in the lens at 0.5 Gy IR compared to higher doses (Kleiman et al. 2007; Worgul et al. 2002; Worgul et al. 2005), suggesting a low dose sensitivity. Here, doses were investigated to clarify if this significance is even greater at the very-low dose range below 100 mGy.

2.1.2 Strains of mice exposed

Figure 2.1: Summary of the four inbred mouse strains used in the studies described in this thesis

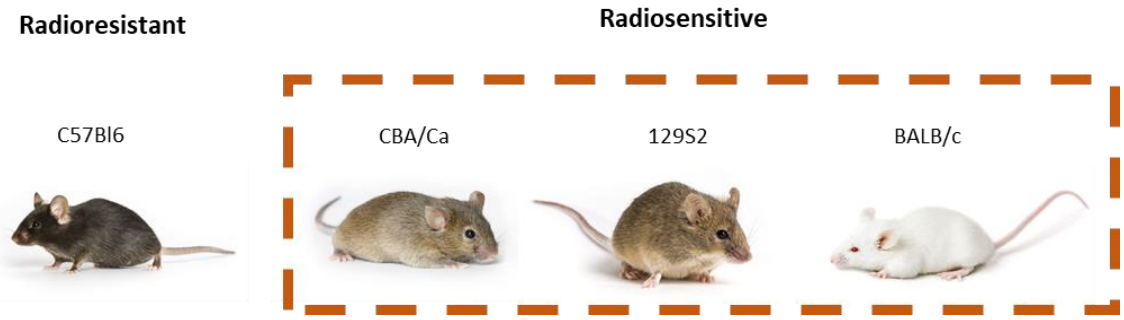

Resistance to IR-induced DNA damage	Reduced post-IR survival rates	Impaired DNA repair (nsSNP on CtIP gene)	Reduced lifespan post-IR
Greater survival ≥1 Gy	Susceptible to IR-induced rAML	Reduced lifespan following IR	Impaired DNA repair (polymorphism in Prkdc gene)
Demonstrated in IR-induced cataract studies previously		Increase in complex chromosomal aberrations post-IR	Low expression of DNA-PKcs (needed during repair)
High natural lens transparency			Genomic instability increase post-IR

Figure 2.1: Different phenotypes of the four strains of mice exposed to IR. The table also highlights key characteristics used for classifying mice as radio-resistant or -sensitive (taken from text below and chapter 1; section 1.6.1 - 4).

Four inbred strains of mice were identified and used in the studies described in this thesis, as summarised in Figure 2.1. C57BL/6 mice are a documented radioresistant strain (Newman et al. 2014) which specifically affects IR-induced DNA damage (Darakhshan et al. 2006; Peng et al. 2009). The strain should survive well following higher (>1 Gy) doses of radiation exposure (Roderick 1963). C57BL/6 mice have previously been identified as a strain of choice in radiation-induced cataract studies (Markiewicz et al. 2015; Wolf et al. 2008). 129S2 mice are more radiosensitive due to a single nucleotide polymorphism affecting a component of the DNA DSB response, the CtIP gene (Makharashvili and Paull 2015). Reduced lifespan and increased chromosomal aberrations following x-irradiation have been reported (Patel et al. 2016). Radiosensitive CBA/Ca mice, similarly, have been observed to have reduced lifespan post-exposure (Patel et al. 2016), a low rate of spontaneous tumour development (Rithidech, Cronkite, and Bond 1999; Brown et al. 2015) and a susceptibility to radiation-induced acute myeloid leukaemia (Boulton et al. 2001; Verbiest, Bouffler, and Badie 2018). Finally, BALB/c mice demonstrated reduced lifespan post-IR exposure (Roderick 1963; Mukherjee, Sainis, and Deobagkar 2014; Newman et al. 2014) and deficient DNA

repair due to a reported polymorphism in the gene encoding DNA-PKcs, as well as a spontaneous mutation in some cases causing cataract and microphthalmia (Bakthavachalu et al. 2010; Kohale et al. 2004), and increased genomic instability (Hamasaki et al. 2007).

C57BL/6 (C57BL/6JOla/Hsd), 129S2 (129S2/SvHsd), BALB/c (BALB/cOlaHsd) and CBA/Ca (CBA/CaOlsHsd) inbred mice were all obtained from Envigo, UK (EnvigoRMS (UK) Ltd., Blackthorn, Bicester, Oxon. OX25 1TP UK). All mice used in this thesis were female, facilitating housing and space requirements in the animal unit of Public Health England (PHE), Chilton. This also eliminated any gender effect that could be expected based on epidemiological studies, thus strengthening power calculations enabling the highest probability of identifying significant low dose IR effects. No breeding of mice took place as part of the studies in this thesis, all mice were bred by the supplier and delivered to PHE at approximately 6-8 weeks of age.

2.1.3 Ethics and licences

Groups of up to five female mice were housed together. The number of mice housed per cage was in accordance with minimum space requirements for mice as outlined by the Code of Practice for the Housing and Care of Animals Bred, Supplied or Used for Scientific Purposes under the Animals (Scientific Procedures) Act 1986 (ASPA). A minimum 200 cm^2 is required for groups of 5 mice. Food (RM3(E), LBS Biotechnology, Hookwood, Surrey. UK) and water were available always. During all studies the health status of the mice was checked daily and recorded. All procedures involving animals were performed in accordance with the Animals (Scientific Procedures) Act 1986 via approved project licencing granted by the UK Home Office (PPL No. PA66E1512). Additional approval from the local Animal Welfare and Ethical Review Body (AWERB) at Public Health England was granted for the duration of this project.

2.1.4 Procedure for mouse exposures

Mice were irradiated *in vivo* whole body at 10 weeks of age, within the reported optimum age bracket of 7 – 10 weeks of age for radiation-induced cataract exposures, where the lens of the mouse is at the earliest 'adult' stage, equivalent to adult human lens exposure (Bannik et al. 2013). Irradiating at the earliest possible adult stage allowed for the longest post-exposure life expectancy. During irradiations, a maximum of five animals per Corex box (Dimensions: L265mm x W230mm x D150mm) were exposed at a time (Figure 2.2). Mice were exposed in the same groups as they were housed. Mice were unrestrained and able to move freely during exposure. X-irradiations took place on site at PHE (Chilton, Oxfordshire UK) whilst gamma irradiations took place at another facility on the same Harwell Campus site, requiring mice to undergo a brief transportation by vehicle

(approximately 2 minutes) to the Medical Research Council's ^{60}Co gamma irradiation facility (Chilton, Oxfordshire UK) (Ainsbury et al. 2017). Following all IR-exposures mice were returned to their home cage within the animal unit of PHE.

Figure 2.2: Corex irradiation and travel box

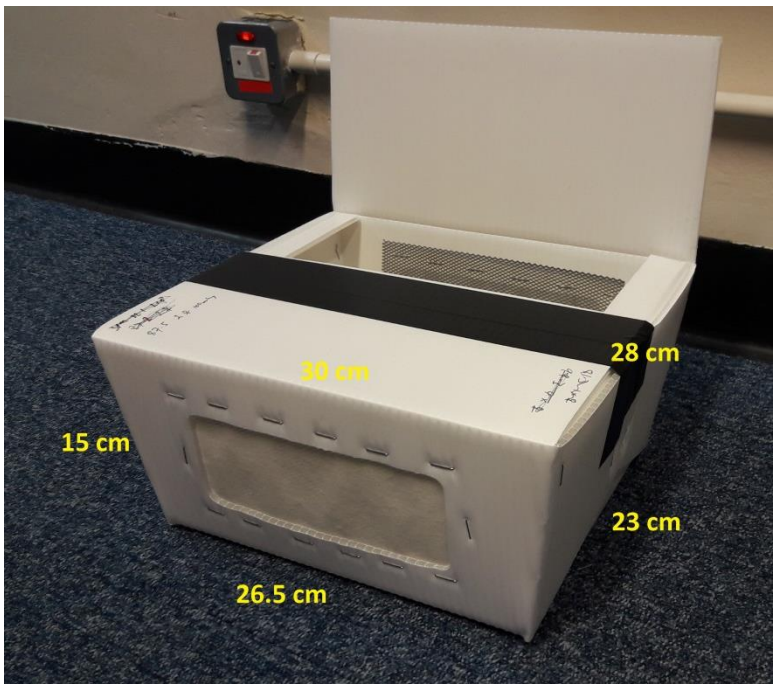

Figure 2.2: Corex transport and exposure boxes used during all irradiations. Boxes contain a layer of substrate to keep the mice enriched during exposure.

2.2 X-radiation exposures

X-irradiations were carried out using a self-contained 250 kVp X-ray unit (CD160/1, AGO X-ray Ltd, Martock UK) with aluminium and copper filtration (~1 mm) containing a Varian NDI-320 source (Figure 2.3). Acute doses of X-rays were delivered at 4.9 mGy or 0.5 Gy min^{-1}. Dosimetry was performed with a calibrated reference ionisation chamber for the exact exposure setup used. Exposures were always monitored using a calibrated UNIDOS E electrometer and 'in-beam' monitor ionisation chamber (all from PTW, Germany) located at source. Correction factors are used to calculate exact dose. Spatial dose uniformity was checked using Gafchromic EBT2 films (Vertec Scientific Ltd., UK) to ensure a homogenous dose was delivered to the entire area of the Corex exposure box (Figure 2.2).

Figure 2.3: X-ray exposure facility at PHE Chilton

Figure 2.3: 250 kVp X-ray unit (CD160/1, AGO X-ray Ltd, Martock UK) located at PHE, Chilton (UK) where all x-irradiations were performed

2.2.1 X-radiation dose-rates

Two dose-rates were used during X-irradiation exposures. Doses delivered at 0.5 Gy/min were achieved using 250 kVp with a current of 13 mA. The Corex mouse boxes (figure 2.2) sit on a Perspex plate situated atop an adjustable table at 60 cm away from the source. This Perspex plate reduces backscatter of electrons. The dose can be monitored using the in-beam electrometer by applying a correction factor of 13 to establish the dose to target. The lower dose-rate of 4.9 mGy/min was delivered by using 250 kVp but reducing the current to 0.2 mA. The adjustable table was removed from the X-ray unit and Corex boxes containing the mice placed on the floor of the X-ray unit atop a Perspex plate. As with the previous dose-rate, a correction factor of 27 can be applied to the electrometer reading to give actual dose. X-radiation dose and dose-rate calibration was performed by Tim Daniels of PHE.

2.3 γ-radiation exposures

During the studies described during this thesis, access to the γ-irradiation facility at MRC Harwell (Figure 2.4) was granted as part of the LDLensRad project, allowing for animal exposures at a range of calibrated doses and dose-rates. Calibration was expertly performed by Dr Mark Hill and

James Thompson of Oxford University. Source decay factors were calculated as per date of exposure, therefore each date of exposure had a slightly different exposure time.

2.3.1 ^{60}Co source and setup of exposure chamber

Doses of 0.5, 1 and 2 Gy were delivered via horizontal geometry at dose-rates of 0.3, 0.063 and 0.014 Gy/min (Table 2.1). The irradiation system is calibrated and traceable to national standards. All doses were delivered to within 5% accuracy. Most of this error comes from the difference in the size of the mice compared to the standard build-up cap that is used (18.6mm diameter). The ^{60}Co air-kerma correction factor (from the calibration certificate) and then an air-kerma to tissue correction factor of 1.113 (the same correction factor as used by Dalke *et al.* (2018)) were used. All irradiations took place at room temperature, and were whole body *in vivo* exposures to all mice. A combination of 1, 2 or 4 ^{60}Co sources were used to achieve dose-rates of 0.014, 0.063 and 0.3 Gy/min respectively.

Figure 2.4: ^{60}Co source(s) and exposure set up at MRC Harwell

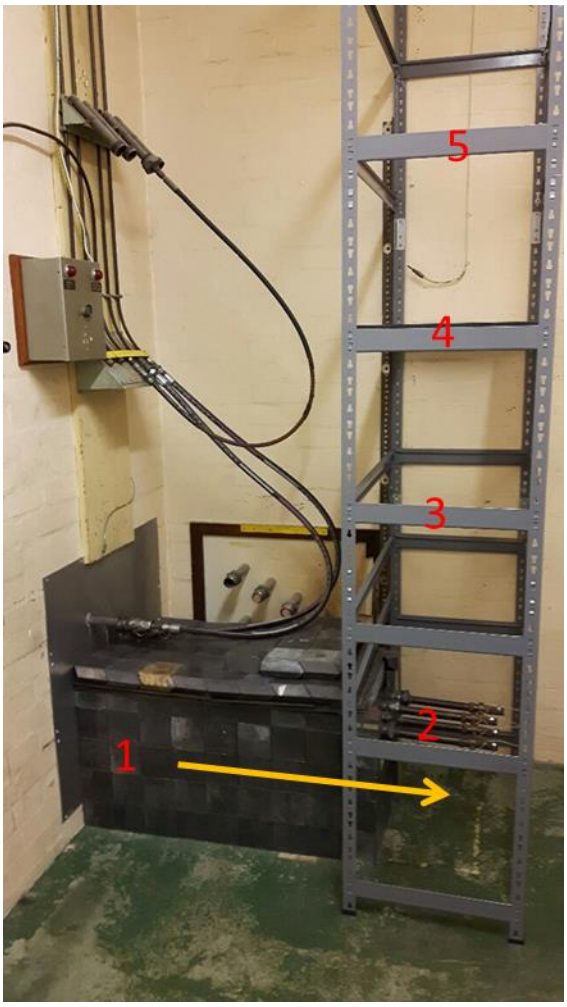

Figure 2.4: ^{60}Co y-radiation exposure cell 3 at the MRC Harwell. Sources are stored externally and travel into the cell (1) through wall travelling through a lead tunnel to the exposure position (2). Bottom shelf (3) delivers 0.3 Gy/min using sources A, B, C and D. Middle shelf (4) delivers 0.063 Gy/min using sources B and C. Top shelf (5) is used to deliver 0.014 Gy/min using source C.

Figure 2.5: Shelf with Perspex 'window' used during exposures

Figure 2.5: Wooden shelf used during exposures. The shelf had a Perspex 'window' on which the Corex exposure boxes were placed. The shelf could be moved to slot into the various shelf brackets to achieve the different dose-rates.

2.3.2 ^{60}Co dose-rates

The different dose-rates of the γ-irradiation were achieved by altering the number of sources used during the exposure, and the distance of the mice away from the sources. As mentioned, three dose-rates were calibrated for the ^{60}Co source(s). Table 2.1 shows the three dose-rates and the time of exposure taken to administer each dose of 0.5, 1 and 2 Gy. The time of exposure to deliver doses greater than 0.5 Gy, using the lowest calibrated dose-rate of 14 mGy/min, was not permissible under the local Home Office project licence and local ethical approval granted for the current study.

Table 2.1: Exposure times for ^{60}Co doses for 300, 63 and 14 mGy/min dose-rates

Dose (Gy)	300 mGy/min	63 mGy/min	14 mGy/min
0.5	1.5 min	7.1 min	39 min
1.0	3.1 min	14.4 min	N/A
2.0	6.3 min	29.2 min	N/A

Table 2.1: Table of exposure times for each dose delivered for each of the calibrated dose-rates.

2.4 Isolation of the lens epithelium

In vivo irradiations ensured the exposure of the lens and its subsequent response to IR occurred under natural conditions. Following exposure, the mice had a post-exposure time of either 30 minutes, 1, 2, 4 or 24 hours in which to allow the lens to respond to the effects of IR.

2.4.1 Sacrifice and eye extraction

Upon reaching the relevant time point, mice were sacrificed via schedule one method of carbon dioxide (CO_2) was performed as per local Home Office Licence. Once cessation had been confirmed, the entire eye was removed using curve tipped tweezers. A small amount of pressure was applied to the upper and lower socket of the eye using the open tweezers allowing it to protrude forward. The curve tipped tweezers were then able to grip the underside of the eye, either side of the optic nerve. The whole eye was easily extracted by gently being pulled outwards. This technique maintains the attachment of the optic nerve, which is useful for easy orientating the eye allowing for small slit to be cut in the back of the eye just above the optic nerve using a scalpel blade and dissecting microscope.

2.4.2 Preparation and fixation of the lens

The eyes were then placed in formaldehyde (4% concentration diluted in phosphate buffered solution (PBS)) (Formaldehyde and PBS: Sigma-Aldrich, Dorset, UK.) and left for approximately 90 minutes at room temperature, to allow the fixative to penetrate the inner tissue and the lens. The fixation time is critical and cannot deviate; over or under fixation results in poor isolation of the epithelium and poor immunofluorescent staining. Following fixation, the formaldehyde was removed and replaced with PBS for overnight storage at 4^{o}C. The PBS was then removed and replaced with fresh PBS containing 0.02% sodium azide solution (to reduce contamination of the tissue) and stored at 4^{o}C prior to microdissection and immunofluorescence staining.

2.4.3 Isolation of the lens epithelial monolayer

2.4.3.1 Microdissection and flat mounting

Once fixed, an eye was held firmly with forceps and the tissue cut to gently reveal and extract the lens. The lens was firm to the touch once fixed and the tissue around the lens can be easily manipulated around the location of the lens so as not to damage the lens itself. Once isolated from the rest of the tissue, the lens was transferred to a small acrylamide disc, orientated with the front of the lens facing down, and then lightly slit across the back in an 'X' shape using the scalpel blade (Figure 2.6). Each corner of the monolayer was then peeled back using fine watchmaker

forceps and pinned flat using 2 mm butterfly pins (Watdon, Eastbourne, UK). It should be noted that this process of pinning the entire epithelium in a single piece, as documented by previous studies (Wu et al. 2014; Markiewicz et al. 2015), represents the 'textbook' approach. The epithelium is a single cell thick monolayer and once removed from the lens is very fragile. The epithelium tears easily creating small pieces of the monolayer (Figure 2.7, image A), which were still able to be pinned down and processed. The lens epithelium was kept suspended in PBS to ensure it did not dry out.

Figure 2.6: The isolated mouse lens during microdissection of the lens epithelium

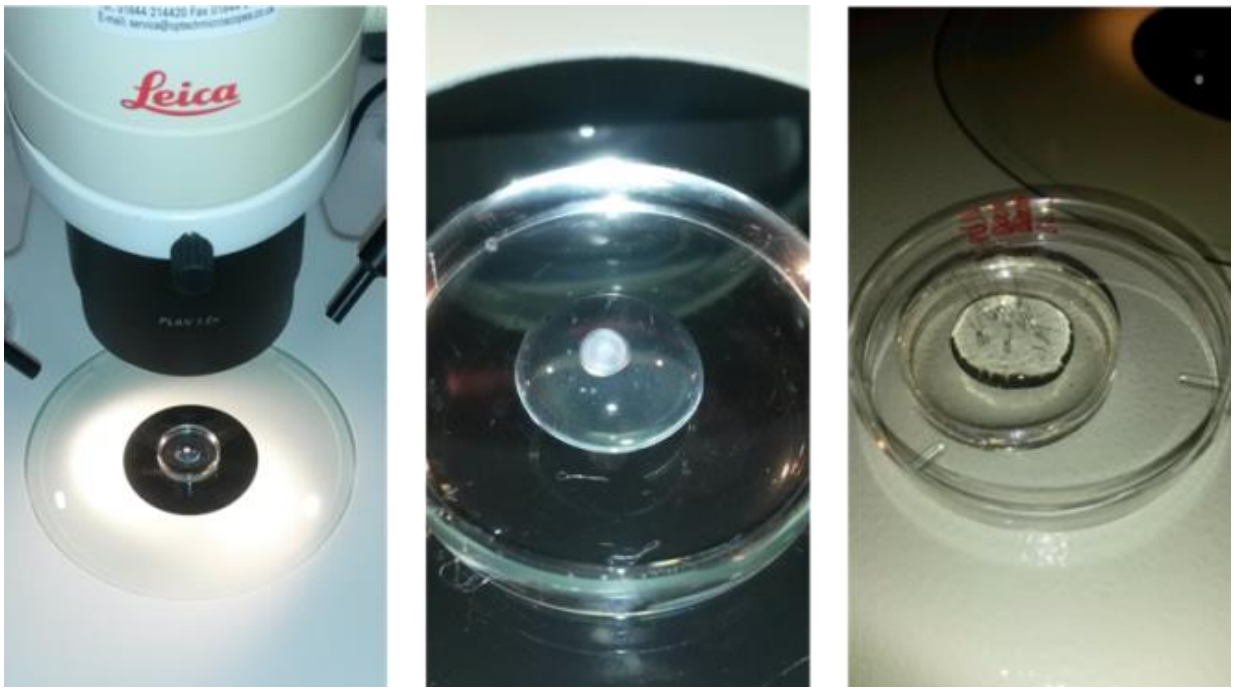

Figure 2.6: Microdissection process of the lens and isolation of the epithelium. Lenses were isolated and suspended in PBS. The epithelium was then delicately removed and pinned onto polyacrylamide discs in preparation for immunofluorescent staining.

Figure 2.7: Isolated portions of the lens epithelium stained with DAPI

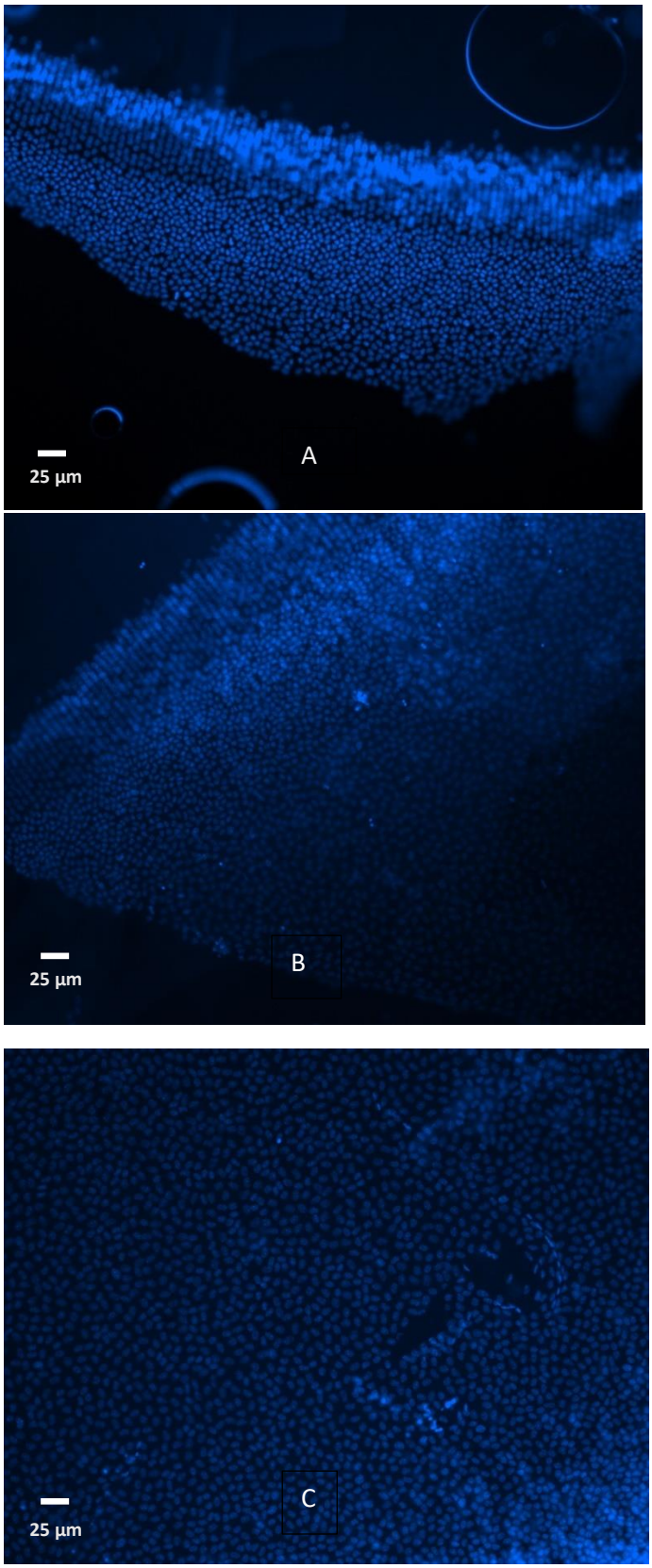

Figure 2.7: Pieces of epithelium (captured at 10x magnification). The delicate nature of the monolayer leaves it prone to tearing, resulting in pieces of various sizes. Here are two pieces of the peripheral region, with meridional rows still attached (A and B), and the central region (C) with some small tears as described.

2.5 Immunofluorescent staining for 53BP1 foci and Ki67 positive LECs

For immunofluorescent staining of the epithelia, the monolayers were first permeabilised with 0.5 % Triton-X 100 (TX) (Sigma Aldrich, Dorset, UK) for 10 minutes (mins), and then incubated at room temperature (RT) with 1 % (w/v) bovine serum albumin (BSA, Fisher Scientific, Loughborough, UK) diluted in PBS for ~30 mins. The primary anti-53BP1 (Abcam, Cambridge, UK) antibody was diluted in 1% (w/v) BSA at 1:500. Anti-53BP1 was incubated on epithelia for 45 mins at RT. The primary antibody was removed and the epithelia incubated with 1% BSA for 5 mins, repeated three times. A secondary antibody together with 200 nm/ml 4', 6-diamidino-2-phenylindole (DAPI, Roche Diagnostics, Burgess Hill UK) was diluted 1:500 (Goat anti-rabbit or anti-mouse IgG depending on primary antibody, Alexa Fluor 555, both from Invitrogen, Paisley UK) in 1% (w/v) BSA and incubated on the epithelia for 30 mins. The secondary antibody was then replaced with PBS to remove excess and this was repeated at least twice. Using fine watchmaker forceps, epithelia were transferred to microscope slide and dried in the dark. Once dried slides were mounted in Prolong gold antifade (Invitrogen, Paisley UK) and the coverslip sealed using nail varnish. Slides were typically left overnight before analysis.

Table 2.2: List of reagents and their sources described within this thesis

Reagent	Source	Dilution
Formaldehyde	Sigma-Aldrich, Dorset, UK	4% (PBS)
Triton-X	Sigma-Aldrich, Dorset, UK	0.5% (PBS)
BSA	Fisher Scientific	1% (PBS)
PBS (tablets)	Sigma-Aldrich, Dorset, UK	1 tablet in 200ml distilled H_2O
Anti-53BP1	Abcam, Cambridge, UK	1:500 (BSA)
AlexaFluor 555 GaM or GaR	Invitrogen, Paisley, UK	1:500 (BSA)
Prolong Gold Antifade	Invitrogen, Paisley, UK	N/A

Table 2.2: All reagents used during the studies described within this thesis, with supplier information and working dilution used.

Proliferative marker Ki67 was detected using a conjugated fluorescently labelled monoclonal antibody (SolA15) with FITC (ThermoFisher Scientific, UK). This antibody was applied alongside the primary 53BP1 antibody, or independently during the primary antibody application step, whereby only DAPI needed applying during the secondary antibody stage.

Figure 2.8: Immunofluorescent staining of Ki67 positive cells and 53BP1 foci in LECs

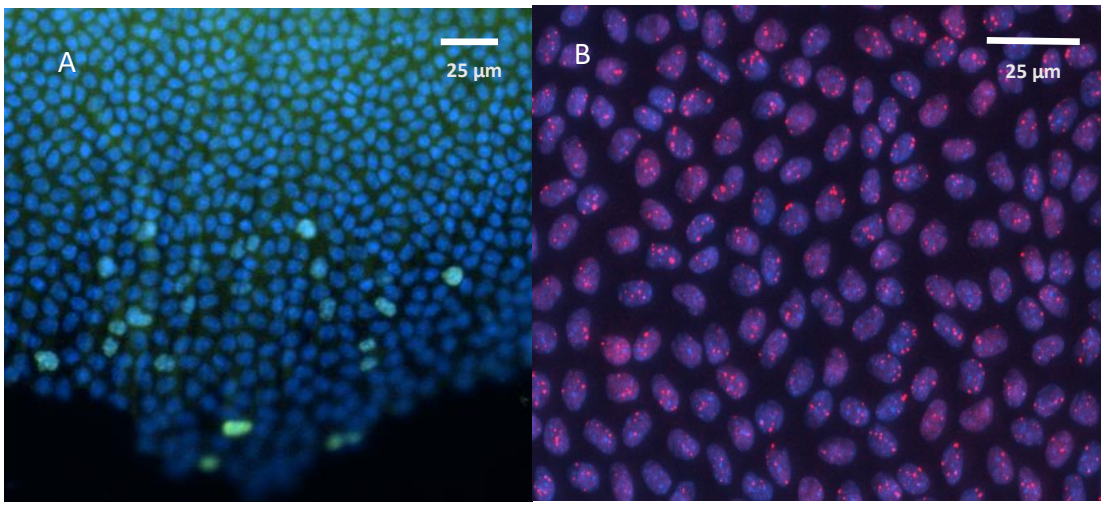

Figure 2.8: DAPI (blue) stained LECs of the peripheral region of the lens epithelial monolayer. Proliferating cells (Ki67 positive, green stain) are clearly visible (image A). The immunofluorescent staining of 53BP1 foci (red dots) are demonstrated (image B).

Figure 2.9: Dual immunofluorescent staining of both Ki67 and 53BP1 in LECs

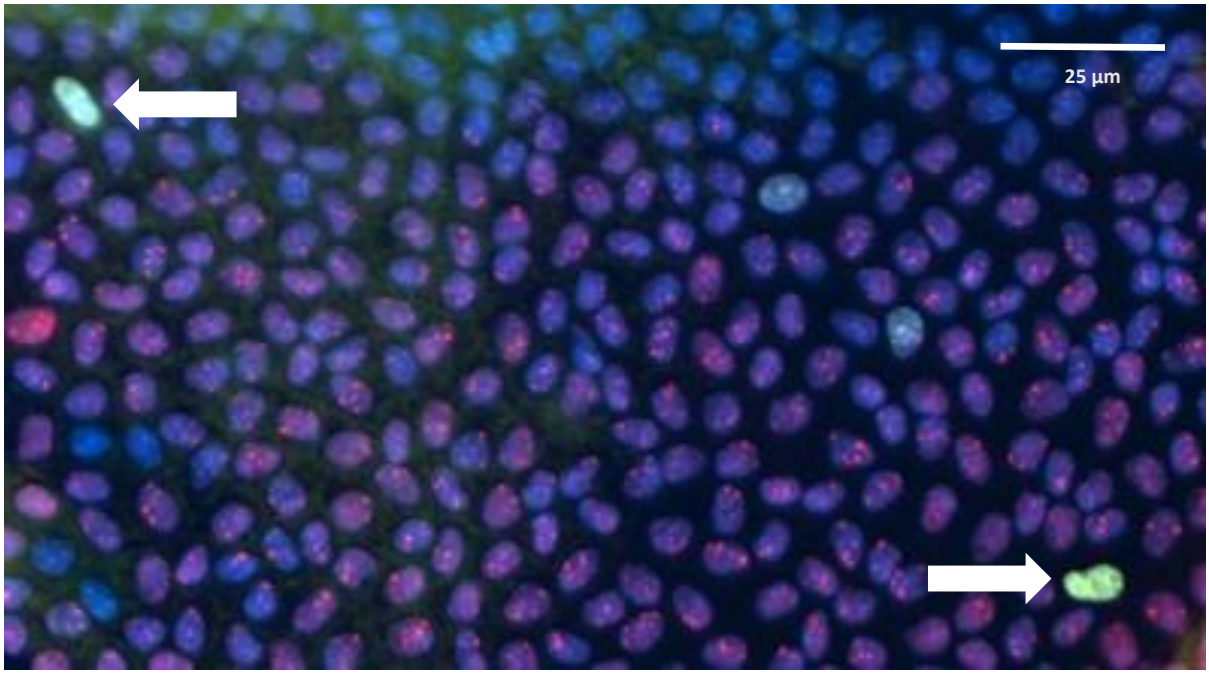

Figure 2.9: Immunofluorescent labelling of both 53BP1 foci (red) with proliferative LECs positive for Ki67 (Green cells, arrowed) alongside a nuclear DAPI counterstain (blue).

2.6 Fluorescence microscopy

Once lens epithelia were prepared as per the protocol as described above, they were imaged at x20 magnification using a Nikon Optiphot 2 fluorescence inverted microscope (located at PHE, Chilton) equipped with separate filters to visualise DAPI, AlexaFluor555 (using TxRed) and

FITC. A minimum of 200 and 350 cells were targeted to be scored for the central and peripheral regions respectively per data point where possible (see chapter 2, section 2.11) (Markiewicz et al. 2015). From these initial data, power and sample size testing was also carried out, based on a significance level of 0.05 and a power of 0.8 to ensure foci were scored in a large enough number of cells for comparative statistics to be applied. Regions of the epithelia were identified based on location within the epithelium and morphological differences. These morphological differences seen under DAPI nuclear staining allowed for the distinction of central region and the more compact and dense peripheral region LECs.

Figure 2.10: Nikon Optiphot 2 fluorescence inverted microscope used during this thesis

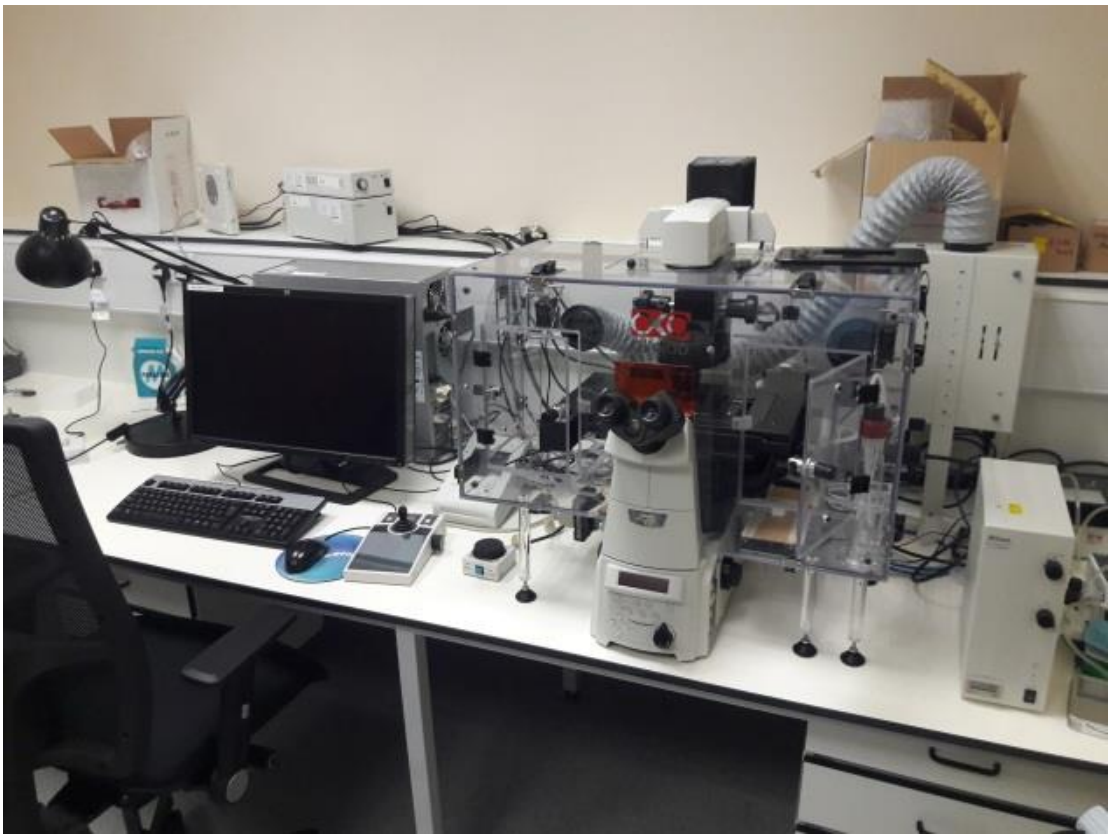

Figure 2.10: The Nikon Optiphot 2 fluorescence inverted microscope used to image the isolated epithelial monolayers of the lens during the studies described in this thesis.

The cellular organisation of the lens epithelium can be divided into regions based upon cell morphology and compartmentalisation of cell proliferation and division. During the studies within this thesis, the central and peripheral regions of the epithelia are analysed separately for comparison. Both regions were identified based on their location within the epithelia and morphological differences which could be seen under fluorescent microscopy (figure 2.10).

2.7 Identification of epithelia region

Using the nuclear stain, DAPI, the central region LECs can be identified as they have a slightly larger nucleus with a fainter DAPI stain. The cells within this region are also less compact than their peripherally located counterparts. Peripheral region LECs are easy to identify, due to the region being narrow in the mouse lens epithelium. They are typically still attached to the meridional rows and are visibly more compact, with a stronger DAPI expression. Figure 2.11 demonstrates this morphological difference clearly. Identification of the two regions is clearly much more straightforward when the whole lens epithelium remains intact (Wu et al. 2015), but experience indicates that this is rarely possible on such small and fragile murine lenses. Nevertheless, each region could be classified sufficiently for analysis during the studies described in this thesis.

Figure 2.11: Comparison of the central and peripheral regions of the lens epithelium

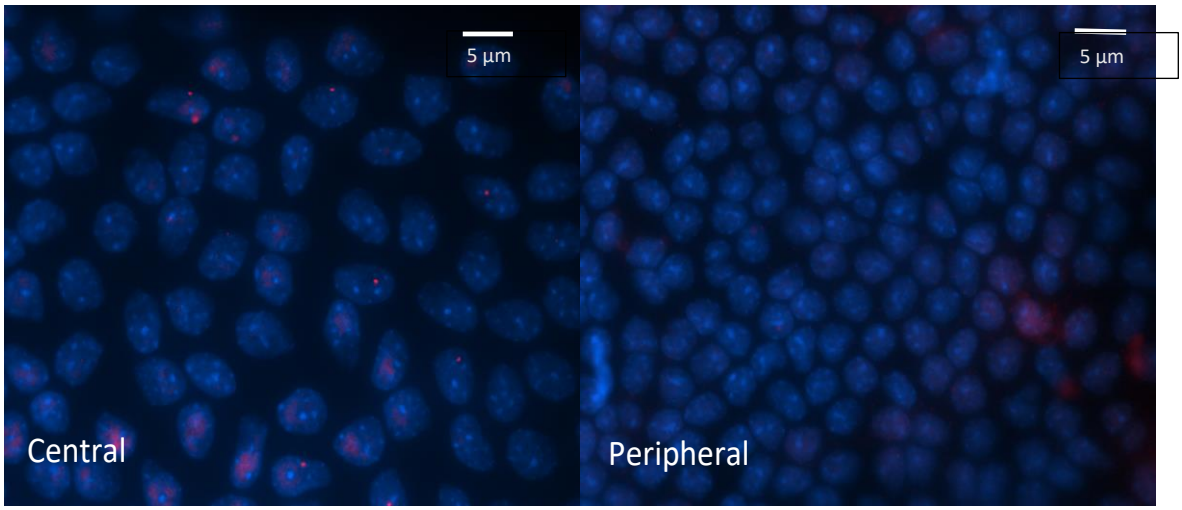

Figure 2.11: DAPI (blue) and 53BP1 foci (red dots) stained LECs from the central and peripheral regions of the epithelial monolayer.

The identification of central and peripheral LECs allowed for the potential differential response of cellular proliferation and DNA damage repair to be analysed using Ki67 and 53BP1 immunofluorescent staining, respectively.

2.8 53BP1 foci scoring and criteria used

RIF (radiation-induced foci) immunofluorescence assays using microscopy provide a well-established and sensitive technique for the quantification of DSBs (Rothkamm et al. 2015). However the assay required some interpretation due to a possible lack of consistency in staining quality and the formation of aggregate formation via non-specific protein staining (Barnard, Bouffler, and Rothkamm 2013). To this end, it is important to have a clear criterion for foci scoring

– particularly important when using automated scoring or image analysis software. Such criteria may include foci size, intensity of the focus signal and general morphology of the foci itself. Non-specific staining can also result in small 'speckles' but these are not 'true' foci. Setting a scoring criterion eliminates these variables, and using a manual scoring method, such as during this study, makes interpretation easier as the eye became trained to recognising true foci. During this study, foci size was not recorded, large or small foci were both recorded as a single focus routinely. Figure 2.12 demonstrates the number of foci scored in some example LECs.

Figure 2.12: 53BP1 foci within central region LECs

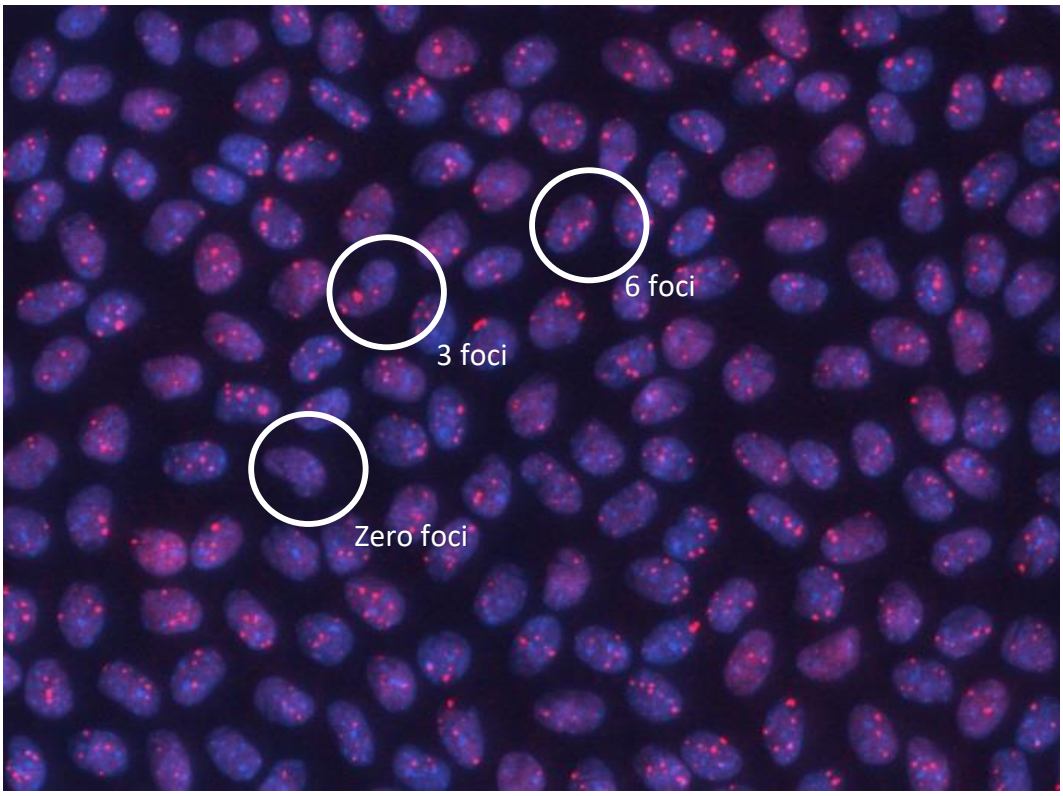

Figure 2.12: Example of 53BP1 scoring in immunofluorescently stained central region LECs.

2.9 Ki67 positive cells

To measure the activity of proliferation, there are a number of well characterised and commonly used markers to identify cycling cells including Ki67, Proliferating Cell Nuclear Antigen (PCNA) and minichromosome maintenance proteins (MCM) (Jurikova et al. 2016). Of these candidate markers, Ki67 was chosen to identify LEC that are undergoing a mitotic phase of cell cycle. Ki67 is commonly used to detect proliferative activity in tumour cells, particularly during breast cancer diagnosis (Denkert et al. 2015; Jurikova et al. 2016; Bosch et al. 2017; Li et al. 2015). Ki67 is a non-histone nuclear cortex protein, involved in the early stages of RNA synthesis (Penault-Llorca and Radosevic-Robin 2017). It was identified relatively recently in 1983, and found to be present

in proliferation cells within a Hodgkin lymphoma cell line (Gerdes et al. 1983). Ki67 is expressed throughout the nucleus of cells during G1, S, G2 and M cycling phases (only absent in G0, or quiescent state cells) (Penault-Llorca and Radosevic-Robin 2017; Miller et al. 2018). Ki67 is one of the most robust biomarkers used in immunohistochemistry, showing consistently strong signalling under an array of fixation procedures (Penault-Llorca and Radosevic-Robin 2017).

During these studies, the recommended scoring of Ki67 was followed, whereby the number of positively stained LECs are expressed as a percentage of positively stained cells against the total number of cells (Penault-Llorca and Radosevic-Robin 2017). Ki67 has recently been demonstrated as a proliferation index marker during a digital image analysis study aiming to improve scoring throughput (Koopman et al. 2018). The method applied to the analysis of proliferating LEC during this study incorporates digital image analysis to then manually scored Ki67 positive cells against total number of cells to produce a proliferation index in the form of a percentage.

2.10 Lifespan eye lens imaging for cataract monitoring

Previously, murine lens opacity analysis relied on the slit lamp method, whereby lenses are graded manually by the operator to distinguish the degree of opacity (Merriam and Focht 1962; Duncan 1981; Barraquer et al. 2017; Chylack et al. 1993). The slit lamp works by a narrow slit of light projected onto the cornea of the eye, allowing several objects to be visualised, including the lens. This image is viewed 'live' through an eye piece and the operator can move the lamp form side to side to look at multiple angles of the lens. The slit lamp is considered one of the most important diagnostic instrument in ophthalmic practice (Blumenthal and Serpetopoulos 1998).

Images can be captured on a computer system. The quantification of lens opacity is less accurate than Scheimpflug; historically lens opacity is then graded on a scale to represent the degree of opacity. Slit lamp tends to be an analysis of back scattering, whereas the visually impairing effects tend to be from forward scattering of light (van den Berg 2018). One of the main problems with this approach to analysing lens opacity comes from individual variability in grading, and also that there is no standardised approach to grading, with a number of different scales being used across operators including, for example, Merriam-and-Focht (Merriam and Focht 1962), LOCS III (Chylack et al. 1993) and more recently BCN 10 (Gali, Sella, and Afshari 2019; Barraquer et al. 2017). Cataract grading systems have evolved over the decades, which can make comparisons to retrospective studies more difficult (Gali, Sella, and Afshari 2019). The many scoring methods used to classify opacities using slit lamp-based observations have made it difficult to compare different studies and different species (Eaton et al. 2017). Slit lamp settings are also not standardised, with image quality and therefore analysis deteriorating substantially when settings of the device are not

optimised (Blumenthal and Serpetopoulos 1998). Image quality and therefore lens opacity grading are directly related to ocular settings on the device (Blumenthal and Serpetopoulos 1998).

Murine models are the most commonly used in-vivo tool for IR-induced cataractogenesis investigation, however other rodents including rabbits (Cogan and Donaldson 1951; Worgul, Medvedovsky, and Merriam 1981) and rats (Kocer et al. 2007; Zintz and Beebe 1986) have often been used. It was in rats that the first standardised grading system for classifying cataract formation was developed (Merriam and Focht 1962).

Increased incidence of cataract following IR exposure have been observed in 'radiosensitive' ATM homozygous and heterozygous mice (Worgul et al. 2005; Worgul et al. 2002; Hall et al. 2006) as well as Mrad9 haploinsufficient mice (Kleiman et al. 2007). These studies all report that cataract begin to form at around 4 weeks post-exposure to 0.5 Gy IR. These cataract were graded using the Merriam and Focht (Merriam and Focht 1962) cataract grading scale by using the aforementioned slit lamp. These studies contributed towards the lens dose limit threshold recommended by the ICRP of 0.5 Gy for acute exposures (Stewart et al. 2012)

2.10.1 The Scheimpflug imaging system

The Scheimpflug imaging system became an established technique for measuring lens opacity and has demonstrated a high-throughput capability in murine cataract studies thanks to recent improvements in image analysis, as well as being used specifically in IR-induced cataract studies (Puk, de Angelis, and Graw 2013; Dalke et al. 2018). The technique was developed for imaging the anterior segment of the eye, with the ability to image starting at the anterior cornea, and continuing through to the posterior of the lens surface (Rosales et al. 2010). The system works by the imaging equipment projecting a narrow slit of blue light onto the eye (produced by a vertical LED 475 nm wavelength in the Pentacam system used in this study). The resulting image formed by the computer can visualise the lens due to a large depth of focus captured due to the tilted image plane (Rosales et al. 2010).

2.10.2 Aim of this study as a modification from previous studies

The aim of the Scheimpflug imaging study was to detect radiation-induced opacities and possible cataract in mice exposed to both 0.063 and 0.3 Gy/min dose-rates of IR, delivering doses of 0.5, 1 and 2 Gy (Table 2.1). These doses and dose-rates were identical to the exposures observing the DNA damage and repair responses and proliferation effects of LECs 4 and 24 hours post-exposure (see chapter 4). A relationship between early radiation-induced effects to DSB repair and cellular proliferation in the LECs, and cataract progression and manifestation *in vivo* in these mice

can identify a possible link between the two end points and identify whether early effects in the LECs can be used as a predictor of cataract manifestation. Due to the higher radiation doses and dose-rate used here compared to a recent study by (Dalke et al. 2018), a shorter 'lifespan' period is used in which to monitor the mice. In this study, monthly imaging on both lenses of each mouse was performed for 18 months post-irradiation, reduced from 24 months (Dalke et al. 2018) to increase survival. The effect of dose-rate was investigated by delivering each dose at two dose-rates. The use of a more 'radioresistant' strain, the C57BL/6 (Newman et al. 2014), compensates for the increased doses (1 and 2 Gy). The strain has shown higher survival rates following 1 Gy and greater doses compared to CBA/Ca and 129S2 strains, essential qualities needed during the 18 month observation period (Roderick 1963) ensuring maximal lifespan. Previous studies investigating the effects of IR on the lens demonstrate the suitability and reproducibility of this strain (Barnard et al. 2018; Markiewicz et al. 2015; Wolf et al. 2008). C57BL/6 mice have black fur and a higher natural lens transparency, both qualities enhance the effectiveness of Scheimpflug imaging and analysis (Puk, de Angelis, and Graw 2013).

A total of 120 C57BL/6 female mice were used during this lens opacity lifespan monitoring study, followed for 18 months (first observation starting at 4 weeks post-irradiation of ^{60}Co gamma radiation).

Table 2.3: Numbers of mice used for each exposure group for lifespan imaging (chapter 6)

Dose-rate	Control	0.5 Gy	1 Gy	2 Gy
0.3 Gy/min	30	10	10	10
0.063 Gy/min	30	10	10	10

Table 2.3: Number of mice used for each dose and dose-rate. Note that 10 control animals were allocated to each dose and sham exposed alongside

The group sizes for exposures were dictated by using existing data from a similar study that used a maximum dose of 0.5 Gy (Dalke et al. 2018), based on formal post-hoc power analysis for a power of 80%. This determined that group sizes of n=19 lenses or 10 mice would allow detection of a statistically significant difference of 2% or 5% transparency in the lens, respectively ($p \leq 0.05$). In this study, n=10 mice were used, with the results of 20 lenses per group pooled together.

2.10.3 Procedure for imaging

Prior to lens imaging, the pupils were dilated using a mydriatic, 1% w/v atropine eye drops (Martindale Pharma, UK). One drop of atropine was administered to each eye by 'scruffing' the

mouse, which pulled back the skin between the shoulder blades and head reducing the mouse's ability to close its eyelids. The drop was gently placed on the cornea and any excess atropine was removed using a tissue. The mouse was then returned to the home cage and left approximately 10 – 15 minutes prior to imaging to allow sufficient dilation of the pupil.

To reduce stress, and as per local ethical considerations (Home Office licence PA66E1512 and AWERB committee), mice were given a short-term general anaesthetic prior to imaging. The mice were placed in a clear Perspex chamber that allowed them to be constantly observed. Using medical grade oxygen (BOC, UK), the isoflurane liquid was released from the precision vaporiser (Fortec, UK). Each mouse was observed until the rate of breathing had sufficiently slowed. The time taken was observation dependant, but approximately 2-3 minutes was usually sufficient. The mouse was then carefully moved to a polystyrene platform fashioned to facilitate imaging using the Pentacam (see figure 2.13). Marked on the platform was a pre-calibrated distance from the camera which allowed the eye to be quickly orientated and positioned. The 475 nm slit of light was set to the vertical position (figure 2.13), and the mouse eye was lined up so that the slit of light sat in the centre of it. To ensure optimal focus of the eye, the software gives adjustment directions to centre the eye.

Figure 2.13: Pentacam Oculus Scheimpflug system

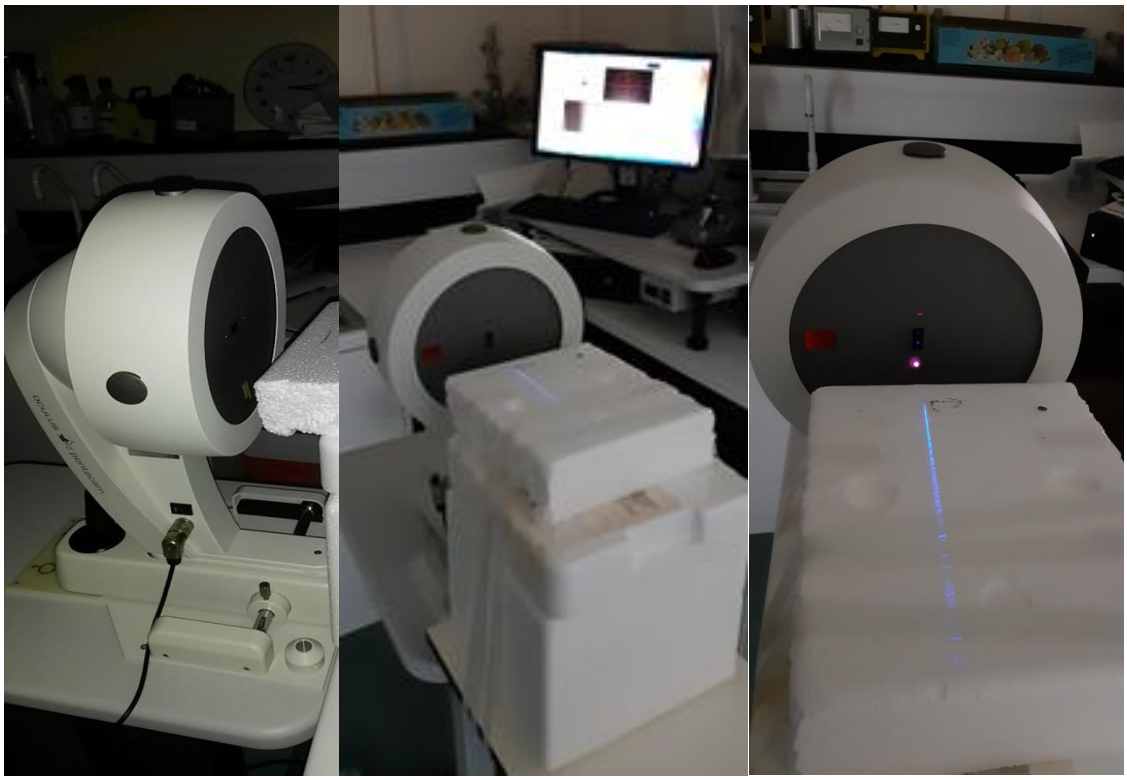

Figure 2.13: Pentacam by Oculus Scheimpflug system, with homemade polystyrene platform for quick orientation of the mouse eye to the camera. The 475nm blue slit of light is visible, allowing for quick orientation of the eye in preparation for imaging.

Figure 2.14: Lens densitometry measurements

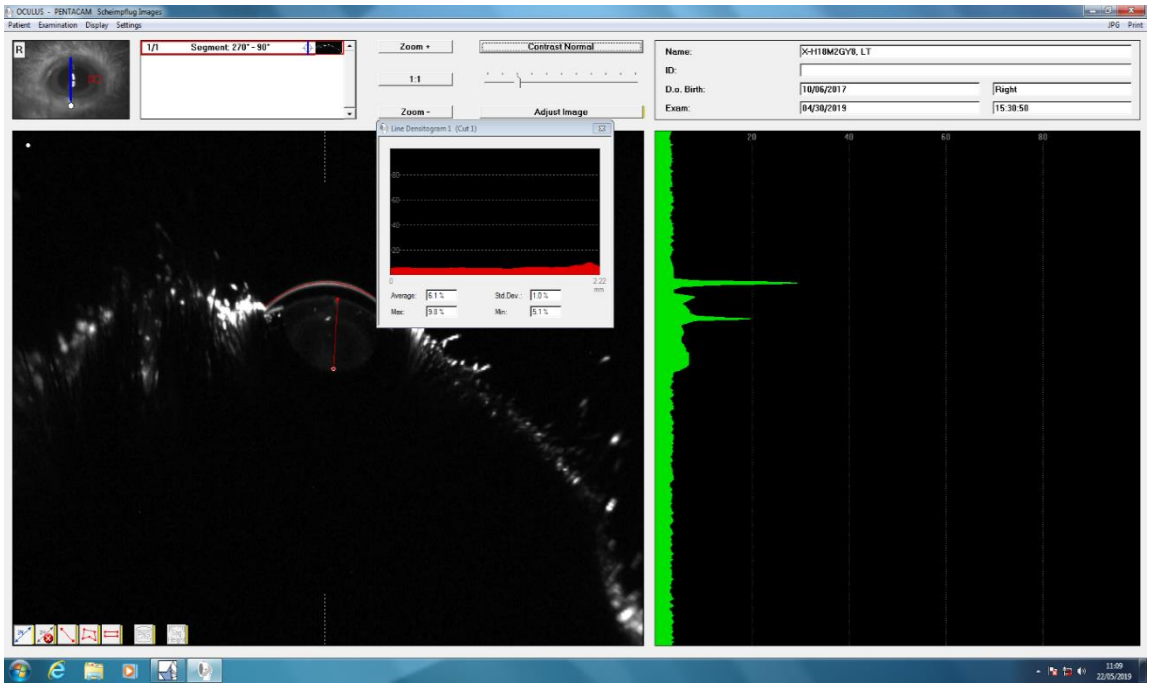

Figure 2.14: Mouse lens densitometry measurement taken at 17 months post-exposure to 2 Gy γ-radiation delivered at a dose-rate of 0.3 Gy/min.

This study used a Pentacam digital camera system (Oculus, Germany) which is essentially the same as used in previous studies first described by a research group at the German Mouse Clinic (Fuchs et al. 2011) and their advice was sought on the best system to install for this project at Public Health England (Fuchs et al. 2011; Dalke et al. 2018; Puk, de Angelis, and Graw 2013). Each mouse was entered into the system as a 'patient', and once added, the operator could re-select for each new monthly image, to build up a library of images throughout the 18 month study period. The software allows the operator to select whether the left or right eye is imaged, therefore during the period in this study, two observations are performed each month, one for each eye. The Images had to be captured manually as the automatic start function was not possible when imaging such small eyes as per previous studies (Fuchs et al. 2011). Prior to starting the Scheimpflug imaging for this study, training was provided by Dr Claudia Dalke at Helmholtz Zentrum, Munich, Germany. The protocol used in the present study was designed by Dr Dalke's research group, described in a previous lifetime study of the lens in mice (Dalke et al. 2018). Images must be captured in a darkened room, with all lights turned off and windows covered to avoid reflection off the cornea. Inevitably some glare remained due to the computer monitor and background light. This often results in a small white dot in the lens (figure 2.14).

2.10.4 Interpretation of measurements

The Pentacam system includes a software package from the manufacturer, which was used for the interpretation and analysis of the images. The software has many functions that can be performed, all optimised for the (much larger) human eye examinations for which it is calibrated. When a suitable image was obtained from the mouse eyes in this study, the function 'densitometry along a line' was used to select the region of the lens to be analysed for lens opacity. Firstly, the contrast of the lens was adjusted so that the border of the lens is visible (as the lens is transparent). This tool allows a red line to be plotted across the lens, from anterior to posterior surfaces, and it was along this line that the software calculates the measurement. The line was drawn approximately through the middle of the lens, avoiding the white dot caused by reflection (figure 2.14). Once a line has been drawn across the lens, several values are presented by the software. The mean, maximum and minimum values were recorded for each image following this analysis. These values represent the percentage opacity of the lens.

2.11 Statistical analysis

2.11.1 Normality testing

Normality testing is required when a sample size is larger, and are certainly an important requirement when using ANOVA analysis, and other parametric tests, as this method relies on normal distribution of data. Therefore, normality testing can confirm this, allowing for accurate and reliable conclusions to be drawn based on the data set and variables used (Ghasemi and Zahediasl 2012).

All data were tested for normality using Anderson-Darling testing, which compares the empirical cumulative distribution function (ECDF) of each data set used within this project with a distribution expected assuming the data were normal. This testing produces a p-value which can indicate where the data are significantly normal or not. Anderson Darling testing is also performed to confirm data are normal (Nelder 1989). All data are normal unless stated otherwise. All data generated and used for analysis within this project showed no evidence of being non-normally distributed.

The number of mice required to perform the various studies and experiments during this thesis was substantial, thus generating a large amount of data, and in varying formats. Regardless of the endpoint, each experimental design aimed to identify the influence of dose, rose rates, strain or time-point post-exposure. These sections of this chapter outline and explain the justification for the use of the various statistical methods that were applied to the data to interpret the significant

effects and interactions that were identified. All statistical analysis of the results presented during the studies described in this thesis were performed using Minitab® 17 software.

2.11.2 Analysis of Variance

General Linear Model Analysis of Variance (ANOVA) is one of the most commonly used statistical tests amongst scientists, used to compare the difference between the effects of three or more levels of a factor, including any 'noise' or error (Ip 2007). If the ANOVA does reveal a significant difference, based on p-value, then further post-hoc testing can reveal where this significance lies (for example using Tukey pair-wise analysis). Tukey pairwise comparisons (Tukey 1949) can identify which factor levels are significantly different from others (Currell and Dowman 2009). Tukey pairwise comparisons can compare all possible pairs of means to determine where the differences from a large ANOVA output lie. The ANOVA is essentially an analytical tool for investigating the sources of variation, or variability of the data, that might be contributing to the final variations within the experimental data (Currell and Dowman 2009; Fry 1999) such as the data generated during this project. The ANOVA model makes some assumptions, including the independence of cases. This assumption of the model is used to simplify the statistical analysis of data. The model also assumes normality of the data, that is that the distribution of the residuals is normal, and the equality of variances. Unless otherwise stated, there was no evidence of departure from normality or significant deviation from the other assumptions detected, thus making ANOVA appropriate for use in statistical analysis during the studies described in this thesis.

Therefore, given the above information, ANOVA analysis was used throughout this thesis, as it represents the most appropriate method for analysing the data generated.

2.11.3 Normalised means and error

Where stated in studies, means were normalised against the sham-irradiated controls and then also presented with normalised standard errors which were calculated by adjusting the original standard errors using the sum of squares method. The exact method of normalisation in each case where it has been used is stated in the each of the relevant results chapters.

2.12 Power calculations

The power of an experiment is essentially a measure of how successful the experiment(s) was at confirming the existence of a significant effect within the factors of the experimental design (Currell and Dowman 2009). Power calculations, or sample size calculations, can therefore give the researcher a target or minimum quantity of a factor to be analysed to accept or reject a hypothesis.

The use of power calculations during this the studies making up this thesis have been used in two distinct ways. The number of animals required per experimental group during both the short-term investigation of DNA damage and repair and the effects of IR on proliferation, as well as the longer term Scheimpflug imaging study. Power calculations can also be performed pot-hoc at the end of the study, to confirm whether the power is sufficient to accept significant findings. This is often a beneficial practice due to initial power calculations performed prior to the experiment can not necessarily be based on exactly similar data, particularly when the researcher is trialling a new technique or method, as has been the case during these studies.

Power calculations are also an important feature in animal research. In the UK, the application of the 3R's (replace, refine and reduce) must be demonstrated to all projects involving animals where possible. Power calculations, as used during this study, have dictated the minimum sample size needed for significance of results with 5% chance of type 1 error (false positive), and 20% chance of type 2 (false negative) error (giving power at 80%), thus reducing the number of animal used and refining the experiment.

2.12.1 Scoring of 53BP1 foci

For the analysis of DNA damage and repair foci, a minimum of 200 and 350 cells were needed to be scored for the central and peripheral regions respectively per data point. From these initial data, power and sample size testing was also carried out, based on a significance level of 0.05 and a power of 0.8 to ensure foci were scored in a large enough number of cells for comparative statistics to be applied.

2.12.2 Scoring of Ki67 positive LECs

The quantification of LEC proliferation was performed by using the biomarker Ki67. The number of positive cells was converted into a percentage of cells in each region, termed a proliferative index. Unlike with DNA damage, there were no previous data of Ki67 positive cell frequency scored within the LECs, therefore power calculations were performed once data had already started to be collected. 2 sample t-test sample size calculations were performed based on a power of 0.8, with results indicating in most cases the number of lenses analysed should be sufficient to detect any significant effect of the factors investigated (dose, dose-rate, region and time).

2.12.3 Lifespan Scheimpflug imaging cohort

As well as short-term investigation of IR-induced DNA damage and proliferation up to 24 hours post-exposure, female C57Bl/6 mice were kept and observed over an 18 month period. During this period, Scheimpflug imaging of the lens of each mouse was performed, a technique which allows the quantitative analysis of the lens density and therefore offers an unbiased statistical evaluation. As previously described, this observation was carried out on each mouse monthly, to track the appearance and development of cataracts. Power calculations confirmed group sizes of n=19 (referring to individual lenses) or 10 mice allow detection of a statistically significant difference of 2% or 5% transparency to be observed, respectively ($p \leq 0.05$).

3. Low dose DNA damage and repair response across four murine strains

The aim of this chapter was to investigate the low-dose response of LECs to IR and identify a potential radiosensitivity. There was a need to identify a suitable model to investigate the biological effects in the LECs at such low doses. Genetic effects are thought to be of greater influence following low dose rather than high dose IR exposure (Kleiman et al. 2007). Appendix A accompanies this chapter.

3.1 Strain dependency

To investigate the influence of strain, four inbred mouse strains were investigated; radioresistant C57BL/6 mice were exposed alongside radiosensitive 129S2, CBA/Ca and BALB/c mice (Newman et al. 2014; Darakhshan et al. 2006; Peng et al. 2009; Roderick 1963; Wolf et al. 2005; Makharashvili and Paull 2015; Patel et al. 2016; Rithidech, Cronkite, and Bond 1999; Boulton et al. 2001; Verbiest, Bouffler, and Badie 2018; Hamasaki et al. 2007), as previously identified (see introduction; 1.6.3, 1.6.3.1) and analysed as per chapter 2 (Materials and Methods). Mice were sacrificed at 1, 2, 4 and 24 hours post-exposure and the lenses fixed and immunofluorescently stained for 53BP1 foci as per chapter 2: Materials and Methods.

3.2 Spontaneous 53BP1 foci

To observe any low dose response of LECs to DNA damage and repair, understanding the natural baseline or spontaneous background levels of 53BP1 is important. The baseline 53BP1 foci levels for all four inbred strains were compared in table 3.1. Post-hoc power analysis revealed the need for larger groups than expected.

Table 3.1: Baseline mean 53BP1 foci/cell in LECs found in all strains

Strain	Central region mean foci/cell ± SE	Peripheral region mean foci/cell ± SE
C57BL/6	0.004 ± 0.002	0.002 ± 0.002
CBA/Ca	0.039 ± 0.019	0.007 ± 0.007
129S2	0.044 ± 0.044	0.011 ± 0.011
BALB/c	0.010 ± 0.005	0.027 ± 0.008

Table 3.1: The mean baseline 53BP1 foci per cell from sham-irradiated control C57BL/6, CBA/Ca, 129S2 and BALB/c inbred mice. Both the central and peripheral regions of the epithelium were analysed separately with standard error.

Baseline 53BP1 foci levels revealed an extremely low frequency of spontaneous foci particularly in the C57BL/6 strain, demonstrated in table 3.1 (see also table A.1), with mean number

of 53BP1 foci per cell being 0.004 ± 0.002 and 0.002 ± 0.002 for central and peripheral epithelia regions respectively. The other three strains investigated; BALB/c, CBA/Ca and 129S2; showed greater mean spontaneous 53BP1 foci/cell compared to C57BL/6 mice in the central lens epithelia region. The central region appeared to demonstrate higher values of mean foci/cell compared to the peripheral region in all strains except for BALB/c. However, despite these observations, no significant differences between strains or regions ($p > 0.05$) was observed.

3.3 Low dose exposures

The effects of low IR doses of 10 and 25 mGy exposures were analysed at 1, 2, 4 and 24 hours post-exposure in all four strains of mice and are demonstrated in figures 3.1 and 3.2 respectively (see Appendix A).

Figure 3.1: Mean 53BP1 foci/cell in LECs of four mouse strains exposed to 10 mGy 1 – 24 hours post-exposure

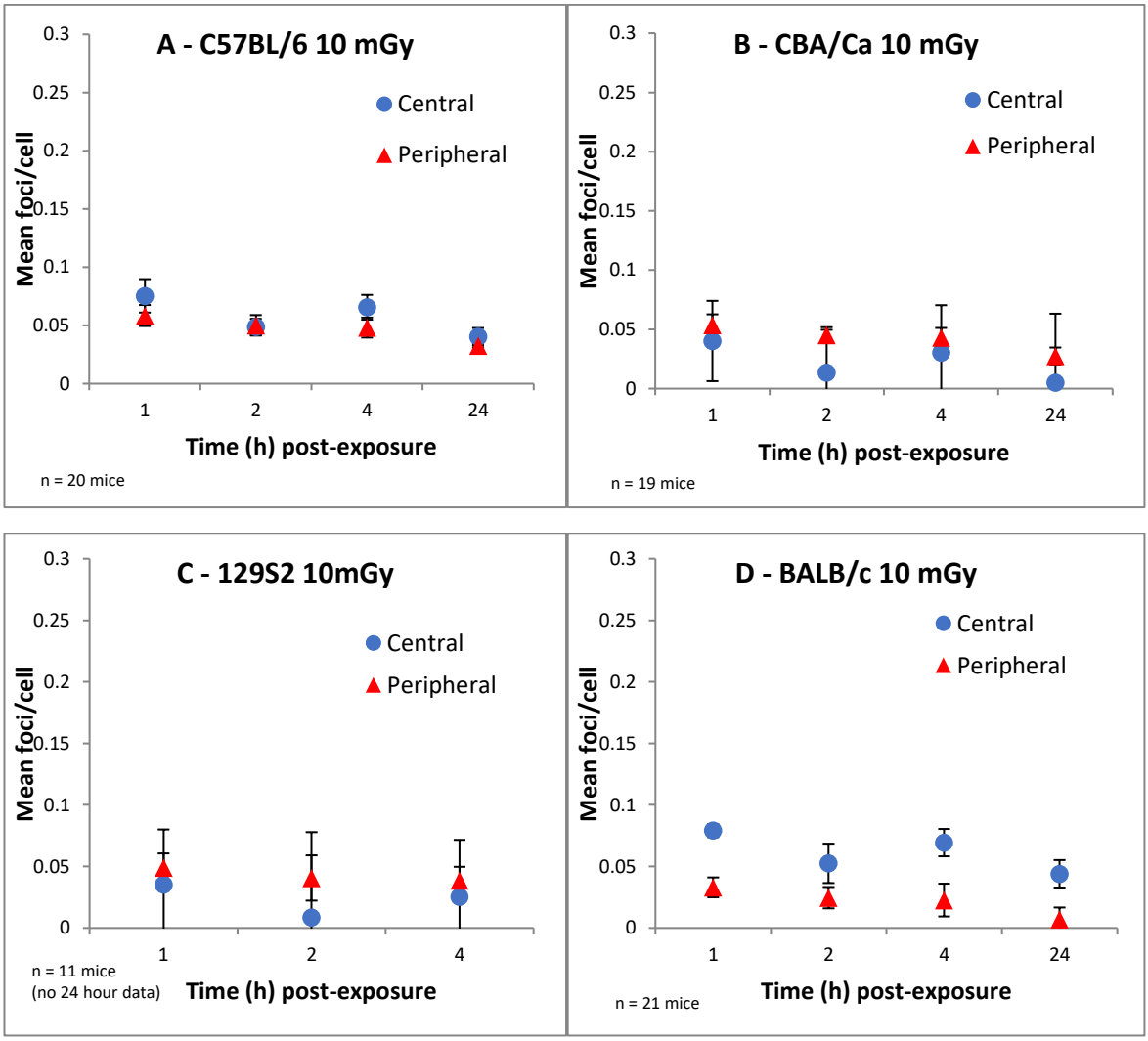

Figure 3.1: Mean 53BP1 foci/cell from the central and peripheral regions of the lens epithelia of C57BL/6 (A), CBA/Ca (B), 129S2 (C) (1 – 4 hours only) and BALB/c (D) mice exposed to 10 mGy x-radiation up to 24 hours post-exposure. See appendix A for data set.

Figure 3.2: Mean 53BP1 foci/cell in LECs of four mouse strains exposed to 25 mGy 1 to 24 hours post-exposure

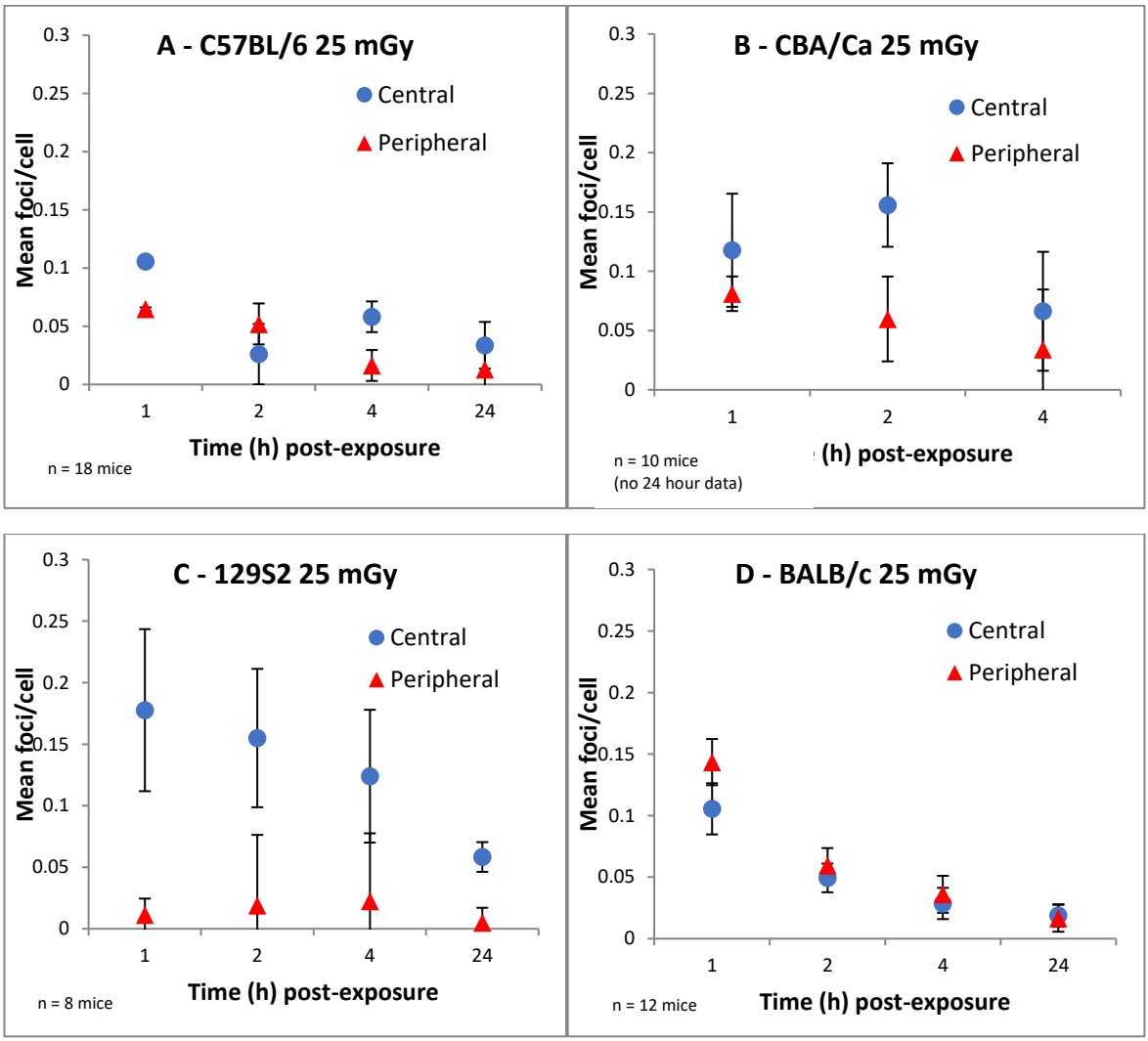

Figure 3.2: Mean 53BP1 foci/cell from the central and peripheral regions of the lens epithelia of C57BL/6 (A), CBA/Ca (B), 129S2 (C) and BALB/c (D) mice exposed to 25 mGy x-radiation up to 24 hours post-exposure. See appendix A for data set.

Figures 3.1 and 3.2 show the comparison of 53BP1 mean foci/cell frequencies in all four strains up to 24 hours post-exposure. The samples were normalised against the sham-irradiated controls (see Materials and Methods; 2.14) and then also presented with normalised standard errors which were calculated by adjusting the original standard errors using the sum of squares method. There was a noticeable difference in mean 53BP1 foci/cell frequency between both central and peripheral regions of the epithelia, with region of the lens epithelium statistically significant (ANOVA $p = < 0.001$). Both CBA/Ca and 129S2 strains showed a greater frequency of mean 53BP1 foci/cell expression in the central compared to the peripheral region of lens epithelium

at 25mGy (figure 3.2). It is noteworthy that C57BL/6 and BALB/c demonstrated the smallest error in each region across most dose and time points (figures 3.1 and 3.2).

All four strains compared demonstrated statistically significant different number of radiation-induced 53BP1 foci/cell from each other (ANOVA $p = 0.002$). Both BALB/c and C57BL/6 demonstrated increased numbers of 53BP1 foci/cell one hour post-exposure when compared to two hours following 25 mGy (figure 3.2), however this difference was less noticeable following 10 mGy (figure 3.1). Tukey pairwise comparisons revealed that both C57BL/6 and CBA/Ca strains were significantly different from one another ($p = 0.003$) in terms of 53BP1 foci/cell, but neither different from 129S2 or BALB/c strains. No statistically significant difference was observed between sham and 10 mGy, although the 25 mGy dose was significant from control ($p < 0.001$) and from 10 mGy ($p < 0.002$). The central region of the lens epithelium showed significantly different mean 53BP1 foci/cell compared to those of the peripheral region ($p < 0.001$). Further comparisons using this analysis revealed only control and 25 mGy 1 hour post-exposure is significantly different from all other time points regarding mean 53BP1 foci/cell ($p \leq 0.01$).

3.4 Residual un-repaired 53BP1 foci

To consider whether repair kinetics differed between strains, the percentage of un-repaired DSBs were calculated (Figure 3.3), using one hour time point as maximal foci induction as this is the earliest post-exposure time point used in this study (the closest approximation of maximal foci presentation within this study, although foci occur much earlier, within minutes of exposure). Percentages greater than 100% represent greater mean 53BP1 foci/cell at later time points, particularly noticeable in the 129S2 strain (figure 3.3). Standard error is given (as a percentage) to highlight, particularly in this 129S2 stain, the large degree of variation, possibly accounting for increased foci frequencies at later time points post-exposure.

Figure 3.3: Percentage of residual un-repaired 53BP1 foci in all strains up to 24 hours post-exposure to 10 and 25 mGy X-irradiation (normalised to control/sham-irradiated)

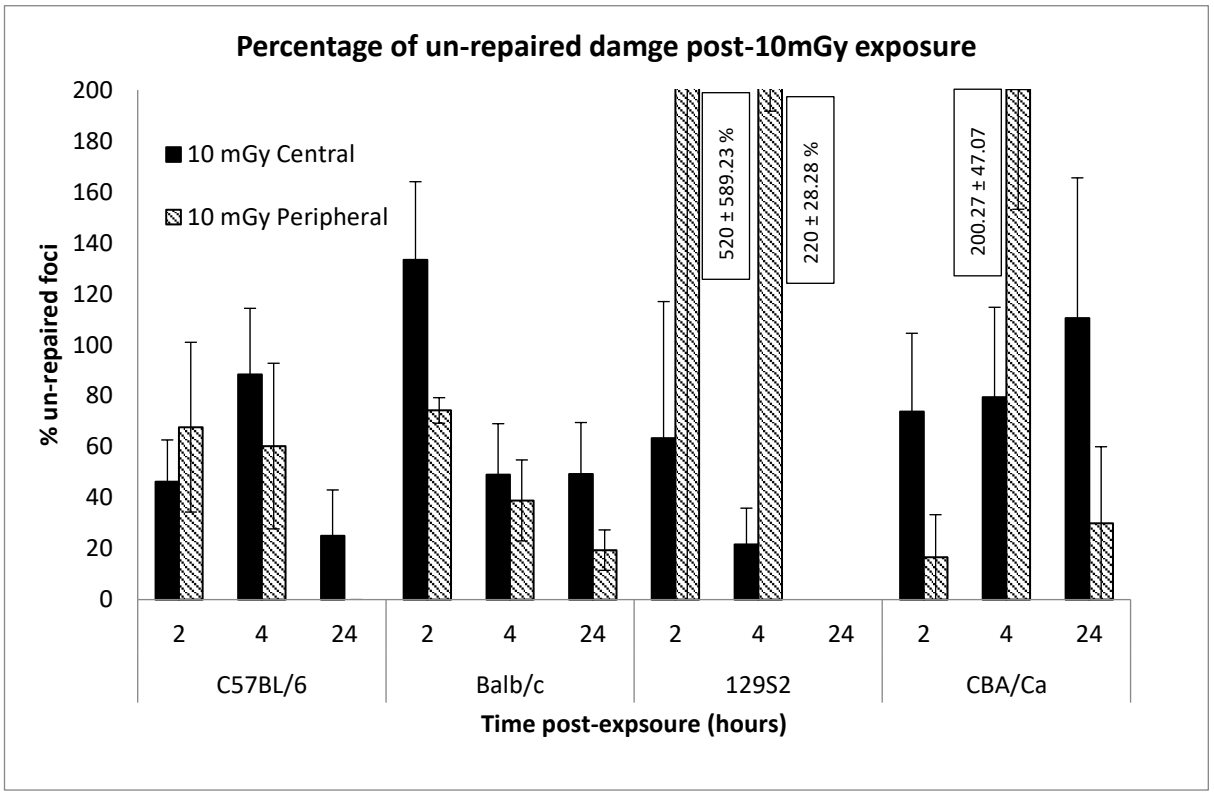

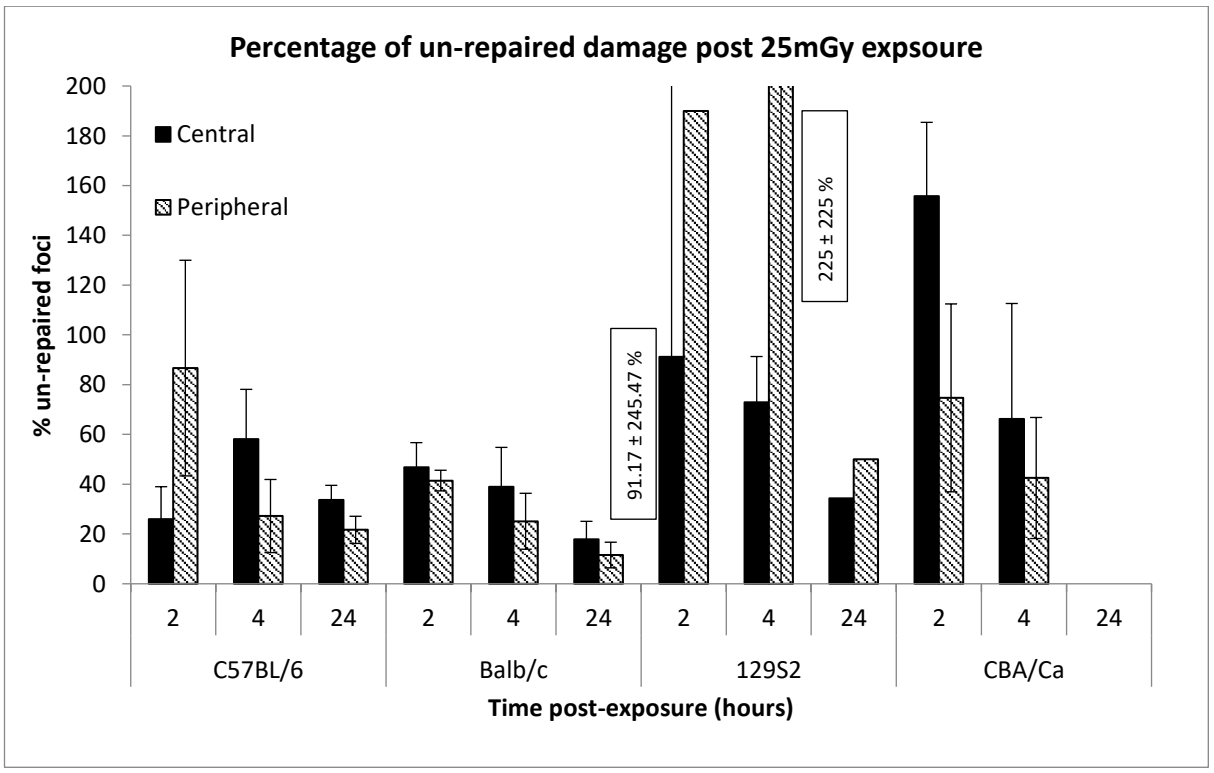

Figure 3.3: Percentage of unrepaired 53BP1 foci in four inbred strains of mice up to 24 hours post-exposure to 10 and 25 mGy x-radiation normalised to control/sham irradiated mice. Error bars represent percentage standard error.

From the first one-hour time point the residual or unrepaired foci at the latter time points were calculated. ANOVA indicated a statistical significance of strain only (p=0.020). More consistent rates of repair were observed in the C57BL/6 and BALB/c strains compared to the other strains, and this was noticeable in Figure 3.2 particularly at 25 mGy, where 24-hour post-exposure mean 53BP1 foci/cell counts were close to baseline. Interestingly the BALB/c strain showed a higher rate of repair at 25 mGy dose but showed a much lower rate of repair after 10 mGy exposures. At 24 hours post exposure to 10 mGy, central region LECs had 0.044 ± 0.011 foci/cell remaining compared to 0.018 ± 0.009 foci/cell post-25 mGy exposure at the same time point, where baseline frequencies were 0.01 (Figure 3.1). This was not seen in the C57BL/6 strain, with similar numbers of unrepaired foci/cell at both 10 and 25 mGy exposures. C57BL/6 showed a greater number of residual foci/cell in the peripheral compared to the central region of the lens epithelium. BALB/c had a higher number of residual foci/cell in the central compared to the peripheral region at 10 mGy only, with the difference between regions negligible at 25 mGy. 129S2 mice showed an extremely high percentage of un-repaired foci/cell in the peripheral region at both doses, remaining for up to 4 hours post-exposure.

3.5 Discussion

The aim of this chapter of the thesis was primarily to identify suitable inbred murine strain(s) that can be used in the investigation of low dose radiation effects in the lens epithelium. DNA DSB repair marker 53BP1 was used to analyse the damage response to IR in four murine strains. Inbred strains were of interest as these represented a cost effective and efficient means of investigating such effects.

All mice used throughout these investigations were irradiated whole body *in vivo* at 10-weeks of age, which has been estimated as the earliest age at which the lens has developed to adulthood (Bannik et al. 2013). The methods employed here (the isolation of lens epithelia and flat-mounting of the monolayer) offered an experimental approach for *in vivo* analysis of the lens and LECs compared to primary cell culture performed *in vitro* (Bannik et al. 2013) as well as histological techniques which cannot always be achieved on mature lenses, albeit methodologies are subject to the chosen endpoint. The lens epitheliums were fixed and analysed at several time points post-exposure, allowing for both early repair and residual damage to be captured (also referred to as fast and slow repair kinetics).

The data strongly suggested that the BALB/c strain demonstrates a lens-specific radio-sensitivity at low doses. Figures 3.1 and 3.2 support this observation best, showing a clear induction and repair kinetics of 53BP1 foci/cell at one hour, gradually reducing towards 24 hours. The inter-

individual variation in some of the strains, particularly the 129S2 and CBA/Ca, indicated that mice even of the same inbred strain and received from the same supplier may suggest that these strains are not as genetically identical to one another as expected, raising further potential concerns if they were to be compared to the same strain from a difference supplier.

The LECs located in the central region of the epithelial monolayer appeared to repair 53BP1 foci at a faster rate than those induced in the peripherally located LECs at one hour post-exposure within the C57BL/6 strain at both doses of IR, but this was not the case in CBA/Ca strain mice (see figure 3.3). This region of the monolayer has shown sensitivity to oxidative stress compared to the peripherally located counterparts when exposed to hydrogen peroxide (Reddan et al. 1995). IR-induced damage generates reactive oxygen species (ROS) which in turn cause secondary oxidative damage in the lens, inducing LEC apoptosis demonstrated *in vitro* (Song, Guo, and Bi 2018). Therefore, it is possible that the increased response observed in the central region LECs may be influenced by this. Furthermore, no observable reduction in foci between two and four hour time points was seen, suggesting a slower or delayed repair response at this dose. This observation was evidenced in the CBA/Ca strain, due to the lower induction of repair in the initial one hour time point. Repair kinetics appeared closer to linear with a steady decline in residual foci presentation from 1 hour continuing through to 24 hours post-exposure. This was an interesting observation, perhaps contradicting findings in other tissue types. The central LECs, as mentioned earlier, comprise largely of metabolically active but quiescent cells, containing DNA at a more relaxed state (Kallingappa et al. 2016) leaving them more sensitive to damage during IR exposure. DNA at such a relaxed state should result in less repairable DNA DSBs following exposure (Lomax, Folkes, and O'Neill 2013). This would support the initial increase in DSBs at one hour, but these would be expected to persist at 24 hours which was only the case for BALB/c mice exposed to 10 mGy.

C57BL/6 are one of the most commonly used murine strains in IR related studies reported in the literature, many of which reported them to be radio-resistant compared to other strains (Newman et al. 2014). The C57BL/6 mice have shown resistance to radiation-induced DNA damage during comparison to the CBA/Ca strain of mice (Darakhshan et al. 2006; Peng et al. 2009). C57BL/6 have shown greater survival rates following 1 Gy and higher doses of IR when compared to CBA/Ca and 129S2 strains, both used in this study due to being more radiosensitive (Roderick 1963). This property made the C57BL/6 strain particularly useful positive-control for higher dose investigations by improving the likelihood of maximum lifespan, needed for observable cataract due to the long latency for manifestation, which is a drawback of many mouse studies due to the relatively limited lifespan of mice. The C57BL/6 strain had previously been used specifically in lens research (Wolf et al. 2008; Markiewicz et al. 2015) for radiation induced cataract as well as also being demonstrated

as the most suitable strain for long term lens imaging due to a higher transparency of the lens during Scheimpflug imaging (Puk, de Angelis, and Graw 2013). At the time of writing, there were limited reports referencing the natural incidence levels of cataract in these mice strains, apart from the widely used C57BL/6 strain, but even these had a variable incidence (Richard S. Smith 1995) making the effects of low dose IR-induction difficult to study long term. The C57BL/6 mice showed a strong age-related tendency to develop cataract, and so were thought to be a relevant human cataract model due to similar cataract incidence documented (Banks et al. 2015).

Besides the C57BL/6 strain, the other three strains within this study were more classically radiosensitive. 129S2 mice are known to carry a nonsynonymous single nucleotide polymorphism (nsSNP) located within the C-terminal interacting protein, CtIP, gene, a crucial component of the DNA DSB repair response (Makharashvili and Paull 2015). These 129S2 strain of mice therefore would be expected to be deficient or at least hindered in DNA repair capabilities in general following DSB induced by IR. This was supported by recent findings (Patel et al. 2016) which identified this strain as being radiosensitive after being observed to have a reduced lifespan following x-irradiation exposure. They also demonstrated increased frequencies of complex chromosomal aberrations after exposure, supporting the strain's radiosensitive status (Patel et al. 2016).

The CBA/Ca mice used in this study also demonstrate a similar post-irradiation survival rate as 129S2 strain (Patel et al. 2016). CBA/Ca mice had been documented as having an extremely low frequency of spontaneous tumour development (Rithidech, Cronkite, and Bond 1999; Brown et al. 2015). They also showed susceptibility to radiation-induced acute myeloid leukaemia (rAML) (Boulton et al. 2001). The BALB/c strain had been previously described as radiosensitive due to a reduced lifespan following IR exposure (Roderick 1963; Mukherjee, Sainis, and Deobagkar 2014; Newman et al. 2014). This strain contains polymorphisms in the gene known as Prkdc (encoding with DNA-dependent protein kinase, catalytic subunit: DNA-PKcs); consequently, DNA repair via non-homologous end joining is hindered in this strain (Okayasu et al. 2000). Interestingly, it is also the DNA-PKcs that is undetectable in severe combined immune deficiency (scid) mice, with this deficiency thought to be a contributing factor to the radiosensitivity of the strain (Danska et al. 1996). However, the effect of this deficiency in the BALB/c compared to scid mice was clearly less pronounced (Okayasu et al. 2000). BALB/c mice were known to have a lower expression frequency of DNA-PKcs due to the Prkdc gene polymorphism, as well as reduced enzyme activity of DNA-dependant protein kinase (DNA-PK) compared to other commonly used strains. BALB/c were also characterised by a spontaneous mutation in some animals causing dense cataract and microphthalmia (Kohale et al. 2004; Bakthavachalu et al. 2010). An increased genomic instability had been suggested due to an observed increased micronuclei detection (fragments of

chromosomes not incorporated into one of the nuclei during division) following x-irradiation had influenced the BALB/c 'radiosensitive' classification (Hamasaki et al. 2007). DNA DSB repair in both the C57BL/6 and BALB/c mouse lenses seem similar based on what has been observed in the results presented in this chapter. Although NHEJ had been hypothesised to play a contributing role to cataract formation *in vitro*, the results of this study suggested a lesser dependence of repair using NHEJ in the lens *in vivo* (Smith et al. 2015), particularly in both the C57BL/6 and BALB/c strains.

Doses of IR as low as 20 mGy had previously been shown to induce DNA DSBs and their subsequent repair in flat mounted lens epithelia (Markiewicz et al. 2015), similarly to the methods of this study (see chapter 2), and the data presented in this chapter demonstrated a lowering of the detectable dose limit to 10 mGy. Such a lowering of detectability was promising and closer to the low dose exposures that occur during occupational and medical exposures (albeit occurring across a broad spectrum of dose-rates (Barnard et al. 2016)) often used in low dose epidemiological analysis of radiation cataract. There had been a need for a low-dose biological and experimental models to complement and support epidemiological studies in trying to understand the underlying mechanisms, and indeed that was one of the research questions of this thesis. Interestingly, the low doses exposed during this study suggested a greater sensitivity of the central rather than the peripheral LECs in all strains apart from the BALB/c.

Analysing DNA damage and the formation and repair of 53BP1 foci as a potential precursor for cataract formation following radiation exposure could provide useful mechanistic information, however a direct link to cataractogenesis and opacity formation is yet to be firmly established. Although the role of DNA damage repair had been hypothesised to play a role it the induction of cataract, this had been mostly limited to *in vitro* analysis (Smith et al. 2015) to underpin the exact mechanism(s). However, as discussed in chapter 1 (section 1.6.2), heterozygous *Ercc1*, Atm and Rad9 knockout mice have demonstrated susceptibility to IR-induced cataract (Kunze et al. 2015; Kleiman et al. 2007; Worgul et al. 2002). Whilst the role of 53BP1 is by no means exclusive to radiation-induced DSBs (discussed at length within the introduction, chapter 1), and its interaction with other proteins (Mayca Pozo et al. 2017; Bartova et al. 2018), there was a strong dose-response relationship with its expression post-exposure seen in the results of this chapter and also in a previous study (Markiewicz et al. 2015). As discussed, 53BP1 foci have been shown to be induced by replication stress, occurring during DNA replication (Fernandez-Vidal, Vignard, and Mirey 2017). The depletion of 53BP1 results in cell cycle arrest (Gupta et al. 2014), highlighting its role beyond being simply a DNA DSB repair marker. It is possible that this could have a minor influence compared to the stronger dose response, particularly in the peripheral region of the lens epithelium, where cell proliferation is occurring more readily. However, no significant increase in

peripheral LEC mean 53BP1 foci/cell was observed in control lenses compared to that of the central LECs, suggesting that the increased rate of proliferation in peripheral LECs was relatively low and by no means are all LECs actively dividing. It may also indicate that the influence of proliferation on 53BP1 foci formation was not as influential in LECs compared to other cell and tissue types. Mrad9 and Atm (both important in maintaining genomic stability) deficient models had shown a greater incidence of cataract formation post-exposure, indicating these proteins as potential determinants or precursors of lens opacification (Kleiman et al. 2007) and again supporting the important role of DNA damage repair (Smith et al. 2015).

Genes which are transcriptionally active in cancer cells are known to be more susceptible to accumulating mutations (Supek and Lehner 2017). In the lens, this would include transcriptionally active genes coding for important proteins such as crystallins (Khan et al. 2015), responsible for the eventual transparency of the LFCs. It was the peripherally located LECs that were slower to repair DSBs (Markiewicz et al. 2015) and this was supported by the results presented in this chapter. The peripheral LEC and the nucleated, differentiating LFCs are where this transcriptional activity is occurring as previously mentioned, and so a slow or delayed repair response could be detrimental to effective cell differentiation. The inter-relationship of DNA repair and transcriptional regulation (Petroni et al. 2016; Lieberman et al. 2017) was therefore an important consideration for understanding the results of this study and the wider mechanism(s) of IR-induced cataract and interpreting the hypothesis of the role of DNA damage and repair from *in vitro* studies (Smith et al. 2015) as well as understanding the effects of low dose radiation in IR-induced cataract epidemiological studies. The DNA repair process was thought to involve the decondensation, or compaction, of chromatin and the eviction of histones at the site of DSB (Bakkenist and Kastan 2015), indicative of mechanistic differences between DNA repair in transcriptionally inactive and active chromatin regions which have yet to be determined for lens cell differentiation.

It was important to also consider the fact that different individuals do not show the same gene-by-environment effects (Lewis et al. 2017) adding a further dimension to the understanding of the complexity of IR-induced cataract and the difficulties in identifying a mechanistic pathway(s). This also applied to different mouse strains such as those in this study, where each strain showed considerable genetic variation (Doran et al. 2016) and differed markedly in their background of genomic rearrangements (Chen et al. 2016). The findings of this study are therefore of importance in understanding human cohorts in a more controlled fashion to translate these findings. The mechanistic inter-relationship of DNA repair, transcription, replication and chromatin condensation state as discussed here make it clear that they are likely all contributing factors, with probable

dependence upon each other, to IR-induced lens opacification and cataract. These make the appearance of a common phenotypic endpoint, namely cortical or posterior subcapsular cataract as described in literature (Worgul et al. 2005; Little 2013; Ainsbury et al. 2016) as the iconic signatures of IR exposure more remarkable given the complexity and lack of understanding of the biological inputs described here. It was therefore very important to determine the strain dependency for IR-induced lens opacification in the mouse.

The results of this study indicated better repair following 25 mGy exposures in all strains. This was more noticeable and consistent in BALB/c mice. This 'better repair' seen in the LECs of the BALB/c was somewhat contradictory to what was known about radiosentivity in human tumour cell lines, where radioresistant tumour tissue in culture repaired DNA damage much faster (Taneja et al. 2004; Lomax et al. 2013). However, little was known about the response of LECs to IR, especially in *in vivo* rather than *in vitro*. 53BP1 had been demonstrated to show a significant dose response relationship within *in vivo* irradiated lens epithelia, but not in foetal human LECs cultured and exposed *in vitro*, highlighting the importance of mouse-based lens studies (Markiewicz et al. 2015). However, there was a lack of significance of dose following 10 mGy exposures. The seemingly efficient repair of damage in the BALB/c was striking when considering the small standard error associated. Arguably, the 129S2 strain could present a similar repair profile, although given the contrasting large error in this strain, it remains unclear. However, both strains were known to be radiosensitive due to ineffective repair mechanisms (as stated earlier), with BALB/c proving the more reliable and reproducible strain for use in further investigations of low dose damage in LECs. Repair response and efficiency may not be the same at high and lower dose radiation exposures (Rothkamm and Lobrich 2003).

During the investigation of background spontaneous 53BP1 foci/cell, the power within this study fell short of ideal power numbers. In most cases the power was probably around 20%, which means that there was a ~ 80% chance for false negative results. This was largely due to the substantial standard error seen between individuals of the same mouse strain, particularly 129S2. A total of 29 lenses (15 mice) would be required to have enough power for statistical significance of lens epithelia region, compared to just 5 lenses needed for the same significance in BALB/c mice, which had substantially smaller standard error. This was more apparent in the post-hoc power calculations for comparison of baseline 53BP1 mean foci/cell when comparing strains. C57BL/6 and BALB/c, both demonstrated the smallest standard error, needing a power of 12 lenses for statistical significance, whereas, for example, 1901 lenses would be required for power to compare C57BL/6 and 129S2 mice. This highlights the need for identification of appropriate and reproducible strains, regardless of 'inbred' status.

The investigations of this chapter have allowed for the identification of the most suitable murine model(s) to investigate the effects of IR at low doses using the formation and repair of DSBs visualised as 53BP1 repair foci as an indicator of LEC damage. These investigations confirm what was generally accepted in the literature, that strain dependant differences in DNA DSB yields are as large as exposure dependant differences. Genetic susceptibility in response to radiation in the lens, is also of greater significance at low dose exposures (Worgul et al. 2005). The conclusions from this chapter support the known radiosensitive nature of the lens compared to other tissues, which was certainly influenced by genetic factors, demonstrated in these results by the significantly different responses of different inbred strains to radiation-induced DNA damage and repair in the lens epithelia. These also suggest that the structure and cellular distribution of the lens may not be uniform from strain to strain (unpublished cell density data from the LDLensRad project) and that this lack of uniformity may also translate to the human population. Therefore, biological and/or mechanistic findings must be interpreted. Whilst comparing the four strains, BALB/c mice were identified as a lens-specific radiosensitive model for quantitative analysis of radiation-induced DNA damage and repair following low-dose exposure. The conclusion from the data is that BALB/c are an optimum model for evaluating the DNA damage and repair effects of IR, where such doses are significantly effective. However, the genotype of this strain (polymorphism inhibiting repair) must be considered when making conclusions and applications to human cohorts. Further to this, the less radiosensitive C57BL/6 strain should be the model of choice in higher dose and longer-term studies as these mice demonstrate the same small margins of inter- and intra- individual variability as the BALB/c strain. It may not be that the lens is radiosensitive, but rather a different mechanism of repair is occurring in this tissue compared to the others during *in vivo* exposure to IR. Further work is needed to fully understand this response as discussed in chapter 7 (section 7.7).

4. Dose and dose-rate response of DNA damage and repair in the lens epithelium

The influence of dose-rate in radiation cataractogenesis had not been extensively studied. One recent epidemiological investigation suggested that protracted radiation exposure increases radiation-induced cataract risk: cumulative doses of radiation <100 mGy received by US radiologic technologists over an extended period were associated with increased excess hazard ratios for cataract development. However, there were few mechanistic studies to underpin such observations. Low-dose radiation-induced DNA damage in LECs had been proposed as a possible contributor to cataract formation and thus visual impairment.

In this chapter, the effect of three dose-rates of ^{60}Co γ-radiation (as described in chapter 2: Materials and Methods, sections 2.3.1 and 2.3.2) on residual 53BP1 repair foci in the LECs following *in vivo* whole body exposure of female C57BL/6 strain mice are explored. The strain had proven suitability and was a reproducible and cost effective model for investigating DNA damage and repair in the lens epithelium as described in chapter 3 (Barnard et al. 2018). Data for peripheral blood lymphocytes (well characterised in biodosimetry studies) were also analysed with the same 53BP1 foci marker for direct comparison from the same animals to better understand the specific lens tissue sensitivity to DNA damage and repair.

This chapter focused on the dose response of the LECs to doses 0.5, 1 and 2 Gy at dose-rates of 0.063 and 0.3 Gy/min. An additional dose-rate of 0.014 Gy/min was investigated to deliver the lowest dose of 0.5 Gy. DSBs visualised through 53BP1 repair foci were counted and analysed at 4 and 24 hours post-exposure (see chapter 2; Materials and Methods). Appendix B accompanies this chapter.

4.1 Dose response

During this study, 53BP1 repair foci were analysed 4 and 24 hours post-exposure. These foci were counted at a further 30 minutes post-exposure following a single dose of 0.5 Gy IR to demonstrate that the LECs display the same characteristic dose response of DNA DSB repair as seen in blood lymphocytes (Horn, Barnard, and Rothkamm 2011), demonstrated in Figure 4.1.

Figure 4.1: DNA damage repair following 0.5 Gy exposure 30 minutes to 24 hours post-exposure

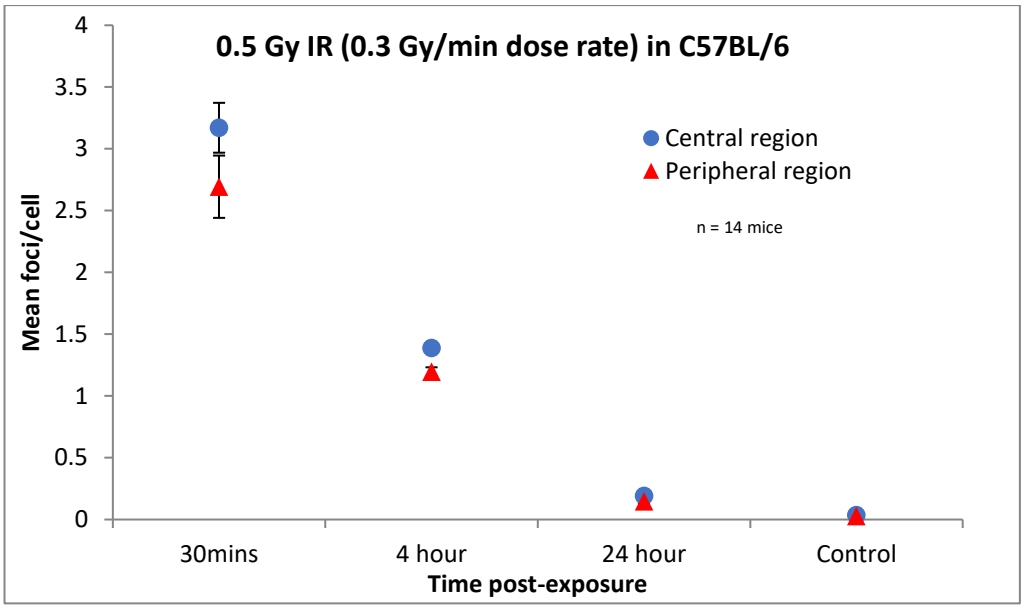

Figure 4.1: DNA damage repair as measured by residual 53BP1 foci from in-vivo irradiated lens epitheliums. Both central and peripheral regions are plotted at 30 mins – 24 hours post-exposure

The mean number of residual 53BP1 foci declined from 30 minutes to 24 hours post-exposure. Central and peripheral region LECs responded similarly (figure 4.1), with no statistical significance of region, but a statistical significant decline in 53BP1 mean foci/cell with time ($p = 0.001$). This confirmed the time-dependant response of mean foci/cell. Post-hoc Tukey comparison confirmed all post-exposure time points were significantly different from each other ($p = \leq 0.015$), except sham-irradiated controls and 24 hour post-exposure time point ($p = 0.8$).

4.2 Dose-rate effect in lymphocytes

Peripheral blood lymphocytes were isolated from 17 female C57BL/6 mice exposed to 0.5 and 1 Gy at three dose-rates; 0.014 (0.5 Gy only), 0.063 and 0.3 Gy/min (see chapter 2: Materials and Methods). The response of the lymphocytes was important and a control for confirmation of dose-rate effects in lymphocytes, as seen in previous studies (Turner et al. 2015). The yield of 53BP1 DSB repair foci were counted at 24 hours post-exposure and plotted with standard error (SE) bars (Figure 4.2), alongside sham-irradiated control mice. All post-irradiation samples had greater foci yields than controls ($p \leq 0.001$). At the lower 0.5 Gy dose exposed, there was a reduction in mean 53BP1 foci/cell from 0.3 to 0.063 Gy/min. This reduction continued down from 0.063 to 0.014 Gy/min. When the delivered dose was increased to 1 Gy, the same reduction in mean 53BP1 foci/cell was observed from 0.3 to 0.063 Gy/min. Figure 4.2 demonstrates a further lowering of

mean 53BP1 foci/cell (0.23 ± 0.026) at 0.5 Gy, when delivered at an even lower dose-rate of 0.014 Gy/min, compared to both the 0.3 and 0.063 Gy/min dose-rate exposures for 0.5 Gy. Performing ANOVA on these results revealed a statistical significant influence of both variables dose and dose-rate (both $p \leq 0.001$) on 53BP1 foci in lymphocytes at 24 hours post exposure.

Figure 4.2: Mean 53BP1 foci/cell in peripheral lymphocytes exposed to 0.5 and 1 Gy at three dose-rates 24 hours post-exposure

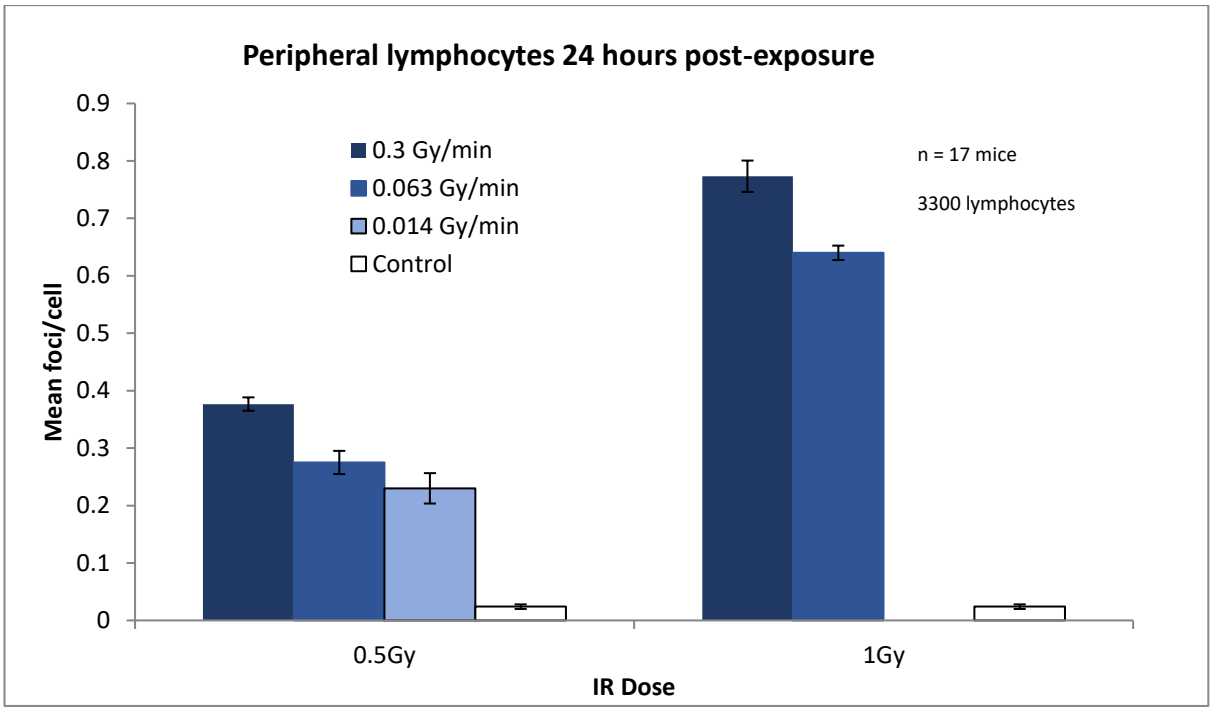

Figure 4.2: Mean 53BP1 foci/cell in the peripheral blood lymphocytes of mice exposed to 0.5 and 1 Gy (plus shame-irradiated controls) 24 hours post-exposure to 3 different dose-rates. For data set see Appendix B.

4.3 Dose-rate effect in the LECs

53BP1 foci were evaluated in the LECs of the central and peripheral regions, as in previous studies (Barnard et al. 2018; Markiewicz et al. 2015) but on a much larger scale in terms of numbers (Appendix B, table B.2). Mean 53BP1 foci/cell were analysed at 4 and 24 hours following exposure to doses of 0.5, 1 and 2 Gy irradiation at 0.3 and 0.063 Gy/min ^{60}Co γ-IR (Figure 4.3). No significant effect of time, region, dose or dose-rate was observed in the sham-irradiated control mice. A reduction of mean foci/cell frequencies was seen at all doses between 4 to 24 hours suggesting repair of DSBs. Doses delivered at 0.3 Gy/min yielded fewer detectable foci than at 0.063 Gy/min in LECs. As mentioned, a lower dose-rate of 0.014 Gy/min was included but limited to only one dose, 0.5 Gy, due to mouse exposure time constraints. Figure 4.3 compared all three dose-rates

(0.014, 0.063 and 0.3 Gy/min) when delivering 0.5 Gy. The further reduction of dose-rate (0.014 Gy/min) further increased detectable mean 53BP1 foci/cell frequencies in both regions at 4 and 24 hours post-exposure.

Figure 4.3: Dose-rate response of LECs when exposed to 0 – 2 Gy at 0.014, 0.063 and 0.3 Gy/min

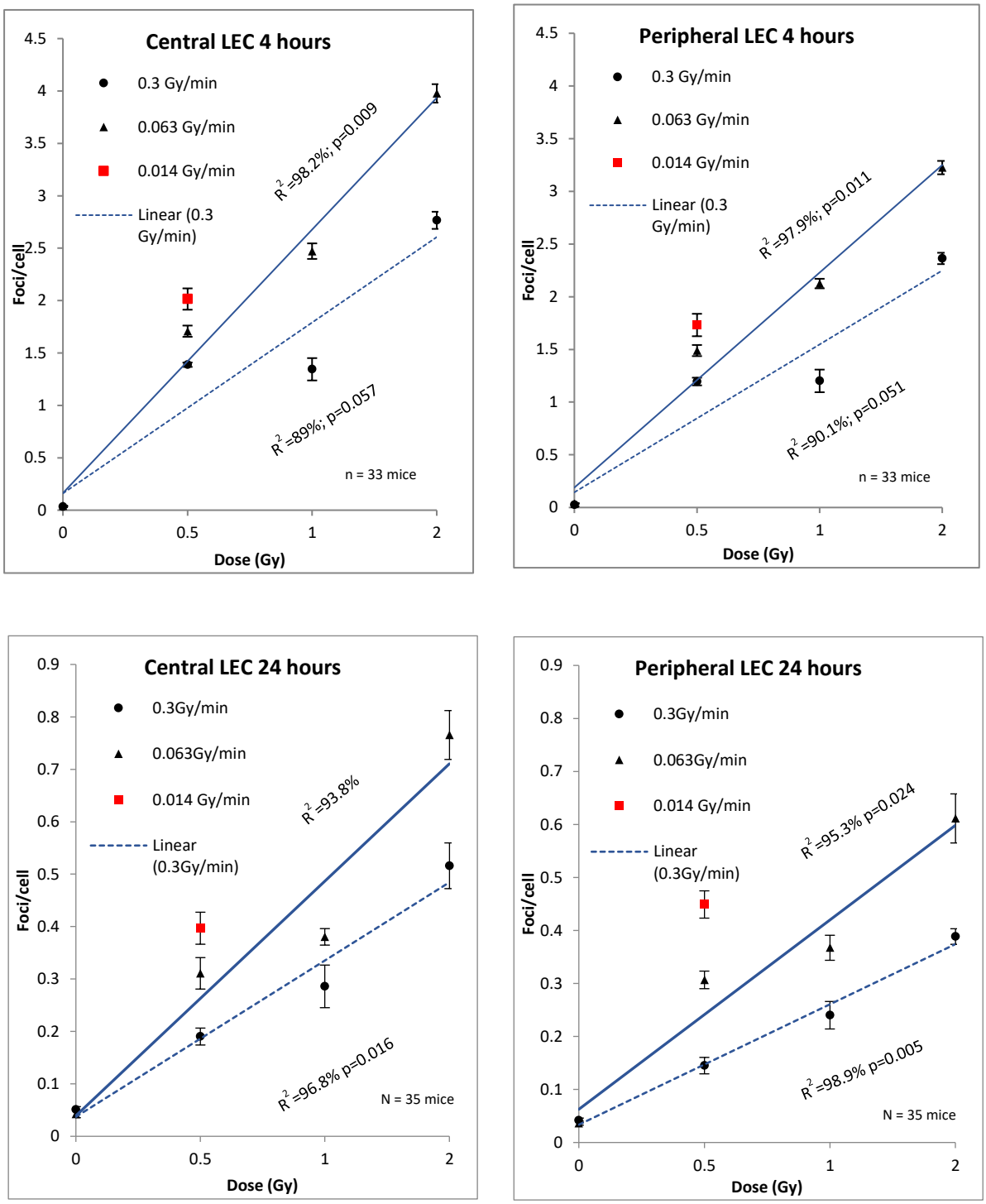

Figure 4.3: Response of mean 53BP1 foci in the central and peripheral region of the lens epithelium following expose to different dose-rates of IR. Linear fits are plotted with SE bars. For data set, see Appendix B.

To perform statistical analysis on these data, a variety of General Linear ANOVA Models were applied and tested, finally a non-hierarchical model with a third order interaction for the variables within these results of dose, dose-rate and time were used as this gave the best fit overall. All three variables were found to significantly affect mean residual foci/cell yields ($p \leq 0.001$), with the interaction between dose, dose-rate and time being statistically significant ($p < 0.001$). These values indicated DNA damage results must be considered in the context of dose, dose-rate and time post-exposure. Only the region of the lens epithelium lacked statistical significance ($p = 0.079$), although significantly different residual foci/cell yields had been previously observed between regions at lower total doses as presented in the chapter 3 comparing multiple murine strains. Tukey's pairwise testing further revealed that all doses were statistically significant from each other and from sham-irradiated controls, except between doses 0.5 and 1 Gy ($p = 0.339$). For all three doses, the intermediate dose-rate of 0.063 Gy/min showed a significantly higher frequency of mean foci/cell compared to the higher dose-rate of 0.3 Gy/min ($p = 0.001$). At 0.5 Gy the residual foci/cell yield at the additional dose-rate of 0.014 Gy/min was significantly different from those at 0.3 Gy/min ($p = 0.014$). There was no significant difference between the two lower dose-rates ($p = 0.696$) at 0.5 Gy 24 hours after exposure.

4.4 Discussion

IR induced DNA damage producing DSBs happens very rapidly post-exposure, with repair starting to occur within minutes (Horn, Barnard, and Rothkamm 2011; Rothkamm and Horn 2009). This early initiation of repair was commonly modelled in samples irradiated *ex vivo* using cell lines or isolated cells such as lymphocytes. However, the exposures used in this study were whole-body *in vivo*, which came with some practical restrictions in terms of very early DSB repair modelling. Therefore 30 minutes post-exposure represented the earliest time point that could be practically and reproducibly achieved. The results of this study supported the time-dependant response of DNA DSB repair foci (figure 4.1).

The observed inverse dose-rate effect in the lens epithelium was evident at both 4 and 24-hour post-exposure. The limited biological evidence for an inverse dose-rate effect in the lens had recently been summarised by Hamada *et al.* (Hamada 2016), suggesting there might be a dose-rate effect at low-LET exposures. Moreover this inverse dose-rate effect would only be observed with high-LET neutron radiation (Worgul et al. 1993). It should also be noted that standard errors associated with mean foci/cell were small during this study, a previously observed characteristic of both the radiosensitive BALB/c and the less sensitive C57BL/6 strains (see chapter 3) (Barnard et al. 2018). Further, post-hoc statistical testing demonstrated a clear trend of higher mean foci/cell with

higher doses, shorter times and, to some extent, lower dose-rates. Dose-rate reduction, and increased duration of exposure generally reduce the biological effects of ionising radiation (Hall 1973) as observed in the lymphocytes of both this study (figure 4.2) and in Turner et al. (Turner et al. 2015), where less DNA damage foci were detected.

The somewhat unexpected finding of this study may be explained when considering the statistical interaction effects. This additional feature of the observed data, i.e., the statistically significant interaction between time (post-exposure), dose and dose-rate, as well as between dose and time, both with strongly significant p-values of < 0.001. Interaction analysis such as these are not commonly considered during such studies, but the results here were clear. This analysis was justified due to the large error observed within the sum of squares from ANOVA testing when the interaction effect was not included. Dose, dose-rate and time were biologically known to have interactions and indeed it appears from these data that residual 53BP1 foci frequencies were influenced by all three.

The dose-rates used in this study were not low in comparison to the generally accepted definition of <5 mGy/h (ICRP 2007a), below which single track events predominate. The choice of dose-rates in this study were driven chiefly by the availability of suitable exposure facilities (MRC Harwell) and the dose and dose-rate ranges within which the source could be reliably calibrated. However, the data presented here supported the hypothesis (Little et al. 2018; Hamada 2017b) that there was a tissue dependant dose-rate effect in the lens that is not seen within the lymphocytes. Reducing dose-rate from 0.3 to 0.063 Gy/min was found to significantly increase the number of detectable residual DSBs within LEC DNA, which raised the question of the effects of protracted low dose-rate exposures on the lens. More investigations are required to establish the influence of both IR dose-rate and energy of the radiation on the DDR of LECs.

Whilst this study considered one response to IR exposure, i.e. DNA damage assessed by 53BP1 repair foci, recent findings suggested this pathway has a role in IR-induced cataractogenesis (Barnard et al. 2018; Markiewicz et al. 2015; Kunze et al. 2015; Osnes-Ringen et al. 2013). Based on the dose responses seen for both Rad51 and 53BP1 foci in a previous study, both HR and NHEJ repair mechanisms respectively, appeared to be active in LECs (Markiewicz et al. 2015). It has been suggested that a combination of IR-induced effects could be responsible for cataract induction, adding to a ‘cataractogenic load’ (Ainsbury et al. 2016; Alice Uwineza and Hamada 2019) concept and the data presented in this chapter supported this view of damage accumulation. Un-repaired DNA damage in LECs could lead to altered cell proliferation (Markiewicz et al. 2015), which could in turn have a detrimental effect on cell differentiation. The results of this chapter also suggested

that IR-induced damage may accumulate as evidenced by the persistence of foci 24 hours post-exposure across the lens epithelium (Figure 4.3). The suggestion of progenitor cells residing in the lens epithelium (Lin et al. 2016; Oka et al. 2010; Zhou et al. 2006) would potentially pose a particularly sensitive target for IR-induced DNA damage depending on where they reside.

Another possible mechanistic explanation for the results of this chapter relate to the role(s) of lens epithelium-derived growth factor (LEDGF) (hypothesis illustrated in Figure 4.4) and eyes absent (EYA) proteins. LEDGF is expressed in greater concentration across the central region of the lens epithelium (Kubo et al. 2003), where it has been shown to protect the cells against oxidative damage (Singh et al. 1999) and DNA damage induced via peroxide and UVB (Matsui et al. 2001; Fatma et al. 2001). The expression of LEDGF is lost towards the equator of the lens, where the peripheral region LECs are located (Kubo et al. 2003) resulting in slower repair. This is important to the results of this chapter, as LEDGF has DNA binding properties (Singh et al. 2006) and is involved in the DNA DSB repair response pathway following γ-radiation exposure (Li and Wang 2017). Recent proteomic and RNA sequencing data revealed higher levels of DNA repair proteins 53BP1, MRE11 and Rad50 in the murine lens epithelium compared to fibre cells (Zhao et al. 2019), but the fact that the peripheral epithelium was more sensitive to IR (Markiewicz et al. 2015) suggested that LEDGF might play a key role in this differential sensitivity between the central and peripheral regions of LECs. EYA, a phosphatase required along with Pax6 and Six3 transcription factors that are essential for eye development (Purcell et al. 2005), is also needed for DNA repair as it dephosphorylates H2AX (Krishnan et al. 2009). Both LEDGF (El Ashkar et al. 2018; Singh et al. 1999) and EYA (Xu et al. 1997) are also required for LEC differentiation into LFCs. The data in this chapter indicated that DNA repair is dependent upon IR dose and dose-rate.

Figure 4.4: The influence of LEDGF on DNA repair in the lens epithelium

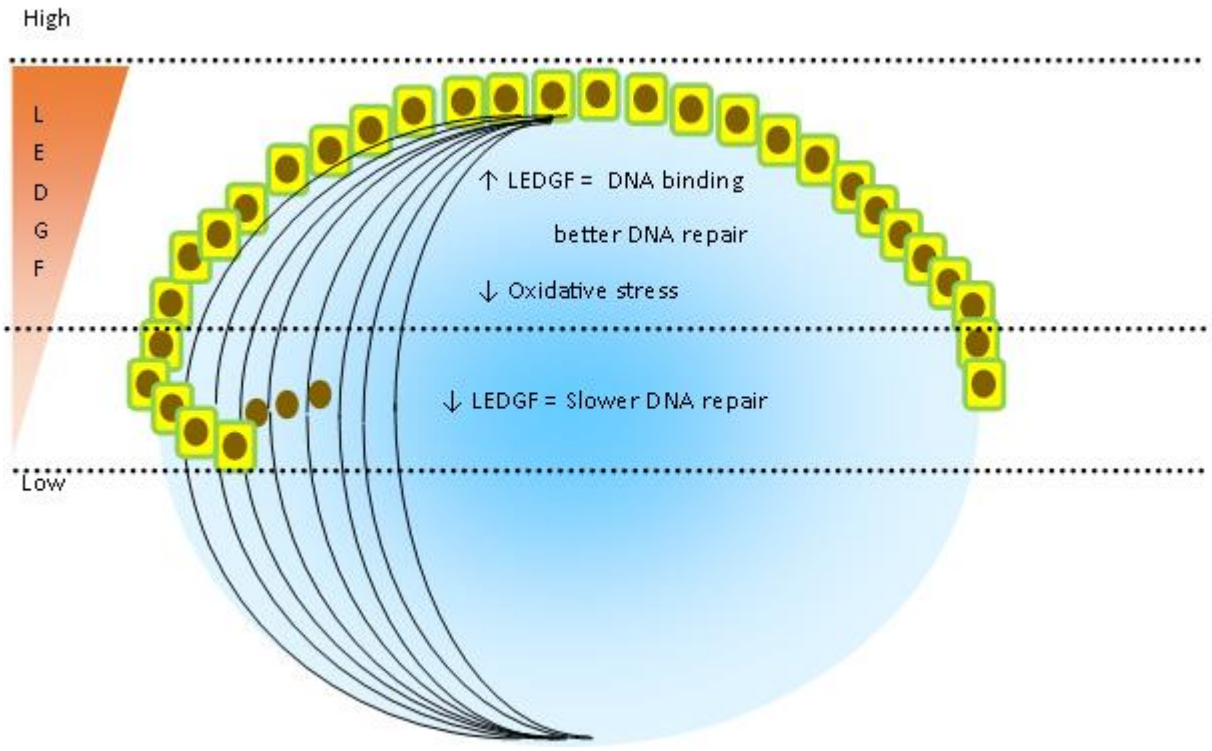

Figure 4.4: The concentration of LEDGF across the lens epithelium and the hypothesised differential influence on DNA damage repair within centrally and peripherally located LECs.

In terms of the findings of this chapter, data can be interpreted to indicate that peripheral LECs are balancing the processes of cell differentiation and DNA DSB repair. At the lower dose-rates, the 53BP1 foci persist (DSBs remain unrepaired) whilst differentiation proceeds (hypothesised). At higher dose-rates, DNA repair is favoured over differentiation with DSBs being repaired and detectable 53BP1 foci decreasing with time. The decreased expression of LEDGF around the peripheral region LECs could help explain the slower repair of DNA damage seen within the results of this chapter at the lower dose-rate (Figure 4.3). The presence of 53BP1 foci indicate that DNA repair was progressing, as a decrease in mean 53BP1 foci/cell with time for both peripheral and central regions of the lens epithelium was also observed.

Inverse dose-rate effects generally occur in instances whereby a continuous low dose-rate exposure to IR allows cells to cycle, but the cells hit a G2-phase block, resulting in cell death (Hall 1973). Although cell death does occur in LECs, this is very low, there were no reported instances of increased LEC death post-IR exposure (Ainsbury et al. 2016). Lifetime loss of LECs due to cell death in humans occurring over many decades may have some subsequent effect on LEC differentiation and lens transparency (Charakidas et al. 2005). One proposed mechanism of the inverse dose-rate effect is a failure of LECs to arrest damaged cells and stop their progression into G2 cell cycle phase.

This would make the peripheral LECs a particular target of the inverse dose-rate effect (Hamada 2016) as it is here that proliferating cells are concentrated (see chapter 5) (Wu et al. 2015). A consequence of delaying DSB repair is that secondary effects accrue and affect lens cell differentiation itself (Hamada 2016; Hamada et al. 2014). This was broadly summarised in the 'cataractogenic load' concept, where genetic, lifestyle and environmental factors were recognised as co-inducers of age-related cataract (Alice Uwineza and Hamada 2019). IR-induced damage therefore compounds the lens aging process by further increasing this 'load' to accelerate aging and the appearance of age-related cataract. This study of an inverse dose-rate effect therefore fuels further debate on IR effects upon the lens and strengthens arguments for regular monitoring in occupational contexts (Bouffler 2012; Barnard et al. 2016; Ainsbury 2014).

Observing an inverse dose-rate effect would typically be expected when a low dose-rate is significantly reduced, towards a protracted exposure. However, the data presented here suggested an inverse dose-rate effect within three different acute exposures. The inverse dose-rate effect is not well understood despite being reported in several studies, but was thought to result from a hyper radiosensitivity of cells to low dose exposure, due to failure to arrest in G2 (Marples 2004) (Lian et al. 2015). However, this was reported at doses below 30 cGy (300 mGy), which are lower than the doses used in this chapter. One of the limitations of this dose-rate investigation study was the ability to expose mice for longer periods of time, which would have allowed for higher doses and even lower dose-rates to be investigated. This was due to local Home Office project licence restrictions, although this can be modified for future studies. Therefore, currently this chapter can only conclude the inverse dose-rate effect was observed across all three dose-rates at one dose, 0.5 Gy.

The findings from this study represented the first *in vivo* experimental investigation of dose-rate effects in the LECs of the mouse eye lens and presented the first evidence suggesting that LECs and lymphocytes respond differently to dose-rate variation in terms of DNA damage repair. Levels of residual DNA damage foci observed in LECs increased with reduced dose-rate, unlike in the peripheral blood lymphocytes from the same animals. This supported the hypothesis that the lens has an unusual DNA damage response to IR compared to other tissues. The data indicate an inverse dose-rate effect in the LECs using residual 53BP1 foci as a marker for DSBs, and it was hypothesised that this residual damage contributes to cataractogenesis. This study evidenced the importance of determining the cell-specific effects of low dose and low dose-rate IR exposures upon DNA repair in target tissues and showed that the response can be cell and tissue specific due to, for instance, competing processes such as cell proliferation and differentiation in a dose-rate dependant manner

as observed in cell-based studies (Truong et al. 2018; Rothkamm and Lobrich 2003; Anglada et al. 2019).

5. The effects of IR on LEC proliferation

As outlined in chapter 1 (section 1.3), the role of LECs in maintaining continual lens growth and function via proliferation (and subsequent differentiation) to supply new LFCs is critical. Disruption to this process can have severe consequences. This chapter presents the findings of IR-induced proliferation effects in the LECs of *in vivo* exposed mice (see chapter 2: Materials and Methods).

As previously described in chapter 2: section 2.9, LEC proliferation was measured by recording the proportion of cycling cells, as detected by Ki67 staining (Bosch et al. 2017; Denkert et al. 2015; Jurikova et al. 2016). This was then converted into a mean percentage of Ki67 (mitotic) positive cells in both central and peripheral epithelia regions of the monolayer. Ki67 is a well-characterised marker for proliferation, particularly in the classification and grading of tumour growth (Bosch et al. 2017; Denkert et al. 2015; Jurikova et al. 2016; Li et al. 2015; Miller et al. 2018; Penault-Llorca and Radosevic-Robin 2017). Appendix C accompanies this chapter.

5.1 The response of Ki67 with time

To confirm that LEC proliferation does not occur earlier than the 4 and 24 hours post-exposure times used throughout this thesis, a time response was performed using the dose of 0.5 Gy ^{60}Co IR at a dose-rate of 0.3 Gy/min (figure 5.1, table C.1). Female C57BL/6 mice were sacrificed and immunostained as per protocols described (see chapter 2: Materials and Methods), with time points post-exposure including an earlier 30 minutes, as well as 4 and 24 hours post-exposure alongside sham-irradiated control mice. The number of Ki67 positive cells were counted and analysed, with mean percentages shown in figure 5.1. Both the central and peripheral region LECs were analysed separately but plotted together demonstrating the observed differential response (figure 5.1).

General linear ANOVA revealed there was a statistically significant higher percentage of Ki67 positive cell frequency in the peripheral region compared to the central region of the lens epithelium ($p=0.009$; figure 5.1). No time point was significant from sham-irradiated control, which suggested no effect of 0.5 Gy IR inducing changes in cell proliferation at up to 24 hours. Some fluctuation was observed in the peripheral region whereby the percentage of Ki67 positive LECs appeared to decline from control to 4 hours post-exposure, returning to a value similar to control after 24 hours. The percentage of Ki67 positive LECs within the central region did not appear to change across all time points and clearly demonstrated smaller standard error, most likely due to a

much lower frequency of cells undergoing cell cycle, which is known to occur in the central region of the lens epithelium.

Figure 5.1: Time response (0 – 24 hours) of proliferation by Ki67 positive LECs exposed to 0.5 Gy

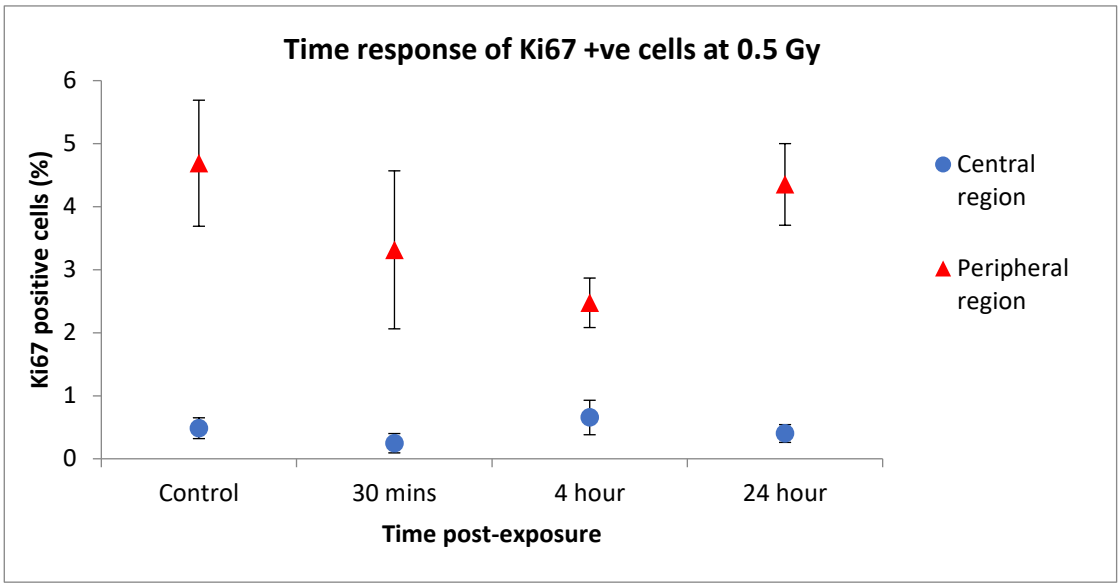

Figure 5.1: Time response of Ki67 positive cells (%) in both the central and peripheral region located LEC following 0.5 Gy exposure to IR at 0.3 Gy/min. Error bars represent standard error.

5.2 Low dose response of LECs

Female mice from two inbred strains (37 in total), the radioresistant C57BL/6 and the radiosensitive BALB/c, were identified as highly suitable candidate strains for comparison (see chapter 3 results. Figure 5.2 demonstrates the observed response of Ki67 positive cell percentage in the lens epithelium following exposure to doses 10, 25, 50, 100 and 1000 mGy x-radiation. The mice were sacrificed at 24 hours post-exposure as described in chapter 2: Materials and Methods.

Figure 5.2: Low dose response of LEC proliferation (10 – 1000 mGy)

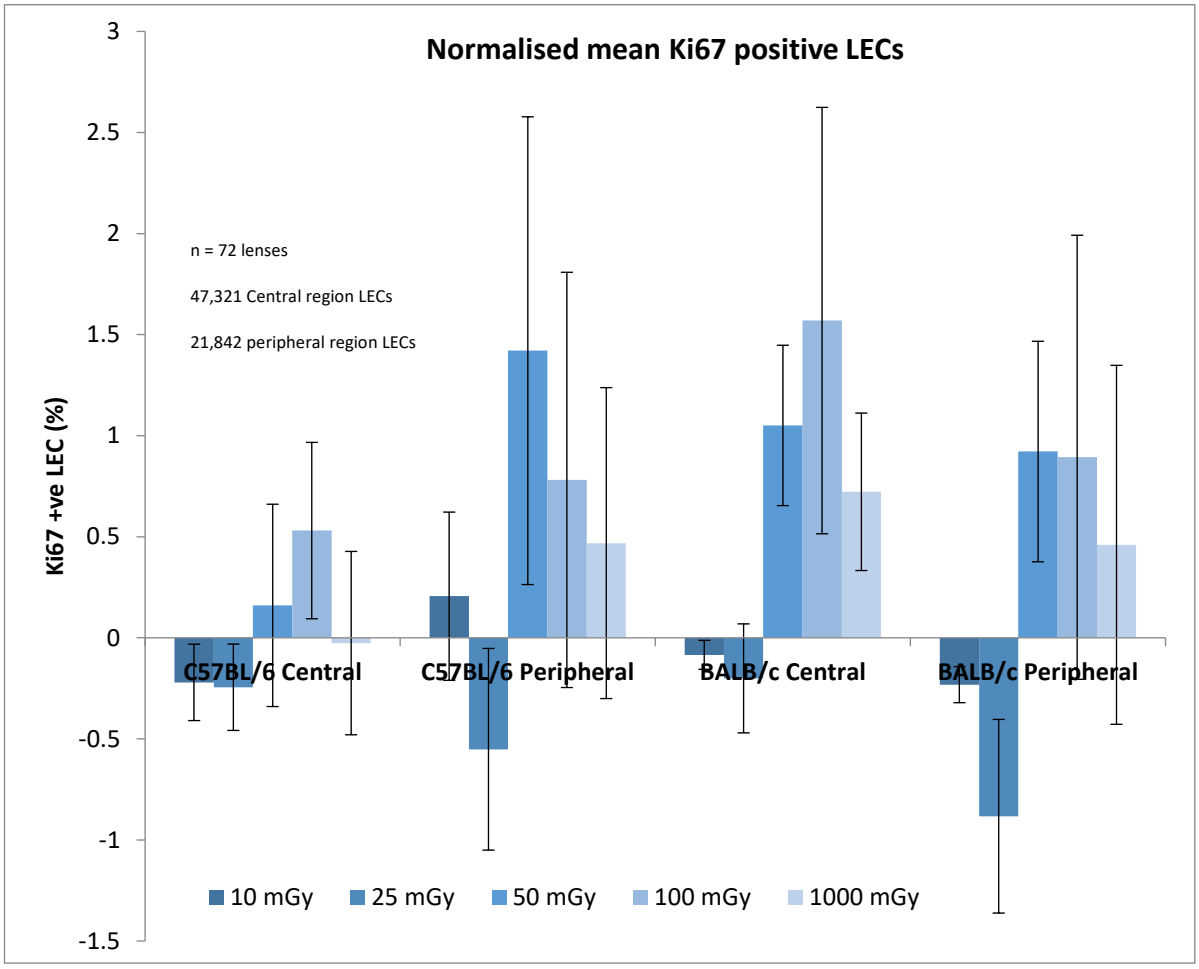

Figure 5.2: Normalised mean percentage of Ki67 positive cells analysed in both central and peripheral region LEC in C57BL/6 and BALB/c. Error bars are normalised standard error.

ANOVA revealed very strong significance of all variables, with both central and peripheral regions of the epithelium and IR dose significant ($p = <0.001$). C57BL/6 and BALB/c were statistically significant from each other ($p = 0.003$). There was no significant interaction effect between strain and the central or peripheral region of the lens epithelium, nor between epithelia region and dose. Within the variable of dose, all six individual doses were post-hoc tested further using Tukey pairwise comparisons (see chapter 2: Materials and Methods section: 2.11). A table of significant dose to dose interactions are presented (table 5.1), most notably the two lowest doses of 10 and 25 mGy were not statistically significant from control, but each have significantly lower percentage of Ki67 positive LECs than 50 and 100 mGy (all $p = \leq 0.004$). Normalising the effect of IR upon mean Ki67 positive LECs was performed by subtracting the sham-irradiated control percentage from that of the exposed mice (see Chapter 2; section 2.11). This allowed the results to be visualised most clearly (see Figure 5.2). The lowest doses of 10 mGy, and more obviously 25 mGy, showed a noticeable trend of a reduction in Ki67 positive cells post-exposure compared to higher doses. This

effect was not seen in the statistically significantly higher Ki67 percentage of LECs at 50 mGy and the higher doses.

Table 5.1: Significant low dose (10 – 1000 mGy) differences

Doses (mGy)	p-Value
Control and 50	0.009
Control and 100	0.005
10 and 50	0.004
10 and 100	0.002
25 and 50	0.000
25 and 100	0.000
25 and 1000	0.01
500 and 1000	0.035

Table 5.1: Significant outcomes from Tukey's Pairwise comparison mean Ki67 positive LECs exposed to low doses of IR in both strains and both central and peripheral regions of the lens epithelia.

5.3 Dose and dose-rate response

During the investigation of dose and dose-rate influence, 74 female C57BL/6 mice were exposed to 0.5, 1 and 2 Gy ^{60}Co radiation (including time-matched sham-irradiated controls) and sacrificed at 4 and 24 hours post-exposure (see chapter 2: Materials and Methods). ANOVA testing of the data revealed central and peripheral region of the epithelium being highly significant (p = >0.001) with the central region LECs expressing statistically significantly less Ki67 positive cells than those located within the peripheral region. Dose was highly significant (p = 0.003), which prompted further post-hoc Tukey's pairwise analysis. This confirmed sham-irradiated controls and 2 Gy exposed mice were significant from each other (p = 0.008), with 2 Gy also being significant from 0.5 Gy (p = 0.034). Figures 5.3 (A-D) demonstrate this data, with central and peripheral lens epithelia regions plotted separately, and for each time point post-exposure.

The effect of dose-rate had a highly statistically significant effect on the DNA damage and repair response in LECs (see chapter 4). Therefore, the doses exposed during this study were also delivered at both 0.063 and 0.3 Gy/min ^{60}Co radiation to investigate whether such an effect would also be present in the response of LEC proliferation.

Figure 5.3: LEC proliferation response 4 and 24 hours post-exposure to 0 – 2 Gy delivered at 0.063 and 0.3 Gy/min

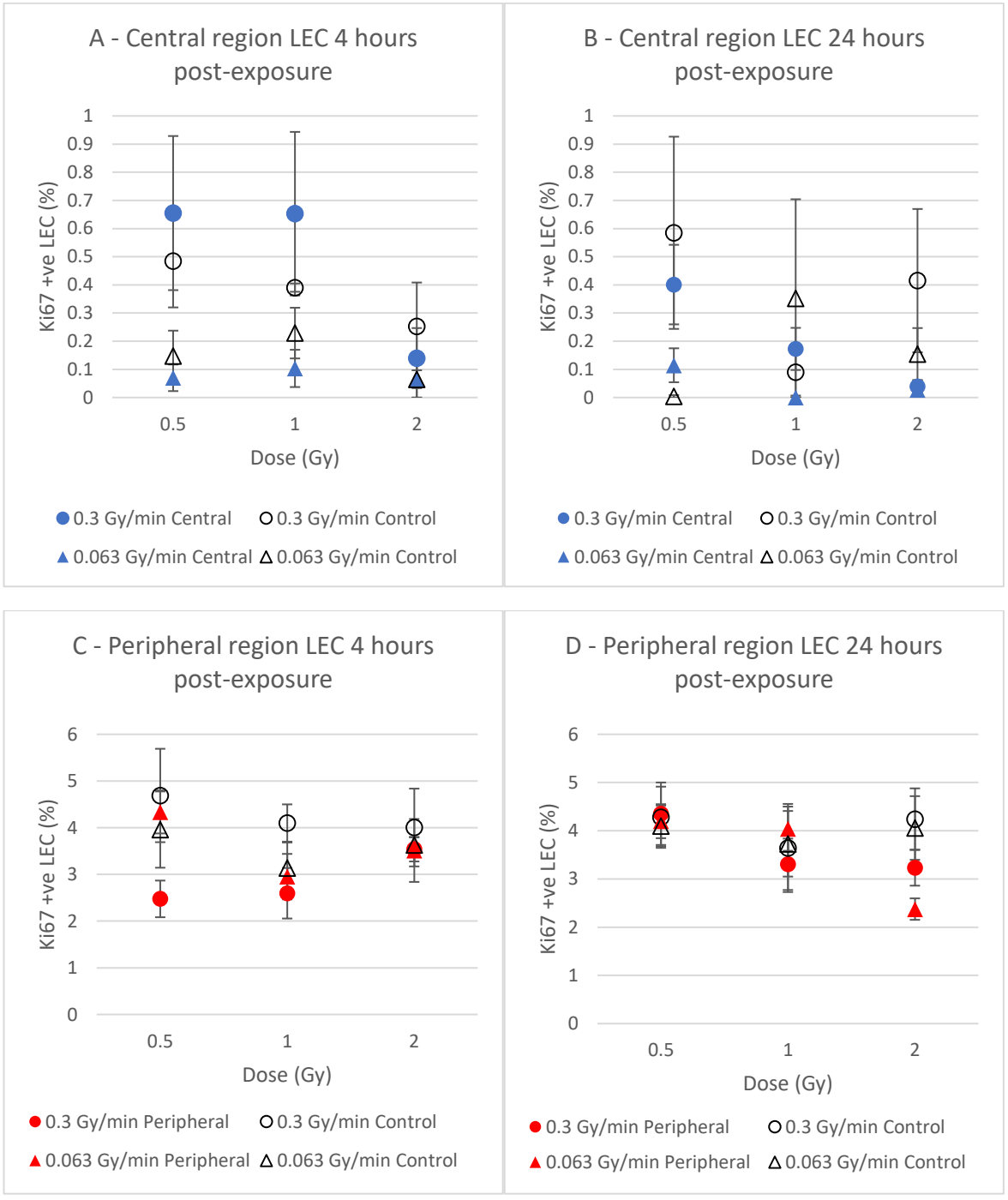

Figure 5.3: Mean percentage of Ki67 positive cells in the central region of the lens epithelium 4 (A) and 24 (B) hours, and the peripheral region at 4 (C) and 24 (D) hours post-exposure to 0.5, 1 and 2 Gy IR at two dose-rates with time matched sham-irradiated controls. Error bars represent standard error. Note the change in y-axis scale from central to peripheral regions. (n = 68 mice; central LECs = 70,215; peripheral LECs = 54,408).

Figure 5.4: Post-hoc Tukey comparisons between 0 – 2 Gy doses

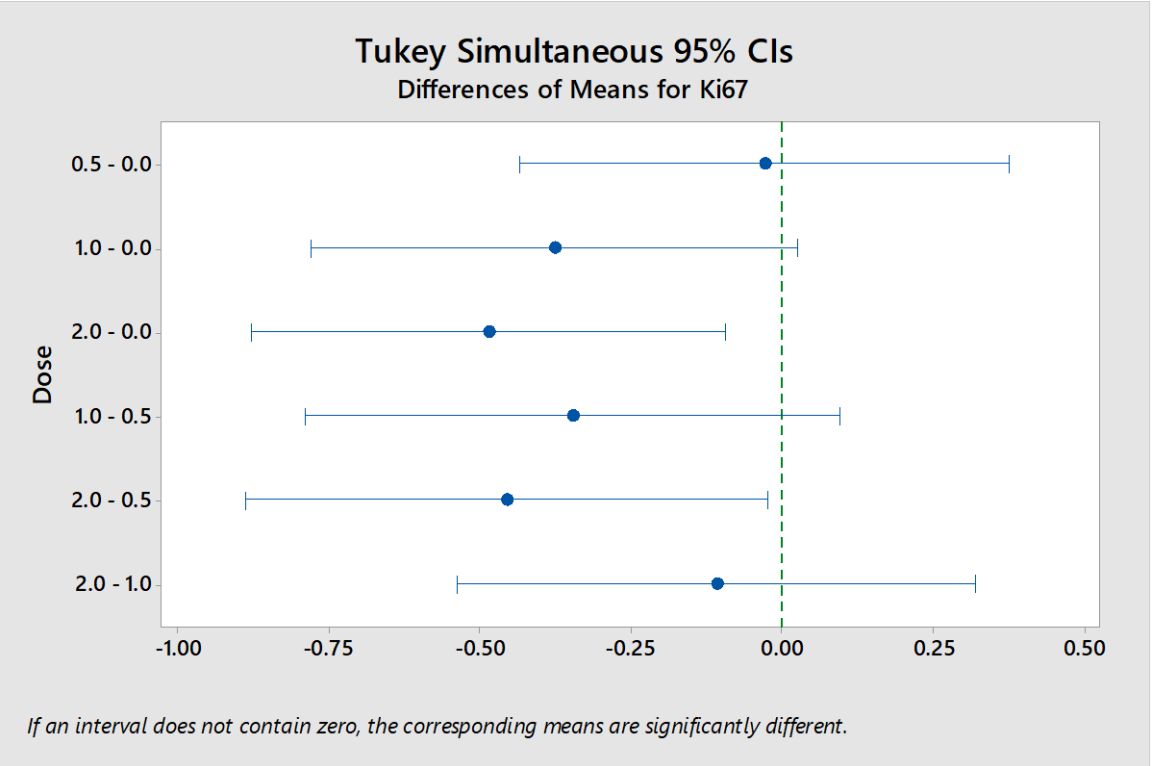

Tukey Simultaneous Tests for Differences of Means

Difference of Dose Levels	Difference of Means	SE of Difference	Simultaneous 95% CI	T-Value	Adjusted P-Value
0.5 - 0.0	-0.018	0.155	(-0.415, 0.380)	-0.11	0.999
1.0 - 0.0	-0.379	0.153	(-0.772, 0.014)	-2.47	0.064
2.0 - 0.0	-0.489	0.149	(-0.872, -0.107)	-3.28	0.006
1.0 - 0.5	-0.361	0.169	(-0.795, 0.073)	-2.14	0.141
2.0 - 0.5	-0.472	0.165	(-0.896, -0.047)	-2.85	0.022
2.0 - 1.0	-0.110	0.164	(-0.531, 0.310)	-0.67	0.907

Individual confidence level = 98.92%

Figure 5.4: Tukey comparison of dose reveals significantly reduced Ki67 positive cells at 2 Gy from sham/control (p = 0.006), and reduced at 2 Gy from 0.5 Gy (p = 0.022).

The statistical analysis of these data for 2 Gy exposure observed a significant decline in Ki67 positive cell percentage in the lens epithelium post-exposure (figure 5.4). The significance of lens epithelia region (central or peripheral) as revealed by initial ANOVA analysis (p = >0.001) suggested some further interaction analysis with other variables should be performed. Interestingly, dose-rate and LEC region were found to have a very close to significant interaction (p = 0.054). Performing post-hoc Tukey comparison revealed the breakdown of these interactions. There were clear significant P-values occurring within the various combinations of interactions. For example,

both dose-rates had a significantly different effect on the central compared to the peripheral region of LECs (p = >0.001).

Figure 5.5: Post-hoc Tukey comparisons of dose-rate (0.063 and 0.3 Gy/min) and LEC region interactions

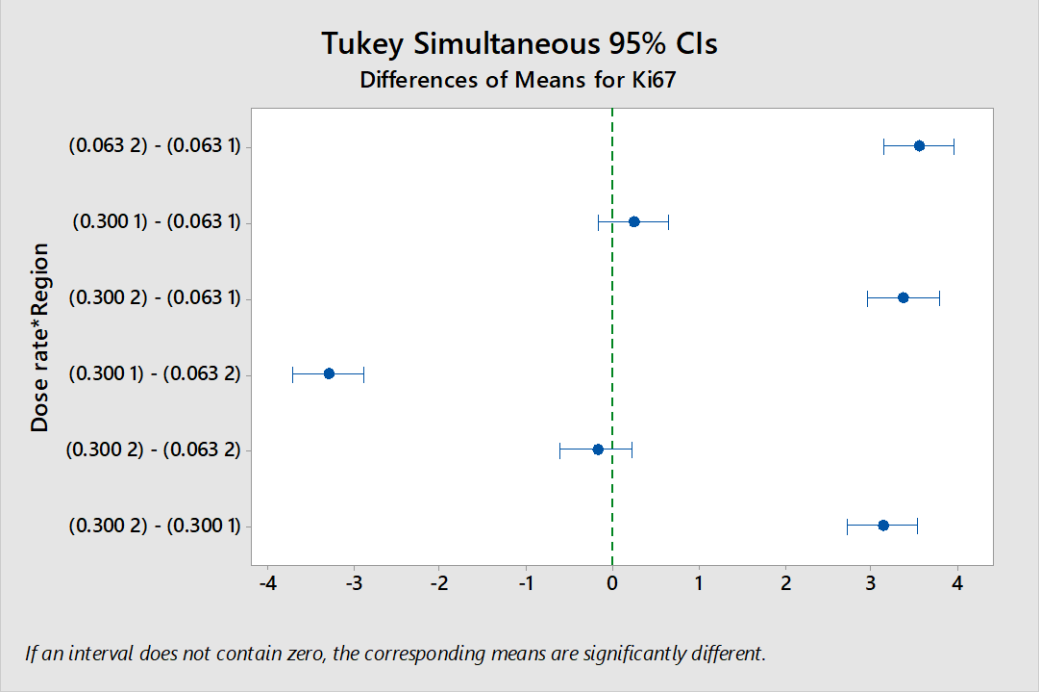

Tukey Simultaneous Tests for Differences of Means

Difference of Dose rate*Region Levels	Difference of Means	SE of Difference	Simultaneous 95% CI	T-Value	Adjusted P-Value
(0.063 2) - (0.063 1)	3.551	0.160	(3.140, 3.962)	22.16	0.000
(0.300 1) - (0.063 1)	0.243	0.158	(-0.163, 0.650)	1.54	0.416
(0.300 2) - (0.063 1)	3.360	0.161	(2.946, 3.774)	20.83	0.000
(0.300 1) - (0.063 2)	-3.308	0.159	(-3.717, -2.899)	-20.75	0.000
(0.300 2) - (0.063 2)	-0.191	0.160	(-0.602, 0.221)	-1.19	0.633
(0.300 2) - (0.300 1)	3.117	0.158	(2.711, 3.523)	19.69	0.000

Individual confidence level = 98.92%

*1 = Central, 2 - Peripheral

Figure 5.5: Post-hoc Tukey pairwise comparison results from dose-rate and lens epithelium region interactions. Several significant p-values from interactions are revealed.

5.4 Discussion

The influence of IR on LEC proliferation within the lens epithelium was not fully understood (Ainsbury et al. 2016). Whilst IR had been demonstrated to influence the lens epithelium (Markiewicz et al. 2015) using proliferation markers, the response of proliferation activity following doses at different dose-rates had not been previously investigated, although an effect had been

hypothesised (Hamada 2017b) (see also chapter 1; section 1.7.3). As discussed and outlined at length throughout chapter 1, the lens was often referred to as a radiosensitive tissue. More recently this had been attributed not to IR-induced cell killing, but because of excessive proliferation and subsequent abnormal differentiation, impaired DNA repair kinetics and non-targeted effects, to name a few (Hamada 2017b) effects following radiation exposure to the lens. It had previously been reported that radiation-induced effects upon LEC proliferation in the lens epithelium of mouse lenses were observable at 24 hours post-exposure (Markiewicz et al. 2015) following x-irradiation.

The identification and scoring of the central and peripheral regions (see chapter 2; section 2.7) of the epithelium were performed due to the known differences in proliferative activity of both (Duncan 1981), which suggested the response of each region to IR may be different given the cell cycle states of the LECs residing within them. The data from C57BL/6 mice in this chapter supported the known organisation of the epithelium (Duncan 1981), with the centrally located LECs having a much lower percentage of proliferating cells, measured here by identifying LECs positive for Ki67 expression following immunofluorescent staining (chapter 2; section 2.9), with the percentage of Ki67 positive cells being greater in the peripheral region. Whilst the peripheral region LECs were known to cycle at an increased rate with a greater number of cells in cycle, this rate was still relatively low, at around 4% as confirmed by the findings of this study and demonstrated in figures 5.1 and 5.3.

Cellular proliferation was reported to be a fairly slow process, with proliferating LECs dividing once every 17 – 20 days (Griep 2006). Whilst proliferative activity was significantly lower in the central region, there were clearly a small number of cells detected as being within cell cycle (Griep 2006). Proliferating cells were certainly known to be radiosensitive (Bakkenist and Kastan 2015; Costes et al. 2010), as discussed throughout chapter 1. Of the few studies that documented the effects of IR *in vivo*, low doses were first shown to increase LEC proliferation in rabbit lenses following x-irradiation 1952 (Von Sallmann 1952). An over proliferation of LECs followed by an adjustment period where proliferation rate returns to 'normal' was observed post-exposure. In 1980, it was suggested that IR-induced cataract occurred due to a 'pathological morphogenesis' in peripheral region LECs following x-radiation. This hypothesis suggested that mitotic changes in LECs demonstrated by abnormal cell densities in this peripheral region resulted in cataract formation. The data of this chapter supported the theory of central region LEC retaining some proliferative ability (Griep 2006), as Ki67 positivity remained above zero (figures 5.1 and 5.3). Proliferation in the LECs was thought to be abundant across the entire epithelium during embryogenesis and development of the lens but becomes compartmentalised quickly to the germinative zone in the

peripheral region (Chapter 1; section 1.3.2). However, when central region LECs were explanted into *in vitro* culture from 10 day old postnatal rats, a burst of cell proliferation was observed (McAvoy and McDonald 1984).

Radiation-induced cataract is possibly driven by altered proliferation or disorganisation of meridional rows in the epithelium. This was first observed during early studies exposing frogs to high doses of x-radiation, which discovered that IR-induced cataract was almost always preceded by a disorganisation of the meridional rows of the lens epithelium (Hayden et al. 1980). When proliferation was inhibited by hypophysectomy (removal of the pituitary gland), irradiation had no effect on the organisation of the meridional rows on the very edge of the lens epithelium. The researchers concluded that IR-induced cataractogenesis must be a result of a mitosis driven formation of abnormal LFCs due to damage or changes to the LECs in the meridional rows (Hayden et al. 1980). Acute X-ray exposure (although relatively lethal dose) of rabbit lenses also resulted in the disarrangement, along with nuclear changes, of LFCs in the bow of the lens as well as well as the peripheral region LECs approximately 1 week post-exposure (von Sallmann 1950). Furthermore, three weeks post-exposure revealed a decrease in the number of cells within this peripheral region, suggesting a lack of cell repopulation (von Sallmann 1950). Exposure of rabbit eyes to very high 15 Gy doses of x-rays resulted in complete inhibition of cell proliferation (as measured by mitotic divisions) as early as 30 minutes post-exposure and lasting several days (Von Sallmann 1952). Proliferation returned thereafter, and continued to increase to an overcompensation around one week later and lasting for approximately a further week. This proliferation 'overshoot', and then readjustment, acts as a catch-up mechanism attempting to regain lost mitotic divisions.

These observations have all supported the hypothesis for a substantial role of proliferation in cataractogenesis, particularly within the peripheral LECs, which are critical for the formation of new and healthy LFCs (Hayden et al. 1980), thus maintaining the growth and replenishment of the lens throughout life. Alteration from normal LEC proliferation rates can be detrimental to the organisation of the epithelium, particularly the meridional rows, leading to cataractogenesis (Hayden et al. 1980).

Inhibiting LEC proliferation had been demonstrated to give an increased radioprotection of the lens (Hayden et al. 1980; Rothstein et al. 1982). Following the induction of DSBs, DNA repair takes precedence. If LECs became damaged due to IR exposure, continuing to proliferate damaged, un-repaired or un-repairable cells would be disadvantageous in LECs, and in LFCs where proteolysis and protein synthesis are still active. As the amount of DNA damage and cell injury induced by IR

increases with dose, proliferation decreases as a protective measure against complex and un-repaired damage within the LECs, which was observed at around 1 Gy (Markiewicz et al. 2015) and up to lethal doses (von Sallmann 1950). Upon induction of DNA DSBs, tumour suppressor protein p53 levels increased within the cell, proportionally to the amount of damage the cell experienced (Levine 1997). This activation of p53 not only facilitates the repair of damage, but also has downstream repercussions influencing cell cycle check points and whether the cell continues to repair, continues to cycle or undergoes apoptosis (Levine 1997; Lieberman et al. 2017; Wride 2011). In the lens, p53 deficiency had been demonstrated to disrupt the lens capsule and the posterior migration of the lens epithelium (Wride 2011; Ikeda et al. 1999). The significant reduction in proliferation presented in this chapter agreed with previous studies following >1Gy IR exposures, which have demonstrated a decreased proliferative activity in the peripheral region of the lens epithelium (Markiewicz et al. 2015; Miller and Riley 1987; von 1950). This also supported the earlier work of von Sallmann (Von Sallmann 1952, 1950) where much higher doses of IR demonstrate a lasting inhibition of proliferation and cell disorganisation which preceded cataract formation. However, the observed suppression of proliferation to sub-control levels was curious at doses of 10 and 25 mGy at 24 hours post-exposure, although not statistically significant. This low-dose inhibition of proliferation suggested a non-linear response to IR. Extrapolating these results from those of the doses above 1 Gy, where proliferation is also inhibited to the point of cell disarrangement and morphological changes in early LFCs within the lens bow, would suggest that the dose range of 10 – 25 mGy may produce a similar disarrangement, which was thought to precede cataractogenesis. However, 50 and 100 mGy doses of heavy ion radiation had been demonstrated to induce meridional row disorganisation in the lenses of mice in two separate studies, at 64 weeks and 16 months post-exposure when irradiated at 3 – 4 months, slightly older than the ages used in the presented results of this chapter (Worgul et al. 1993; Tao et al. 1994). Therefore, the disorganisation of the meridional rows cannot be attributed to an induction or inhibition of proliferation, but certainly a general disruption to normal proliferation rates was clear based on the limited studies currently available.

5.4.1 Dose response of proliferation

Unexpectedly, the response of the central region LECs in the radiosensitive BALB/c strain appeared to show a slightly increased proliferation rate compared to the peripheral region. The response of the central region LECs in the C57BL/6 strain showed minimal response at the higher doses. The DNA damage and repair response was significantly strain dependant during the results of chapter 3. Exposure to 50 and 100 mGy induced a significantly increased response of Ki67 positive cells from that of control, 10 and 25 mGy exposures. The general trend of the results in

this chapter was the response to 25 mGy, and to a lesser extent 10 mGy, IR was statistically lower than from doses above 50 mGy. Low dose x-radiation (20 – 75 mGy) had been demonstrated to promote proliferation in lung fibroblast and lung cancer cells *in vitro* (Liang et al. 2016) as well as in bone marrow cells in mice *in vivo* (Jiang et al. 2008). The results of this chapter suggested a similar response of LECs that showed increased proliferation, peaking at 50 mGy and remaining moderately increased at 100 mGy, before decreasing at 1 Gy in a non-linear or bimodal action (hypothesised by figure 5.6).

Figure 5.6: Hypothesised bimodal/non-linear response of LEC proliferation

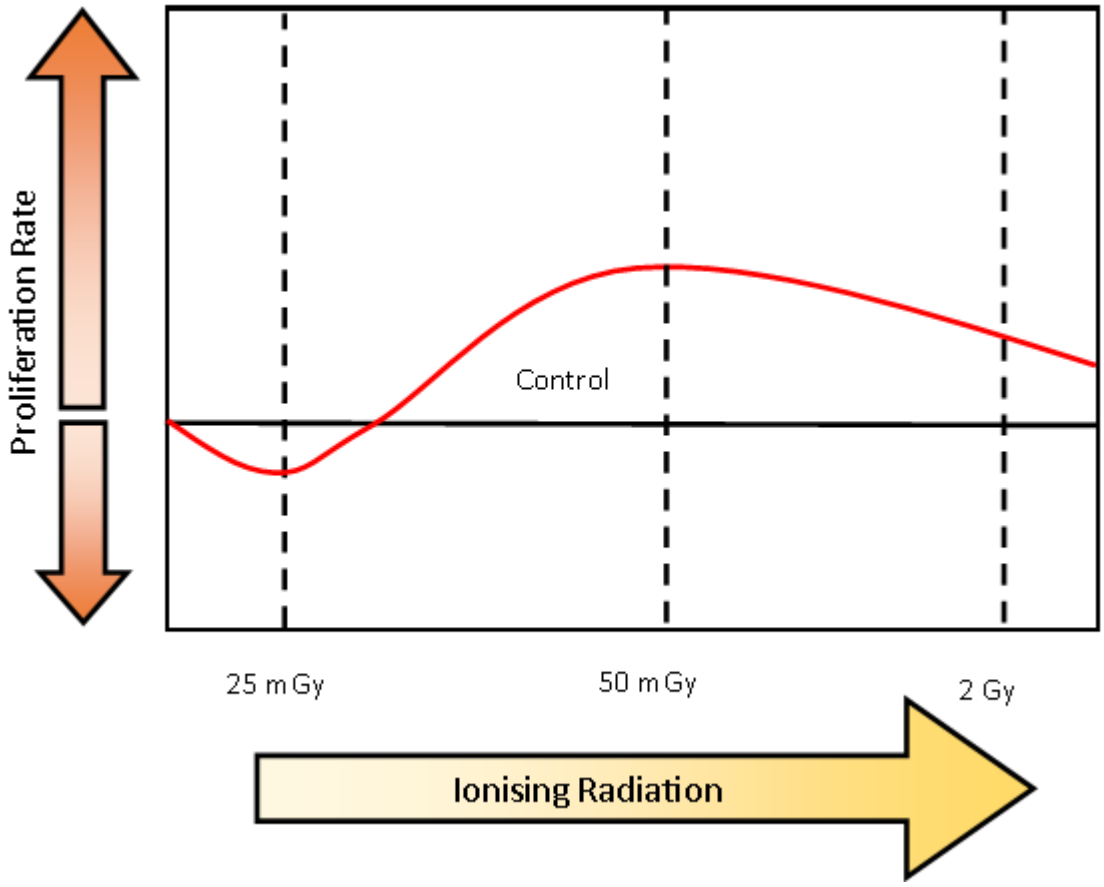

Figure 5.6: Representation of the hypothesised bimodal or non-linear response of proliferation to IR exposure adapted from the observed Ki67 responses seen in the LECs during this study. An initial inhibition or suppression of proliferation at 25 mGy, with an induction of proliferation peaking at 50 mGy prior to declining towards control rates.

The influence of IR dose on proliferation within the lens, whilst not fully understood, had been increasingly investigated, particularly with regards to low dose exposures such as those used during this chapter and the extent of the influence upon the lens epithelium. The potential influence of

dose-rate had been less discussed and investigated, but should be considered the next logical question given the uncertainty around low dose acute exposures.

The statistically significant effect at 2 Gy reducing the mean percentage of proliferating LECs in comparison to 0.5 Gy exposed mice and sham-irradiated controls suggested that this highest dose could represent a threshold, around which LEC proliferation decreases as a protective mechanism inhibiting the division of cells with complex or unrepaired DNA damage, as previously discussed. This proposed hypothesis (visualised by figure 5.6) could certainly be extrapolated from the high dose studies discussed which appeared to inhibit LEC proliferation completely. However, low doses of IR, particularly between 25 – 1000 mGy, as demonstrated during this study and in others (Markiewicz et al. 2015), were demonstrated to increase cell proliferation, supporting a non-linear or bimodal response hypothesis (figure 5.6). It had been suggested that this increase in proliferation could be an effort to repopulate cells lost due to cell cycle arrest or apoptosis (Von Sallmann 1952). Interestingly, proliferation had previously been observed to decrease in the lens epithelium as early as 30 minutes to 24 hours post-exposure, declining at around 1 Gy dose and reducing further to control values at 2 Gy when analysing EdU uptake and cyclin-D1 expression (Markiewicz et al. 2015). This was further supported by an observed significant increase in LEC density in both central and peripheral regions, increasing up to 250 mGy, but reducing at 1 and 2 Gy 24 hours post-exposure. This hypothesis is challenged when proliferation (analysed using Ki67 proliferative index) had been reported to increase following acute 3 Gy IR exposure in Ptch1 heterozygous mice, however this mutant demonstrated an increased proliferation of LECs naturally and mice were exposed at P2 and P10, young ages where proliferation was known to be at a higher frequency (De Stefano et al. 2015).

A previous study demonstrated increased levels of cyclin D1, thought to be involved in the signalling and induction of proliferation alongside DNA repair, following 100 and 250 mGy x-radiation exposure (Markiewicz et al. 2015). At higher doses (1 and 2 Gy) this effect was not observed. The results presented in this chapter suggested a similar pattern of activity, with a dose of 50 mGy inducing LEC proliferation significantly, but effects at 1 Gy not being significant. The significant increase in proliferating cells from control at 50 and 100 mGy ($p=0.009$ and 0.005 respectively) suggested a non-linear dose response, peaking at these doses. The non-linear response of the lens to IR had been recently suggested in other studies (Barnard et al. 2018; Markiewicz et al. 2015; Little et al. 2018), and the results of this chapter would support a similar mechanism. Whilst suppression of proliferation was observed following 10 and 25 mGy exposure, this striking observation was not significant from control, but these lower doses were significant from the higher doses. Whilst a significant effect of 2 Gy from control was observed (an increase

in proliferation at 4 hours, but a decrease at 24 hours), this p-value of 0.041 is very close to non-significance, with margins between SE being extremely close. In this low dose range, perhaps the most striking observation was the apparent suppression of cell proliferation at 25 mGy, coupled with the significant increase at 50 mGy (p=0.009).

5.4.2 Dose-rate influence on the response of proliferation

The use of both 0.063 and 0.3 Gy/min dose-rates during the exposures had allowed for some interesting discussion on the matter. During statistical analysis, only dose (p = 0.003) and region (central or peripheral) (p = >0.001) were significant during the initial ANOVA, with dose-rate not significant (p = 0.618). However, when interactions between the variables were analysed, dose-rate and lens epithelia region interactions stood out as being on the cusp of significance at p = 0.054. Therefore, dose (a significant certainty) and dose-rate (a strong possibility) influence LEC proliferation in a way that depends on whether the target cells were in the central or peripheral region of the epithelium. Regardless of statistical significance, post-hoc comparisons were performed on dose-rate and region interactions (figure 5.8). Whilst this interpretation of the data can be difficult to fully comprehend, the observation nevertheless was an interesting one, considering that the initial ANOVA revealed no significance of dose-rate, only epithelia region, however the interaction between both regions and the dose-rates suggested an effect tantalisingly close to significance (p = 0.054), which must be noteworthy regardless of lacking statistical significance. Several significant interactions between region and dose were revealed by post-hoc testing (figure 5.8).

Although this influence of dose-rate was more clearly demonstrated within the response of DNA damage (see chapter 4), the effect of dose-rate has a strong possibility to influence rates of LEC proliferation in the lens epithelium. Both regions of the epithelium are classified essentially by their proliferative activity, with the peripheral region housing the large majority of cycling cells, whilst the central region, though not completely devoid of cycling cells, is comprised mostly of less active quiescent cells.

The data and findings presented in this chapter confirmed significant effects of dose and epithelia region influencing the response of LEC proliferation activity within the lens epithelium. Although the hypothesised influence of IR dose-rate was less conclusive and an outright effect cannot be supported by these investigations, deeper interactions between dose-rate and lens epithelial region present a promising focus for further investigation.

It should be noted that there was a large amount of variance particularly visible at low doses in these data (see standard error bars in all figures), with inter-individual differences within cell proliferation rates being potentially higher than anticipated. However, the strains used during this project were inbred and therefore should be less genetically diverse than a human cohort would be as a result. Although the data have sufficient power, this low dose variance would likely suggest much larger numbers of mice would needed to detect significance that would certainly strengthen the findings. Nonetheless, the results presented suggest that LEC proliferation rates respond to radiation in a non-linear fashion (visualised by figure 5.7), supporting previous studies and hypothesis (Hamada 2017b). Whilst the influence of dose-rate remains unclear, each region of the lens epithelium is likely to be responding differently depending on the dose-rate at which exposure to a given dose of IR has been delivered.

All murine exposures during these studies were performed during the morning. This was to provide consistency whilst minimising the potential influence of circadian rhythm in the LECs (Wiechmann and Summers 2008), which has been suggested to affect the LECs by a diurnal rhythm in terms of mitotic division (von Sallmann and Grimes 1966). Given the time points post-exposure during this study, potential influence of circadian rhythm was a difficult aspect to manage; mice exposed in the morning may be sacrificed in the afternoon if they are part of a 4 hour time point, for example. Similarly, mice as part of a 24 hour time point post-exposure would be sacrificed the following morning. The influence of time of death, i.e. morning or afternoon, may have some impact on these data. However, the exact role of circadian rhythm has not been extensively studied or defined in the lens. Melatonin, a hormone demonstrated to influence circadian rhythm, is found in the lens and has had a suggested role in maintaining LEC function and proliferation, also potentially acting as a protector to cataract formation given its known antioxidant properties (Wiechmann and Summers 2008). The role of melatonin is not fully understood but would be expected to have an influence during IR exposure, whether significant or not.

Both C57BL/6 and BALB/c strains of mice were exposed during this study, classified as radioresistant and radiosensitive, respectively, as discussed during chapter 1; section 1.6.3.1. The radio-susceptibility status of each strain is derived primarily from observations of radiation-induced effects such as survivability, DNA damage repair efficiency and related tumour frequencies. Repair deficiency, as seen in the BALB/c mice, could have in influence of cell cycle efficiency and rates, for example 53BP1 is known to be involved not only in DNA damage repair but also in cell cycle progression via checkpoints (Fradet-Turcotte et al. 2013; Gupta et al. 2014; Levine 1997). Therefore, it is possible a repair deficient strain can have abnormal cellular proliferation activity. Strain is significant within this study (and during the DNA damage and repair response, chapter 3),

which would suggest that there is a genetic influence in IR-induced proliferation effects in the lens epithelium also.

During this study, both x- and γ-radiation exposures were used, therefore the low dose data were analysed separately from the higher dose dose-rate comparison data. Whilst a significant effect at such doses from both radiation sources was not expected, the data were not pooled as a precaution. However, both sources of radiation were calibrated to the same standard by the same persons as described during chapter 2: Materials and Methods. The variability of scoring from lens epithelium to lens epithelium should have little impact on the data, however, the monolayer tears easily (see chapter 2, section 2.4.3 and 2.4.3.1) therefore the amount of tissue recovered and analysed from each lens can vary. Low powered images were captured and scored remotely, and whilst bias was avoided, there was the possibility for images of better quality staining to be captured. The variability of the epithelial pieces that were isolated and stained were also one of the reasons why it was not possible to automate the imaging process. To minimise any further possible variability, reagents used during the immunofluorescent staining were kept constant by using the same products, suppliers and batches.

To summarise the key findings of this study, the data appeared to support the hypothesis of a non-linear or bimodal response of proliferation to IR in the lens epithelium. Whilst the peripheral region of the lens epithelium contained many proliferating cells, the minority of cycling cells remaining in the central region appear to respond to IR also. The interaction between dose-rate and lens epithelial region suggested there was greater investigation to be performed, with a differential response of both central and peripheral region potentially being dose-rate dependant, rather than simply dose dependant.

6. Lifespan imaging of the lens

In addition to investigating the early (≤ 24 hours post-exposure) effects of IR on the DNA damage response of LECs (chapters 3 and 4), and changes to their proliferation behaviour (chapter 5), the potential detection and progression of lens opacities to cataracts was monitored using the Scheimpflug imaging system and lens densitometry analysis (see chapter 2; section 2.10). Scheimpflug imaging had previously been demonstrated to be an accurate and precise technique to detect lens opacity changes and monitor cataractogenesis (Dalke et al. 2018; Fuchs et al. 2011; Puk, de Angelis, and Graw 2013). Scheimpflug imaging decreases scorer variability (Blumenthal and Serpetopoulos 1998; Eaton et al. 2017; van den Berg 2018) and allows for the grading of lens opacity by the well characterised LOCS III classification scale (Pei et al. 2008).

A total of 120 female C57BL/6 mice were whole body γ-irradiated at 10 weeks of age (see chapter 2, section 2.1). Only female mice were used during this study, as gender effects were not expected (Dalke et al. 2018) and this allowed many mice to be housed more efficiently. Each eye of the irradiated mice was imaged at monthly intervals for 18 months. Both the left and right eye of each animal was imaged approximately 1 week apart at every month. The mean lens density measurement was used as a measure of opacity across the lens, although minimum and maximum values were also recorded (Dalke et al. 2018) for each lens at every timepoint. Appendix D supplements this chapter or results.

6.1 Mouse survival

The C57BL/6 strain was selected for use in this study due to its radioresistant nature, facilitating the survival of the mice following up to 2 Gy irradiation (Newman et al. 2014; Roderick 1963) (see chapter 2, section 2.1). Mice that did not survive the 18 month observation period were recorded and post-mortems performed where possible (as reported in table 6.1).

Table 6.1: Time and probable cause of death for mice that did not survive to 18 months during lens lifespan imaging

Mouse	Date irradiated	Dose	Dose-rate	Date of death	Cause
A (RB)	18/12/2017	Control	0.3 Gy/min	29/01/2018	Non-recovery from scruffing
F (RT)	18/12/2017	Control	0.3 Gy/min	08/05/2019	Inflamed ears with broken skin
F (RB)	18/12/2017	Control	0.3 Gy/min	03/04/2019	Inflamed ears with broken skin
H (LT)	18/12/2017	1 Gy	0.3 Gy/min	04/02/2019	Leg paralysis
J (LT)	19/12/2017	Control	0.3 Gy/min	26/01/2019	Bowel tumour
L (LT)	19/12/2017	2 Gy	0.3 Gy/min	15/11/2019	Trauma, pale, very unwell and lethargic
M (RB)	19/12/2017	Control	0.063 Gy/min	10/04/2019	Dramatic weight loss and loss of energy
O (RB)	19/12/2017	0.5 Gy	0.063 Gy/min	17/04/2019	Loss of muscle tone, very weak

Table 6.1: A total of eight C57BL/6 mice did not survive the 18-month Scheimpflug observation period. Each mouse has a reported cause of death where possible.

During the observation period, a total of 8 mice were lost prematurely (Table 6.1), 6.66 % of the initial cohort of mice. Probable cause of death and post-mortem results revealed no obvious trend for a cause of death. Most notably, two mice which were cage-mates did develop (and eventually sacrificed as a result) an unusual skin condition around the ears and across the tops of the head. This condition presented itself initially as a small rash which worsened over time until the skin became very inflamed, broken and sore. Both mice developed the condition at a similar age. This condition had not previously been observed in the PHE animal housing facility, and could potentially have been a result of mice grooming their heads after the atropine drops were added prior to Scheimpflug imaging. However, it was not certain that this was the cause as it would have been expected to be seen in a greater number of mice (as all mice underwent the same procedure). Also noteworthy was the lack of radiation-induced premature death, with five of the eight mice who did not survive to 18 months being sham-irradiated controls rather than IR exposed. Nonparametric distribution analysis using the Kaplan-Meier method were performed on the survival data from the cohort of mice (figure 6.1) to identify any statistical significance or interaction between variables and mouse survival (Goel, Khanna, and Kishore 2010). The comparison of survival curves revealed no significant difference between each condition, with Log-Rank and Wilcoxon P-values being similar at 0.639 and 0.636 respectively. This indicates that the premature deaths did not significantly affect the data.

Figure 6.1: Survival plot for all 120 lifespan imaging C57BL/6 mice

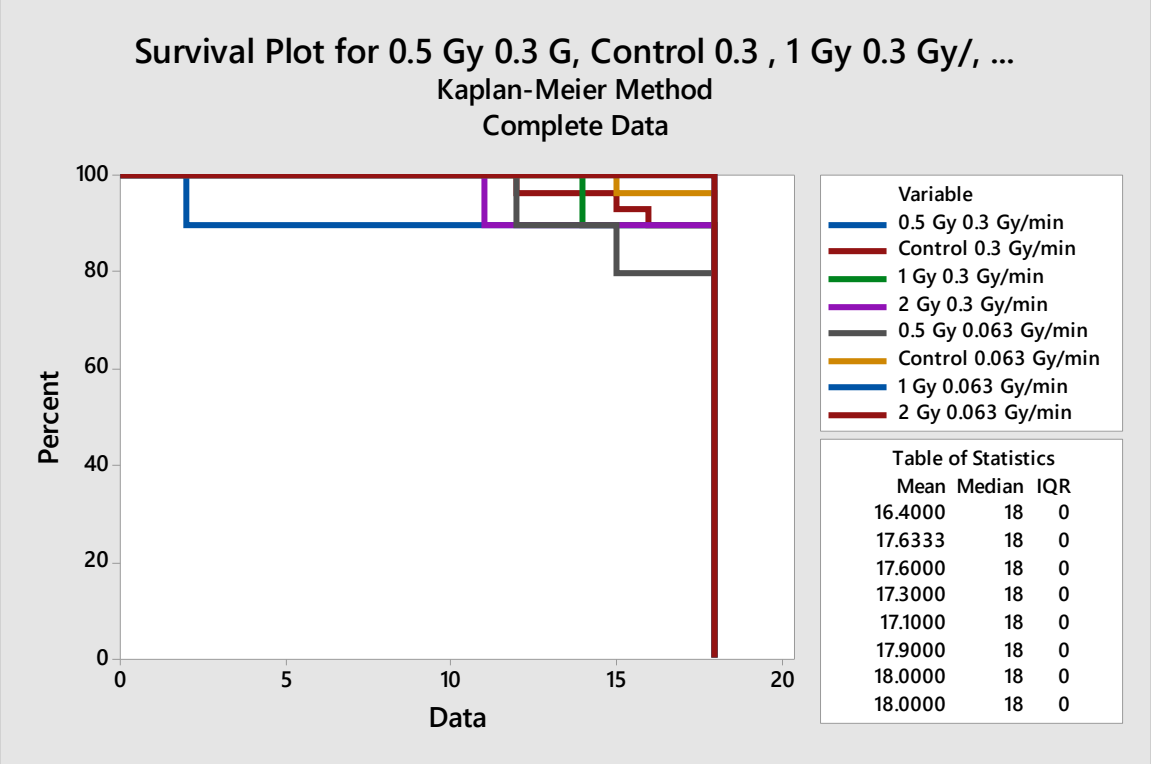

*Figure 6.1: Kaplan-Meier survival plot of mouse survival under all exposure conditions, including controls. Note were all mice sacrificed at 18 months. *'Data' = month post-exposure*

6.2 Scheimpflug lens densitometry results

Mean lens density measurements were collected from each lens monthly, over a period of 18 months post-exposure. The data are plotted for the three doses of 0.5, 1 and 2 Gy (including sham-irradiated control mice) when delivered by either 0.3 Gy/min (figure 6.2) or 0.063 Gy/min (figure 6.3). Mean lens density at the earliest post-exposure measurement, one month, demonstrated approximately 5 – 5.25% lens opacity for both dose-rates. A clear increase in mean lens opacity from first to last month could be seen in both graphs, and in all doses including sham-irradiated control mice. As is clear from both figure 6.2 and 6.3, the standard error bars plotted for each data point showed a considerable amount of cross over.

Table 6.2: Mean lens density following 0.3 Gy/min exposures to 0 – 2 Gy

Month post-exposure	Control	0.5 Gy	1 Gy	2 Gy	Control SE	0.5 Gy SE	1 Gy SE	2 Gy SE
1	5.14	5.08	4.87	5.14	0.06	0.08	0.08	0.13
2	5.30	5.01	5.10	5.10	0.07	0.10	0.09	0.07
3	5.16	5.17	5.11	5.21	0.05	0.11	0.07	0.09
4	5.21	5.14	5.16	5.23	0.05	0.07	0.11	0.14
5	5.22	5.22	5.03	5.31	0.05	0.09	0.06	0.08
6	5.37	5.25	5.30	5.38	0.06	0.11	0.09	0.12
7	5.51	5.39	5.41	5.35	0.05	0.10	0.14	0.09
8	5.49	5.56	5.71	5.63	0.47	0.32	0.11	0.10
9	5.63	5.46	5.61	5.77	0.07	0.08	0.41	0.08
10	5.79	5.74	5.92	5.64	0.06	0.11	0.11	0.13
11	6.13	6.08	5.92	6.10	0.08	0.11	0.10	0.16
12	6.02	6.14	6.00	6.16	0.09	0.13	0.10	0.11
13	6.06	6.10	6.14	6.20	0.07	0.12	0.13	0.30
14	5.92	5.78	5.92	5.84	0.13	0.16	0.11	0.19
15	6.29	6.13	6.46	6.28	0.14	0.19	0.23	0.22
16	6.19	6.28	6.16	5.80	0.08	0.16	0.09	0.11
17	6.41	6.16	6.30	6.32	0.14	0.18	0.19	0.12
18	6.39	6.37	6.20	6.43	0.08	0.10	0.15	0.13

Table 6.2: Mean lens density measurements over the 18 month observation period of mice exposed to 0.5, 1 and 2 Gy (and sham irradiated controls) with 0.3 Gy/min. Standard errors are also given.

Figure 6.2: Mean lens density in mice exposed to 0 – 2 Gy at 0.3 Gy/min

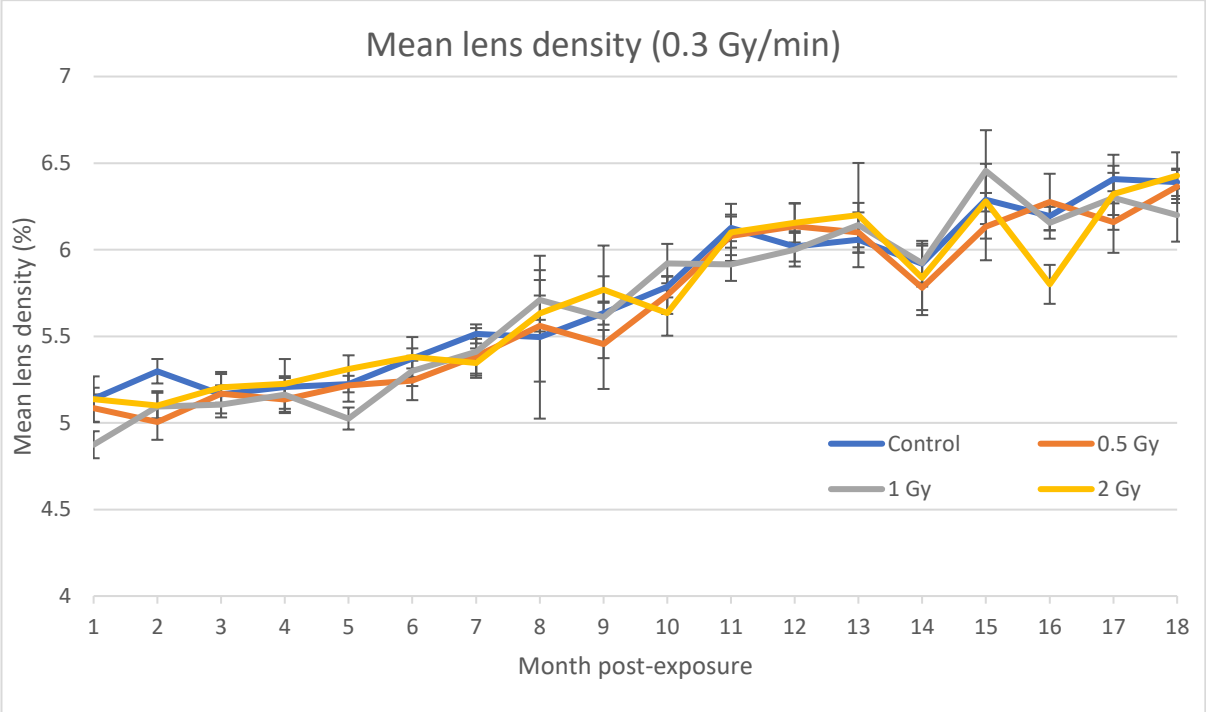

Figure 6.2: Mean lens density results from Scheimpflug imaging of mice exposed to 0.3 Gy/min doses, with standard error bars. General increase in lens opacity over time for all doses and sham-irradiated controls. Month post-exposure and dose statistically significant (p = <0.001 and p = 0.002 respectively).

Table 6.3: Mean lens density following 0.063 Gy/min exposures to 0 – 2 Gy

Month post-exposure	Control	0.5 Gy	1 Gy	2 Gy	Control SE	0.5 Gy SE	1 Gy SE	2 Gy SE
1	5.05	5.19	5.28	5.02	0.05	0.10	0.06	0.13
2	5.31	5.19	5.14	5.37	0.05	0.07	0.11	0.08
3	5.28	5.27	5.44	5.17	0.05	0.10	0.08	0.08
4	5.15	5.28	5.34	5.30	0.44	0.10	0.10	0.12
5	5.41	5.05	5.21	5.33	0.06	0.07	0.08	0.08
6	5.29	5.25	5.26	5.81	0.05	0.10	0.09	0.07
7	5.44	5.36	5.44	5.59	0.42	0.08	0.07	0.13
8	5.58	5.46	5.57	5.72	0.07	0.08	0.08	0.11
9	5.66	5.58	5.78	5.84	0.37	0.11	0.09	0.15
10	5.73	5.75	5.80	5.98	0.07	0.11	0.14	0.13
11	6.02	6.16	6.06	6.06	0.07	0.14	0.08	0.10
12	5.94	5.61	6.25	6.15	0.59	0.11	0.12	0.20
13	6.10	5.97	6.15	5.95	0.07	0.45	0.13	0.63
14	5.81	5.95	5.78	6.12	0.09	0.22	0.12	0.17
15	6.15	6.12	6.39	6.67	0.09	0.16	0.13	0.14
16	6.25	6.16	5.99	6.40	0.08	0.14	0.11	0.20
17	6.37	6.23	6.14	6.37	0.08	0.12	0.11	0.57
18	6.41	6.56	6.37	6.49	0.08	0.14	0.12	0.12

Table 6.3: Mean lens density measurements over the 18 month observation period of mice exposed to 0.5, 1 and 2 Gy (and sham irradiated controls) with 0.063 Gy/min. Standard errors are also given.

Figure 6.3: Mean lens density of mice exposed to 0 – 2 Gy at 0.063 Gy/min

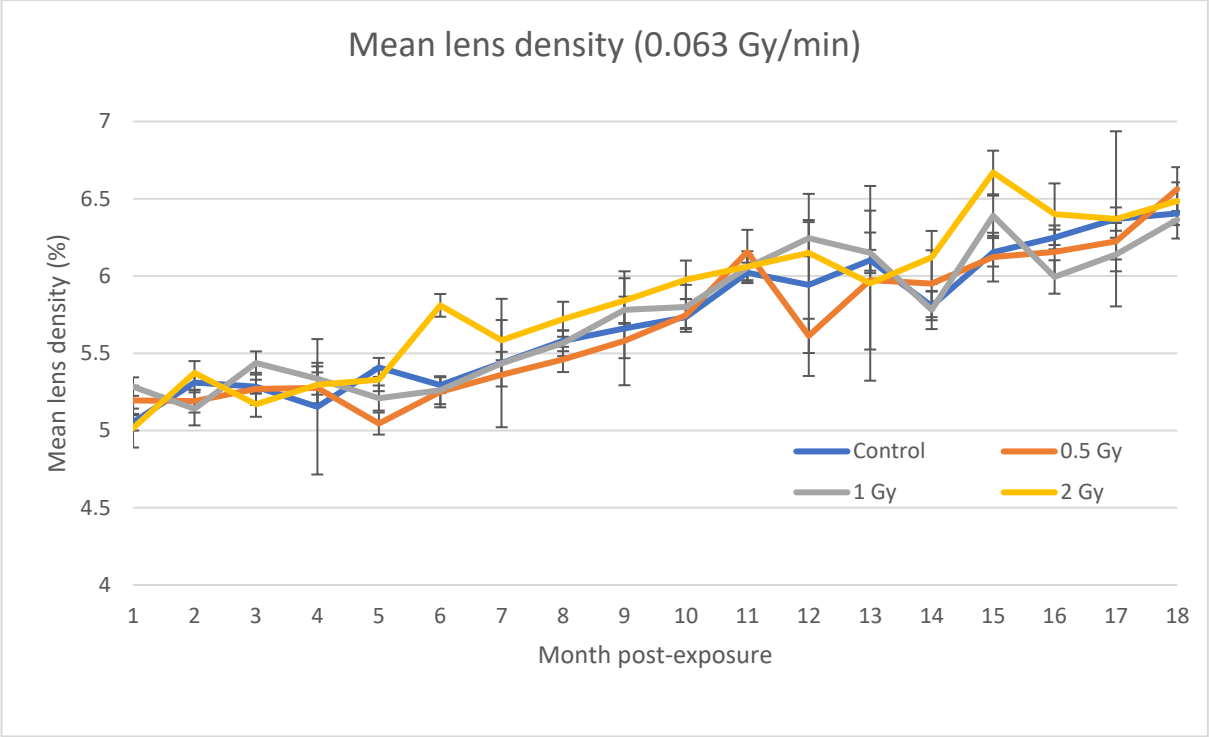

Figure 6.3: Mean lens density results from Scheimpflug imaging of mice exposed to 0.063 Gy/min doses, with standard error bars. General increase in lens opacity over time for all doses and sham-irradiated controls. Month post-exposure and dose statistically significant (p = <0.001 and p = 0.002 respectively).

In total, 3,896 lens images, or data points, were generated and lens density measurements calculated from during the observational period. Using general linear ANOVA, the mean lens density data were analysed for statistical significance across all variables; month (post-exposure; 1 - 18), dose (Control, 0.5, 1 and 2 Gy) and dose-rate (0.063 or 0.3 Gy/min). Month post-exposure proved strongly significant (p = <0.001), confirming an age-related increase in mean lens density across all doses and within both dose-rates. Interestingly, dose was also strongly significant (ANOVA p = 0.002). Further post-hoc Tukey pairwise comparisons revealed this was due to a statistically significant difference between 0.5 and 2 Gy in both dose-rates, but not with any other dose or from control. Figures 6.5 and 6.6 present this observation clearly, with both 0.5 and 2 Gy doses only plotted for each dose-rate. The statistically significant increase of mean lens density following 2 Gy exposure appeared more prominent with the 0.063 Gy/min dose-rate. Dose-rate was significant at p = 0.01, prompting further interaction analysis. This revealed a significant interaction between dose and dose-rate (dose*dose-rate) with p = 0.018. Post-hoc Tukey pairwise analysis of dose*dose-rate interaction revealed 2 Gy delivered at 0.063 Gy/min being significant from all other doses and from the higher 0.3 Gy/min dose-rate. Therefore, delivering 2 Gy IR at 0.063 Gy/min significantly increased mean lens density compared to sham-irradiated control mice,

and compared to 2 Gy delivered at the higher dose-rate of 0.3 Gy/min, which did not increase mean lens density.

Figure 6.4: Post-hoc Tukey comparison of dose*dose-rate significant interactions in lifespan imaging mice

Grouping Information Using the Tukey Method and 95% Confidence

Dose*Dose rate	N	Mean	Grouping	
2.0 0.063	327	5.83795	A	
1.0 0.063	330	5.74535	A	B
0.0 0.300	945	5.73442		B
0.0 0.063	988	5.72465		B
2.0 0.300	320	5.71562		B
1.0 0.300	328	5.67466		B
0.5 0.063	323	5.67341		B
0.5 0.300	335	5.67166		B

Means that do not share a letter are significantly different.

Figure 6.4: Tukey comparison grouping results from the significant interaction between dose and dose-rate revealed by general linear ANOVA. 2 Gy delivered at 0.063 Gy/min is statistically significant form all other dose and dose-rate combinations, except for 1 Gy delivered at 0.063 Gy/min.

Figure 6.5: Comparison of mean lens density in mice exposed to 0.5 and 2 Gy significant doses at 0.063 Gy/min

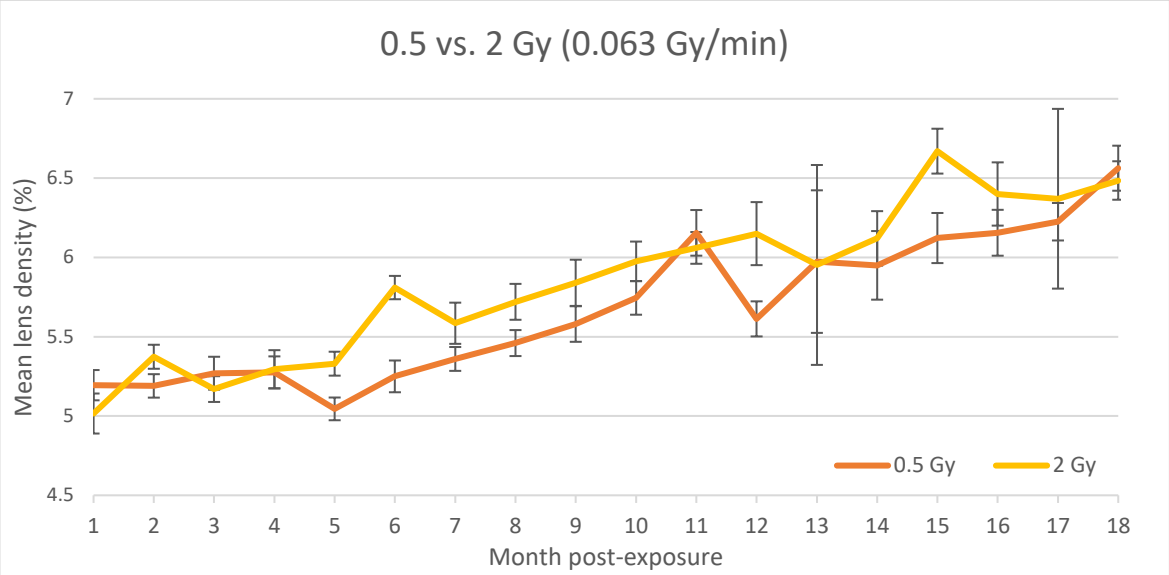

Figure 6.5: Mean lens density (%) following 0.5 and 2 Gy doses delivered at 0.063 Gy/min plotted against each other over the 18-month observation period. Both doses are statistically different from one another (p = 0.002)

Figure 6.6: Comparison of mean lens density in mice exposed to 0.5 and 2 Gy significant doses at 0.3 Gy/min

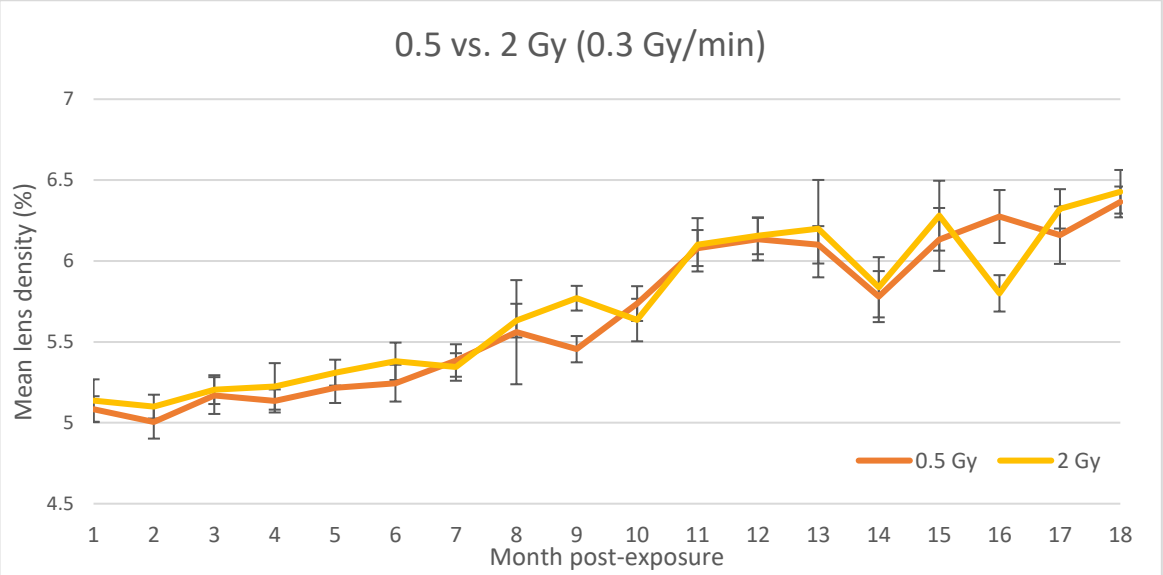

Figure 6.6: Mean lens density (%) following 0.5 and 2 Gy doses delivered at 0.3 Gy/min plotted against each other over the 18-month observation period. Both doses are statistically different from one another (p = 0.002)

The most significant variable was month post-exposure. This effect was very clear from the data, presented in all the graphs here. The first five months of observations showed no significant increase in mean lens density, but at the sixth month, significant increases were seen in both dose-rates at all doses. Figure 6.7 demonstrates this most clearly, using Tukey grouping information for all 18 months.

Figure 6.7: Tukey comparison of month post-exposure

Grouping Information Using the Tukey Method and 95% Confidence

Month	N	Mean	Grouping
18	217	6.39490	A
17	217	6.31630	A B
15	114	6.27879	A B C
16	197	6.17025	B C D
13	228	6.08044	C D
11	234	6.06504	D E
12	233	6.01761	D E
14	111	5.87554	E F
10	235	5.77881	F G
9	236	5.65817	G H
8	236	5.57078	H I
7	238	5.44471	I J
6	237	5.35132	J K
5	237	5.25054	K L
3	235	5.22414	K L
2	236	5.22374	K L
4	235	5.20682	K L
1	220	5.09396	L

Means that do not share a letter are significantly different.

Figure 6.7: Tukey comparison of mean lens density versus month post-exposure. No significant change is seen in the first 5 months, followed by a steady significant increase in mean lens opacity up to 18 months post-exposure.

6.3 Discussion

Kleiman *et al.* (Kleiman et al. 2007) previously demonstrated, whilst not using Scheimpflug but slit-lamp imaging, the detection of IR-induced cataract following 0.5 Gy x-irradiation in approximately 50% of WT mice, and in a greater percentage in DNA repair deficient heterozygous mutant mice. The dose of 0.5 Gy was therefore chosen as the upper 'positive' control dose in the lifespan imaging study by Dalke *et al.* (Dalke et al. 2018) more recently. This lifespan study by Dalke *et al.* (Dalke et al. 2018) was investigating the effects of dose limit on detectable cataract formation using the more sensitive Scheimpflug imaging system. With 0.5 Gy identified as the positive control, reduced doses of 0.125 and 0.063 Gy were also incorporated during exposures of DNA deficient (heterozygous Ercc2 mutants (Kunze et al. 2015)) mice. During the Dalke *et al.* (Dalke et al. 2018)

study, mice were also imaged monthly for a period of 24 months as opposed to the 18 month period undertaken in the study presented in this chapter. Reducing the observation period to 18 months counteracted the possible increase in mortality predicted with higher (1 and 2 Gy) whole body IR-exposure doses, however C57BL/6 have demonstrated higher rates of survival compared to other strains following >1 Gy IR-exposure (Roderick 1963). Coincidently, even radiosensitive and DNA repair deficient Ercc2 mutant mice showed approximately 75% population survival at 18 months following 0.5 Gy irradiation (Dalke et al. 2018). Whilst this percentage does not seem dramatic, it is a significant reduction of lifespan compared to control. Historic studies of IR-induced cataract have tended to perform focused irradiation of the eye (Kleiman et al. 2007) where damage is localised to the lens, however whole body irradiations such as those used during this thesis could inevitably have resulted in higher mortality rates due to secondary health effects such as cancers and tumours. By using a strain demonstrated to resist some of the IR-related (Barnard et al. 2018; Carreras et al. 2019; Mukherjee, Sainis, and Deobagkar 2014; Roderick 1963) effects improved the probability of the mice surviving the duration of the observation period. C57BL/6 mice have a black fur coat which had been identified as the most suitable phenotype for achieving the best imaging results using the Scheimpflug system (Fuchs et al. 2011; Puk, de Angelis, and Graw 2013).

Previous studies of IR-induced cataract in mice have used radiosensitive heterozygous mutants Atm and Mrad9 (Kleiman et al. 2007; Worgul et al. 2002; Worgul et al. 2005; Hall et al. 2006), and more recently the *Ercc2*/Xpd heterozygous mutants (Dalke et al. 2018; Kunze et al. 2015). Whilst these heterozygous mutants were chosen as they were identified as being susceptible to IR-induced cataract, they were not necessarily representative of the human population. Therefore, the use of an inbred strain of mice was deemed more representative (Carreras et al. 2019).

The Scheimpflug technique was established as the grading classification of choice for human with most animal models using slit lamp imaging. Later, not only grading of cataract formation, but the monitoring of opacity progression was made possible using more a more advanced imaging technique; the Scheimpflug system. This technique was again first demonstrated in animals using rats (Hockwin et al. 1984), and quickly demonstrated by direct comparison to slit lamp grading in mice (Takizawa and Sasaki 1986). In the last decade, Scheimpflug imaging had been successfully adapted from human to mouse lens analysis, most notably it had been implemented in the German Mouse Clinic (Munich, Germany) to track lens density and opacification increases in the mouse models (Puk, de Angelis, and Graw 2013; Kunze et al. 2015; Dalke et al. 2018; Fuchs et al. 2011). Scheimpflug imaging is a considerable improvement to measure the progression of lens opacity *in vivo* in a more accurate and quantitative way (Dalke et al. 2018). Many studies of

radiation-induced cataract in animals over that past few decades have used the slit-lamp system to score and grade lens opacity and cataract. Use of the Scheimpflug imaging system for the study of radiation-induced cataract has predominantly been demonstrated by, as previously mentioned, the German Mouse Clinic. Most recently, a lifetime study was performed using B6C3F1 wild type and B6RCF1 *Ercc2* heterozygous mutant mice following whole body acute low-dose ^{60}Co gamma exposure to doses from 0.063 to 0.5 Gy (Dalke et al. 2018) revealed some interesting results. As previously mentioned, the *Ercc2* gene is involved in DNA repair (Kunze et al. 2015). Homozygous *Ercc2* mutants show development of both cortical and nuclear cataracts, hence why this model was chosen essentially as a positive control for radiation-induced cataract. The study performed monthly imaging of both male and female mice from both mutant and WT, up to 24 months post-irradiation. The researchers grouped the lens density data into 'first four' and 'last four' months to reduce heterogeneity in the data. Whilst no effect of genotype was seen in that study ($p = 0.414$), the study could detect a dose-dependent increase in lens opacity of around just 1% at the highest dose of 0.5 Gy. However, this 1% increase in (maximum) lens opacity relates to a LOCS III score much less that that considered clinically to be visually impairing. This study by Dalke *et al.* (Dalke et al. 2018) represented a comprehensive approach to investigating radiation-induced lens opacity using the Scheimpflug imaging system to quantify opacity in a way more accurate and precise than previously used techniques. The lack of cataract induction even at the highest dose of 0.5 Gy (a dose previously reported to induce cataract rapidly) could suggest that the strain of mice used (*Ercc2 +/-*) were radioresistant at 0.5 Gy, although this is unlikely as radiation-induced cancers and chromosomal aberrations increased, along with a general shortening of lifespan suggesting that these mice were significantly affected by this dose (Dalke et al. 2018). As has been discussed from earlier studies using the slit lamp, 0.5 Gy of IR exposure resulted in cataract formation in DNA repair deficient mice, as observed and graded via slit lamp. However, the Scheimpflug has not been demonstrated to support these previous studies using its more advanced densitometry image analysis. This could be due to the low dose-rate at which the dose was delivered. Dalke *et al*. (Dalke et al. 2018) used a dose-rate of 0.063 Gy/min, with Worgul *et al*. (Worgul et al. 2002; Worgul et al. 2005) and Kleiman *et al*. (Kleiman et al. 2007) using 0.5 Gy/min (Hall *et al*. (Hall et al. 2006) do not specify dose-rate). It is concluded that an increase in dose-rate, dose and alternative strain could explain the differences in results for future studies.

The aim of the study presented in this chapter was not to replicate those previous studies by Dalke *et al.* (Dalke et al. 2018), but to modify and adapt the methodologies to identify the effects of not only dose, but dose-rate, upon mean lens opacity changes. Since the potential influence of dose-rate had been much hypothesised (Hamada 2017b; Little et al. 2018) and known to be

significant in the DNA damage response of LECs (see chapter 4), it was important to incorporate a second higher dose-rate of 0.3 Gy/min alongside the replicated existing dose-rate of 0.063 Gy/min. Whilst the study by Dalke *et al.* (Dalke et al. 2018) exposed mice to a series of low doses (0.063, 0.125 and 0.5 Gy), the limited lifespan of a mouse may well have been a factor in the lack of significant dose effects in mean lens density measurements. Therefore, whilst retaining 0.5 Gy as the lowest dose, 1 and 2 Gy doses were also incorporated not only to hopefully decrease the latency period of cataract induction, but also to include higher doses as positive controls of IR. With increasing exposure doses, there was an inevitable increased risk to mouse mortality rates, therefore, a radioresistant strain of mice was chosen, the C57BL/6, which had been demonstrated to survive such doses of IR particularly well (Barnard et al. 2018; Mukherjee, Sainis, and Deobagkar 2014; Roderick 1963).

A group size of 19 mice was previously identified as adequate for detecting a statistically significant 2% opacity change between mice (Puk, de Angelis, and Graw 2013).

The 6.6 % premature loss of mice, regardless of irradiation or dose, was much lower than the losses seen in the previous 2018 study by Dalke *et al.* (Dalke et al. 2018), where a loss of ~25% of mice had occurred after 18 months, albeit B6RCF1 (F1 hybrid of C3H and C57BL/6) WT and *Ercc2*$^{+/-}$ mice were used as opposed to the more radioresistant C57BL/6 used in this study. Aside from the statistically significant dose and dose-rate findings, the significantly higher survival of the C57BL/6 mice presented here suggested the use of this radioresistant strain was highly justified. Although not statistically significant, the study by Dalke *et al.* (Dalke et al. 2018) observed an increased survivability of mice exposed to 0.063 Gy compared to sham-irradiated controls. It was perhaps then noteworthy that five of the eight premature deaths from this study were sham-irradiated controls rather than irradiated mice.

The data presented in this chapter demonstrated a mean lens density/opacity of around 5 - 5.25% in all the 14-week-old C57BL/6 mice, the age of the mice during the first observation, one month post-exposure when they were 10 weeks of age. This value was almost identical to mean lens density previously observed in B6RCF1 mice lenses at one month post-exposure (Dalke et al. 2018), which increased by about 1.5% after 18 months. The findings here supported both the initial mean lens density value and an almost identical age-related increase in mean lens density as previously reported (Dalke et al. 2018) using a C57BL/6 hybrid strain. A 5% mean lens opacity was also reported in similarly aged 2-month-old inbred C57BL/6 (Puk, de Angelis, and Graw 2013). After 12 months, these unirradiated C57BL/6 mice were observed to have had an increase of around 1% mean lens density, which was supported by observations in the study presented here. This increase

in lens density is thought to be due to faint nuclear opacities or slight cortical opacities that develop due to aging (Dalke et al. 2018; Puk, de Angelis, and Graw 2013). These similarities in results from multiple previous studies suggested a very strong reproducibility of the Scheimpflug imaging technique, which is promising for future study comparisons and also for results generated from the LDLensRad consortium (https://www.researchgate.net/project/LDLensRad-the-European-CONCERT-project-starting-in-2017-Towards-a-full-mechanistic-understanding-of-low-dose-radiation-induced-cataracts).

These significant findings of dose ($p = 0.002$) and dose-rate ($p = 0.01$) influencing mean lens density, as well as revealing that these significant variables can be attributed to the significant interactions between dose and dose-rate ($p = 0.018$), have identified that mice exposed to 2 Gy IR at a dose-rate of 0.063 developed an increased mean lens opacity, potentially leading to cataract manifestation, compared to sham-irradiated controls. This result was particularly striking as exposure to 2 Gy and the higher 0.3 Gy/min dose-rate yields no such significance, therefore the lower dose-rate had a greater potency on the opacity of the lens.

The mean lens density data plotted in figures 6.2, 6.3, 6.5 and 6.6 have standard error bars included. There are clearly some minor perturbations from month to month, which were also observed in the study by Dalke *et al*. (2018) (Dalke et al. 2018). Lens densitometry measurements are not automated, that is, the user must manually select the line along which the measurement is calculated. This changes from image to image, as described in Chapter 2: section 2.10, to allow for the exclusion of the reflection spot. To limit variability, the same 'scorer' was used to analyse all images. Post-hoc power calculations comparing months 1 and 18 (2 Gy 0.3 Gy/min for example here) revealed a significantly lower sample size of just 7 animals (actual power 0.81) was required for significance of month. However, using the same 2 Gy (0.3 Gy/min) exposure group, for month to month (9 and 10 months for example) perturbations to be significant, a sample size of 338 would be required.

The findings of this study are important, but it is also key to take into consideration the properties of the technique that could influence variability. The reliability and repeatability of lens densitometry data were accepted as being very high (Kirkwood et al. 2009; Weiner et al. 2014) in human patients, however it should be noted the system is not calibrated for animal use. The human lens is smaller in relation to the entire eye and sits at the anterior of the eye, behind the cornea. However, in mice, the lens is much larger in relation to the eye and appears to fill the entire ocular space behind the cornea. Therefore, the back of the lens sits much further back very close to the

retina. Even during maximum dilation of the eye, the back of the lens was not always visible during imaging.

Historically, PSC were thought to be induced by IR, but more recently it is thought that IR accelerates the process of age-related cataract, or add to the 'cataractogenic load', which can also include cortical and nuclear cataract development (Alice Uwineza and Hamada 2019; Ainsbury et al. 2016; Ainsbury et al. 2009). During the capture of lens images using the Scheimpflug imaging system, it was apparent that there is some variation in image quality, particularly the proportion of the lens that was visible during image acquisition due to inter-individual differences in the mice. Therefore, opacities or cataracts developing in the posterior region of the lens may not be observable in all lens images using the Scheimpflug system. However, using the measurement of mean, rather and maximum, lens density was most likely to detect opacities developing in the lens cortex or nucleus. In terms of the significance of the results presented here, the increased mean lens density occurring post-exposure to 2 Gy (0.063 Gy/min) was potentially an IR induced acceleration of early cortical or nuclear age-related cataract. It was important to remember that the Pentacam Scheimpflug imaging system is optimised for human rather than rodent lenses.

Whilst this significant finding was particularly interesting as it occurred only at a lower dose-rate, it is important to remember that an increase of 2% mean lens density is expected as an aging effect in mice (Puk, de Angelis, and Graw 2013). However, the natural density of the lens had been increased because of IR exposure in the data presented here due to the significance from sham-irradiated control animals. To fully appreciate these results presented and to give some perspective, the comparison between Pentacam Scheimpflug imaging systems and the LOCS III grading criteria needs to be understood. Such investigations have revealed that the LOCS III grading method was a highly satisfactory scoring method which could be applied to Scheimpflug images to interpret the results (Pei et al. 2008). Furthermore, according to the LOCS III criterion of 14.1% lens opacity for a type 2 cataract in humans, which had been defined as the beginning for vision impairment according by Pei *et al*. (Pei et al. 2008), this should be the value of opacity required for cataract classification during this study.

Whilst doses as low as 0.5 Gy had previously been demonstrated to induce cataract in mice (Hall et al. 2006; Kleiman et al. 2007; Worgul et al. 2002; Worgul et al. 2005) deemed more radiosensitive, it should be reiterated, as previously discussed, that these previous reports of IR-induced cataract were analysed using slit-lamp rather than Scheimpflug imaging, and classified using the Merriam-and-Focht scoring system (Merriam and Focht 1962). This system was developed using very high dose and localised (rather than whole body) exposures to the lens, up to

40 and 50 Gy. At such doses, severe changes to the mitotic activity of LECs in the lens epithelium occur, particularly the peripheral region occur, which are much less pronounced at lower doses (Dalke et al. 2018). The Scheimpflug imaging system is substantially more advanced and enabled the sensitive quantification of opacities accurately, as oppose to the less sensitive grading system that slit lamp analysis is restricted to.

The IR-induced increase in means lens opacity evidenced not only a significant effect of dose but suggested an inverse dose-rate effect due to no significant effects being seen in 0.3 Gy/min exposures. Whilst this increase in mean lens density was still a long way from being a classified IR-induced cataract, this was the first evidence of an inverse dose-rate sensitivity of the lens to IR-induced lens opacity.

7. Additional discussion and conclusions

To understand fully the important findings in these studies (table 7.1), a return to the four research questions which this thesis aimed to address can provide a broader context and perspective:

7.1 ***The effects of low dose IR exposure are not fully understood within the lens. Evidence suggests a possible differential response at low compared to high dose IR. The DNA damage response at low doses are investigated across four strains of mice in-vivo to determine the effect of low dose IR in inducing DNA DSBs and repair in the lens epithelium. Strain dependency of the lens in response to IR can help to explain population variance and individual susceptibility. Genetics are thought to have a greater influence in low dose IR response. Thus, the hypothesis to be investigated in this thesis is that low dose IR impacts the DNA damage response in the lens epithelium in a genetic-dependant manner.***

Low dose exposures of four murine strains revealed radioresistant C57BL/6 and radiosensitive BALB/c mice were the most suitable for analysing the radiation-induced DNA damage response in the lens epithelium (see chapter 3). The analysis of DNA damage via 53BP1 foci in flat-mounted lens epitheliums had only recently been reported (Markiewicz et al. 2015), but not employed for large scale studies. 53BP1 showed a significant dose response in LECs, and was strongly strain dependant. Both C57BL/6 and BALB/c represent the most useful models for investigating the effect of low dose radiation on the DNA damage response of the lens epithelium. This study justified the need for identifying a suitable mouse strain(s) to ensure findings can be relied upon in a practical and reproducible way. Chapter 3 evidences not only the different levels of variance within difference inbred strains, but also the differential response between the central and peripheral region LECs which may also suggest different cellular organisation from strain to strain; region is not significant across all strains (supported by unpublished LDLensRad data from other endpoints). These findings support genetic sensitivity being more critical than the exposure at low doses of IR in the lens (Kleiman et al. 2007), crucial in understanding the variable outcomes in occupational exposure studies. This study would also support the idea of the lens not being as radiosensitive as previously thought (Dalke et al. 2018), but that a different mechanism of repair of different dependence on known repair systems may occur that is not seen in other studied tissues.

7.2 ***The effect of not only dose but also dose-rate is not well understood. The ICRP recommend dose limits but do not make comment on the delivery of that dose. Recent epidemiological studies suggest the effects of low versus high dose-rate may not be uniform in IR-induced cataract. Thus, the hypothesis to be investigated in this thesis is whether using***

multiple dose-rates to ascertain whether the in vivo DNA damage response is dose and/or dose-rate dependant.

In chapter 4, the most surprising and striking effect was the inverse dose-rate response of DNA damage and repair in the LECs, but not in lymphocytes collected from the same animals. An inverse dose-rate response in the lens had been hypothesised recently but lacked biological evidence (Little et al. 2018; Hamada 2016). The results suggested that, whilst the role of IR-induced DNA damage and repair may not be exclusively responsible for cataractogenesis, the inverse dose-rate response was observed for both DNA repair foci (described in chapter 4) and observed in mean lens opacity increase (described in chapter 6). It is hypothesised that reduced DNA repair efficiency at lower dose-rates may be due to the influence of growth factors present across the lens but not in uniform concentrations, creating a differential response between central or peripheral LECs. LEDGF is the best example of this, as discussed, where peripheral region LECs are exposed to lower concentrations than the central region LECs (Kubo et al. 2003), contributing towards a slower DNA repair response in the peripheral region. The involvement of LEDGF requires *in vivo* endpoints rather than *in vitro* models to accurately test this hypothesis. In terms of the inverse dose-rate response of DNA repair in the LECs seen in this thesis, low dose-rates allow 53BP1 foci to persist/remain unrepaired in the proliferating peripheral region LECs, allowing for proliferation and differentiation to continue. When dose-rates were higher, DNA repair is favoured and so proliferation and differentiation are supressed. The statistical significance of dose-rate was further compounded/evidenced by interaction analysis, where dose and dose-rate must be considered in the context of one another, rather than as independent variables.

7.3 ***LEC proliferation and differentiation are naturally well-regulated and controlled, a characteristic essential for lens function. The impact of IR on LEC proliferation behaviour has been demonstrated in historic studies, however the impact of dose and dose-rate in proliferation has not been well described. Thus, the hypothesis to be investigated in this study is whether IR causes disruption to normal proliferation behaviour, suggesting subsequent aberrant differentiation and cell migration.***

IR-induced cataractogenesis has been suggested to occur due to altered LEC proliferation. Therefore, cycling LECs largely residing in the peripheral region of the lens epithelium were most at risk of IR. This study confirmed that most Ki67 positive cells were indeed located in the peripheral region of the lens epithelium (chapter 5). A dose of 2 Gy significantly reduced the mean percentage of Ki67 positive cells compared to sham-irradiated controls. An observed suppression of proliferation at 10 and 25 mGy doses (although not significant from control) was seen. The

investigation of IR-induced effects of LEC proliferation was conducted up to 24 hours post-exposure. Whilst statistically significant effects were seen, including interactions between dose-rate and lens epithelia region, no significant time response was seen. A hypothesis for a non-linear or bimodal response has been proposed, further investigation is needed to support this hypothesis more fully. Whilst previous studies suggest a role of altered proliferation during IR-induced cataractogenesis (Von Sallmann 1952; Von Sallmann, Grimes, and Mc 1962), this was not observed at the low doses of this study. Changes in lens aspect have been reported post-exposure to low doses (Markiewicz et al. 2015) which coincide with non-linear responses of EdU incorporation and cyclin-D1 expression. However, lens aspect changes were seen 10 months after irradiation, along with cell density changes at 24 hours. Lens aspect ratio could be explained by an increased volume of LECs around the lens equator, leading to significantly different lens shape. Therefore, the increase in cell density in the peripheral region would most likely be due to an increase in cell proliferation, but with progeny cells not able to immediately differentiate.

7.4 *Scheimpflug imaging is a proven sensitive technique for quantifying and tracking lens opacity in mice. This technology allows for the monitoring of lens opacity in vivo in mice over a period. Dose-rate effects have never previously been addressed using this method, and current studies can be significantly modified to offer an optimum study for detection of IR induced cataract whilst using the same exposure conditions and those used to investigate early DNA damage, repair and cell proliferation effects. Thus, the hypothesis to be investigated during this study is that dose and dose-rate impact upon lens opacities over time.*

The 'tracking' of lens opacity over an 18-month period for a total of 120 mice generated almost 4,000 images for analysis, representing a large and substantial data set (see chapter 6). Mean lens opacity was statistically significantly increased in mice exposed to 2 Gy IR at the lower dose-rate of 0.063 Gy/min using statistical analysis of interaction comparisons (as described in chapter 6). No effect in mean lens opacity was seen in mice exposed to any dose (0.5 – 2 Gy) at the higher 0.3 Gy/min dose-rate. Whilst the increased lens opacity was not observed in doses lower than 2 Gy, this was likely due to lower doses requiring a latency period greater than the period followed in the study. A lens sensitivity to lower dose-rate supports a role of impaired DNA DSB repair in cataractogenesis and support the theory of radiation cataract being due to an increased cataractogenic load accelerating age-related cataract (Alice Uwineza and Hamada 2019).

7.5 Key conclusions to the research questions

The statistically significant interaction of lens epithelia region with dose-rate seen in IR-induced LEC proliferation (described in chapter 5), as well as the differential response of central

and peripheral LECs to IR-induced DNA damage and repair (as reported in chapter 4) suggested that the effect of a given dose of IR must be considered in the context of the dose-rate at which it was delivered. At low doses of IR, DNA repair appears better/more efficient at 25 mGy compared to 10 mGy in all four strains of mice used in the study. It is possible that doses <25 mGy do not produce sufficient damage to promote quick and effective repair of breaks in LEC and so proliferation and differentiation continue with no significant alteration. However, although small reductions in proliferation were commonly observed, no statistically significant reduction in proliferation at 10 or 25 mGy compared to control was seen. A non-linear/bimodal response of LEC proliferation to IR is proposed. This hypothesis can explain the reduction in proliferation following 2 Gy irradiation, where the amount of damage generated is too great to remain unrepaired, therefore repair is favoured and proliferation/differentiation reduces. This reduction in proliferation may result in an over-proliferating phase at later time points, as documented in previous studies demonstrating proliferation 'catch-up' (Von Sallmann 1952), although limited time-course data are available to conclude this fully. Central and peripheral region LECs repaired IR-induced DNA damage at different efficiencies, with dose-rate having a significant contribution to the repair efficiency of a given dose. DNA repair following low dose IR exposure appears to be less efficiently repaired than that delivered at higher doses. This thesis suggests that low dose and low dose-rate favour a less efficient DNA repair response in a differential manner across the lens epithelium.

Whilst this conclusion required further substantiation, it can be strengthened in the context of other endpoints and warrants further investigation (see upcoming section 7.7).

To summarise the key findings from studies previously presented in this thesis:

Table 7.1: Main findings from each of the four results chapter 3-6.

Chapter	Key Finding(s)
Research question 1; Chapter 3. The effects of low dose IR exposure in the DNA damage response of LECs	• Highly strain dependant • C57BL/6 and BALB/c most suitable strains • Differential response of lens epithelial region
Research question 2; Chapter 4. The dose response and dose-rate effect on the DNA damage response from IR in LECs	• Inverse dose-rate response in LECs but not in lymphocytes • Dose and dose-rate must be considered in context of each other
Research questions 3; Chapter 5. The effects of IR on LEC proliferation	• Non-linear/bimodal response of Ki67 • Suppression of proliferation at low dose • Suppression of proliferation at 2 Gy
Research question 4; Chapter 6. The effect of IR dose and dose-rate on lens opacity	• 2 Gy statistically higher mean lens opacity than 0.5 Gy at both dose-rates • 2 Gy delivered at 0.063 Gy/min (interaction) significantly increases mean lens opacity

7.6 Limitations

Many of the experiments and investigations carried out within this thesis featured novel methods of analysis, where little or no published data were previously available upon which to base power calculations needed to guide the required number of animals. The use of post-hoc power calculations was a valuable statistical tool, allowing for refinements to follow-up investigations, as well as aiding the reproducibility of the results. Power calculations for new experimental approaches are often a best-guess as they are based on similar data or similar tissues studied. The effects of low dose IR across four murine strains (chapter 3) within this thesis is an excellent example of this, where post-hoc power revealed the true number of animals needed for statistical power at such low dose investigations. In some cases, post-hoc power calculation results were surprising, with the recommended lenses needed being > 1,900 to statistically significantly differentiate this strain from C57BL/6 for example, in terms of 53BP1 repair foci response. However, the number of lenses needed to give power to statistically significantly differentiate between C57BL/6 and BALB/c was substantially lower, at 12 lenses. This study highlights the inter-

individual variation in response within inbred mice strains which was in some cases larger than expected, identifying the most suitable strain is crucial. This also raised a concern of cross-comparing one study to another where the same strain has been used but perhaps from different suppliers. Chapter 3 demonstrated the negative impact on statistical analysis and power of experiments different strains of mice can have, with choice of strain needing further consideration in radiation cataract studies in general. Of course, the number of animals required is not always practical and in some cases impossible given the scale of the study. However, the identification of a reproducible and less variable strains allowed for more efficient and focused investigations. Whilst statistically significant changes to LEC proliferation are seen at 24 hours post-exposure, further experiments need to characterise the time-course response in greater depth post-exposure.

Whilst the inverse dose-rate effect of both LEC DNA damage response and in mean lens opacity were significant, it is important to remember that the dose-rates used during these studies are rather acute, with exposures no longer than 39 minutes (see chapter 2; 2.3.2 and table 2.1). Low dose-rates are generally accepted to be delivered at <5 mGy/h. Inverse dose-rate response is more typically seen at protracted and continuous dose-rates, rather than those used during the studies in this thesis. Local ethical restrictions resulted in only 0.5 Gy exposure delivered at a further lower dose-rate of 0.014 Gy/min. Future studies can amend this restriction to allow the inverse dose-rate response to be further supported at even lower dose-rates and multiple doses.

Whilst the proliferation and repair markers used in chapters 3, 4 and 5 (53BP1 and Ki67) only represent one specific marker each, they were identified as the most suitable to detect the desired responses. Further markers could be analysed such as histone-H3 in the case of proliferation, or γH2AX/RAD51 for DSBs and also damage signalling pathways e.g. Atm, to further support the hypothesis of this thesis. Isolation of the lens epithelium varied from lens to lens, as did the quantity of material extracted and the way in which it was immunofluorescently labelled. Therefore, the method of flat mounting cannot be automated currently. Furthermore, the monolayers were imaged and analysed manually, which could lead to bias in image quality selection. Samples were anonymised as afar as possible and scorer bias considered.

The influence of circadian rhythm was considered, particularly in chapter 5 investigating the effect of IR on LEC proliferation, and any potential impact of this effect was minimised. As such, all mice were exposed during the morning. However, depending on the post-exposure time point, this could mean mice were sacrificed in the morning or afternoon. The time of sacrifice could have some impact on the results presented, although the role of circadian rhythm in LECs is not well known. The data for lower and higher doses could not be pooled due to the use of both x- and γ-

radiation, use of one radiation source could have strengthened the data during statistical analysis and potentially allow pooling of results.

7.7 Relevance for radiation protection, impact, and future work:

The observation of an inverse dose-rate effect in the lens epithelium was one of the most striking findings reported in this thesis. Whilst there were limitations with mouse exposures, preventing higher dose and/or lower dose-rate irradiations, there was an obvious need for further investigation. Reducing dose-rates further to protracted levels such as those seen in nuclear accidents, space exploration and possibly medical occupational limits would be extremely valuable to underpin the potential impact of low dose-rate sensitivity of the lens and what this means for workers and those likely to be exposed. Further investigations can help to better model excess risk of cataract during IR exposure, and add further biological and mechanistic evidence to support the hypothesis. Similarly, the studies of this thesis have been able to detect low dose DNA damage and repair response in the lens epithelium of mice exposed to 10 and 25 mGy. However, to achieve statistical significance at low dose, larger number of animals will be required, and a strain with a consistent response. Genetic background can impact the efficiency of the DNA damage response, and potentially other endpoints, at low dose exposures. This is a critical consideration when considering population variance and human occupational cohorts. Persons are known to have different radiosensitivity, which may affect IR-induced cataract susceptibility. The identification of such a strain can allow for further low dose investigations to be performed reliably and practically. Further reduction of doses, getting closer to those seen in occupational and medical exposure settings should be possible given the improved power calculations which can now be performed based on the results presented in this thesis.

This thesis had used one marker each to analyse DNA damage and repair and/or proliferation; 53BP1 and Ki67 respectively. Whilst these markers were selected carefully and represent ideal candidates, up- and/or down-stream markers for both would further strengthen the understanding of the role of these pathways in radiation-induced cataractogenesis. Later time points beyond 24 hours can support the proposed hypothesis for a non-linear or bimodal response of proliferation in the LECs. With post-hoc power testing, many experiments can be refined and power improved now that preliminary data has been collected. Further experiments should include time points beyond 24 hours. This would confirm whether 24 hours post-exposure was too premature for proliferative changes to occur. If no further effects are induced when observed, this could strengthen the hypothesis proposed within this thesis. Whilst the proposed hypothesis needs further evidence to support its existence *in vivo*, the results allow for further experiments to be focused. The statistically significant decrease in Ki67 positive LECs following a 2 Gy exposure would

suggest that the result of this dose could be further explored and the activity of proliferation characterised across a much longer time course to more fully understand the effect.

Low dose-rate occupational eye exposures have been shown to carry an excess risk for cataract in a US radiologic technologist study (Little et al. 2018). The inverse dose-rate effect in both early DNA damage repair (up to 24 hours post-exposure) and in mean lens opacity increase would supports the excess risk biologically. Eye lens exposure doses need to be considered in the context of the dose-rate at which they are delivered, as this may be a critical factor in lens radiosensitivity. This is not only the case for biological and mechanistic studies of the lens, but also epidemiological studies in the future should not overlook the potential importance of dose-rate when analysing occupational and medical exposure cohorts. These data are highly relevant for those occupational and medical workers routinely exposed to low dose IR at low dose-rates. Furthermore, the observed inverse dose-rate effect led to greater effects with continuous low dose-rates, which are more typical of occupational exposures by comparison with higher dose-rate/acute exposure. Whilst early DNA damage alone is unlikely to be the sole cause of radiation-induced cataract, its likely contribution to the cataractogenic load concept is further supported by the lens opacity increases being seen only at the lower dose-rate.

The ICRP state that cataracts are a 'tissue reaction' with an assumed threshold of 500 mSv (Hamada and Fujimichi 2014), no effects are expected at sub-threshold doses. The results from the studies in this thesis would not support the idea of a threshold in radiation-induced cataract. Rather, the conclusions from this thesis provide evidence that IR effects in the lens are due to stochastic processes given the strong strain dependency and dose and dose-rate influence upon DNA repair. A full understanding of the interactions between DNA damage response, LEC proliferation and lens opacity change is still unclear, definitive conclusions cannot be made without further investigation to ensure radiation protection of the lens is fully fit for purpose now and in the future.

8. Appendices:

DOI:10.20348/STOREDB/1112/1221

References:

'1990 Recommendations of the International Commission on Radiological Protection'. 1991. *Ann ICRP*, 21: 1-201.

Agency, International Atomic Energy. 2011. *Cytogenetic Dosimetry: Applications in Preparedness for and Response to Radiation Emergencies*.

Ainsbury, E. A., S. Barnard, S. Bright, C. Dalke, M. Jarrin, S. Kunze, R. Tanner, J. R. Dynlacht, R. A. Quinlan, J. Graw, M. Kadhim, and N. Hamada. 2016. 'Ionizing radiation induced cataracts: Recent biological and mechanistic developments and perspectives for future research', *Mutat Res*, 770: 238-61.

Ainsbury, E. A., S. D. Bouffler, W. Dorr, J. Graw, C. R. Muirhead, A. A. Edwards, and J. Cooper. 2009. 'Radiation cataractogenesis: a review of recent studies', *Radiat Res*, 172: 1-9.

Ainsbury, E., C. Badie, S. Barnard, G. Manning, J. Moquet, M. Abend, A. C. Antunes, L. Barrios, C. Bassinet, C. Beinke, E. Bortolin, L. Bossin, C. Bricknell, K. Brzoska, I. Buraczewska, C. H. Castano, Z. Cemusova, M. Christiansson, S. M. Cordero, G. Cosler, S. D. Monaca, F. Desangles, M. Discher, I. Dominguez, S. Doucha-Senf, J. Eakins, P. Fattibene, S. Filippi, M. Frenzel, D. Georgieva, E. Gregoire, K. Guogyte, V. Hadjidekova, L. Hadjiiska, R. Hristova, M. Karakosta, E. Kis, R. Kriehuber, J. Lee, D. Lloyd, K. Lumniczky, F. Lyng, E. Macaeva, M. Majewski, S. Vanda Martins, S. W. McKeever, A. Meade, D. Medipally, R. Meschini, R. M'Kacher, O. M. Gil, A. Montero, M. Moreno, M. Noditi, U. Oestreicher, D. Oskamp, F. Palitti, V. Palma, G. Pantelias, J. Pateux, C. Patrono, G. Pepe, M. Port, M. J. Prieto, M. C. Quattrini, R. Quintens, M. Ricoul, L. Roy, L. Sabatier, N. Sebastia, S. Sholom, S. Sommer, A. Staynova, S. Strunz, G. Terzoudi, A. Testa, F. Trompier, M. Valente, O. V. Hoey, I. Veronese, A. Wojcik, and C. Woda. 2017. 'Integration of new biological and physical retrospective dosimetry methods into EU emergency response plans - joint RENEB and EURADOS inter-laboratory comparisons', *Int J Radiat Biol*, 93: 99-109.

Ainsbury, E.A., Bouffler, S., Cocker, M., Gilvin, P., Holt, E., Peters, S., Slack, K., Williamson, A. 2014. 'Public Health England survey of eye lens doses in the UK medical sector', *Journal of Radiological Protection*, 34: 15-29.

Al-Haj, A.N., Lobriguito, A.M., Al-Gain, I. . 2015. 'Staff eye doses in a large medical centre in Saudi Arabia: are they meeting the new ICRP recommendations?', *Radiat Prot Dosimetry*, 165: 294-8.

Alice Uwineza, Alexia A. Kalligeraki, Nobuyuki, and Miguel Jarrin Hamada, Roy A. Quinlan. 2019. 'Cataractogenic load – a concept to study the contribution

of ionizing radiation to accelerated aging in the eye lens', *Mutation Research/Reviews in Mutation Research*, 779: 68-81.

Andley, U. P. 2007. 'Crystallins in the eye: Function and pathology', *Prog Retin Eye Res*, 26: 78-98.

Andley, U. P., J. S. Rhim, L. T. Chylack, Jr., and T. P. Fleming. 1994. 'Propagation and immortalization of human lens epithelial cells in culture', *Invest Ophthalmol Vis Sci*, 35: 3094-102.

Anglada, T., J. Repulles, A. Espinal, M. A. LaBarge, M. R. Stampfer, A. Genesca, and M. Martin. 2019. 'Delayed gammaH2AX foci disappearance in mammary epithelial cells from aged women reveals an age-associated DNA repair defect', *Aging (Albany NY)*, 11: 1510-23.

Asaithamby, A., and D. J. Chen. 2009. 'Cellular responses to DNA double-strand breaks after low-dose gamma-irradiation', *Nucleic Acids Res*, 37: 3912-23.

Attigah, N., K. Oikonomou, U. Hinz, T. Knoch, S. Demirel, E. Verhoeven, and D. Bockler. 2016. 'Radiation exposure to eye lens and operator hands during endovascular procedures in hybrid operating rooms', *J Vasc Surg*, 63: 198-203.

Augusteyn, R. C. 2008. 'Growth of the lens: in vitro observations', *Clin Exp Optom*, 91: 226-39.

Azizova, T. V., N. Hamada, E. S. Grigoryeva, and E. V. Bragin. 2018. 'Risk of various types of cataracts in a cohort of Mayak workers following chronic occupational exposure to ionizing radiation', *Eur J Epidemiol*, 33: 1193-204.

Babizhayev, M. A., A. I. Deyev, and L. F. Linberg. 1988. 'Lipid peroxidation as a possible cause of cataract', *Mech Ageing Dev*, 44: 69-89.

Babizhayev, M. A., K. S. Vishnyakova, and Y. E. Yegorov. 2011. 'Telomere-dependent senescent phenotype of lens epithelial cells as a biological marker of aging and cataractogenesis: the role of oxidative stress intensity and specific mechanism of phospholipid hydroperoxide toxicity in lens and aqueous', *Fundam Clin Pharmacol*, 25: 139-62.

Babizhayev, M. A., and Y. E. Yegorov. 2010. 'Telomere attrition in lens epithelial cells - a target for N-acetylcarnosine therapy', *Front Biosci (Landmark Ed)*, 15: 934-56.

Bains, S. K., K. Chapman, S. Bright, A. Senan, M. Kadhim, and P. Slijepcevic. 2019. 'Effects of ionizing radiation on telomere length and telomerase activity in cultured human lens epithelium cells', *Int J Radiat Biol*, 95: 54-63.

Bakkenist, C. J., and M. B. Kastan. 2015. 'Chromatin perturbations during the DNA damage response in higher eukaryotes', *DNA Repair (Amst)*, 36: 8-12.

Bakthavachalu, B., S. Kalanke, S. Galande, B. Ramanamurthy, P. Parab, K. N. Kohale, and V. Seshadri. 2010. 'Dense cataract and microphthalmia (dcm) in BALB/c mice is caused by mutations in the GJA8 locus', *J Genet*, 89: 147-54.

Balagurumoorthy, P., S. J. Adelstein, and A. I. Kassis. 2011. 'Novel method for quantifying radiation-induced single-strand-break yields in plasmid DNA highlights 10-fold discrepancy', *Anal Biochem*, 417: 242-6.

Banks, G., I. Heise, B. Starbuck, T. Osborne, L. Wisby, P. Potter, I. J. Jackson, R. G. Foster, S. N. Peirson, and P. M. Nolan. 2015. 'Genetic background influences age-related decline in visual and nonvisual retinal responses, circadian rhythms, and sleep', *Neurobiol Aging*, 36: 380-93.

Bannik, K., U. Rossler, T. Faus-Kessler, M. Gomolka, S. Hornhardt, C. Dalke, O. Klymenko, M. Rosemann, K. R. Trott, M. Atkinson, U. Kulka, and J. Graw. 2013. 'Are mouse lens epithelial cells more sensitive to gamma-irradiation than lymphocytes?', *Radiat Environ Biophys*, 52: 279-86.

Barnard, S., S. Bouffler, and K. Rothkamm. 2013. 'The shape of the radiation dose response for DNA double-strand break induction and repair', *Genome Integr*, 4: 1.

Barnard, S. G., E. A. Ainsbury, R. A. Quinlan, and S. D. Bouffler. 2016. 'Radiation protection of the eye lens in medical workers-basis and impact of the ICRP recommendations', *Br J Radiol*, 89: 20151034.

Barnard, S. G. R., J. Moquet, S. Lloyd, M. Ellender, E. A. Ainsbury, and R. A. Quinlan. 2018. 'Dotting the eyes: mouse strain dependency of the lens epithelium to low dose radiation-induced DNA damage', *Int J Radiat Biol*: 1-9.

Barraquer, R. I., L. Pinilla Cortes, M. J. Allende, G. A. Montenegro, B. Ivankovic, J. C. D'Antin, H. Martinez Osorio, and R. Michael. 2017. 'Validation of the Nuclear Cataract Grading System BCN 10', *Ophthalmic Res*, 57: 247-51.

Bartova, E., S. Legartova, J. Krejci, P. Reznickova, A. S. Kovarikova, J. Suchankova, R. Fedr, E. Smirnov, M. Hornacek, and I. Raska. 2018. 'Depletion of A-type lamins and Lap2alpha reduces 53BP1 accumulation at UV-induced DNA lesions and Lap2alpha protein is responsible for compactness of irradiated chromatin', *J Cell Biochem*.

Bassnett, S. 2009. 'On the mechanism of organelle degradation in the vertebrate lens', *Exp Eye Res*, 88: 133-9.

Behrens, R. 2015. 'Monitoring the eye lens: how do the international organisations react?', *Radiat Prot Dosimetry*, 164: 75-8.

Bekker-Jensen, S., and N. Mailand. 2010. 'Assembly and function of DNA double-strand break repair foci in mammalian cells', *DNA Repair (Amst)*, 9: 1219-28.

Bilski, P., Bordy, J-M., Daures, J., Denoziere, M., Fantuzzi, E., Ferrari, P., Gualdrini, G., Kopec, M., Mariotti, F., Monteventi, F., Wach, S. . 2011. 'The new EYE-D™ dosemeter for measurements of Hp(3) for medical staff', *Radiation Measurements*, 46: 1239-42.

Bitarafan Rajabi, A., Noohi, F., Hashemi, H., Haghjoo, M., Miraftab, M., Yaghoobi, N., Rastgou, F., Malek, H., Faghihi, H., Firouzabadi, H., Asgari, S., Rezvan, F., Khosravi, H., Soroush, S., Khabazkhoob, M. 2015. 'Ionizing Radiation-Induced Cataract in Interventional Cardiology Staff', *Res Cardiovasc Med*, 4: e25148.

Blakely, E. A., K. A. Bjornstad, P. Y. Chang, M. P. McNamara, E. Chang, G. Aragon, S. P. Lin, G. Lui, and J. R. Polansky. 2000. 'Growth and differentiation of human lens epithelial cells in vitro on matrix', *Invest Ophthalmol Vis Sci*, 41: 3898-907.

Blumenthal, E. Z., and C. N. Serpetopoulos. 1998. 'On focusing the slit-lamp: Part I. An inaccurate ocular setting--what is there to lose?', *Surv Ophthalmol*, 42: 351-4.

Bosch, D. E., M. R. Kilgore, R. A. Schmidt, P. E. Swanson, M. H. Rendi, and O. H. Chang. 2017. 'Comparison of Proliferation Markers Ki67 and Phosphohistone-H3 (pHH3) in Breast Ductal Carcinoma In Situ', *Appl Immunohistochem Mol Morphol*, 25: 543-47.

Bouffler, S., Ainsbury, E., Gilvin, P., Harrison, J. 2012. 'Radiation-induced cataract: the Health Protection Agency's response to the ICRP statement on tissue reactions and recommendation on the dose limit for the eye lens', *Journal of Radiological Protection*, 32: 479-88.

Boulton, E., H. Cleary, D. Papworth, and M. Plumb. 2001. 'Susceptibility to radiation-induced leukaemia/lymphoma is genetically separable from sensitivity to radiation-induced genomic instability', *Int J Radiat Biol*, 77: 21-9.

Broughton. J., Cantone, M.C., Ginjaume, M., Shah, B. . 2013. 'Report of Task Group on the implications of the implementation of the ICRP recommendations for a revised dose limit to the lens of the eye', *Journal of Radiological Protection*, 33: 855-68.

Brown, N., R. Finnon, G. Manning, S. Bouffler, and C. Badie. 2015. 'Influence of radiation quality on mouse chromosome 2 deletions in radiation-induced acute myeloid leukaemia', *Mutat Res Genet Toxicol Environ Mutagen*, 793: 48-54.

Brown, Nicholas Phelps, and Anthony J. Bron. 1996. *Lens disorders : a clinical manual of cataract diagnosis* (Butterworth Heinemann: Oxford).

Bruchmann, I., Szermerski, B., Behrens, R., Geworski, L. . 2015. 'Impact of radiation protections means on the dose to the lens of the eye while handling radionuclides in nuclear medicine', *Z Med Phys*.

Bu, L., Y. Jin, Y. Shi, R. Chu, A. Ban, H. Eiberg, L. Andres, H. Jiang, G. Zheng, M. Qian, B. Cui, Y. Xia, J. Liu, L. Hu, G. Zhao, M. R. Hayden, and X. Kong. 2002. 'Mutant DNA-binding domain of HSF4 is associated with autosomal dominant lamellar and Marner cataract', *Nat Genet*, 31: 276-8.

Burdak-Rothkamm, S., K. Rothkamm, and K. M. Prise. 2008. 'ATM acts downstream of ATR in the DNA damage response signaling of bystander cells', *Cancer Res*, 68: 7059-65.

Carinou, E., M. Ginjaume, U. O'Connor, R. Kopec, and M. Sans Merce. 2014. 'Status of eye lens radiation dose monitoring in European hospitals', *J Radiol Prot*, 34: 729-39.

Carreras, E., M. Velasco de Andres, M. Orta-Mascaro, I. T. Simoes, C. Catala, O. Zaragoza, and F. Lozano. 2019. 'Discordant susceptibility of inbred C57BL/6 versus outbred CD1 mice to experimental fungal sepsis', *Cell Microbiol*, 21: e12995.

Cemusova, Z., Ekendahl, D., Judas, L. . 2015. 'Assessment of eye lens doses in interventional radiology: a simulation in laboratory conditions.', *Radiat Prot Dosimetry*.

Chang, P. Y., K. A. Bjornstad, E. Chang, M. McNamara, M. H. Barcellos-Hoff, S. P. Lin, G. Aragon, J. R. Polansky, G. M. Lui, and E. A. Blakely. 2000. 'Particle irradiation induces FGF2 expression in normal human lens cells', *Radiat Res*, 154: 477-84.

Chang, P. Y., K. A. Bjornstad, C. J. Rosen, M. P. McNamara, R. Mancini, L. E. Goldstein, L. T. Chylack, and E. A. Blakely. 2005. 'Effects of iron ions, protons and X rays on human lens cell differentiation', *Radiat Res*, 164: 531-9.

Charakidas, A., A. Kalogeraki, M. Tsilimbaris, P. Koukoulomatis, D. Brouzas, and G. Delides. 2005. 'Lens epithelial apoptosis and cell proliferation in human age-related cortical cataract', *Eur J Ophthalmol*, 15: 213-20.

Chen, Z., K. Gowan, S. M. Leach, S. S. Viboolsittiseri, A. K. Mishra, T. Kadoishi, K. Diener, B. Gao, K. Jones, and J. H. Wang. 2016. 'Unexpected effects of different genetic backgrounds on identification of genomic rearrangements via whole-genome next generation sequencing', *BMC Genomics*, 17: 823.

Chodick, G., Bekiroglu, N., Hauptmann, M., Alexander, B. H., Freedman, D. M., Doody, M. M., Cheung, L. C., Simon, S. L., Weinstock, R. M., Bouville, A., Sigurdson, A. J. 2008. 'Risk of cataract after exposure to low doses of ionizing radiation: a 20-year prospective cohort study among US radiologic technologists', *American Journal of Epedimiology*, 168: 620-31.

Chua, M. L., and K. Rothkamm. 2013. 'Biomarkers of radiation exposure: can they predict normal tissue radiosensitivity?', *Clin Oncol (R Coll Radiol)*, 25: 610-6.

Chumak, V. V., B. V. Worgul, Y. I. Kundiyev, N. M. Sergiyenko, P. M. Vitte, C. Medvedovsky, E. V. Bakhanova, A. K. Junk, O. Y. Kyrychenko, N. V. Musijachenko, S. V. Sholom, S. A. Shylo, O. P. Vitte, S. Xu, X. Xue, and R. E. Shore. 2007. 'Dosimetry for a study of low-dose radiation cataracts among Chernobyl clean-up workers', *Radiat Res*, 167: 606-14.

Chylack, L. T., Jr., J. K. Wolfe, D. M. Singer, M. C. Leske, M. A. Bullimore, I. L. Bailey, J. Friend, D. McCarthy, and S. Y. Wu. 1993. 'The Lens Opacities Classification System III. The Longitudinal Study of Cataract Study Group', *Arch Ophthalmol*, 111: 831-6.

Ciraj-Bjelac, O., Rehani, M., Minamoto, A., Sim, K.H., Liew, H.B., Vano, E. 2012. 'Radiation-induced eye lens changes and risk for cataract in interventional cardiology', *Cardiology*, 123: 168-71.

Clutton, S. M., K. M. Townsend, C. Walker, J. D. Ansell, and E. G. Wright. 1996. 'Radiation-induced genomic instability and persisting oxidative stress in primary bone marrow cultures', *Carcinogenesis*, 17: 1633-9.

Coeytaux, K., E. Bey, D. Christensen, E. S. Glassman, B. Murdock, and C. Doucet. 2015. 'Reported radiation overexposure accidents worldwide, 1980-2013: a systematic review', *PLoS One*, 10: e0118709.

Cogan, D. G., and D. D. Donaldson. 1951. 'Experimental radiation cataracts. I. Cataracts in the rabbit following single x-ray exposure', *AMA Arch Ophthalmol*, 45: 508-22.

Costes, S. V., I. Chiolo, J. M. Pluth, M. H. Barcellos-Hoff, and B. Jakob. 2010. 'Spatiotemporal characterization of ionizing radiation induced DNA damage foci and their relation to chromatin organization', *Mutat Res*, 704: 78-87.

Currell, Graham, and Antony Dowman. 2009. 'Essential mathematics and statistics for science'.

Dalke, C., F. Neff, S. K. Bains, S. Bright, D. Lord, P. Reitmeir, U. Rößler, D. Samaga, K. Unger, H. Braselmann, F. Wagner, M. Greiter, M. Gomolka, S. Hornhardt, S. Kunze, S. J. Kempf, L. Garrett, S. M. Hölter, W. Wurst, M. Rosemann, O. Azimzadeh, S. Tapio, M. Aubele, F. Theis, C. Hoeschen, P. Slijepcevic, M. Kadhim, M. Atkinson, H. Zitzelsberger, U. Kulka, and J. Graw. 2018. 'Lifetime study in mice after acute low-dose ionizing radiation: a multifactorial study with special focus on cataract risk', *Radiat Environ Biophys*, 57: 99-113.

Danska, J. S., D. P. Holland, S. Mariathasan, K. M. Williams, and C. J. Guidos. 1996. 'Biochemical and genetic defects in the DNA-dependent protein kinase in murine scid lymphocytes', *Mol Cell Biol*, 16: 5507-17.

Darakhshan, F., C. Badie, J. Moody, M. Coster, R. Finnon, P. Finnon, A. A. Edwards, M. Szluinska, C. J. Skidmore, K. Yoshida, R. Ullrich, R. Cox, and S. D. Bouffler. 2006. 'Evidence for complex

multigenic inheritance of radiation AML susceptibility in mice revealed using a surrogate phenotypic assay', *Carcinogenesis*, 27: 311-8.

Dauer, L. T., E. A. Ainsbury, J. Dynlacht, D. Hoel, B. E. K. Klein, D. Mayer, C. R. Prescott, R. H. Thornton, E. Vano, G. E. Woloschak, C. M. Flannery, L. E. Goldstein, N. Hamada, P. K. Tran, M. P. Grissom, and E. A. Blakely. 2017. 'Guidance on radiation dose limits for the lens of the eye: overview of the recommendations in NCRP Commentary No. 26', *Int J Radiat Biol*: 1-9.

Day, R. C., and C. W. Beck. 2011. 'Transdifferentiation from cornea to lens in Xenopus laevis depends on BMP signalling and involves upregulation of Wnt signalling', *BMC Dev Biol*, 11: 54.

De Stefano, I., B. Tanno, P. Giardullo, S. Leonardi, E. Pasquali, F. Antonelli, M. Tanori, A. Casciati, S. Pazzaglia, A. Saran, and M. Mancuso. 2015. 'The Patched 1 tumor-suppressor gene protects the mouse lens from spontaneous and radiation-induced cataract', *Am J Pathol*, 185: 85-95.

Delaye, Mireille, and Annette Tardieu. 1983. 'Short-range order of crystallin proteins accounts for eye lens transparency', *Nature*, 302: 415.

Denkert, C., J. Budczies, G. von Minckwitz, S. Wienert, S. Loibl, and F. Klauschen. 2015. 'Strategies for developing Ki67 as a useful biomarker in breast cancer', *Breast*, 24 Suppl 2: S67-72.

Di Paola, M., Bianchi, M., Baarli, J. . 1978. 'Lens opacification in mice exposed to 14-MeV neutrons', *Radiation Research*, 73: 340-50.

Dickey, J. S., F. J. Zemp, A. Altamirano, O. A. Sedelnikova, W. M. Bonner, and O. Kovalchuk. 2011. 'H2AX phosphorylation in response to DNA double-strand break formation during bystander signalling: effect of microRNA knockdown', *Radiat Prot Dosimetry*, 143: 264-9.

Ding, D., Y. Zhang, J. Wang, X. Wang, D. Fan, L. He, X. Zhang, Y. Gao, Q. Li, and H. Chen. 2016. 'gamma-H2AX/53BP1/pKAP-1 foci and their linear tracks induced by in vitro exposure to radon and its progeny in human peripheral blood lymphocytes', *Sci Rep*, 6: 38295.

Doran, A. G., K. Wong, J. Flint, D. J. Adams, K. W. Hunter, and T. M. Keane. 2016. 'Deep genome sequencing and variation analysis of 13 inbred mouse strains defines candidate phenotypic alleles, private variation and homozygous truncating mutations', *Genome Biol*, 17: 167.

Duncan, George. 1981. *Mechanisms of cataract formation in the human lens* (Academic Press: London; New York).

Eaton, J. S., P. E. Miller, E. Bentley, S. M. Thomasy, and C. J. Murphy. 2017. 'Slit Lamp-Based Ocular Scoring Systems in Toxicology and Drug Development: A Literature Survey', *J Ocul Pharmacol Ther*, 33: 707-17.

Edwards, A. A., and D. C. Lloyd. 1998. 'Risks from ionising radiation: deterministic effects', *J Radiol Prot*, 18: 175-83.

El Ashkar, S., J. Schwaller, T. Pieters, S. Goossens, J. Demeulemeester, F. Christ, S. Van Belle, S. Juge, N. Boeckx, A. Engelman, P. Van Vlierberghe, Z. Debyser, and J. De Rijck. 2018. 'LEDGF/p75 is dispensable for hematopoiesis but essential for MLL-rearranged leukemogenesis', *Blood*, 131: 95-107.

Eldred, J. A., L. J. Dawes, and I. M. Wormstone. 2011. 'The lens as a model for fibrotic disease', *Philos Trans R Soc Lond B Biol Sci*, 366: 1301-19.

Fatma, N., E. Kubo, P. Sharma, D. R. Beier, and D. P. Singh. 2005. 'Impaired homeostasis and phenotypic abnormalities in Prdx6-/-mice lens epithelial cells by reactive oxygen species: increased expression and activation of TGFbeta', *Cell Death Differ*, 12: 734-50.

Fatma, N., D. P. Singh, T. Shinohara, and L. T. Chylack, Jr. 2001. 'Transcriptional regulation of the antioxidant protein 2 gene, a thiol-specific antioxidant, by lens epithelium-derived growth factor to protect cells from oxidative stress', *J Biol Chem*, 276: 48899-907.

Fernandez-Vidal, A., J. Vignard, and G. Mirey. 2017. 'Around and beyond 53BP1 Nuclear Bodies', *Int J Mol Sci*, 18.

Feuerhahn, S., and J. M. Egly. 2008. 'Tools to study DNA repair: what's in the box?', *Trends Genet*, 24: 467-74.

Fradet-Turcotte, A., M. D. Canny, C. Escribano-Diaz, A. Orthwein, C. C. Leung, H. Huang, M. C. Landry, J. Kitevski-LeBlanc, S. M. Noordermeer, F. Sicheri, and D. Durocher. 2013. '53BP1 is a reader of the DNA-damage-induced H2A Lys 15 ubiquitin mark', *Nature*, 499: 50-4.

Freeman, G. 1963. 'LENS REGENERATION FROM THE CORNEA IN XENOPUS LAEVIS', *J Exp Zool*, 154: 39-65.

Frey, DG. 2014. 'Radiation Cataracts: New Data and New Recommendations', *American Journal of Roentgenology*, 203.

Froger, A., D. Clemens, K. Kalman, K. L. Nemeth-Cahalan, T. F. Schilling, and J. E. Hall. 2010. 'Two distinct aquaporin 0s required for development and transparency of the zebrafish lens', *Invest Ophthalmol Vis Sci*, 51: 6582-92.

Fry, John C. 1999. *Biological data analysis : a practical approach* (IRL Press at Oxford University Press: Oxford).

Fuchs, H., V. Gailus-Durner, T. Adler, J. A. Aguilar-Pimentel, L. Becker, J. Calzada-Wack, P. Da Silva-Buttkus, F. Neff, A. Gotz, W. Hans, S. M. Holter, M. Horsch, G. Kastenmuller, E. Kemter, C. Lengger, H. Maier, M. Matloka, G. Moller, B. Naton, C. Prehn, O. Puk, I. Racz, B. Rathkolb, W. Romisch-Margl, J. Rozman, R. Wang-Sattler, A. Schrewe, C. Stoger, M. Tost, J. Adamski, B. Aigner, J. Beckers, H. Behrendt, D. H. Busch, I. Esposito, J. Graw, T. Illig, B. Ivandic, M. Klingenspor, T. Klopstock, E. Kremmer, M. Mempel, S. Neschen, M. Ollert, H. Schulz, K. Suhre, E. Wolf, W. Wurst, A. Zimmer, and M. Hrabe de Angelis. 2011. 'Mouse phenotyping', *Methods*, 53: 120-35.

Fujii, N., T. Nakamura, Y. Sadakane, T. Saito, and N. Fujii. 2007. 'Differential susceptibility of alpha A- and alpha B-crystallin to gamma-ray irradiation', *Biochim Biophys Acta*, 1774: 345-50.

Fujimichi, Y., and N. Hamada. 2014. 'Ionizing irradiation not only inactivates clonogenic potential in primary normal human diploid lens epithelial cells but also stimulates cell proliferation in a subset of this population', *PLoS One*, 9: e98154.

Fujimoto, M., H. Izu, K. Seki, K. Fukuda, T. Nishida, S. Yamada, K. Kato, S. Yonemura, S. Inouye, and A. Nakai. 2004. 'HSF4 is required for normal cell growth and differentiation during mouse lens development', *Embo j*, 23: 4297-306.

Gali, H. E., R. Sella, and N. A. Afshari. 2019. 'Cataract grading systems: a review of past and present', *Curr Opin Ophthalmol*, 30: 13-18.

Gerdes, J., U. Schwab, H. Lemke, and H. Stein. 1983. 'Production of a mouse monoclonal antibody reactive with a human nuclear antigen associated with cell proliferation', *Int J Cancer*, 31: 13-20.

Ghasemi, A., and S. Zahediasl. 2012. 'Normality tests for statistical analysis: a guide for non-statisticians', *Int J Endocrinol Metab*, 10: 486-9.

Goel, M. K., P. Khanna, and J. Kishore. 2010. 'Understanding survival analysis: Kaplan-Meier estimate', *Int J Ayurveda Res*, 1: 274-8.

Gong, Z., Y. W. Cho, J. E. Kim, K. Ge, and J. Chen. 2009. 'Accumulation of Pax2 transactivation domain interaction protein (PTIP) at sites of DNA breaks via RNF8-dependent pathway is required for cell survival after DNA damage', *J Biol Chem*, 284: 7284-93.

Gorin, M. B., S. B. Yancey, J. Cline, J. P. Revel, and J. Horwitz. 1984. 'The major intrinsic protein (MIP) of the bovine lens fiber membrane: characterization and structure based on cDNA cloning', *Cell*, 39: 49-59.

Gralek, M., K. H. Chrzanowska, K. Kanigowska, and B. Kocyla-Karczmarewicz. 2011. '[Ocular findings in Nijmegen breakage syndrome]', *Klin Oczna*, 113: 153-5.

Griep, A. E. 2006. 'Cell cycle regulation in the developing lens', *Semin Cell Dev Biol*, 17: 686-97.

Gupta, A., C. R. Hunt, S. Chakraborty, R. K. Pandita, J. Yordy, D. B. Ramnarain, N. Horikoshi, and T. K. Pandita. 2014. 'Role of 53BP1 in the regulation of DNA double-strand break repair pathway choice', *Radiat Res*, 181: 1-8.

Gwon, A. 2006. 'Lens regeneration in mammals: a review', *Surv Ophthalmol*, 51: 51-62.
Hall, E. J., and D. J. Brenner. 1991. 'The dose-rate effect revisited: radiobiological considerations of importance in radiotherapy', *Int J Radiat Oncol Biol Phys*, 21: 1403-14.
Hall, E. J., B. V. Worgul, L. Smilenov, C. D. Elliston, and D. J. Brenner. 2006. 'The relative biological effectiveness of densely ionizing heavy-ion radiation for inducing ocular cataracts in wild type versus mice heterozygous for the ATM gene', *Radiat Environ Biophys*, 45: 99-104.
Hall, Eric J. 1973. *Radiobiology for the radiologist* (Hagerstown, Md. : Medical Dept., Harper & Row, [1973] ©1973).
Hamada, N. 2016. 'Ionizing radiation sensitivity of the ocular lens and its dose rate dependence', *Int J Radiat Biol*: 1-11.
———. 2017a. 'Ionizing radiation response of primary normal human lens epithelial cells', *PLoS One*, 12: e0181530.
———. 2017b. 'Ionizing radiation sensitivity of the ocular lens and its dose rate dependence', *Int J Radiat Biol*, 93: 1024-34.
Hamada, N., and Y. Fujimichi. 2014. 'Classification of radiation effects for dose limitation purposes: history, current situation and future prospects', *J Radiat Res*, 55: 629-40.
———. 2015. 'Role of carcinogenesis related mechanisms in cataractogenesis and its implications for ionizing radiation cataractogenesis', *Cancer Lett*, 368: 262-74.
Hamada, N., Y. Fujimichi, T. Iwasaki, N. Fujii, M. Furuhashi, E. Kubo, T. Minamino, T. Nomura, and H. Sato. 2014. 'Emerging issues in radiogenic cataracts and cardiovascular disease', *J Radiat Res*, 55: 831-46.
Hamasaki, K., K. Imai, T. Hayashi, K. Nakachi, and Y. Kusunoki. 2007. 'Radiation sensitivity and genomic instability in the hematopoietic system: Frequencies of micronucleated reticulocytes in whole-body X-irradiated BALB/c and C57BL/6 mice', *Cancer Sci*, 98: 1840-4.
Hammer, G. P., U. Scheidemann-Wesp, F. Samkange-Zeeb, H. Wicke, K. Neriishi, and M. Blettner. 2013. 'Occupational exposure to low doses of ionizing radiation and cataract development: a systematic literature review and perspectives on future studies', *Radiat Environ Biophys*, 52: 303-19.
Hashim, Z., and S. Zarina. 2011. 'Advanced glycation end products in diabetic and non-diabetic human subjects suffering from cataract', *Age (Dordr)*, 33: 377-84.
Hayden, J. H., H. Rothstein, B. V. Worgul, and G. R. Merriam, Jr. 1980. 'Hypophysectomy exerts a radioprotective effect on frog lens', *Experientia*, 36: 116-8.
Hejtmancik, J. F., and A. Shiels. 2015. 'Overview of the Lens', *Prog Mol Biol Transl Sci*, 134: 119-27.
Henry, J. J., and P. A. Tsonis. 2010. 'Molecular and cellular aspects of amphibian lens regeneration', *Prog Retin Eye Res*, 29: 543-55.
Hill, M. A. 2004. 'The variation in biological effectiveness of X-rays and gamma rays with energy', *Radiat Prot Dosimetry*, 112: 471-81.
Hockwin, O., V. Dragomirescu, T. Shibata, H. Laser, and A. Wegener. 1984. 'Long-term follow-up examination of experimental cataracts in rats by Scheimpflug photography and densitometry', *Graefes Arch Clin Exp Ophthalmol*, 222: 20-5.
Hopkins, K. M., W. Auerbach, X. Y. Wang, M. P. Hande, H. Hang, D. J. Wolgemuth, A. L. Joyner, and H. B. Lieberman. 2004. 'Deletion of mouse rad9 causes abnormal cellular responses to DNA damage, genomic instability, and embryonic lethality', *Mol Cell Biol*, 24: 7235-48.
Horn, S., S. Barnard, D. Brady, K. M. Prise, and K. Rothkamm. 2013. 'Combined analysis of gamma-H2AX/53BP1 foci and caspase activation in lymphocyte subsets detects recent and more remote radiation exposures', *Radiat Res*, 180: 603-9.
Horn, S., S. Barnard, and K. Rothkamm. 2011. 'Gamma-H2AX-based dose estimation for whole and partial body radiation exposure', *PLoS One*, 6: e25113.

Huen, M. S., J. Huang, J. W. Leung, S. M. Sy, K. M. Leung, Y. P. Ching, S. W. Tsao, and J. Chen. 2010. 'Regulation of chromatin architecture by the PWWP domain-containing DNA damage-responsive factor EXPAND1/MUM1', *Mol Cell*, 37: 854-64.

ICRP. 2007a. 'Early and Late Effects of Radiation in Normal Tissues and Organs – Threshold Doses for Tissue Reactions in a Radiation Protection Context.', *Annals of the ICRP Publication 103*.

———. 2007b. 'ICRP Publication 103', *Annals of the ICRP*, 37.

ICRP, Ann. 2012. 'ICRP Statement on Tissue Reactions', 1-2: 1-322.

Ikeda, S., N. L. Hawes, B. Chang, C. S. Avery, R. S. Smith, and P. M. Nishina. 1999. 'Severe ocular abnormalities in C57BL/6 but not in 129/Sv p53-deficient mice', *Invest Ophthalmol Vis Sci*, 40: 1874-8.

Ip, E. H. 2007. 'General linear models', *Methods Mol Biol*, 404: 189-211.

Iyengar, L., and F. J. Lovicu. 2017. 'Aqueous humour-induced lens epithelial cell proliferation requires FGF-signalling', *Growth Factors*, 35: 131-43.

Iyengar, L., B. Patkunanathan, O. T. Lynch, J. W. McAvoy, J. E. Rasko, and F. J. Lovicu. 2006. 'Aqueous humour- and growth factor-induced lens cell proliferation is dependent on MAPK/ERK1/2 and Akt/PI3-K signalling', *Exp Eye Res*, 83: 667-78.

Jackson, S. P., and J. Bartek. 2009. 'The DNA-damage response in human biology and disease', *Nature*, 461: 1071-8.

Jacob, S., Boveda, S., Bar, O., Brézin, A., Maccia, C., Laurier, D., Bernier, M.O. 2013. 'Interventional cardiologists and risk of radiation-induced cataract: results of a French multicenter observational study', *International Journal of Cardiology*, 167: 1843-7.

James, E. R. 2007. 'The etiology of steroid cataract', *J Ocul Pharmacol Ther*, 23: 403-20.

Jarrin, M., F. C. Mansergh, M. E. Boulton, L. Gunhaga, and M. A. Wride. 2012. 'Survivin expression is associated with lens epithelial cell proliferation and fiber cell differentiation', *Mol Vis*, 18: 2758-69.

Jiang, H., Y. Xu, W. Li, K. Ma, L. Cai, and G. Wang. 2008. 'Low-dose radiation does not induce proliferation in tumor cells in vitro and in vivo', *Radiat Res*, 170: 477-87.

Jurikova, M., L. Danihel, S. Polak, and I. Varga. 2016. 'Ki67, PCNA, and MCM proteins: Markers of proliferation in the diagnosis of breast cancer', *Acta Histochem*, 118: 544-52.

Kadhim, M. A., S. R. Moore, and E. H. Goodwin. 2004. 'Interrelationships amongst radiation-induced genomic instability, bystander effects, and the adaptive response', *Mutat Res*, 568: 21-32.

Kallingappa, P. K., P. M. Turner, M. P. Eichenlaub, A. L. Green, F. C. Oback, A. M. Chibnall, D. N. Wells, and B. Oback. 2016. 'Quiescence Loosens Epigenetic Constraints in Bovine Somatic Cells and Improves Their Reprogramming into Totipotency', *Biol Reprod*, 95: 16.

Kanao, T., and Y. Miyachi. 2006. 'Lymphangiogenesis promotes lens destruction and subsequent lens regeneration in the newt eyeball, and both processes can be accelerated by transplantation of dendritic cells', *Dev Biol*, 290: 118-24.

Kato, T. A., H. Nagasawa, M. M. Weil, J. B. Little, and J. S. Bedford. 2006. 'Levels of gamma-H2AX Foci after low-dose-rate irradiation reveal a DNA DSB rejoining defect in cells from human ATM heterozygotes in two at families and in another apparently normal individual', *Radiat Res*, 166: 443-53.

Katta, A. V., R. V. Katkam, and H. Geetha. 2013. 'Lipid peroxidation and the total antioxidant status in the pathogenesis of age related and diabetic cataracts: a study on the lens and blood', *J Clin Diagn Res*, 7: 978-81.

Kayastha, F., H. Madhu, A. Vasavada, and K. Johar. 2014. 'Andrographolide reduces proliferation and migration of lens epithelial cells by modulating PI3K/Akt pathway', *Exp Eye Res*, 128: 23-6.

Khan, S. Y., S. F. Hackett, M. C. Lee, N. Pourmand, C. C. Talbot, Jr., and S. A. Riazuddin. 2015. 'Transcriptome Profiling of Developing Murine Lens Through RNA Sequencing', *Invest Ophthalmol Vis Sci*, 56: 4919-26.

Khoury, H.J., Garzon, W.J., Andrade, G., Lunelli, N., Kramer, R., de Barros, V.S., Huda, A. . 2015. 'Radiation exposure to patients and medical staff in hepatic chemoembolization interventional procedrues in Recife, Brazil', *Radiat Prot Dosimetry*, 165: 263-7.

Kim, H., and H. Yim. 2018. '53BP1: A guardian for centrosomal integrity', *Front Biosci (Landmark Ed)*, 23: 1-12.

Kimura, Y., M. Madhavan, M. K. Call, W. Santiago, P. A. Tsonis, J. D. Lambris, and K. Del Rio-Tsonis. 2003. 'Expression of complement 3 and complement 5 in newt limb and lens regeneration', *J Immunol*, 170: 2331-9.

Kirkwood, B. J., P. L. Hendicott, S. A. Read, and K. Pesudovs. 2009. 'Repeatability and validity of lens densitometry measured with Scheimpflug imaging', *J Cataract Refract Surg*, 35: 1210-5.

Kleiman, N. J., J. David, C. D. Elliston, K. M. Hopkins, L. B. Smilenov, D. J. Brenner, B. V. Worgul, E. J. Hall, and H. B. Lieberman. 2007. 'Mrad9 and atm haploinsufficiency enhance spontaneous and X-ray-induced cataractogenesis in mice', *Radiat Res*, 168: 567-73.

Kleiman, N. J., and A. Spector. 1993. 'DNA single strand breaks in human lens epithelial cells from patients with cataract', *Curr Eye Res*, 12: 423-31.

Kleiman, N. J., R. R. Wang, and A. Spector. 1990. 'Hydrogen peroxide-induced DNA damage in bovine lens epithelial cells', *Mutat Res*, 240: 35-45.

Kocer, I., S. Taysi, M. V. Ertekin, I. Karslioglu, A. Gepdiremen, O. Sezen, and K. Serifoglu. 2007. 'The effect of L-carnitine in the prevention of ionizing radiation-induced cataracts: a rat model', *Graefes Arch Clin Exp Ophthalmol*, 245: 588-94.

Kohale, K., A. Ingle, A. Kelkar, and P. Parab. 2004. 'Dense cataract and microphthalmia--new spontaneous mutation in BALB/c mice', *Comp Med*, 54: 275-9.

Koopman, T., H. J. Buikema, H. Hollema, G. H. de Bock, and B. van der Vegt. 2018. 'Digital image analysis of Ki67 proliferation index in breast cancer using virtual dual staining on whole tissue sections: clinical validation and inter-platform agreement', *Breast Cancer Res Treat*, 169: 33-42.

Kosinski-Collins, M. S., and J. King. 2003. 'In vitro unfolding, refolding, and polymerization of human gammaD crystallin, a protein involved in cataract formation', *Protein Sci*, 12: 480-90.

Krishnan, N., D. G. Jeong, S. K. Jung, S. E. Ryu, A. Xiao, C. D. Allis, S. J. Kim, and N. K. Tonks. 2009. 'Dephosphorylation of the C-terminal tyrosyl residue of the DNA damage-related histone H2A.X is mediated by the protein phosphatase eyes absent', *J Biol Chem*, 284: 16066-70.

Kubo, E., D. P. Singh, N. Fatma, T. Shinohara, P. Zelenka, V. N. Reddy, and L. T. Chylack. 2003. 'Cellular distribution of lens epithelium-derived growth factor (LEDGF) in the rat eye: loss of LEDGF from nuclei of differentiating cells', *Histochem Cell Biol*, 119: 289-99.

Kumari, S. S., S. Eswaramoorthy, R. T. Mathias, and K. Varadaraj. 2011. 'Unique and analogous functions of aquaporin 0 for fiber cell architecture and ocular lens transparency', *Biochim Biophys Acta*, 1812: 1089-97.

Kunze, S., C. Dalke, H. Fuchs, M. Klaften, U. Rossler, S. Hornhardt, M. Gomolka, O. Puk, S. Sabrautzki, U. Kulka, M. Hrabe de Angelis, and J. Graw. 2015. 'New mutation in the mouse Xpd/Ercc2 gene leads to recessive cataracts', *PLoS One*, 10: e0125304.

Le Heron, J., Padovani, R., Smith, I., Czarwinski, R. . 2010. 'Radiation protection of medical staff', *European Journal of Radiology*, 76: 20-3.

Lee, J. H., and T. T. Paull. 2007. 'Activation and regulation of ATM kinase activity in response to DNA double-strand breaks', *Oncogene*, 26: 7741-8.

Lett, J. T., A. B. Cox, and A. C. Lee. 1986. 'Cataractogenic potential of ionizing radiations in animal models that simulate man', *Adv Space Res*, 6: 295-303.

Levine, A. J. 1997. 'p53, the cellular gatekeeper for growth and division', *Cell*, 88: 323-31.
Lewis, L., G. E. Crawford, T. S. Furey, and I. Rusyn. 2017. 'Genetic and epigenetic determinants of inter-individual variability in responses to toxicants', *Curr Opin Toxicol*, 6: 50-59.
Li, L. T., G. Jiang, Q. Chen, and J. N. Zheng. 2015. 'Ki67 is a promising molecular target in the diagnosis of cancer (review)', *Mol Med Rep*, 11: 1566-72.
Li, L., and Y. Wang. 2017. 'Cross-talk between the H3K36me3 and H4K16ac histone epigenetic marks in DNA double-strand break repair', *J Biol Chem*, 292: 11951-59.
Lian, Y., J. Xiao, X. Ji, S. Guan, H. Ge, F. Li, L. Ning, and J. Liu. 2015. 'Protracted low-dose radiation exposure and cataract in a cohort of Chinese industry radiographers', *Occup Environ Med*, 72: 640-7.
Liang, X., J. Gu, D. Yu, G. Wang, L. Zhou, X. Zhang, Y. Zhao, X. Chen, S. Zheng, Q. Liu, L. Cai, J. Cui, and W. Li. 2016. 'Low-Dose Radiation Induces Cell Proliferation in Human Embryonic Lung Fibroblasts but not in Lung Cancer Cells: Importance of ERK1/2 and AKT Signaling Pathways', *Dose Response*, 14: 1559325815622174.
Lieberman, H. B., S. K. Panigrahi, K. M. Hopkins, L. Wang, and C. G. Broustas. 2017. 'p53 and RAD9, the DNA Damage Response, and Regulation of Transcription Networks', *Radiat Res*, 187: 424-32.
Lin, H., H. Ouyang, J. Zhu, S. Huang, Z. Liu, S. Chen, G. Cao, G. Li, R. A. Signer, Y. Xu, C. Chung, Y. Zhang, D. Lin, S. Patel, F. Wu, H. Cai, J. Hou, C. Wen, M. Jafari, X. Liu, L. Luo, J. Zhu, A. Qiu, R. Hou, B. Chen, J. Chen, D. Granet, C. Heichel, F. Shang, X. Li, M. Krawczyk, D. Skowronska-Krawczyk, Y. Wang, W. Shi, D. Chen, Z. Zhong, S. Zhong, L. Zhang, S. Chen, S. J. Morrison, R. L. Maas, K. Zhang, and Y. Liu. 2016. 'Lens regeneration using endogenous stem cells with gain of visual function', *Nature*, 531: 323-8.
Little, M. P. 2013. 'A review of non-cancer effects, especially circulatory and ocular diseases', *Radiat Environ Biophys*, 52: 435-49.
Little, M. P., C. M. Kitahara, E. K. Cahoon, M. O. Bernier, R. Velazquez-Kronen, M. M. Doody, D. Borrego, J. S. Miller, B. H. Alexander, S. L. Simon, D. L. Preston, N. Hamada, M. S. Linet, and C. Meyer. 2018. 'Occupational radiation exposure and risk of cataract incidence in a cohort of US radiologic technologists', *Eur J Epidemiol*.
Liu, J., C. G. Chamberlain, and J. W. McAvoy. 1996. 'IGF enhancement of FGF-induced fibre differentiation and DNA synthesis in lens explants', *Exp Eye Res*, 63: 621-9.
Liu, Y. C., M. Wilkins, T. Kim, B. Malyugin, and J. S. Mehta. 2017. 'Cataracts', *Lancet*, 390: 600-12.
Lobrich, M., B. Rydberg, and P. K. Cooper. 1995. 'Repair of x-ray-induced DNA double-strand breaks in specific Not I restriction fragments in human fibroblasts: joining of correct and incorrect ends', *Proc Natl Acad Sci U S A*, 92: 12050-4.
Lomax, M. E., L. K. Folkes, and P. O'Neill. 2013. 'Biological Consequences of Radiation-induced DNA Damage: Relevance to Radiotherapy', *Clinical Oncology*, 25: 578-85.
Louis, C. F., K. C. Hur, A. C. Galvan, E. M. TenBroek, L. J. Jarvis, E. D. Eccleston, and J. B. Howard. 1989. 'Identification of an 18,000-dalton protein in mammalian lens fiber cell membranes', *J Biol Chem*, 264: 19967-73.
Lovicu, F. J., C. G. Chamberlain, and J. W. McAvoy. 1995. 'Differential effects of aqueous and vitreous on fiber differentiation and extracellular matrix accumulation in lens epithelial explants', *Invest Ophthalmol Vis Sci*, 36: 1459-69.
Lovicu, F. J., and J. W. McAvoy. 2001. 'FGF-induced lens cell proliferation and differentiation is dependent on MAPK (ERK1/2) signalling', *Development*, 128: 5075-84.
———. 2005. 'Growth factor regulation of lens development', *Dev Biol*, 280: 1-14.
Makharashvili, N., and T. T. Paull. 2015. 'CtIP: A DNA damage response protein at the intersection of DNA metabolism', *DNA Repair (Amst)*, 32: 75-81.
Malmstrom, T., and R. H. Kroger. 2006. 'Pupil shapes and lens optics in the eyes of terrestrial vertebrates', *J Exp Biol*, 209: 18-25.

Markiewicz, E., S. Barnard, J. Haines, M. Coster, O. van Geel, W. Wu, S. Richards, E. Ainsbury, K. Rothkamm, S. Bouffler, and R. A. Quinlan. 2015. 'Nonlinear ionizing radiation-induced changes in eye lens cell proliferation, cyclin D1 expression and lens shape', *Open Biol*, 5: 150011.

Marples, B. 2004. 'Is low-dose hyper-radiosensitivity a measure of G2-phase cell radiosensitivity?', *Cancer Metastasis Rev*, 23: 197-207.

Martin, C. J. 2011. 'A 20mSv dose limit for the eye: sense or no sense?', *Journal of Radiological Protection*, 31: 385-7.

Martin, M. D., D. B. Danahy, S. M. Hartwig, J. T. Harty, and V. P. Badovinac. 2017. 'Revealing the Complexity in CD8 T Cell Responses to Infection in Inbred C57B/6 versus Outbred Swiss Mice', *Front Immunol*, 8: 1527.

Matsui, H., L. R. Lin, D. P. Singh, T. Shinohara, and V. N. Reddy. 2001. 'Lens epithelium-derived growth factor: increased survival and decreased DNA breakage of human RPE cells induced by oxidative stress', *Invest Ophthalmol Vis Sci*, 42: 2935-41.

Matsuyama, M., H. Tanaka, A. Inoko, H. Goto, S. Yonemura, K. Kobori, Y. Hayashi, E. Kondo, S. Itohara, I. Izawa, and M. Inagaki. 2013. 'Defect of mitotic vimentin phosphorylation causes microophthalmia and cataract via aneuploidy and senescence in lens epithelial cells', *J Biol Chem*, 288: 35626-35.

Mayca Pozo, F., J. Tang, K. W. Bonk, R. A. Keri, X. Yao, and Y. Zhang. 2017. 'Regulatory cross-talk determines the cellular levels of 53BP1 protein, a critical factor in DNA repair', *J Biol Chem*, 292: 5992-6003.

Mc Laughlin, J. P. 2015. 'Some characteristics and effects of natural radiation', *Radiat Prot Dosimetry*, 167: 2-7.

McAvoy, J. W., and C. G. Chamberlain. 1989. 'Fibroblast growth factor (FGF) induces different responses in lens epithelial cells depending on its concentration', *Development*, 107: 221-8.

McAvoy, J. W., and J. McDonald. 1984. 'Proliferation of lens epithelial explants in culture increases with age of donor rat', *Curr Eye Res*, 3: 1151-3.

Medvedovsky, C., Worgul, B.V., Huang, Y., Brenner, D.J., Tao, F., Miller, J., Zeitlin, C., Ainsworth, E.J. . 1994. 'The influence of dose, dose-rate and particle fragmentation on cataract induction by energetic iron ions', *Advances in Space Research*, 14: 475-82.

Menko, A. S., B. M. Bleaken, A. A. Libowitz, L. Zhang, M. A. Stepp, and J. L. Walker. 2014. 'A central role for vimentin in regulating repair function during healing of the lens epithelium', *Mol Biol Cell*, 25: 776-90.

Merriam, G. R., Jr., and E. F. Focht. 1962. 'A clinical and experimental study of the effect of single and divided doses of radiation on cataract production', *Trans Am Ophthalmol Soc*, 60: 35-52.

Michael, R., and A. J. Bron. 2011. 'The ageing lens and cataract: a model of normal and pathological ageing', *Philos Trans R Soc Lond B Biol Sci*, 366: 1278-92.

Miller, I., M. Min, C. Yang, C. Tian, S. Gookin, D. Carter, and S. L. Spencer. 2018. 'Ki67 is a Graded Rather than a Binary Marker of Proliferation versus Quiescence', *Cell Rep*, 24: 1105-12.e5.

Miller, R. C., and E. F. Riley. 1987. 'Recovery of rat lens epithelial cells after total or partial X-irradiation', *Exp Eye Res*, 45: 407-18.

Miller, R. J., T. Fujino, and M. D. Nefzger. 1967. 'Lens findings in Atomic bomb survivors. A review of major ophthalmic surveys at the atomic Bomb Casualty Commission (1949-1962)', *Arch Ophthalmol*, 78: 697-704.

Milligan, J. R., J. Y. Ng, C. C. Wu, J. A. Aguilera, R. C. Fahey, and J. F. Ward. 1995. 'DNA repair by thiols in air shows two radicals make a double-strand break', *Radiat Res*, 143: 273-80.

Mohamed, A., and R. C. Augusteyn. 2018. 'Human lens weights with increasing age', *Mol Vis*, 24: 867-xxx.

Mousseau, T. A., and A. P. Moller. 2013. 'Elevated frequency of cataracts in birds from chernobyl', *PLoS One*, 8: e66939.

Mukherjee, S., K. B. Sainis, and D. D. Deobagkar. 2014. 'F1 hybrids of BALB/c and C57BL/6 mouse strains respond differently to low-dose ionizing radiation exposure', *J Genet*, 93: 667-82.

Nakashima, E., K. Neriishi, and A. Minamoto. 2006. 'A reanalysis of atomic-bomb cataract data, 2000-2002: a threshold analysis', *Health Phys*, 90: 154-60.

Nelder, P. McCullagh and J. A. 1989. *Generalized Linear Models* (CRC Press, Taylor & Francis Group).

Neriishi, K., E. Nakashima, M. Akahoshi, A. Hida, E. J. Grant, N. Masunari, S. Funamoto, A. Minamoto, S. Fujiwara, and R. E. Shore. 2012. 'Radiation dose and cataract surgery incidence in atomic bomb survivors, 1986-2005', *Radiology*, 265: 167-74.

Neumaier, T., J. Swenson, C. Pham, A. Polyzos, A. T. Lo, P. Yang, J. Dyball, A. Asaithamby, D. J. Chen, M. J. Bissell, S. Thalhammer, and S. V. Costes. 2012. 'Evidence for formation of DNA repair centers and dose-response nonlinearity in human cells', *Proc Natl Acad Sci U S A*, 109: 443-8.

Newman, M. R., P. J. Sykes, B. J. Blyth, E. Bezak, M. D. Lawrence, K. L. Morel, and R. J. Ormsby. 2014. 'The methylation of DNA repeat elements is sex-dependent and temporally different in response to X radiation in radiosensitive and radioresistant mouse strains', *Radiat Res*, 181: 65-75.

Noda, Asao. 2017. 'Radiation-induced unrepairable DSBs: their role in the late effects of radiation and possible applications to biodosimetry', *Journal of Radiation Research*, 59: ii114-ii20.

Noon, A. T., and A. A. Goodarzi. 2011. '53BP1-mediated DNA double strand break repair: insert bad pun here', *DNA Repair (Amst)*, 10: 1071-6.

O'Connor, U., Gallagher, A., Malone, L., O'Reilly, G. . 2013. 'Occupational radiation dose to eyes from endoscopic retrograde cholangiopancreatography procedures in light of the revised eye lens dose limit from the International Commission on Radiological Protection', *The British Journal of Radiology*, 86.

Oka, M., C. Toyoda, Y. Kaneko, Y. Nakazawa, E. Aizu-Yokota, and M. Takehana. 2010. 'Characterization and localization of side population cells in the lens', *Mol Vis*, 16: 945-53.

Okayasu, R., K. Suetomi, Y. Yu, A. Silver, J. S. Bedford, R. Cox, and R. L. Ullrich. 2000. 'A deficiency in DNA repair and DNA-PKcs expression in the radiosensitive BALB/c mouse', *Cancer Res*, 60: 4342-5.

Omar, A., Marteinsdottir, M., Kadesjö, N., Fransson, A. 2015. 'On the feasibility of utilizing active personal dosimeters worn on the chest to estimate occupational eye lens dose in x-ray angiography', *Journal of Radiological Protection*, 35: 271-84.

Osnes-Ringen, O., A. O. Azqueta, M. C. Moe, C. Zetterstrom, M. Roger, B. Nicolaissen, and A. R. Collins. 2013. 'DNA damage in lens epithelium of cataract patients in vivo and ex vivo', *Acta Ophthalmol*, 91: 652-6.

Otake, M., Schull, W.J. . 1990. 'Radiation-related posterior lenticular opacities in Hiroshima and Nagasaki atomic bomb survivors based on the DS86 dosimetry system', *Radiation Research*, 121: 3-13.

Panier, S., and S. J. Boulton. 2014. 'Double-strand break repair: 53BP1 comes into focus', *Nat Rev Mol Cell Biol*, 15: 7-18.

Patel, A., J. Anderson, D. Kraft, R. Finnon, P. Finnon, C. L. Scudamore, G. Manning, R. Bulman, N. Brown, S. Bouffler, P. O'Neill, and C. Badie. 2016. 'The Influence of the CTIP Polymorphism, Q418P, on Homologous Recombination and Predisposition to Radiation-Induced Tumorigenesis (mainly rAML) in Mice', *Radiat Res*, 186: 638-49.

Paulson, E., Cheafor, D., Enterline, D., McAdams, P., Yoshizumi, T. 2001. 'CT Fluoroscopy-guided Interventional Procedures: Techniques and Radiation Dose to Radiologists', *Vascular and Interventional Radiology*, 220: 161-7.

Pei, X., Y. Bao, Y. Chen, and X. Li. 2008. 'Correlation of lens density measured using the Pentacam Scheimpflug system with the Lens Opacities Classification System III grading score and visual acuity in age-related nuclear cataract', *Br J Ophthalmol*, 92: 1471-5.

Penault-Llorca, F., and N. Radosevic-Robin. 2017. 'Ki67 assessment in breast cancer: an update', *Pathology*, 49: 166-71.

Peng, Y., N. Brown, R. Finnon, C. L. Warner, X. Liu, P. C. Genik, M. A. Callan, F. A. Ray, T. B. Borak, C. Badie, S. D. Bouffler, R. L. Ullrich, J. S. Bedford, and M. M. Weil. 2009. 'Radiation leukemogenesis in mice: loss of PU.1 on chromosome 2 in CBA and C57BL/6 mice after irradiation with 1 GeV/nucleon 56Fe ions, X rays or gamma rays. Part I. Experimental observations', *Radiat Res*, 171: 474-83.

Peterson, S. R., P. A. Silva, T. J. Murtha, and J. K. Sun. 2018. 'Cataract Surgery in Patients with Diabetes: Management Strategies', *Semin Ophthalmol*, 33: 75-82.

Petroni, M., F. Sardina, C. Heil, M. Sahun-Roncero, V. Colicchia, V. Veschi, S. Albini, D. Fruci, B. Ricci, A. Soriani, L. Di Marcotullio, I. Screpanti, A. Gulino, and G. Giannini. 2016. 'The MRN complex is transcriptionally regulated by MYCN during neural cell proliferation to control replication stress', *Cell Death Differ*, 23: 197-206.

Puk, O., M. H. de Angelis, and J. Graw. 2013. 'Lens density tracking in mice by Scheimpflug imaging', *Mamm Genome*, 24: 295-302.

Purcell, P., G. Oliver, G. Mardon, A. L. Donner, and R. L. Maas. 2005. 'Pax6-dependence of Six3, Eya1 and Dach1 expression during lens and nasal placode induction', *Gene Expr Patterns*, 6: 110-8.

Rafferty, N. S., and K. A. Rafferty, Jr. 1981. 'Cell population kinetics of the mouse lens epithelium', *J Cell Physiol*, 107: 309-15.

Rafnsson, V., E. Olafsdottir, J. Hrafnkelsson, H. Sasaki, A. Arnarsson, and F. Jonasson. 2005. 'Cosmic radiation increases the risk of nuclear cataract in airline pilots: a population-based case-control study', *Arch Ophthalmol*, 123: 1102-5.

Rathmann, N., Kostrzewa, M., Kara, K., Bartling, S., Haubenreisser, H., Schoenberg, S.O., Diehl, S.J. . 2015. 'Radiation exposure of the interventional radiologist during percutaneous biopsy using a multiaxis interventional C-arm CT system with 3D laser guidance: a phantom study', *The British Journal of Radiology*.

Reddan, J. R., and D. C. Dziedzic. 1982. 'Insulin-like growth factors, IGF-1, IGF-2 and somatomedin C trigger cell proliferation in mammalian epithelial cells cultured in a serum-free medium', *Exp Cell Res*, 142: 293-300.

Reddan, J. R., F. J. Giblin, D. C. Dziedzic, B. M. Wirebaugh, and J. L. Peters. 1995. 'Hydrogen peroxide affects specific epithelial subpopulations in cultured rabbit lenses', *Invest Ophthalmol Vis Sci*, 36: 289-99.

Richard S. Smith, John P. Sundberg. 1995. 'Microphthalmia and ocular infections in inbred C57 black mice', *JAX Notes*.

Rithidech, K. N., E. P. Cronkite, and V. P. Bond. 1999. 'Advantages of the CBA mouse in leukemogenesis research', *Blood Cells Mol Dis*, 25: 38-45.

Robinson, M. L. 2013. 'A mechanism for the synergism of FGF- and Wnt-signaling during lens fiber cell differentiation', *Invest Ophthalmol Vis Sci*, 54.

Roderick, T. H. 1963. 'THE RESPONSE OF TWENTY-SEVEN INBRED STRAINS OF MICE TO DAILY DOSES OF WHOLE-BODY X-IRRADIATION', *Radiat Res*, 20: 631-9.

Romanova, K., Vassileva, J., Alyakov, M. . 2015. 'Radiation exposure to the eye lens of orthopaedic surgeons during various orthopaedic procedures', *Radiat Prot Dosimetry*, 165: 310-3.

Rosales, P., A. De Castro, I. Jimenez-Alfaro, and S. Marcos. 2010. 'Intraocular lens alignment from purkinje and Scheimpflug imaging', *Clin Exp Optom*, 93: 400-8.

Rothkamm, K., S. Barnard, J. Moquet, M. Ellender, Z. Rana, and S. Burdak-Rothkamm. 2015. 'DNA damage foci: Meaning and significance', *Environ Mol Mutagen*, 56: 491-504.

Rothkamm, K., and S. Horn. 2009. 'gamma-H2AX as protein biomarker for radiation exposure', *Ann Ist Super Sanita*, 45: 265-71.

Rothkamm, K., I. Kruger, L. H. Thompson, and M. Lobrich. 2003. 'Pathways of DNA double-strand break repair during the mammalian cell cycle', *Mol Cell Biol*, 23: 5706-15.

Rothkamm, K., and M. Lobrich. 2003. 'Evidence for a lack of DNA double-strand break repair in human cells exposed to very low x-ray doses', *Proc Natl Acad Sci U S A*, 100: 5057-62.

Rothstein, H., B. V. Worgul, C. Medvedovsky, and G. R. Merriam, Jr. 1982. 'G0/G1 arrest of cell proliferation in the ocular lens prevents development of radiation cataract', *Ophthalmic Res*, 14: 215-20.

Rühm, W., Woloschak, G.E., Shore, R.E., Azizova, T.V., Grosche, B., Niwa, O., Akiba, S., Ono, T., Suzuki, K., Iwasaki, T., Ban, N., Kai, M., Clement, C.H., Bouffler, S., Toma, H., Hamada, N. . 2015. 'Dose and dose-rate effects of ionizing radiation: a discussion in the light of radiological protection. ', *Radiation and Environmental Biophysics*, 54: 379-401.

Ruiz de Almodovar, J. M., C. Bush, J. H. Peacock, G. G. Steel, S. J. Whitaker, and T. J. McMillan. 1994. 'Dose-rate effect for DNA damage induced by ionizing radiation in human tumor cells', *Radiat Res*, 138: S93-6.

Ruotolo, R., F. Grassi, R. Percudani, C. Rivetti, D. Martorana, G. Maraini, and S. Ottonello. 2003. 'Gene expression profiling in human age-related nuclear cataract', *Mol Vis*, 9: 538-48.

Sanders, J. L., A. Iannaccone, R. M. Boudreau, Y. P. Conley, P. L. Opresko, W. C. Hsueh, S. R. Cummings, R. M. Cawthon, T. B. Harris, M. A. Nalls, S. B. Kritchevsky, and A. B. Newman. 2011. 'The association of cataract with leukocyte telomere length in older adults: defining a new marker of aging', *J Gerontol A Biol Sci Med Sci*, 66: 639-45.

Sandilands, A., A. M. Hutcheson, H. A. Long, A. R. Prescott, G. Vrensen, J. Loster, N. Klopp, R. B. Lutz, J. Graw, S. Masaki, C. M. Dobson, C. E. MacPhee, and R. A. Quinlan. 2002. 'Altered aggregation properties of mutant gamma-crystallins cause inherited cataract', *Embo j*, 21: 6005-14.

Sanson, M., V. Marcaud, E. Robin, C. Valery, F. Sturtz, and B. Zalc. 2002. 'Connexin 43-mediated bystander effect in two rat glioma cell models', *Cancer Gene Ther*, 9: 149-55.

Schey, K. L., R. S. Petrova, R. B. Gletten, and P. J. Donaldson. 2017. 'The Role of Aquaporins in Ocular Lens Homeostasis', *Int J Mol Sci*, 18.

Scully, R., and A. Xie. 2013. 'Double strand break repair functions of histone H2AX', *Mutat Res*, 750: 5-14.

Seals, K.F., Lee, E.W., Cagnon, C.H., Al-Hakim, R.A., Kee, S.T. 2015. 'Radiation-Induced Cataractogenesis: A Critical Literature review for the Interventional Radiologist', *Cardiovascular Interventional Radiology*.

Shafie, S. M., F. R. Barria von-Bischhoffshausen, and J. B. Bateman. 2006. 'Autosomal dominant cataract: intrafamilial phenotypic variability, interocular asymmetry, and variable progression in four Chilean families', *Am J Ophthalmol*, 141: 750-2.

Shui, Y. B., H. Sasaki, J. H. Pan, I. Hata, M. Kojima, Y. Yamada, K. I. Hirai, N. Takahashia, and K. Sasaki. 2000. 'Morphological observation on cell death and phagocytosis induced by ultraviolet irradiation in a cultured human lens epithelial cell line', *Exp Eye Res*, 71: 609-18.

Sidjanin, D., S. Zigman, and J. Reddan. 1993. 'DNA damage and repair in rabbit lens epithelial cells following UVA radiation', *Curr Eye Res*, 12: 773-81.

Silverman, J., H. Takai, S. B. Buonomo, F. Eisenhaber, and T. de Lange. 2004. 'Human Rif1, ortholog of a yeast telomeric protein, is regulated by ATM and 53BP1 and functions in the S-phase checkpoint', *Genes Dev*, 18: 2108-19.

Singh, D. P., E. Kubo, Y. Takamura, T. Shinohara, A. Kumar, L. T. Chylack, Jr., and N. Fatma. 2006. 'DNA binding domains and nuclear localization signal of LEDGF: contribution of two helix-turn-helix (HTH)-like domains and a stretch of 58 amino acids of the N-terminal to the trans-activation potential of LEDGF', *J Mol Biol*, 355: 379-94.

Singh, D. P., N. Ohguro, L. T. Chylack, Jr., and T. Shinohara. 1999. 'Lens epithelium-derived growth factor: increased resistance to thermal and oxidative stresses', *Invest Ophthalmol Vis Sci*, 40: 1444-51.

Smith, A. J., S. S. Ball, K. Manzar, R. P. Bowater, and I. M. Wormstone. 2015. 'Ku80 Counters Oxidative Stress-Induced DNA Damage and Cataract Formation in the Human Lens', *Invest Ophthalmol Vis Sci*, 56: 7868-74.

So, S., A. J. Davis, and D. J. Chen. 2009. 'Autophosphorylation at serine 1981 stabilizes ATM at DNA damage sites', *J Cell Biol*, 187: 977-90.

Song, J., D. Guo, and H. Bi. 2018. 'Chlorogenic acid attenuates hydrogen peroxideinduced oxidative stress in lens epithelial cells', *Int J Mol Med*, 41: 765-72.

Song, S., A. Landsbury, R. Dahm, Y. Liu, Q. Zhang, and R. A. Quinlan. 2009. 'Functions of the intermediate filament cytoskeleton in the eye lens', *J Clin Invest*, 119: 1837-48.

Stewart, D. N., J. Lango, K. P. Nambiar, M. J. Falso, P. G. FitzGerald, D. M. Rocke, B. D. Hammock, and B. A. Buchholz. 2013. 'Carbon turnover in the water-soluble protein of the adult human lens', *Mol Vis*, 19: 463-75.

Stewart, F. A., A. V. Akleyev, M. Hauer-Jensen, J. H. Hendry, N. J. Kleiman, T. J. Macvittie, B. M. Aleman, A. B. Edgar, K. Mabuchi, C. R. Muirhead, R. E. Shore, and W. H. Wallace. 2012. 'ICRP publication 118: ICRP statement on tissue reactions and early and late effects of radiation in normal tissues and organs--threshold doses for tissue reactions in a radiation protection context', *Ann ICRP*, 41: 1-322.

Supek, F., and B. Lehner. 2017. 'Clustered Mutation Signatures Reveal that Error-Prone DNA Repair Targets Mutations to Active Genes', *Cell*, 170: 534-47.e23.

Takata, K., T. Matsuzaki, and Y. Tajika. 2004. 'Aquaporins: water channel proteins of the cell membrane', *Prog Histochem Cytochem*, 39: 1-83.

Takemoto, L., and C. M. Sorensen. 2008. 'Protein-protein interactions and lens transparency', *Exp Eye Res*, 87: 496-501.

Takizawa, A., and K. Sasaki. 1986. 'In vivo observations of cataract development in Emory mouse', *Ophthalmic Res*, 18: 243-7.

Tan, A. G., P. Mitchell, E. Rochtchina, T. Hong, R. G. Cumming, and J. J. Wang. 2012. 'Lens retrodots and vacuoles and their associations with the prevalence and incidence of age-related cataract', *Eye (Lond)*, 26: 568-75.

Tao, F., P. Powers-Risius, E. L. Alpen, C. Medvedovsky, J. David, and B. V. Worgul. 1994. 'Radiation effects on late cytopathological parameters in the murine lens relative to particle fluence', *Adv Space Res*, 14: 483-91.

Tholozan, F. M., and R. A. Quinlan. 2007. 'Lens cells: more than meets the eye', *Int J Biochem Cell Biol*, 39: 1754-9.

Treton, J. A., and Y. Courtois. 1981. 'Evolution of the distribution, proliferation and ultraviolet repair capacity of rat lens epithelial cells as a function of maturation and aging', *Mech Ageing Dev*, 15: 251-67.

Truong, K., S. Bradley, B. Baginski, J. R. Wilson, D. Medlin, L. Zheng, R. K. Wilson, M. Rusin, E. Takacs, and D. Dean. 2018. 'The effect of well-characterized, very low-dose x-ray radiation on fibroblasts', *PLoS One*, 13: e0190330.

Truscott, R. J. 2005. 'Age-related nuclear cataract-oxidation is the key', *Exp Eye Res*, 80: 709-25.

Tseng, A. S. 2017. 'Seeing the future: using Xenopus to understand eye regeneration', *Genesis*, 55.

Tukey, J. W. 1949. 'Comparing individual means in the analysis of variance', *Biometrics*, 5: 99-114.

Turner, H. C., I. Shuryak, M. Taveras, A. Bertucci, J. R. Perrier, C. Chen, C. D. Elliston, G. W. Johnson, L. B. Smilenov, S. A. Amundson, and D. J. Brenner. 2015. 'Effect of dose rate on residual gamma-H2AX levels and frequency of micronuclei in X-irradiated mouse lymphocytes', *Radiat Res*, 183: 315-24.

Upadhya, D., M. Ogata, and L. W. Reneker. 2013. 'MAPK1 is required for establishing the pattern of cell proliferation and for cell survival during lens development', *Development*, 140: 1573-82.

Upton, A. C., K. W. Christenberry, G. S. Melville, J. Furth, and G. S. Hurst. 1956. 'The Relative Biological Effectiveness of Neutrons, X-Rays, and Gamma Rays for the Production of Lens Opacities: Observations on Mice, Rats, Guinea-Pigs, and Rabbits', 67: 686-96.

van den Berg, Tjtp. 2018. 'Intraocular light scatter, reflections, fluorescence and absorption: what we see in the slit lamp', *Ophthalmic Physiol Opt*, 38: 6-25.

Vanhavere, F., Carinou, E., Domienik, J., Donadille, L., Ginjaume, M., Gualdrini, G., Koukorava, C., Krim, S., Nikodemova, D., Ruiz-Lopez, N., Sans-Merce, M., Struelens, L. . 2015. 'Measurements of the eye lens doses in interventional radiology and cardiology: Final results of the ORAMED project.', *Radiation Measurements*, 46: 1243-47.

Vano, E., Sanchez, R.M., Fernandez, J.M. . 2015. 'Estimation of staff lens doses during interventional procedures. Comparing cardiology, neuroradiology and interventional radiology', *Radiat Prot Dosimetry*, 165: 279-83.

Varadaraj, K., S. S. Kumari, and R. T. Mathias. 2010. 'Transgenic expression of AQP1 in the fiber cells of AQP0 knockout mouse: effects on lens transparency', *Exp Eye Res*, 91: 393-404.

Verbiest, T., S. Bouffler, and C. Badie. 2018. 'No equal opportunity for leukemia initiating cells', *Oncotarget*, 9: 37078-79.

von, Sallmann L. 1950. 'Experimental studies on early lens changes after x-ray irradiation', *Trans Am Ophthalmol Soc*: 228-42.

von Sallmann, L. 1950. 'Experimental Studies on Early Lens Changes after X-Ray Irradiation', *Trans Am Ophthalmol Soc*, 48: 228-42.

———. 1952. 'Experimental studies on early lens changes after roentgen irradiation. III. Effect of x-radiation on mitotic activity and nuclear fragmentation of lens epithelium in normal and cysteine-treated rabbits', *AMA Arch Ophthalmol*, 47: 305-20.

von Sallmann, L., and P. Grimes. 1966. 'Effect of age on cell division, 3H-thymidine incorporation, and diurnal rhythm in the lens epithelium of rats', *Invest Ophthalmol*, 5: 560-7.

Von Sallmann, L., P. Grimes, and Elvain N. Mc. 1962. 'Aspects of mitotic activity in relation to cell proliferation in the lens epithelium', *Exp Eye Res*, 1: 449-56.

Weiner, X., M. Baumeister, T. Kohnen, and J. Buhren. 2014. 'Repeatability of lens densitometry using Scheimpflug imaging', *J Cataract Refract Surg*, 40: 756-63.

Wiechmann, A. F., and J. A. Summers. 2008. 'Circadian rhythms in the eye: the physiological significance of melatonin receptors in ocular tissues', *Prog Retin Eye Res*, 27: 137-60.

Wolf, N., W. Pendergrass, N. Singh, K. Swisshelm, and J. Schwartz. 2008. 'Radiation cataracts: mechanisms involved in their long delayed occurrence but then rapid progression', *Mol Vis*, 14: 274-85.

Wolf, N., P. Penn, W. Pendergrass, H. Van Remmen, A. Bartke, P. Rabinovitch, and G. M. Martin. 2005. 'Age-related cataract progression in five mouse models for anti-oxidant protection or hormonal influence', *Exp Eye Res*, 81: 276-85.

Worgul, B V, D J Brenner, C Medvedovsky, G R Merriam, Jr, and Y Huang. 1993. 'Accelerated heavy particles and the lens. VII: The cataractogenic potential of 450 MeV/amu iron ions', *Investigative Ophthalmology & Visual Science*, 34: 184-93.

Worgul, B. V., Y. I. Kundiyev, N. M. Sergiyenko, V. V. Chumak, P. M. Vitte, C. Medvedovsky, E. V. Bakhanova, A. K. Junk, O. Y. Kyrychenko, N. V. Musijachenko, S. A. Shylo, O. P. Vitte, S. Xu, X. Xue, and R. E. Shore. 2007. 'Cataracts among Chernobyl clean-up workers: implications regarding permissible eye exposures', *Radiat Res*, 167: 233-43.

Worgul, B. V., C. Medvedovsky, and G. R. Merriam, Jr. 1981. 'Cataractogenesis in the X-irradiated rabbit eye', *Curr Eye Res*, 1: 275-80.

Worgul, B. V., G. R. Merriam, Jr., and C. Medvedovsky. 1989. 'Cortical cataract development--an expression of primary damage to the lens epithelium', *Lens Eye Toxic Res*, 6: 559-71.

Worgul, B. V., L. Smilenov, D. J. Brenner, A. Junk, W. Zhou, and E. J. Hall. 2002. 'Atm heterozygous mice are more sensitive to radiation-induced cataracts than are their wild-type counterparts', *Proc Natl Acad Sci U S A*, 99: 9836-9.

Worgul, B. V., L. Smilenov, D. J. Brenner, M. Vazquez, and E. J. Hall. 2005. 'Mice heterozygous for the ATM gene are more sensitive to both X-ray and heavy ion exposure than are wildtypes', *Adv Space Res*, 35: 254-9.

Wormstone, I. M., and M. A. Wride. 2011. 'The ocular lens: a classic model for development, physiology and disease', *Philos Trans R Soc Lond B Biol Sci*, 366: 1190-2.

Wride, M. A. 2011. 'Lens fibre cell differentiation and organelle loss: many paths lead to clarity', *Philos Trans R Soc Lond B Biol Sci*, 366: 1219-33.

Wu, J. J., W. Wu, F. M. Tholozan, C. D. Saunter, J. M. Girkin, and R. A. Quinlan. 2015. 'A dimensionless ordered pull-through model of the mammalian lens epithelium evidences scaling across species and explains the age-dependent changes in cell density in the human lens', *J R Soc Interface*, 12: 20150391.

Wu, W., F. M. Tholozan, M. W. Goldberg, L. Bowen, J. Wu, and R. A. Quinlan. 2014. 'A gradient of matrix-bound FGF-2 and perlecan is available to lens epithelial cells', *Exp Eye Res*, 120: 10-4.

Xu, P. X., I. Woo, H. Her, D. R. Beier, and R. L. Maas. 1997. 'Mouse Eya homologues of the Drosophila eyes absent gene require Pax6 for expression in lens and nasal placode', *Development*, 124: 219-31.

Yuan, J. P., L. W. Wang, A. P. Qu, J. M. Chen, Q. M. Xiang, C. Chen, S. R. Sun, D. W. Pang, J. Liu, and Y. Li. 2015. 'Quantum dots-based quantitative and in situ multiple imaging on ki67 and cytokeratin to improve ki67 assessment in breast cancer', *PLoS One*, 10: e0122734.

Yuan, R., L. L. Peters, and B. Paigen. 2011. 'Mice as a mammalian model for research on the genetics of aging', *Ilar j*, 52: 4-15.

Zagorska, A., K. Romanova, J. Hristova-Popova, J. Vassileva, and K. Katzarov. 2015. 'Eye lens exposure to medical staff during endoscopic retrograde cholangiopancreatography', *Phys Med*.

Zhao, Y., P. A. Wilmarth, C. Cheng, S. Limi, V. M. Fowler, D. Zheng, L. L. David, and A. Cvekl. 2019. 'Proteome-transcriptome analysis and proteome remodeling in mouse lens epithelium and fibers', *Exp Eye Res*, 179: 32-46.

Zhou, M., J. Leiberman, J. Xu, and R. M. Lavker. 2006. 'A hierarchy of proliferative cells exists in mouse lens epithelium: implications for lens maintenance', *Invest Ophthalmol Vis Sci*, 47: 2997-3003.

Zimmermann, M., and T. de Lange. 2014. '53BP1: pro choice in DNA repair', *Trends Cell Biol*, 24: 108-17.

Zintz, C., and D. C. Beebe. 1986. 'Morphological and cell volume changes in the rat lens during the formation of radiation cataracts', *Exp Eye Res*, 42: 43-54.